NTNU

Norwegian University of
Science and Technology

Engineered Geothermal Systems

Lars Anders Drange

Master of Science in Product Design and Manufacturing
Submission date: June 2011
Supervisor: Erling Næss, EPT

Norwegian University of Science and Technology
Department of Energy and Process Engineering

NTNU

Norwegian University
of Science and Technology

Department of Energy
and Process Engineering

EPT-M-2011-35

MASTER THESIS

for

Stud.techn. Lars Anders Drange
Spring 2011

Engineered Geothermal Systems

Konstruerte geotermiske systemer

Background and objective.

Deep Geothermal energy reefer to heat that is extracted from boreholes several kilometers deep in the bedrock. Traditionally this has been done in areas where there are naturally occurring hot springs.

Geothermal energy is a renewable energy resource that has some unique features. It is continuous and it can be used as base load. If managed properly it can provide clean energy for electricity and heat production without either emissions or footprint. As it is a local energy resource it also has socio-economical benefits.

With an increased demand for clean energy, geothermal has received interest, but instead of the traditional systems, it is Engineered Geothermal Systems (EGS) that are in focus. The theoretical potential is vast, but for EGS to reach a significant portion of its potential, it must be proven that the concept can be applied independent of site conditions.

Since the geological and thermal structure of the uppermost kilometers of the crust varies geographically, the method or concept is site dependent. This makes EGS a conceptual name for a wide range of ways to utilize geothermal energy. Ranging from single well concepts using the natural permeability of sedimentary basins to systems with multiple wells and artificially constructed fractures in crystalline rock.

There are many ideas in the literature to how an EGS could be constructed, however, only few have been implemented and often with the aim to produce electricity. Since EGS produce at low enthalpy, and typically have a decline of thermal output with time, the production of electricity can be done with binary cycles and by hybridization with other energy sources.

The aim of this thesis will be to first evaluate different EGS concepts, this includes both implemented and published concept. Then determine which concepts that could be constructed based on Norwegian geology. From this, a minimum of one concept will be selected for further studies and a simplified method to simulate the concepts will be developed, the method should be able to capture the long term thermal output from the system. This will then be used as input for evaluation of different topside systems and ways to efficiently utilize the heat, primarily for production of electricity.

The following questions shall be considered in the project work:

1. Literature survey regarding EGS and electricity production from EGS:
   a) Describe and evaluate different EGS concepts available in the literature. Identify positive and negative aspects of each concept. Evaluate the applicability of the concepts to the geological situation in Norway.

   b) Electricity production from EGS and alternatives for integration of EGS with hybrid cycles utilizing other energy resources.

2. Develop a mathematical/numerical model to calculate the thermal output of one or more selected EGS concepts. The model(s) shall be presented and discussed. Uncertainties in the model(s) shall be discussed.

3. Perform calculations on the modeled EGS concepts including top-site utilization analyses, primarily for electricity production. The top-side calculations shall be based on the thermal output from the EGS-model(s) and on hybridization with other energy resources.

4. Perform sensitivity analyses for overall system performance based on specifications that will be made in cooperation with the department of Energy and Process Engineering.

5. Suggestions for further work shall be made with focus on potential technology developments that can improve thermal output of the geothermal system.

Within 14 days of receiving the written text on the master thesis, the candidate shall submit a research plan for his project to the department.

When the thesis is evaluated, emphasis is put on processing of the results, and that they are presented in tabular and/or graphic form in a clear manner, and that they are analyzed carefully. The thesis should be formulated as a research report with summary both in English and Norwegian, conclusion, literature references, table of contents etc. During the preparation of the text, the candidate should make an effort to produce a well-structured and easily readable report. In order to ease the evaluation of the thesis, it is important that the cross-references are correct. In the making of the report, strong emphasis should be placed on both a thorough discussion of the results and an orderly presentation.
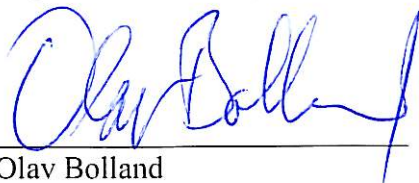
The candidate is requested to initiate and keep close contact with his/her academic supervisor(s) throughout the working period. The candidate must follow the rules and regulations of NTNU as well as passive directions given by the Department of Energy and Process Engineering.

Pursuant to "Regulations concerning the supplementary provisions to the technology study program/Master of Science" at NTNU §20, the Department reserves the permission to utilize all the results and data for teaching and research purposes as well as in future publications.

One – 1 complete original of the thesis shall be submitted to the authority that handed out the set subject. (A short summary including the author's name and the title of the thesis should also be submitted, for use as reference in journals (max. 1 page with double spacing)).

Two – 2 – copies of the thesis shall be submitted to the Department. Upon request, additional copies shall be submitted directly to research advisors/companies. A CD-ROM (Word format or corresponding) containing the thesis, and including the short summary, must also be submitted to the Department of Energy and Process Engineering

Department of Energy and Process Engineering, 6. February 2011

Olav Bolland
Department Head

Erling Næss
Academic Supervisor

Research Advisors: Henrik Holmberg, ph.d.-candidate, EPT/NTNU

Preface

This master thesis was written spring 2011 as a part of my master's degree in Mechanical Engineering at the Norwegian University of Science and Technology, department of Energy and Process Engineering.

The topic is "Engineered Geothermal Systems" and the potential for deep geothermal energy in Norway. The master thesis is written from thermodynamic point of view.

I would like to thank Erling Næss and Henrik Holmberg, my supervisors. Their guidance and knowledge have been critical to my work.

Trondheim June 11, 2011

Lars Anders Drange

Summary

Different concepts for Enhanced Geothermal Systems (EGS) are presented and evaluated according to their potential for medium to large scale power production in Norwegian conditions. Potential locations for geothermal energy in Norway are identified. A fractured EGS with multiple wells situated in a low to medium temperature granitic basement was found to be the concept best suited for medium to large scale power production in Norway.

An Organic Rankine Cycle (ORC) is typically used as the heat conversion cycle in low to medium temperatures. The ORC yields a better thermal performance in these temperatures, compared to flash cycles and Stirling engines. It is also a mature technology and commercially available. Thermal efficiency of the ORC was found to decrease drastically when operated at lower than design temperature.

A numerical model of a fractured EGS was developed using Matlab. The model was able to capture the long term thermal behavior of a EGS. Based on this model was a sensitivity analysis conducted in order to see how responsive the thermal output is to different parameters. Typical ranges of fractured EGS parameters was found in existing literature regarding EGS. Thermo physical properties, such as thermal conductivity and specific heat, are highly dependent on mineral composition and temperature. They can therefore vary several factors between sites. Typical fracture apertures were found to be between 0.2 mm to 3 mm, and dependent on local geological conditions. The thermal output from the fractured EGS was found to be highly sensitive to changes in parameters like fracture aperture, fracture length and fracture spacing.

Geothermal energy is marginal at best, consequently is it vital to extract as much geothermal energy as possible. A typical fractured EGS is therefore designed with a temperature drop of about $10^0C - 15^0C$. The result is that the system is highly sensitive to variations in reservoir parameters. It is therefore critical to obtain accurate estimates and models of the fractured reservoir, and to control the fracture development during stimulation and operation.

A system consisting of a fractured EGS and ORC was found to be extremely sensitive to variations in geothermal temperature. A temperature decrease of 10% yielded a 25% decrease in net work output.

In order to reduce the risk related to the uncertainty of the geothermal temperature over the life time of the EGS is it advisable to combine geothermal energy with an alternative energy source. A hybridization of geothermal energy and a waste combustion plant was found to yield a stable power output regardless of geothermal temperature, and also offered a higher thermal efficiency than a standalone ORC. Geothermal energy could either by used as pre-heat in the waste combustion cycle or a ORC bottoming cycle could be used.

Sammendrag

Forskjellige konsepter for Konstruerte Geotermiske Systemer (KGS) blir gjennomgått og evaluert i forhold til potensialet de har for medium til stor skala produksjon av strøm i Norge. Mulige lokasjoner for dyp geotermisk energi i Norge blir identifisert. Et sprekket KGS med flere brønner i lav til moderat temperatur granitt ble identifisert som det mest sannsynlige geotermiske systemet for medium til stor skala kraftproduksjon i Norge.

Organisk Rankine Syklus (ORC) blir typisk brukt til å konvertere lav til medium temperatur varme til energi. Grunnen er at en ORC har en høyere termisk virkningsgrad ved lave temperaturer, sammenlignet med Flash syklus og Stirling motorer. Teknologien er også moden og kommersiell. Den termiske virkningsgraden til en ORC synker drastisk hvis den geotermiske temperaturen synker under designpunktet.

En numerisk model av et oppsprukket KGS, som fanger den termiske prossesen over levetiden til systemet, ble utviklet i Matlab. En sensitivitetsanalyse ble utført basert på modellen som ble utviklet, for å avdekke hvor følsom produksjonstemperaturen fra en KGS er med tanke på forandringer i reservoaret og driftsbetingelser. Termiske egenskaper til berggrunnen kan varier med en faktor på to til tre, på grunn av store forskjeller i mineralsammensetning av granitt. Sprekkåpningen varier typisk mellom 0.5mm til 3mm, basert på tall fra tidligere studier og er avhengig av lokale geologiske forhold. Den termiske produksjonen fra et KGS er sensitiv for varisjon i parametere som, sprekk bredde, sprekklengde og avstand mellom sprekkene.

Geotermisk energi er i beste fall marginal, noe som gjør at mest mulig energi bør utvinnes fra reservoaret. Det er derfor typisk å designe en KGS med et temperatur fall på 10^0C til 15^0C. Som en følge av dette blir systemet følsomt for forandringer i reservoaret. Nøyaktige estimater og modeller er derfor kritiske for økonomisk drift, samt å kontrollere sprekke dannelser under stimulering og i drift.

Et system bestående av en KGS og en kraftproduserende ORC er sensitivt for forandringer i geotermisk temperatur. Hvis den geotermiske temperaturen synker med 10% synker netto arbeid fra systemet med 25%.

For å redusere risikoen forbundet med usikkerheten i den geotermiske temperaturen over levetiden til systemet bør geotermisk energi kombineres med en annen alternativ energi kilde. Et hybrid system, hvor et søppelforbrenningsanlegg ble kombinert med geotermisk energi, fikk en høyere og mer stabil termisk virkingsgrad enn enslig ORC. Geotermisk energi kan bli brukt til forvarming i en dampsyklus eller i en ORC bunnsyklus.

Contents

List of Figures

III

IV

List of Tables

Nomenclature

Latin letters

$\dot{m}$ Mass flow rate

$\dot{q}$ Specific heat

$\dot{w}$ Specific work

$\vec{F}$ Body forces

f_l Louis friction coefficient

h_1 Specific enthalpy state 1

h_2 Specific enthalpy state 2

h_f Fracture aperture

A   Area

Cp   Specific heat

H   Enthalpy

h   Heat transfer coefficient

K   Permeability

k   Thermal conductivity

L   Length

m   mass

n   Quantity

P   Pressure

Q   Heat

q	Volumetric flow rate
r	Radius
s	Specific entropy
T	Temperature
t	Time
UA	Heat exchanger parameter UA (heat transfer resistance and area)
v	Velocity
W	Width
X	Number of well pairs
z	Hight

Greek letters

β	mass flow of circulation fluid per net produced MW
δL	Pseduo length
ϵ	Surface roughness
η	Efficiency
$\dot{\eta}$	Incrimental efficiency
μ	Dynamic viscosity
ρ	Density
θ	Angle of simulated wellbore zone
ξ	$\delta s/\delta T$

Subscript

0	Initial
C	Cold
c	Cross section
e	External
frac1	Fracture 1

frac2 Fracture 2

geo   Geothermal

H   Hot

i   Inlet

net   Netto from system

th   Thermal

tri   Triangular top site cycle

typ   Typical top site cycle

w   Wellbore

Abbreviations

DFH   Dual fluid hybrid top site cycle

EGS   Enhanced Geothermal Systems

EOR   Enhanced Oil Recovery

HDR   Hot Dry Rock

HEWI Heat Exchanger Within Insulator

HYB   Hybrid top site cycle

ORC   Organic Rankine Cycle

PI   Production Index

PIRSA Government of South Australia Primary Industries and Resources

SAHFA Southern Australian Heat Flow Anomaly

TOUGH2 EGS simulation software

Introduction

Geothermal energy is an abundant renewable energy resources, which could be accessed all over the world. The interest in geothermal energy has grown rapidly as the demand for clean and renewable energy has increased. The potential for geothermal energy is enormous, estimates suggests that geothermal energy resources are 50 000 times larger than the energy of all oil and gas resources in the world [14]. Geothermal energy is predicted to produce around 100 000MW in the USA in 50 years, as of 2008 the production was 2 900MW [14]. The potential for growth is substantial, with the international market for geothermal power possibly exceeding $25 billion over the next 10 to 15 years [14].

Geothermal energy has some unique features. It is continuous and the energy production rate is independent of local weather conditions, which makes geothermal energy ideal as a base load since it provides a stable and predictable energy production. The drawbacks have been, and still are, high investment costs related to drilling and reservoir stimulation, combined with low thermal efficiency due to small temperatures differences. As a result is commercial operation of geothermal power plants only feasible at sites with special geological conditions. Hopefully is this about change as the knowledge and interest in Enhanced Geothermal Systems (EGS) increases.

Enhanced Geothermal Systems (EGS) is a conceptual name for a wide range of geothermal systems where the bedrock have been artificially stimulated in order to increase the permeability in the rock formation. Traditional geothermal power plants uses natural occurring aquifers/hot springs. Where water is produced at high temperatures and power is typically generated from a flash cycle (steam turbine). Such systems require special geological conditions, their potential is therefore limited. Enhanced Geothermal Systems aims to extract heat from dry rock formations, thus drastically increasing the number of potential sites for deep geothermal energy.

Several EGS concepts have been proposed, where the major differences are the number of wells and how the wells are connected. The first study of a EGS, or Hot Dry Rock (HDR)

system, was started in 1974 at Fenton Hill (USA). Since then have several research projects been undertaken in order to better understand the physics of a geothermal reservoir, a few examples are Soultz (France), Rosemanowes (UK) and Fjällback (Sweden). The research have lead to a better understanding about geothermal fields develop and react to changes in pressure, temperature and flow rate among others. As better models are being developed will the risk related to exploration and operation of EGS plants decrease, making EGS an attractive energy alternative at a growing number of locations. However, EGS is still a novel technology and further research is needed.

Problem definition

The thesis will focus on the subsurface process of a deep geothermal power plant. A simplified model of a fractured EGS will be developed in order to better understand the physical behavior of such systems. The results from the EGS model will be used as input in a top-site power cycle simulation. The aim is to better understand the critical factors and mechanisms when operating a deep geothermal power plant. Since this is a conceptual study will the system not be optimized.

Different EGS concepts are described and briefly evaluated in order to build a foundation from which potential EGS concepts applicable for Norwegian conditions can be chosen. Based on the most promising concept is a transient numerical model, both for the EGS and top-site system, developed. It was difficult to obtain software that could simulate/model a EGS, a Finite Volume numerical model was therefore developed using Matlab. This proved to be a time consuming process therefore was only one EGS concept studied in detail.

Only power producing top site cycles are considered, alternative uses such as district heating is not considered. The top site utilization is a continuation of a report written fall 2010, where different top site utilizations options were investigated [15]. Based on this report was it decided to focus on medium to large scale power production.

The thermal output from the EGS reservoir was subjected to a sensitivity analysis, where all reservoir and operating parameters were varied. A complete system, combining a top site cycle and the EGS reservoir, was designed. A sensitivity analysis was performed on the complete system in order to see how the thermal performance of such a system was effected by variations in geothermal reservoir conditions.

Restrictions were imposed by Rock Energy on which types EGS systems that could be investigated, therefore were fractured EGS systems given most attention in this thesis.

Report organization

Different EGS concepts are described and briefly evaluated in Part 1, from which a suitable EGS concept for medium to large power production in Norway is chosen for further study. The geological conditions relevant for a EGS in Norway is presented, and used to evaluate the potential for EGS in Norway. A literature study relevant to modeling a fractured EGS is conducted in Part 1, from which a numerical EGS model is developed. The last section of Part 1 focuses on top site cycles for power production from low to moderate geothermal temperature fields.

In Part 2 is a numerical model that captures the long term thermal output from a EGS developed. The model is discussed in detail in Appendix A and B. The effect of several parameters on the thermal behavior of a fractured EGS is investigated.

A EGS power plant is designed Part 3, where both the fractured reservoir and the top site cycle is modeled. A sensitivity analysis is conducted in order to investigate the effect of variations in the geothermal reservoir conditions on the thermal performance of the system.

Each part is followed by a short summary, presenting the major findings in the respective part.

Part 1

Literature review

This part of the thesis will give the reader an introduction to existing material regarding different aspects of a deep geothermal power plant. The topic have been divided into two major categories; top-site and the geothermal reservoir. Most attention will be given to the geothermal reservoir, or Enhanced Geothermal System, since this is the area of most interest.

Different EGS concepts, both conceptual and existing, will be presented in section 1.1 and 1.2. A overview of existing models for transient heat analysis of a EGS is given in section 1.5, these models will be used as a basis for the EGS model developed in this thesis (part 2). The different EGS concepts and their applicability in Norway are discussed in section 1.3. The most promising top-site systems will be presented and discussed in section 1.6, this is a continuation of the work done in the project thesis fall 2010 [15]. The potential for geothermal energy production in Norway is commented in section 1.3.

The text assumes that the reader is familiar with common geological and reservoir expressions, however a brief introduction and definitions of common expressions are given in appendix E.

1.1 General EGS concepts

The different EGS concepts presented in this thesis have been divided into two main categories, one-well and multiple-well systems. Each category have been divided into subgroups depending on how the wells are connected. An extra category is dedicated to old depleted oil and gas wells, since these wells differ from a greenfield design and are especially interesting from a Norwegian perspective due to the large number of oil wells in the North Sea.

Examples of each system is found in section 1.2.
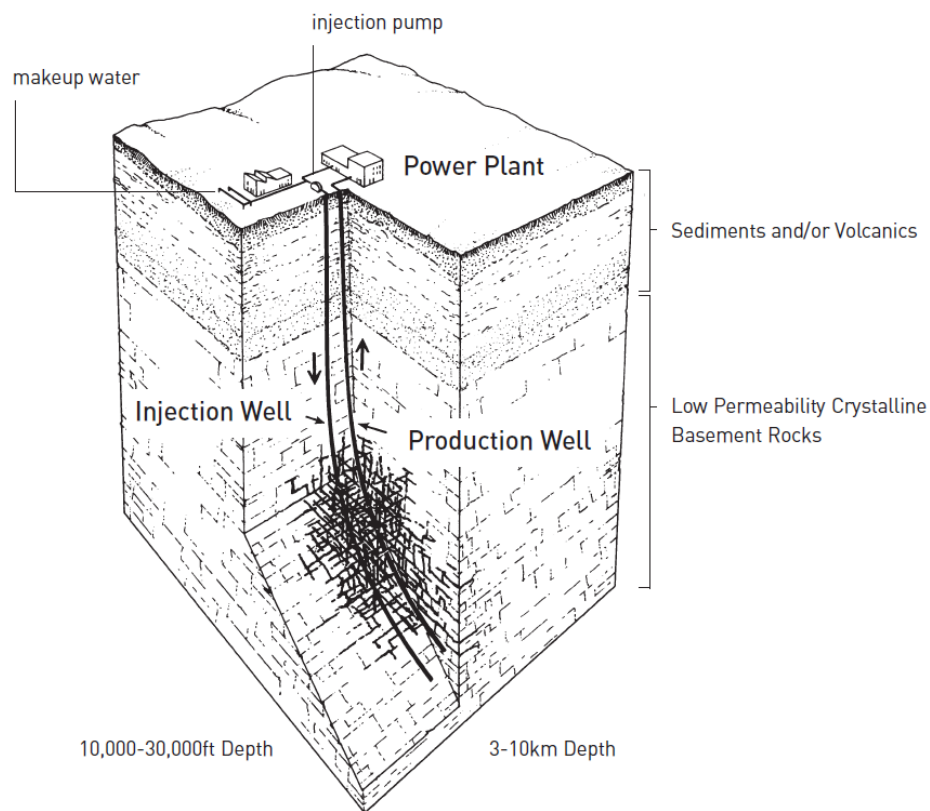
Figure 1.1: Conventional two-well EGS configuration [1]

1.1.1 Single well systems

In single well systems are one wellbore used as both injection and production well, using annular tubing (fig.1.2). Such systems typically have low production rates, due to limitations on heat production imposed by the heat transfer to the well [2]. However, the investment cost is also relatively low since only one well is needed. This makes one well systems ideal for small scale heat production.

Single well systems can be further categorized after how heat is transferred from the rock formation to the working fluid. The main categories are; closed loop downhole heat exchangers (fig.1.2), systems using a secondary circulation fluid (fig.1.6(a)) and systems circulating the working fluid directly in through the rock formation (fig.1.6(b)).

- **Closed loop downhole heat exchangers** are systems where the working fluid is circulated in a closed wellbore annulus, and heat transfer is achieved through conduction between the rock formation and the wellbore casing. Heat transfer in the rock formation is also mainly by conduction, however natural occurring brine could enhance the heat transfer if present. These systems are limited by the heat transfer resistance in the rock formation near the wellbore.

- **Downhole heat exchanger with secondary fluid** are similar to closed loop downhole heat exchangers. However, these systems artificially injects a fluid into the rock formation, in order to improve the heat transfer rate in the rock formation near the wellbore. This fluid is referred to as a secondary fluid. The purpose of the fluid is to decreases the heat transfer resistance in the rock formation, thus increasing heat transfer rates to the wellbore. The secondary fluid is typically circulated due to buoyancy effects, due to temperature gradients in the rock formation. The effect of a secondary fluid depends on the permeability of the rock, an increase in permeability increases the buoyancy driven flow which in turn reduces the thermal resistance in the rock formation. Therefore should low permeability zones be artificially stimulated in order to increase the permeability.

  Such systems typically offers higher heat production rates than closed loop downhole heat exchangers without a secondary fluid.

- **Direct circulation of the working fluid**. A few systems have been proposed where the working fluid are directly circulated in the bedrock (fig.1.6(b)). The GeneSys concepts is such a system, further information regarding the GeneSys project can be

found in section 1.2.2. The advantage with these concepts are lower heat transfer resistance between circulation fluid and the rock formation, since the circulation fluid is in direct contact with the rock. However, due to mineral dissolution could impurities prove to be major problem in surface equipment. A top site heat exchanger between the circulation fluid and the working fluid of the top site cycle is required in order to prevent impurities entering top site equipment, such as the turbine. Such systems typically offers higher heat production rates due to lower thermal resistance and a large surface contact area between the circulation fluid and the rock.
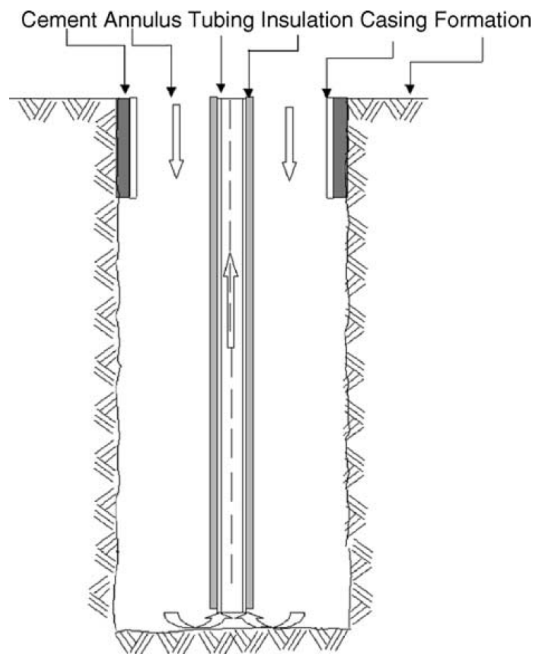
Figure 1.2: Single well with downhole heat exchanger [2]

1.1.2 Multiple well systems

These systems uses different wellbores for injection and production, two or more wells are therefore required in order to circulate the circulation fluid. Multiple well systems can be divided into subgroups after how the wellbores are connected. The different methods that currently exists are; natural fractures/porosity, artificially stimulated fractures or interconnected wells. However, it is rare that natural permeability in the bedrock is high enough to support commercial flow rates, most systems are therefore artificially stimulated.

These systems typically offer higher heat extraction rates than single well concepts. The main reason is the possibility of using multiple wells which will increase the flow rate combined with a larger contact surface area between the circulation fluid and the rock formation. Well spacing typically range from 400 to 1000 meters, which drastically increases the contact surface area between rock and circulation fluid compared to single well systems.

- **Fractured systems** uses fractures, natural and/or artificially induced, in order to connect the wells. The circulation fluid is transported from the injection point to the production point by fractures in the bedrock.

  Fractured systems can be divided into two subgroups; fractures in permeable media and fractures in impermeable media. Fractures in permeable media are typically a fractured EGS situated in porous sedimentary rock. One advantage with such systems are that well-known technology from the oil and gas industry can be applied fairly easily, since most of the oil and gas industry drill and exploit sedimentary formations. Another advantage is that the circulation fluid flow in both the fracture and rock matrix pores. Which reduces the heat transfer resistance, since the heat transfer in the rock matrix is aided by the flow of circulation fluid in the pores. Compared to a impermeable rock formation where the heat transfer is only by conduction through the rock matrix. The disadvantage is typically lower temperatures than in impermeable rock formations, such as granite. The reason is that impermeable rock formations, such as granite, are located below the sedimentary layers and thus have higher temperature due to geothermal gradients. The temperature of the rock formation is critical in order to achieve commercial operation of a EGS, the higher the rock formation temperature is the higher the total thermal efficiency of the system is, see section 1.6. It should be noted that impermeable media refers (in this text) to igneous rock such as granite and not to impermeable sedimentary layers such as clays and shales.

  The design approach shown to give the best connectivity is to first drill the injection well, then stimulate the bedrock and target the second well into the stimulated area at the location giving the lowest loss of circulation fluid [1]. Most EGS sites operating today uses a multiple well fractured system. The drawback with these systems today are leakage of circulation fluid, pressure loss and prediction of fracture propagation.

- **Porous media**. There are few to non EGS sites where natural porosity and per-

meability in the bedrock is large enough to support commercial flow rates, without a excessive pressure drop. Most systems uses a combination of natural porosity and artificially induced fractures, see "fractured systems" above.

- **Interconnected Wells** are systems where the production and injection wells form a closed loop. The differences between interconnected wells and single wells with downhole heat exchanger is that interconnected wells have different wells for production and injection. The result is a larger heat transfer area and the well can support a higher flow rate.

    The advantage with such systems is low leakage rates, fairly easily calculated pressure drop and known fluid flow paths. The disadvantage is increased drilling costs.

1.1.3   Old oil and gas wells

Old oil and gas wells could be used for heat mining. However, most oil and gas wells will need some modifications before they can be used. Single well systems have been investigated, both theoretical and in practice. For example is the test site at the GeneSys project old gas wells, see section 1.2.2 and [3]. Davis et al.(2009) [16] conducted a simplified investigation of abandoned onshore oil wells, they found that a electricity output of 2-3MW could be expected (based on onshore oil wells in southern Texas). It should be noted that transient effects, such as cooling of the rock formation close to the wellbore, is not considered in the study. A output of 3MW should therefore be regarded as a maximum. The reason for the low electricity generation is the same as for "closed loop down hole heat exchanger" systems, since both systems are equal from a thermodynamic perspective. However, since the oil well is already in place should the investment costs be lower than for green field closed loop down hole heat exchanger systems, even if some modifications are required. Making abandoned oil and gas wells more attractive for small scale geothermal energy than greenfield projects.

Studies that have looked at multiple well systems that uses abandoned oil and gas wells as production and injection wells was not found. However, such a system should be possible and have significant lower investment costs than greenfield projects and should be investigated. Abandoned oil and gas field have typically been subjected to several Enhanced Oil Recovery (EOR) treatments, such as water/CO_2 injection, chemical treatments and so on. These treatments have been optimized for oil and gas recovery and could have a drastically impact on water flow and thus the potential for heat mining. Oil and gas fields

are also typically situated in sedimentary regions with relative low temperatures compared to a granite basement (which typically is situated deeper than the sedimentary basin). The geothermal temperature drastically effects the thermal efficiency of the top-site cycle (see section 1.6), the temperature is therefore critical in order achieve a commercial EGS.

Another possibility is that the rock formation could have been artificially heated in order to enhance oil production, resulting in a higher rock formation temperature than estimated by a geothermal gradient. Exploration of oil sand is a example where steam is injected in the bedrock in order to extract oil. In such cases could EGS projects be very interesting, since the geothermal temperature has been artificially increased. Another advantage with this type of system is that the detailed information about the rock formation have been gathered during oil and gas production, and detailed concept studies could be conducted without excessive costs.

Studies on the use of abandoned offshore oil and gas wells was not found.

1.2 Examples of EGS concepts

The EGS sites and concepts presented in the following subsections gives a picture of the range of different concepts that have been proposed for extraction of heat from deep geothermal systems in hot dry rocks. The purpose of this section is to find concepts that can be used for geothermal energy production in Norway. Therefore are only the most relevant projects, sites and concepts briefly presented, in order to form a basis from where the most suitable concepts can be chosen. A more in-depth study of several of the EGS sites was conducted by Jester et.al (2005) [1]. A overview of the different EGS sites worldwide and concepts can be found in appendix C.

Most of the existing EGS sites are based on a multiple well artificially fractured system (table C.1). The reason is that natural fractures and porosity typically cannot support commercial flow rates and interconnected wells are at the moment to costly. Three existing fractured multiple well systems are presented in the following sections; Soultz, Cooper Basin and Paralana.

1.2.1 Multiple well

EGS that have more than one wellbore are presented in the following section.

Soultz

Soultz is a multiple well fracture system in granite and one of the most important European research sites on EGS, where research and measurements have been conducted over the past 20 years.

Two reservoirs have been created in granite, at 3.5km and 5km vertical depths. The successful long term circulation test of the reservoir at 3.5km was followed by drilling a deeper reservoir at 5km. The reservoir at 5km has temperature around 200^oC and consists of three wells, one production well and two injection wells. The production well (GPK3)is situated between the two injection wells, see figure 1.3(b). Through stimulation was a good connection between well GPK2 and GPK3 established, however it was problematic to establish a connection to well GPK4 and it still a ongoing project [1]. The Soultz project demonstrated that large fractured volumes could be created repeatedly in rock containing pre-existing natural fractures that are ready to fail in shear [1].

A four month closed loop flow test conducted in 1997 showed no net circulation fluid losses, once the flow rate had stabilized at 25kg/s. [1]

In 2008 was a ORC power plant (1.5MW) installed. The production temperature was 175^oC at a flow rate of 35 l/s and the injection temperature was 80^oC-90^oC. Optimization of the complete EGS power plant is ongoing. [17]

Cooper Basin

The Cooper Basin project was begun in 2002 and is located in the southern Australia, in the Southern Australian Heat Flow Anomaly (SAHFA). The system is similar to Soultz, with multiple wells in a granite basement, using fractures to connect the wellbores. The plan for the project was to demonstrate feasibility of an EGS system in an area with large volumes of high-temperature (250^0C) and fairly uniform granitic basement. The granitic basement was fractured using hydraulic stimulation.

A scale up to a multiple well system seems feasible, due to horizontal reservoir development, and should make EGS power production competitive with other base-load technologies [1] . For further information please see [1] and [18].

Paralana project

The Paralana project is located in southern Australia, within in the Southern Australian Heat Flow Anomaly (SAHFA). The site is situated in deep sediments (5km), surrounded by granite. The granite is part of the Mount Painter Inlier which has an average heat production ($10 \mu W m^{-3}$), four times higher than average granite [19]. The Paralana project investigates how multiple stimulation in sediments can increase flow rate and heat extraction. The advantage with sediments, compared to granite, is that sediments have a higher natural porosity and permeability allowing higher flow rates, while granite can to some extent be regarded as impermeable.

The concept used at the Paralana site is called Heat Exchanger Within Insulator (HEWI). Where the sediments layer above the granite basement is stimulated, instead of stimulation of the granite basement itself. The advantage is higher flow rates, greater control of fracture propagation and known technology from the oil and gas industry related to stimulation of sediments. The disadvantage is a lower temperature source. For more information see [19].
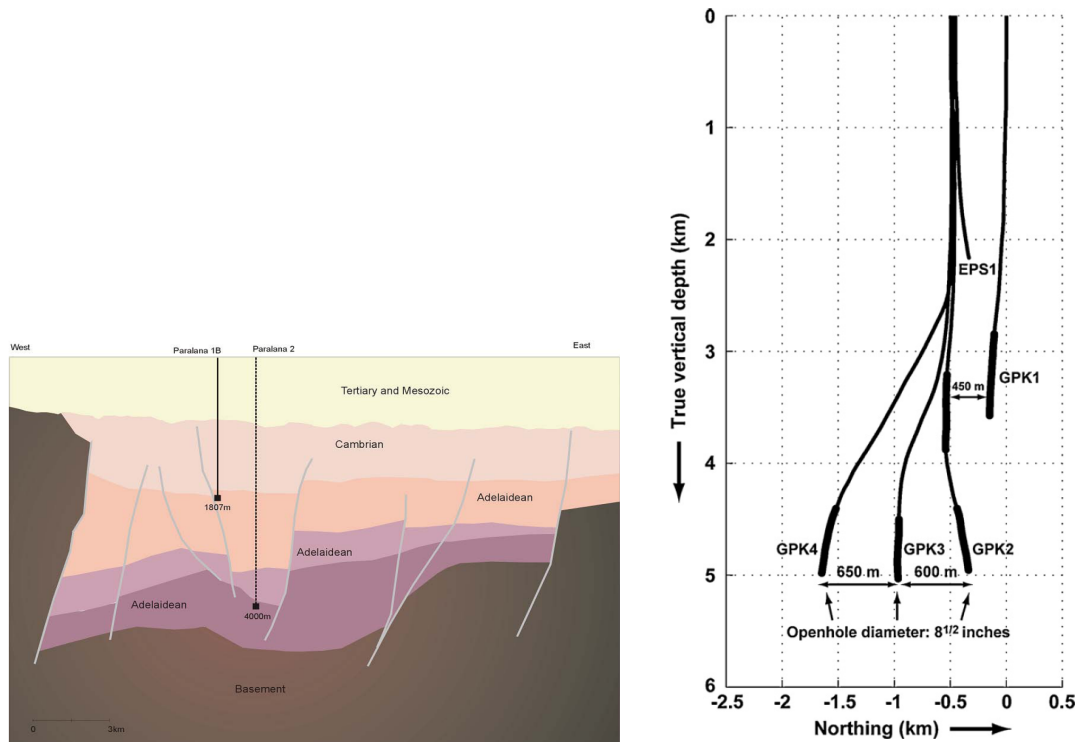
(a) The Paralana project (multiple well fracture system in sediments)

(b) Cross-section through the Soultz reservoir (multiple well fracture system in granite)

Figure 1.3: Two different multiple well EGS concepts

Rock Energy

A interconnected multiple well system have been proposed by the Norwegian company Rock Energy. The injection and production wells are connected, using advanced directional drilling equipment, to form a downhole heat exchanger. Depending on the required heat production can the number of connected wells be increased. The advantage with this approach is a fairly easily predicted heat output, minimal risk of short circuiting (see section 1.4) and stable heat output. The effect is a predictable heat output, which reduces the financial risk. The drawback with this technology is high investments costs related to drilling.

Earth Energy Extraction System

Another concept has been proposed by Geothermex. The Earth Energy Extraction system (triple-E) are based on a multiwell system with several ultra slim injection wells and one
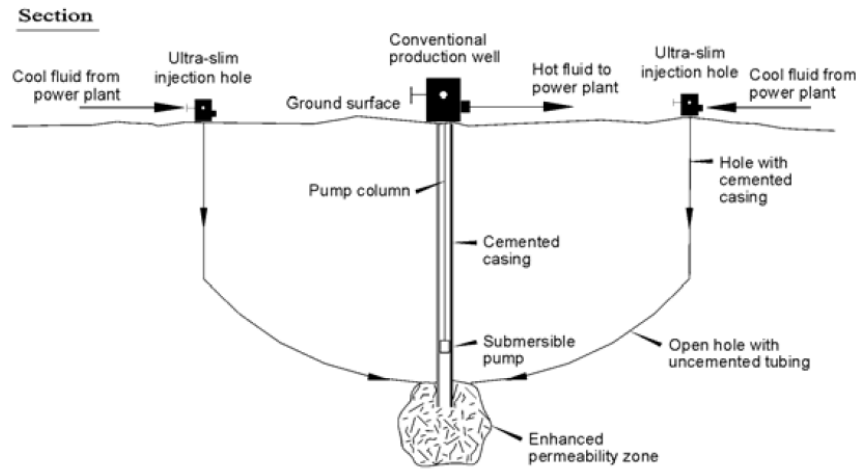
Figure 1.4: Earth Energy Extraction System

production well (fig.1.4). The circulation fluid is preheated in the ultra slim injection wells at low flow rates. The fluid is then further heated up as it travels through fractures and pores to the production well. The distance between where the injection wells are terminated and the production well is small, thus limiting leakage. Advantages with this design are believed to be; low-risk, low-cost and modular (number of wells).

More information can be found in a paper by Sanyal et.al (2005) [20]. The Earth Energy Extraction system is at a conceptual level.

1.2.2 Single well

In this section are concepts based on a single well presented.

GeneSys concept

The GeneSys (Generated Geothermal Systems) concept is a single well system that can produce heat for direct usage from tight sediments for small to medium heat energy demands (2MWh annually) [21]. The system is based on a single well with downhole heat exchanger and a circulation fluid.

An old oil and gas well in the northern Germany were used to the test the concept. In the test was a sandstone layer fractured, by hydraulic stimulation, in order to create a connection to natural faults and fractures. The circulation fluid was reinjected through the annulus and produced through the production tubing. The well could not maintain high enough flow rates over time ($25\ m^3/h$), due to little communication between the injection

and production layer in the geological formation. However, a cycle of injection, warm-up period and production was very promising [3], giving the idea to a huff-puff system (see fig.1.5(b)). Which is a cyclic production scheme that produces heat in given time periods and are idle in the remaining time allowing the rock formation to be reheated.

Three different concepts have emerged from the GeneSys project; deep circulation (fig.1.5(a)), huff-puff (1.5(b)) and two strata (1.5(c)). The deep circulation concept takes advantage of fault zones to communicate between the reinjection and production point. The huff-puff concept uses a stimulated fracture combined with natural drainage to communicate, however flow rates obtained are small and a cyclic process showed to yield the best results for such systems [3]. Two strata concept creates a link/fracture between two permeable layers with a hydraulic fracture, see figure 1.5(c)).

(a) Deep Circulation

(b) Huff Puff

(c) Two Strata
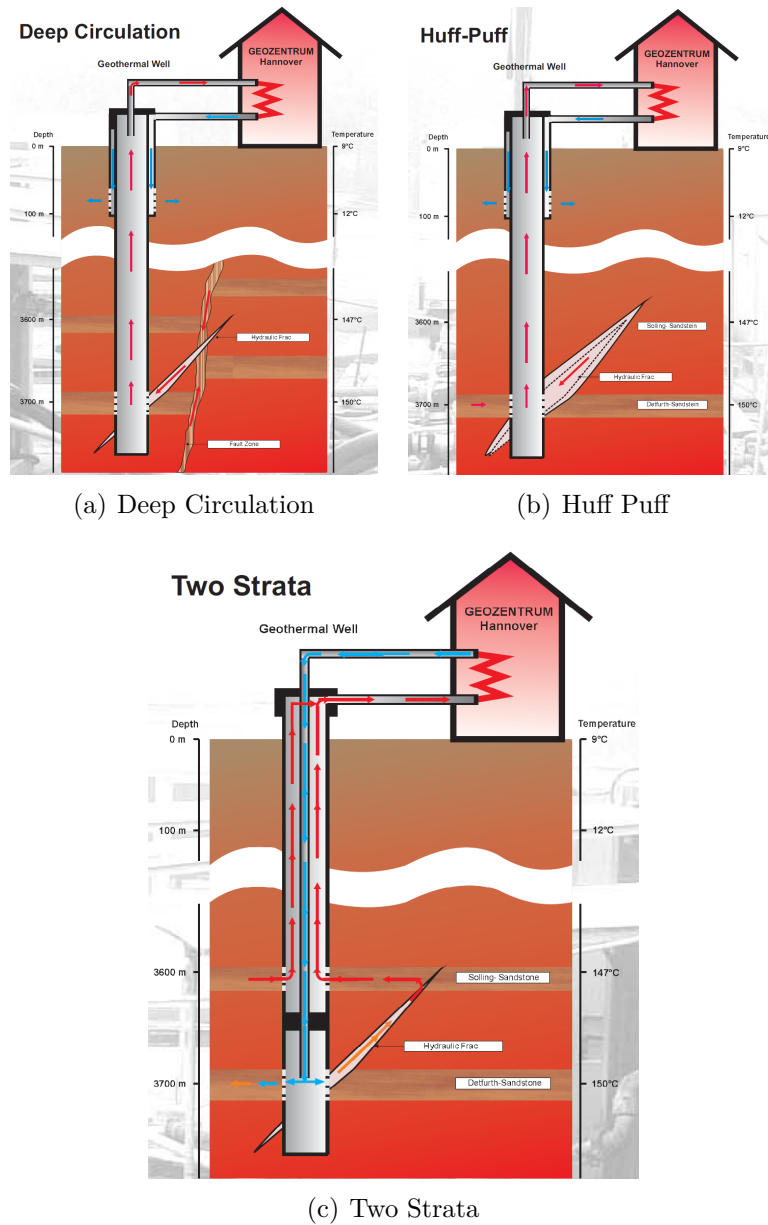
Figure 1.5: Different single well concepts developed by the GeneSys project [3]

Single well with thermosiphon

Wang et.al (2010) [4] proposed a single well design with a downhole heat exchanger (fig.1.6(a)). The working fluid in the power generation cycle is circulated in a closed loop downhole, and a second fluid is circulated in the fractures in order to increase the heat transfer rate. Since the working fluid is circulated in a closed loop will problems related to scaling and fouling in surface equipment be small, if existing at all. The system uses a thermosiphon effect to circulated the working fluid, which renders downhole pumps unnecessary and reduces cost. Simulation of the system shows limited thermal production capacity (530kW) [22], it should be noted that the thermal output increases with an increase in well diameter. The simulation also showed that the key factor determining the thermal production is the flow rate in the fractures.

Due to the low production capacity was other alternatives investigated. The two final alternatives were; circulating the working fluid directly in the fracture (fig.1.6(b)) and a different configuration of the flow pattern inside the wellbore for the two fluid system. It was found that single well systems have better thermal output per well for the same flow rates compared to two well fractured system. However, the problem with a single well that uses a secondary fluid is that the circulation in the fracture is determined by free convection which limits the flow rate and heat transfer rate.

Further information can be found in articles by Wang et.al (2009, 2010) [4, 22].

(a) System with two separated circulation fluids

(b) System with one circulation/working fluid
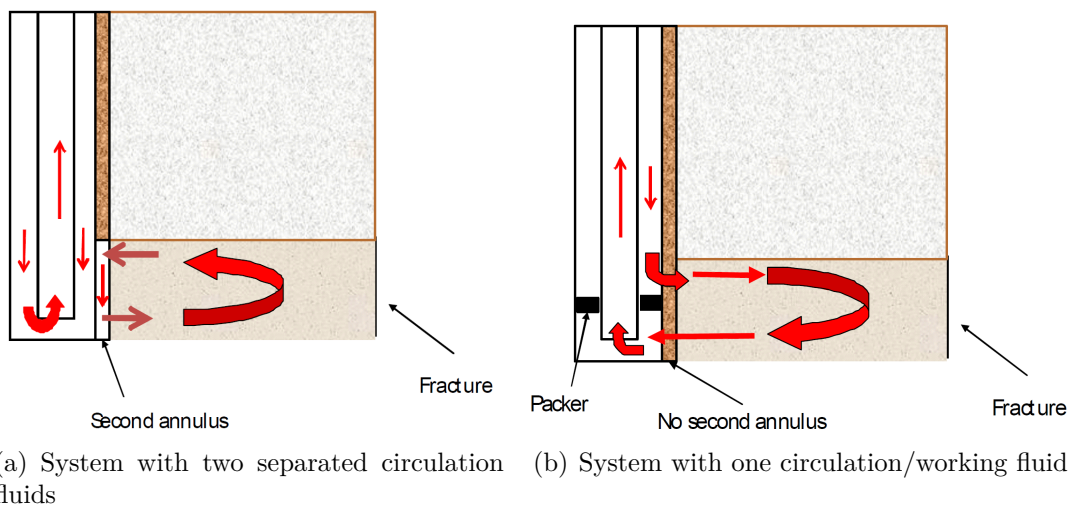
Figure 1.6: Different single well concepts developed by Wang et.al (2010) [4]

1.3 EGS and Norway

1.3.1 EGS potential in Norway

Norway have been categorized as a "cold spot", however recent studies have shown that the heat flow is 25% higher than previously anticipated [23]. Based on these new findings is the average heat flow in the region 50 to 70 mW/m^2 (fig.1.3.1), which is in excellent agreement with data from Sweden [13]. Temperatures at 5km have been calculated based on conditions at 800m deep boreholes, see fig.1.7. The majority of the sites were in the range of 100 to 200 ^0C, which can be classified as medium temperature fields. The heat production in the Norwegian bedrock ranges between 2 - 7 $\mu W/m^3$, where the average is around 2 - 3 $\mu W/m^3$ (fig.1.8(a)). In comparison does the Southern Australian Heat Flow Anomaly (SAHFA) have a average radiogenic heat production of 10 $\mu W/m^3$ [19].

The highest temperatures and heat fluxes are found in the southern part of Norway, which also is the most populated area. These areas have district heating systems and electricity grids in place, which reduces the costs related to infrastructure. Pilot plants should therefore be built in the southern parts of Norway, due to proximity to energy consumers and high geothermal temperatures. High geothermal temperatures are critical in order to achieve economical power generation from geothermal energy (EGS) (see section 1.6).

Based on figure 1.7 and figure 1.3.1 is it evident that potential sites are located in southern parts of Norway. Potential EGS sites are believed to be found in areas where heat producing granite is surrounded by swecogranit with low heat production [24]. Brun [24] targeted Hurdal and Iddefjord as potential EGS sites.
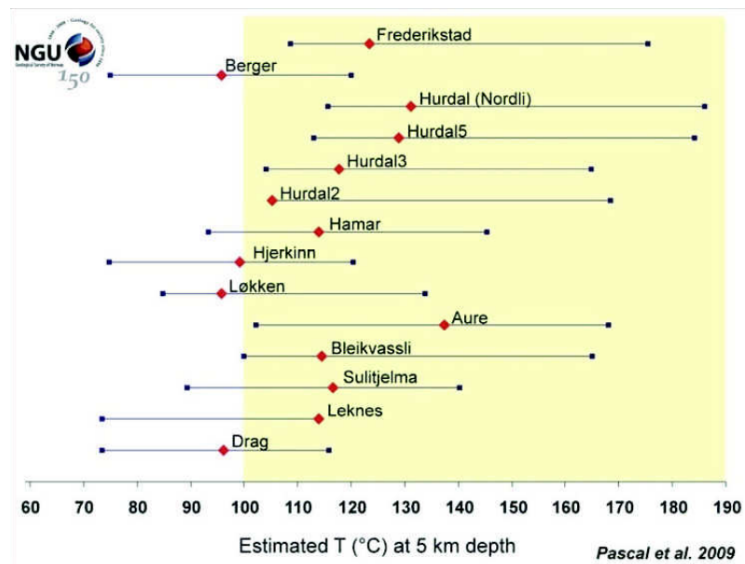
Figure 1.7: Estimated temperature at 5km in Norway, based on 800m deep boreholes [13]
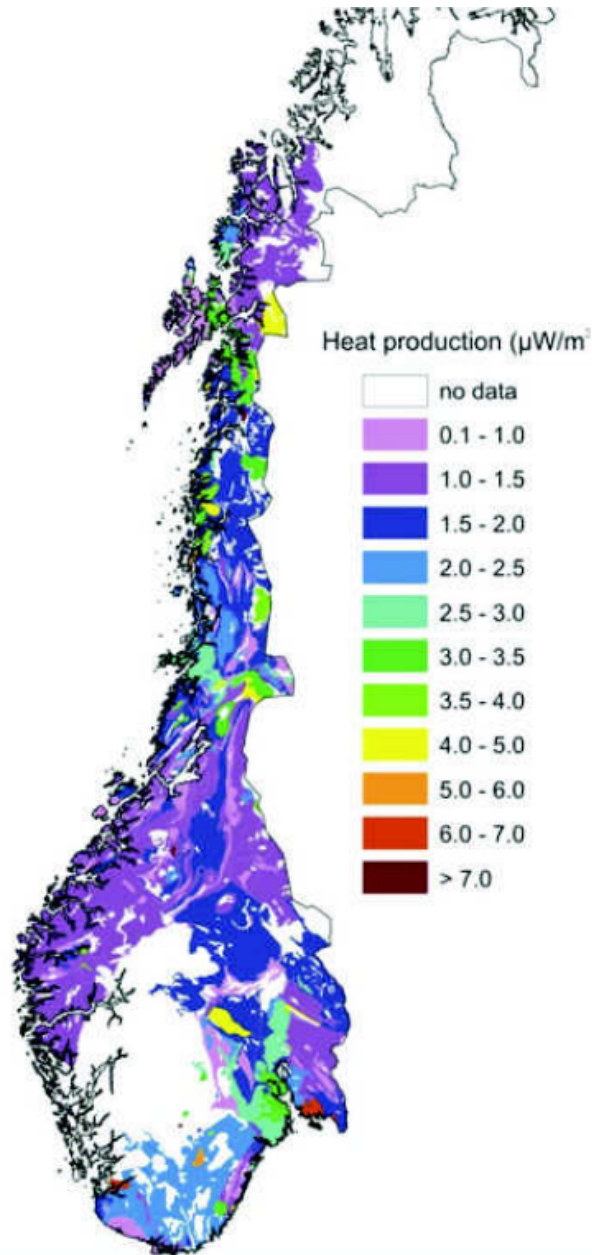
(a) radiogenic heat production in Norway ($\mu W/m^3$) (Slagstad et al. 2009)[23]
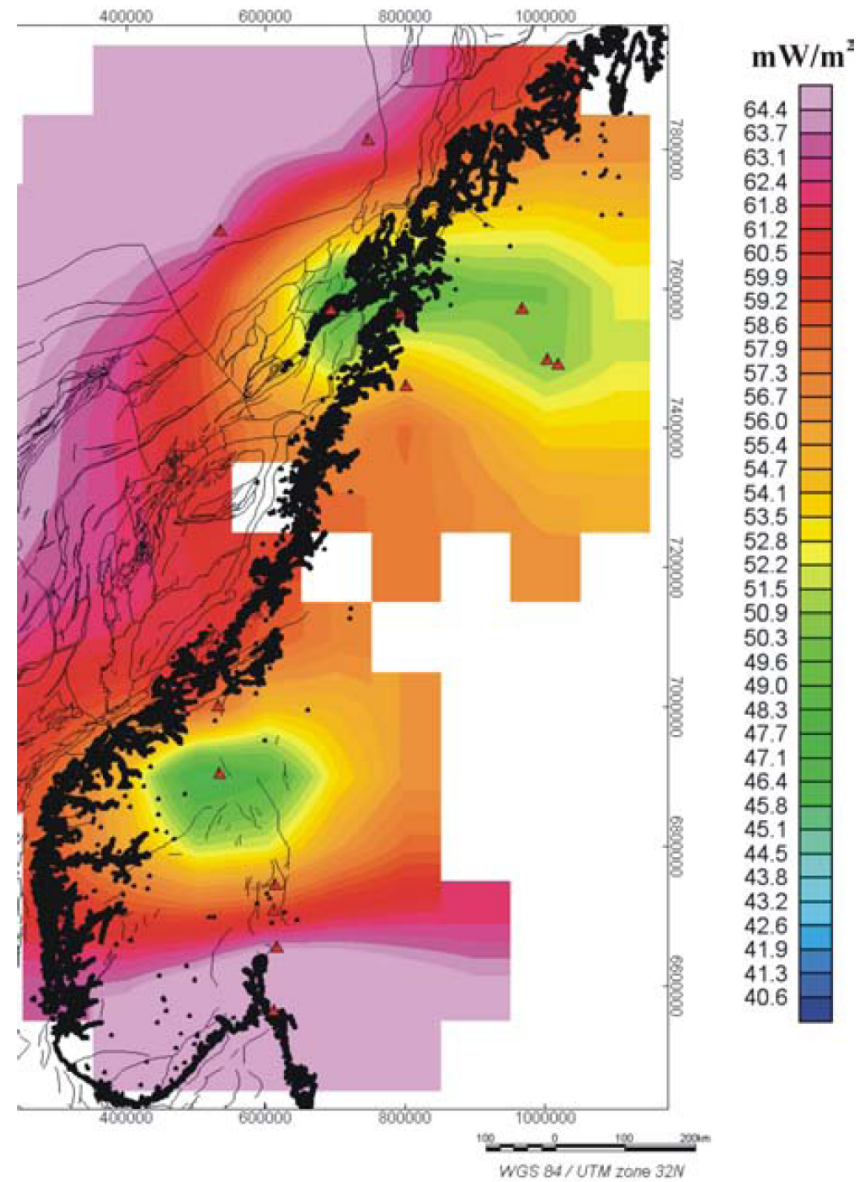
(b) Heat flow in Norway (mW/m^2) [13]

Figure 1.8: Heat production and temperature in Norway

Bedrock types in Norway

A hot and dry bedrock with low porosity and permeability is expected at potential EGS sites in Norway [24]. Figure 1.3.1 shows a simplified geological map of Norway.

1.3.2 Potential EGS concepts in Norway

Numerous EGS concepts exists, with their own advantages and disadvantages. The choice of EGS concept should be determined by the geology and infrastructure at the site, since the optimum EGS concept is highly dependent on local factor such as stress field, fractures, infrastructure etc. It is therefore difficult to recommend a specific concept before a site is targeted. However, some general guidelines can be drawn. A single well system should be chosen for small to medium scale projects, since these offer low investment costs and low heat production. When a medium to large scale project is considered should a multiple well system be used, since it can produce more heat than a single well system.

The scope of this thesis is to investigate large scale electricity production, therefore is a multiple well system selected for further analysis in this thesis. Based on the geothermal gradient and rock types in Norway does a porous media system look unfeasible. A fractured or interconnected well system should therefore be selected. Due to the small temperature gradient and heat production in the Norwegian bedrock would a potential EGS power plant be located in metamorphic or igneous rock, such as granite, which typically is found below (deeper) than sedimentary formations and therefore have a higher temperature.

There are several configurations of a multiple well fractured EGS, where number of wells, spacing between wells, well diameter varies and well configuration varies as these are highly site specific and depends local factors. A site should therefore be found before further specifications are made.

Abandoned offshore oil and gas wells could be potential sites for geothermal energy in the future. However, at the moment does such a project look unfeasible due to the increased costs compared to a onshore project and the fact onshore EGS is still a novel technology. Making commercial exploitation of abandoned offshore oil and gas wells very unlikely in the near future. However, as EGS technology matures could offshore oil and gas wells be attractive.
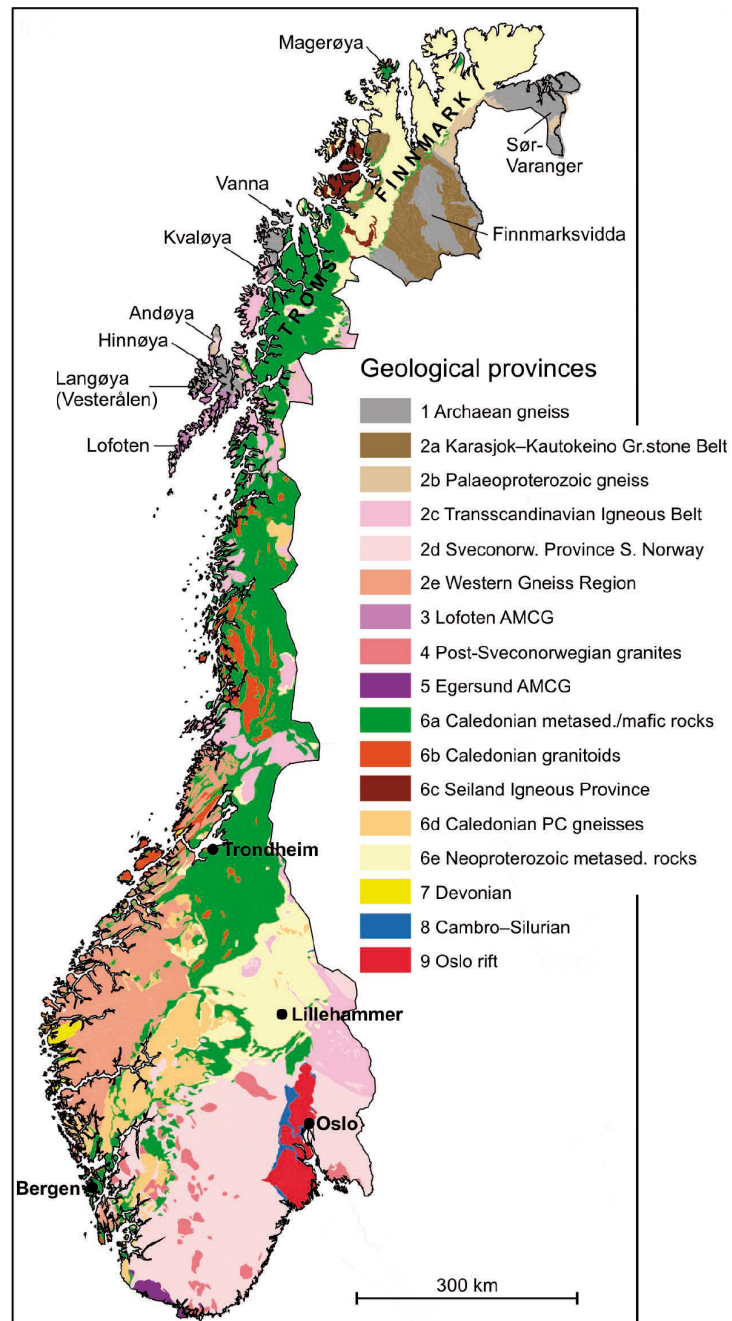
Figure 1.9: Simplified geological map of Norway [5]

1.4 Factors effecting a fractured EGS

In this section are different aspects effecting the productivity of a EGS presented. The focus will be on multiple well systems with fractures, since these systems are the most common systems and the only EGS system on a larger scale that is currently operational. The aspects effecting a thermodynamic model of a EGS system will be presented, such as rock-fluid interactions and fracture development.

This is, however, a brief presentation in order to give a understanding of how the productivity and heat output from a EGS is influenced by different parameters. The report "The Future of Geothermal Energy - Impact of Enhanced Geothermal Systems (EGS) on the United States in the 21st Century" by Tester et.al (2005) provides excellent reading on this topic if a more in-depth analysis is required [1].

Well stimulation

Well stimulation of a geothermal resources is adopted from the oil and gas industry. The basic technology used in the oil and gas industry can also be used with geothermal reservoirs, however there are some important differences. The most important are that geothermal reservoirs require higher flow rates (due to low specific enthalpy) and most geothermal reservoirs are situated in granite or crystalline rock instead of sediments (as most of the oil and gas reservoirs).

The type of well stimulation that should be used is site specific and depends on local factors, however some key points are: Fractures in granite are supported by the self-propping effect, therefore are proppants typically not need in order to keep the fracture open (as fractures in sediments) [25]. The different stimulation options used in crystalline rock/granite are; chemical treatment and thermal fracturing close to the wellbore, while hydraulic stimulation is used to create fractures and increase flow far from the well [26].

A heat production of 5MW per well is need in order for EGS to be competitive (compared to natural hydrothermal systems), which require flow rates of 30 to 100 kg/s depending on fluid temperature [1]. Such high flow rates requires large heat transfer surfaces to heat the fluid up to reservoir temperature.

Propagation of fractures

Since most of the geothermal reservoirs are located in crystalline basement rock are fractures in sediments not commented. Fractures in sediments is also well known from the

oil and gas industry. In crystalline rock is the most effective stimulation achieved through stimulating existing natural fractures and making them fail in shear, not tensile [1]. Therefore is it crucial to determine the orientation of the stress field before stimulation, since most of the fractures will be aligned with the stress field. The pressure needed to shear natural fractures and joints are typically in the range of 2-10 MPa [1], the shear failure increases the hydraulic apertures of the fracture.

The natural fractures that can transport fluid pre-stimulation are the fractures that will be targeted during stimulation [1]. Areas with pre existing fractures should therefore be targeted for EGS.

Circulation of water/fluid through the rock could have long term effects. Long field test have shown some dissolution of rock, specially at high pump pressures, which could lead to short circuiting. Short circuiting occurs when one fracture transport a large portion of the mass flow. The effect of short circuiting is decreased life expectancy and lower fluid temperatures, which could possible render a EGS project non-economical. Short circuiting could also occur if there are large differences in fracture aperture after stimulation. It is therefore important to monitor the fracture propagation during stimulation in order to avoid short circuiting, which could drastically reduce the lifetime of the system.

The fractures formed after stimulation is typically a complex network of fractures. Where direction, fracture aperture changes both within the fracture and between fractures. However, a single fracture model adequately captures thermal recovery through heat conduction from the rock surrounding the reservoir [27].

Circulation fluids

Water, or brine, is commonly used as circulation fluid in EGS. However, other circulation fluids have been proposed. Brown (2000) [28], Pruess (2006) [29] and Atrens et al. (2010) [30] have suggested CO_2 as circulation fluid instead of water. Based on the analysis conducted by Brown [28] and Pruess [29] does CO_2 show several advantages over water as circulation fluid. The most important advantages are; large buoyancy drive due to significant wellbore density differences which reduces the parasitic losses related to pumping compared to water, the inability of CO_2 to dissolve and transport minerals which eliminates scaling in surface equipment. However, major uncertainties remain with regard to chemical interactions between fluid and rock [29]. Both papers find CO_2 superior to water with regard to heat mining.

Atrens et al (2010) [30] investigated a two wellbore CO_2 thermosiphon system. They

found that such a system underperforms from a exergy point of view, compared to a water based system. The two main reasons are lower heat capacity and lower density of CO_2 in the production wellbore. If large wellbore diameters are used, or if the EGS is situated in a high impedance reservoir, then the difference between a water based and CO_2 based system is small.

Water is the circulation fluid that is commonly used. CO_2 have several advantages compared to water but major uncertainties still exists regarding CO_2 as circulation fluid, and further investigation is required before CO_2 can be used on a commercial level.

Pressure drop

The expected pressure drop in a EGS varies depending on rock type, fracture aperture, fracture length, reservoir depth and mass flow. The pressure drop in a EGS could therefore vary a great deal. Remoroza et al (2011) [31] used a reservoir pressure between 20 and 50 MPa and a pressure drop of 2MPa across the fracture. However, pressure drops of $10 - 20$ MPa have also been used. The pressure drop used in different studies are tabulated in table D.1.

A fracture network has a complex flow pattern, due to flow through pores and interconnected fractures. In addition is the fracture aperture highly irregular along the fracture, which could cause sudden pressure changes in the flow. Most of the work done on pressure drop calculation have either used simplified friction factor relationship or assuming the fracture to be a highly porous structure and applying Darcy's law.

The performance of a geothermal well is also often measured using a "Productivity Index", which is the mass flow rate per unit pressure drop ($PI = q/\Delta P$). Measurements at Soultz showed a net 3-day single-well productivity index of 4 to 5 l/s/MPa.

Leakage

Every EGS that are based on fractures experience leakage of circulation fluid. The Ogachi project (Japan) had a leakage rate of 97% at the most, after stimulation had the leakage rate dropped down to 75% [1]. While the EGS at Rosemanowes had leakage rate of about 37% during a circulation test with 25kg/s [1]. It is critical to limit the leakage in order to avoid increased costs due to the excess amounts of circulation fluid needed.

Tests at Soultz have showed that the leakage rate can approach zero. A four month closed loop flow test conducted in 1997 showed no net circulation fluid losses, once the flow rate had stabilized at 25kg/s [17].

Due to potential water leakage from a geothermal reservoirs could EGS projects be prohibited due to the environmental interest. Especially if water resources are limited or if the geothermal reservoir is situated near vulnerable areas.

Measurements

Due to the relative high temperatures in deep geothermal reservoirs are accurate measurements a problem. The main problem is that the most of the equipment is made for the oil and gas industry and cannot handle the high temperatures found in these reservoirs. However, it is expected that increased interest in geothermal energy will make it possible to manufacture equipment that can be used in high temperatures at a reasonable price.

Rock-fluid interaction

The circulation fluid could interact with the rock, either dissolving or depositing minerals depending on flow regime and local rock conditions. Non-Condensable Gases (NCG) may also react with the circulation fluid, which could cause problems with top-site equipment. Contamination of the circulation fluid could also change the thermodynamic properties of the fluid, the impact on estimates will most likely vary with degree and type of contaminants. Little is known about the long term effects of fluid-rock interactions and further research is needed.

Questions that needs answers are: Will mineral deposition over time diminish connectivity and increase pressure drop? Is mineral dissolution going to create short circuits or improve pressure drop? Where will mineral deposition and dissolution occur? Can we use rock-fluid interactions to characterize the performance of the reservoir? [1]

Thermal breakthrough

There is only a finite amount of energy that can be extracted from the reservoir, the theoretical amount is given by $Q = m_{rock}Cp_{rock}\left(T_{initial} - T_{inlet}\right)$. However, it is not practical to extract all the heat stored in the reservoir. The fracture outlet temperature will start to drop below the initial rock temperature and approach the fluid inlet temperature after a given time. A vertical thermal gradient will develop in the rock matrix due to the thermal resistance in the rock, which results in a lower temperature at rock matrix interface than further away from the fracture. Another way of putting it is that a thermal front advances through the reservoir, this can be seen in figure 1.10(b). This means that all the energy in

27

$$\Theta = \frac{\rho_f C_f b}{\rho_r C_r D}$$
$$\tau = \frac{\lambda t}{\rho_r C_r D^2}$$
ρ = density ((r)ock, (f)luid)
D = fracture spacing
C = specific heat ((r)ock, (f)luid)
b = fracture aperture
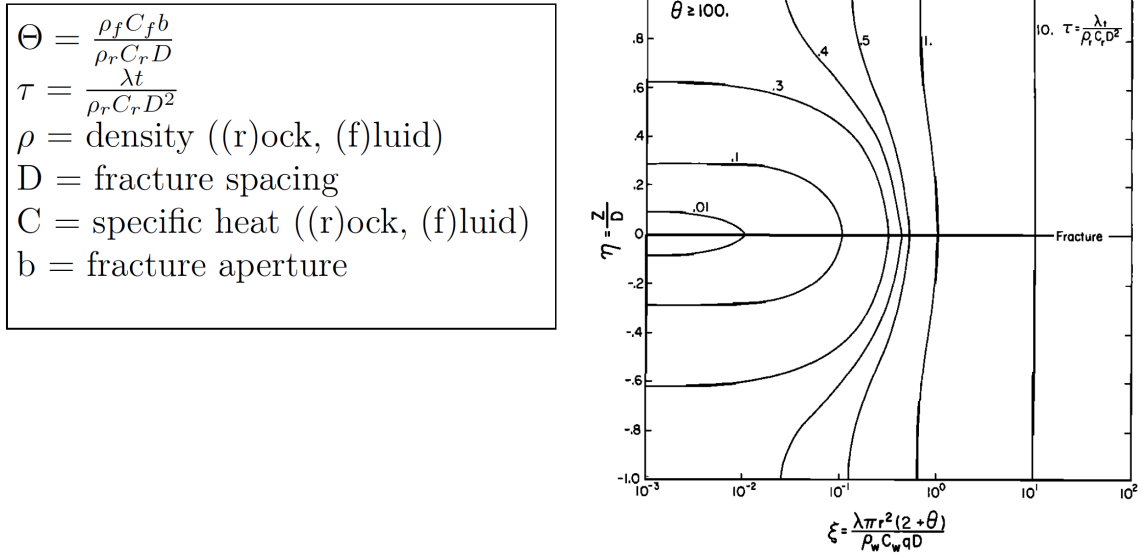
(a) Figure 1.10(b) nomenclature   (b) Average thermal front propagation as a function of dimensionless parameters [32]

Figure 1.10: Average thermal front propagation profiles taken from Bodvarson et al. (1982) [32]

the reservoir cannot be extracted before the fluid outlet temperature have dropped below economical production temperatures. When the production temperature starts to drop below the initial rock temperature is the reservoir said to have reached thermal breakthrough or thermal breakdown.

Bodvarson et al (1982) [32] investigated the development of a thermal front in a fractured geothermal reservoir. The analysis was based on a analytical solution of a horizontal fracture with constant aperture with rock matrix extending a finite length in vertical direction. The most important assumptions done in the analysis was; purely radial flow, initially temperature T_0 everywhere in the rock matrix, uniform temperature distribution in vertical direction in the fracture, rock matrix is impermeable, horizontal conduction is neglected, negligible heat transfer resistance between rock/fluid and constant physical properties.

The dimensionless solution is plotted in figure 1.10(b), the nomenclature used is given in figure 1.10(a). The figure shows how the thermal front propagates in the rock matrix as function of time. The term thermal front shown in figure 1.10(b) is the average isotherm in the rock matrix.

Bodvarson et al (1982) [32] defines three distinct behaviors in a fractured geothermal

reservoir; early time behavior, intermediate time behavior and late time behavior. At early times will the cold water front advance along the fracture as if no rock matrix is present. At intermediate times will the rock matrix start to conduct heat to the fracture and slow down the advancement of the cold front along the fracture. Late time behavior is identified by communication between fractures, which means that the heat flow in the rock matrix is effected by the other fractures in the system. This topic is discussed in detail in [32], the relevance for this thesis is the identification of different time periods and how the thermal front advances in a geothermal reservoir.

1.5 Mathematical modeling of a fractured EGS

In this section will different methods to model heat transfer and flow in a fractured EGS reservoir be presented and discussed.

The choice of method depends on required accuracy, available reservoir data and which parameters that are studied. For preliminary studies are simple models that does not require detailed reservoir properties used, and average reservoir properties are typically used. As potential sites have been identified are more detailed models used in order predict the production rates and behavior of the system more accurate, however these models require detailed reservoir data. Which in turn means drilling of wells and costly measurements in order to obtain the data. However, old oil and gas wells can deviate from this procedure, since these reservoirs have been studied thoroughly during oil and gas exploration which allows for detailed models without a large increase in costs.

1.5.1 Basics

The fundamental theoretical background for a model of heat transfer in a fractured EGS is presented in this section. Giving a background for the more complex models presented later.

The governing equations in a classical heat transfer problem, without chemical reactions are; The conservation of mass (eq.1.1), conservation of momentum (eq.1.2) and conservation of energy (eq.1.3).

$$\frac{\delta \rho}{\delta t} + \nabla_0 \left(\rho \vec{v} \right) = 0 \tag{1.1}$$

$$\rho \left[\frac{\delta \vec{v}}{\delta t} + \vec{v}_0 \nabla \vec{v} \right] = -\nabla P + \mu \nabla^2 \vec{v} + \rho \vec{F} \tag{1.2}$$

$$\rho C p \left[\frac{\delta T}{\delta t} + \vec{v}_0 \nabla T \right] = k \nabla^2 T + Q_0 \tag{1.3}$$

Steady state conduction through a solid is given by Fourier's law. Which can be applied directly to heat transfer through a solid, such as impermeable rock.

$$\dot{q} = -k A_c \nabla T \tag{1.4}$$

Fluid flow through a porous media can be assumed to follow Darcy's law (eq.1.5) at low Reynolds numbers (based on the pore size) [33]. For higher Reynolds numbers could

a modified version of Darcy's equation be used.

$$-\nabla P = \frac{\mu \vec{v}}{K} \tag{1.5}$$

The temperature at a given depth in sediments and in a conductive system can be estimated by eq. 1.6 [34]. Where T_0 is surface temperature, Q_e is equilibrium conductive heat flow and Kc is conductivity (as a function of depth).

$$T(z) = T_0 + \int (Q_e/Kc)dz \tag{1.6}$$

Representation of fractures

Fractures provide most of the reservoir permeability in a Enhanced Geothermal Systems, while most of the heat reserves are stored in the rock matrix. In some special cases where the reservoir is a high permeability reservoir could the ratio between flow in the rock matrix and in the fracture be small. However, flow through fractures is always likely to dominate the convective contribution.

There are two main alternatives in modeling a fracture dominated system, either model the fractures explicit or modify the hydrologic parameters (implicit method). The last approach involves drastic simplification of the problem. The fracture system is simplified to flow in porous media, where the permeability is increased in order to account for the fractures. This is often referred to as the effective continuum method. Due to the high degree of simplification are the results only applicable when the fracture spacing is sufficiently small [35]. Which typically is not the case in a EGS.

The other approach is to model each fracture explicit, which both require detailed information of the reservoir and computer capacity due to the complex calculations. The dual porosity model (fig.1.11(a)) is such a model. Where the fractures are represented as spaces between the porous matrix blocks. The temperature in each block is assumed to be uniform. Limitations with this representation are that the fractures divides the reservoir into blocks of uniform size and the transient flow between the matrix and blocks is not correctly represented [36]. The MINC (Multiple Interacting Continua) formulation addresses the latter issue by discretisation each matrix block [36, 35].

(a) Idealized dual porosity model of a frac-   (b) MINC (Multiple Interacting Continua) [36]
tured porous medium [35]
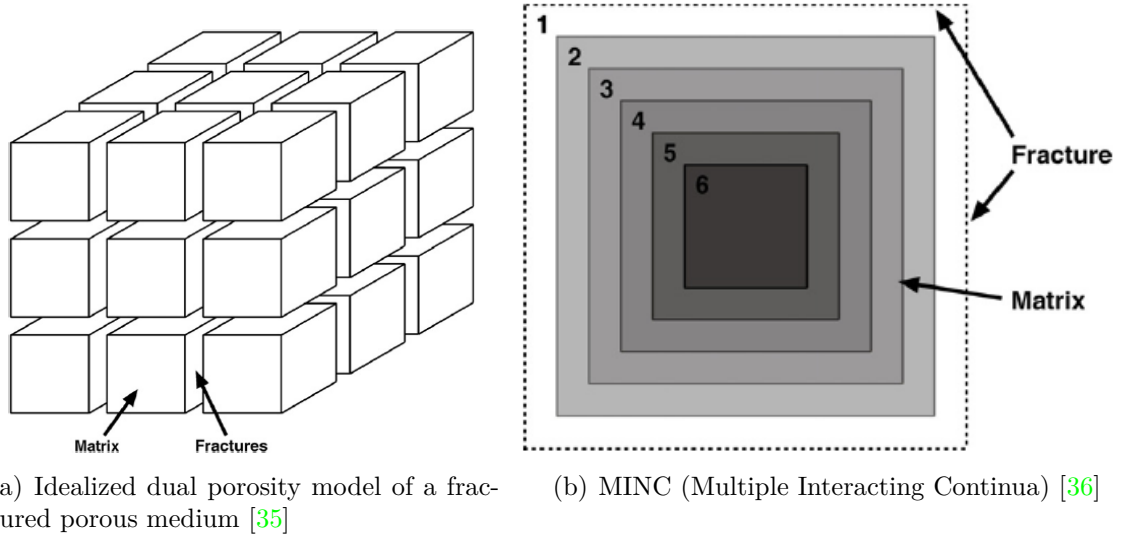
Figure 1.11: Models dealing with fracture representation

Heat transfer in fractures

Flow and heat transfer in fractures are problematic, due to the wide range of fracture systems, fracture aperture, fracture roughness and geometry. However, some simplifications can be done in order to create a model that gives an impression of how the system behaves. Either by modeling the fracture network with an increased permeability of a porous media (implicit approach), or modeling the fractures explicit. Due to decrease in accuracy for the implicit method when the fracture spacing increases should a implicit method be used when modeling a typical fractured EGS.

The heat transfer between the rock matrix and circulation fluid in a fracture is determined by the heat transfer coefficient. However, it has proven difficult to find a exact relationship for the heat transfer coefficient in a fracture. Zhao conducted an experiment on core samples in order to determine the heat transfer coefficient. Zhao et al. (1993) [37] found the heat transfer coefficient in joints to follow the relationship given in eq.1.7, the results from the experiment can be seen in fig.1.12. The relation given below is found from linear regression of the result in the experiment conducted by Zhao et al. (1993) [37].

$$h = A\vec{v}^B \tag{1.7}$$

$$A = 543 \pm 52$$

$$B = 0.90 \pm 0.03$$

32
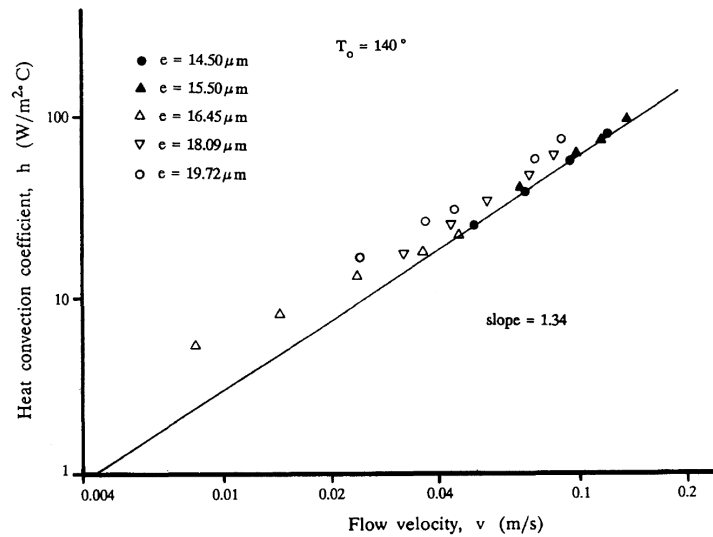
Figure 1.12: Variation of average heat transfer coefficient with flow velocity at a rock temperature of $140^0 C$ [37]

The heat transfer coefficient found by Zhao underpredicts the heat transfer coefficient by a factor of 10-15 compared to classical analytical solutions of integral flows (flat plates, squares, circles). Since no explanation is given by Zhao for the large difference is the result regarded as unreliable and should be used with care.

A report by Ogino et al (1999) [38] concludes that the forced convection between flowing water and the fracture surface has an important role in the heat transfer mechanism only in the early stage of heat extraction and the heat transfer resistance between rock/fluid can be assumed to be negligible in all practical cases. This assumptions is frequently used in the literature when the heat transfer in a fractured EGS is modeled.

Pressure drop

The pressure drop in a fractured reservoir varies greatly, and is dependent on the fracture network, rock properties, mass flow, well spacing and circulation fluid properties. Due to large variety of fractured reservoirs have several methods been used to estimate the pressure drop. There are basically three different approaches used in the literature; modeling the pressure drop using a effective permeability (effective continuum method), model the system with different permeability for the fracture and the matrix (effective porous continuum. method, used in the TOUGH2 EGS simulation software [39]) or model the pressure drop using a appropriate friction factor and assuming flow between flat plates (used by

33

Cibich [40] in a EGS model developed for PIRSA[1] Petroleum and Geothermal Group)

The fluid flow is in assumed to follow Darcy's law in practically all papers and reviews that have been investigated. TOUGH2, the software most often used to simulate EGS, uses a effective fracture permeability in order to estimate the pressure drop. Non-Darcy flow could occur in a reservoir, example turbulent flow, however based on the literature review is this rarely (if at all) considered when calculating the pressure drop. Typical ranges of flow rate, fracture aperture, permeability and friction factor used in the literature is found in Appendix D.

The effective continuum method (implicit method) offers a simple way to estimate the pressure drop, typically using a effective permeability from reservoir tests. However, the model is unable to account for or predict mass flow distribution in the reservoir. The dual porosity model (fig 1.11(a)) uses two different permeabilities, one for the fracture and one for the rock matrix, and it its therefore able to account for mass flow distribution in the reservoir and to a certain degree predict flow pattern. Cibich developed a pressure drop model assuming that flow in a fracture could be modeled using flow between flat plates and an appropriate friction factor. There are however few investigations of regarding friction factors in fracture flow. Cibich based his work on a friction factor developed by Louis (1969) in "A study of Groundwater in jointed rocks and its influence on the stability of rock masses". The friction factor used by Cibich [8] is $f_l = 1 + 3.1 \left(\epsilon/h_f\right)^{1.5}$, where ϵ is surface roughness and h is fracture aperture. The model developed by Cibich is used by PIRSA Petroleum and Geothermal Group as a model for a fractured EGS [41].

Chemical reactions

Rock-fluid interactions such as dissolving or depositing of minerals can be modeled using mass transfer and chemistry. Such models are incorporated in the most common simulation software used in EGS modeling, such as TOUGH2. However, in a pre-study of EGS concepts are the extra detail introduced by such models not necessary.

1.5.2 EGS models

EGS models range from simplified analytical approaches to complex numerical simulation programs. A short description of the different methods is given below.

---

[1]Government of South Australia Primary Industries and Resources

Analytical models

A few simplified analytical EGS models have been published. Obviously cannot these models be used for detailed modeling of a EGS. However, they are useful in order to understand the physical behavior of a EGS and conceptual studies.

Sutter et al (2011) [27] developed a analytical solution for a fracture based on works done by Gringerarten et al (1975) and Wunder and Murphy (1978). The model developed is a 2D transient solution of the temperature in the rock formation. The temperature of the circulation fluid is assumed to be equal to the temperature rock formation temperature at the interface between the circulation fluid and rock formation. A more in-depth study of the model can be found in section A.2.1 (Appendix A).

A similar analytical model is also developed by Cheng et al (2001) [42].

Lumped parameter analysis

Lumped parameter models are simple models that reflects some of the physical processes in a producing geothermal reservoir. Such models are good at a conceptual level, when little is known about the reservoir formation.

They typically assume that the rock formation is isentropic and homogenous, which is a major simplification. At least in porous rocks, such as certain types of sediments. The circulation fluid is typically assumed to be single phase. A common approach is also to model the effect of fractures by increasing the effective permeability of the reservoir, the effective continuum method (see subsection "representation of fractures in section 1.5). More advanced models model the fractures explicit as "tunnels" in the rock formation. Heat transfer between the rock matrix and circulation fluid is either modeled using a heat transfer coefficient or assuming that the heat transfer coefficient can be neglected. The latter is the most common approach, and it is valid approximation in any practical case [27]. Zhao [43] conducted experiments in order to determine the heat transfer coefficient, however the results seems to be erroneous as the heat transfer coefficient is underestimated by a factor of 10-15 compared to analytical solutions.

Wellbore models

Wellbore models that include heat transfer are common in the oil and gas industry. Models range from the classical solution of Ramey (see appendix A) to complex numerical programs. Choice of model depends on the detailed required and computer power available.

However, the classical solution by Ramey have shown to yield good results except for the first transient period and is therefore the most practical solution for a conceptual study. Ramey's solution is a analytical solution and require little computer power, which makes it easy and efficient to use.

Complex numerical simulation programs

Sanyal et al. (2010) [44] presented an overview of the state-of-the-art numerical simulation software for EGS. A list of necessary and desirable features that should be included in a EGS/HDR program are [44]

- Explicit representation of the fractures

- Fracture opening as a function of effective stress

- Shear deformation and associated jacking of the fractures

- A relationship between fracture aperture and fracture conductivity, including the potential for turbulent flow in the fractures

- "Channeling" and thermo-elastic effects

- mineral deposition and dissolution

- A tracer module

- Two-phase flow and the consequent complexities of phase change, relative permeability, capillary pressure effects, etc.

TOUGH2 is the most common simulation tool used to model EGS reservoirs [36]. It is a general-purpose numerical simulation program written in Fortran for multi-phase, multi-component fluid and heat flow in porous and fractured media [44]. TOUGH2 is developed by Karsten Pruess et al at Lawrence Berkeley National Laboratory. PetraSim is a commercial computer code with a graphical interface that uses TOUGH2 as base code.

Comsol is graphical program based on the Finite Element Method (FEM) which offers a simple and user friendly interface, and can be used to model simplified EGS reservoirs at a conceptual level. The combination of the heat transfer module and the Earth Science module can model heat transfer in porous medium, however it cannot model fractures in a comprehensive way (as TOUGH2). Model stability problems have been reported when

long time scales are used [24]. However, Comsol is developing software that can be used to model a EGS [personal communication].

1.6   Top site utilization

Top site utilization of geothermal energy was investigated in the project thesis [15] leading to the master thesis. Different alternatives, ranging from district heating to electricity generation, were studied. This master thesis will build upon work done on power production cycles in the project thesis. The findings in the project thesis will be briefly reviewed and followed by a more in-depth study of potential power cycles and issues related to power production from dry geothermal reservoirs.

1.6.1   Potential top site cycles

This subsection builds upon the work conducted in the project thesis, where different top site utilization concepts were investigated. The findings regarding electricity generated cycles are briefly reviewed and forms a basis from where potential top site cycles for a EGS power plant can be chosen. Alternative top site utilization methods, such as district heating and process heat are not considered in this thesis.

The bulk of the cost related to a EGS power plant is the investment cost, operational costs of a EGS power plant is only a small portion of the total cost. The cost of the power plant and underground system is therefore critical in achieving a commercial EGS power plant. The critical parameter is therefore cost per MW ($/MWe) and not thermal efficiency of the system. However, a cost analysis is not inside the scope of this paper and the focus will therefore be on thermal performance of the system.

There are several power cycles that can be used to extract heat from low to medium temperatures ($100^0C - 200^0C$). The most common cycles used for geothermal energy, and other low/medium temperature sources, are; flash cycles, Organic Rankine Cycles, Kalina cycle and Stirling engines. There are a multitude of different optimization designs for each cycle type, depending on site specific conditions. Top site cycles for geothermal energy can be regarded as a mature technology, there are several operational geothermal power cycles. The majority of these cycles are based convective geothermal reservoir (aquifers), with typically high pressures and temperatures. However, there is a increasing number of HDR systems. HDR systems are typically situated in low to medium temperature reservoir and a binary cycles is often preferred. Table 1.13 shows different low-temperature operating binary power plants. Cycle type, working fluid and gross capacity is tabulated. The table is taken from Franco et al (2009) [6].

Binary power plants, or Organic Rankine Cycles, are typically preferred as the top site

Small binary power plants using low-temperature geothermal resources or non-conventional working fluids (data from various open-file sources).

Plant and location	T_{geo} (°C)	Cycle	Working fluid	Gross capacity (kWe)	Specific brine consumption $[(\text{kg s}^{-1})\,\text{MW}^{-1}]$	Cooling tower
Nigorikawa, Japan	140	Rankine	R114	1000	50	Wet
Otake, Japan	130	Rankine	Isobutane	1000	14.7	Wet/dry
Husavik, Iceland	124	Kalina	NH_3–H_2O	1700	53	Wet
Nagqu, China	110	Rankine	Isopentane	1000	69	Dry
Altheim, Austria	106	Rankine	C_5F_{12}	1000	86	Dry
Wabuska, CA, USA	104	Rankine	Isopentane	1750	34.3	Wet
Chena Hot Spring, AK, USA	74	Rankine	R134a	400	57.9	Wet/dry
Kutahya-Simav, Turkey	145	Rankine with superheat	R124	2900	42	Wet

T_{geo}: geothermal fluid temperature.

Figure 1.13: Small binary power plants using low temperature geothermal resources or non-conventional working fluids [6]

cycle for low to medium temperatures. Binary cycles are more efficient than flash cycles in moderate temperature ranges [45]. Stirling Engines are typically not built for large scale power production, however they could be interesting for small scale geothermal power production. The Kalina cycle is a type of ORC that uses a water-ammonia mixture as working fluid. The Kalina cycles do show a 20%-40% increase in theoretical thermal efficiency, compared to other ORC [46]. However, based on measurements done on operational plants are the difference in thermal efficiency negligible [46]. The Kalina cycle is also patented. A ORC is therefore typically used with moderate geothermal reservoirs. The ORC is studied in detail in section 1.7.

Different ORC's

Several Organic Rankine Cycles have been studied and the optimum design (with respect to thermal performance) varies depending on the geothermal resource and available top site resources (cooling water and other energy sources). The thermal efficiency of a standalone ORC is between $9-14\%$ for a geothermal temperature between 100^0C-200^0C. Franco et al. (2009) [6] conducted a optimization study of ORC with several different working fluids and temperature ranges, the results are tabulated in figure 1.22. The thermal efficiency was found to range between $10\%-11\%$ for any optimized solution, regardless of working fluid. A typical ORC is shown in figure 1.14(a), however more complex designs have been proposed with several pressure levels, superheater and pre-heater, internal heat exchanger. Since the range of geothermal temperatures and cooling water temperature between different sites will the optimum thermal design differ depending on local conditions. A single optimum design does not exist.

Another possibility is to combine geothermal energy with another renewable energy resources in a hybrid plant. Two such systems was investigated by Gozdur [47], the same cycles were also investigated in the project thesis and the results from that analysis can be

found in Appendix F. The two hybrid cycles are shown in figure 1.14(b) and figure 1.14(c). The hybrid cycle where geothermal water is used as pre-heat in a waste combustion plant with a Rankine cycle that uses water as working fluid showed to yield a thermal efficiency of about 20%. The hybrid plant also provided a stable thermal efficiency and energy output for variation in the geothermal temperature. The reason is that the fluctuations in geothermal energy was countered by increasing or decreasing the amount of energy from the waste combustion. The other alternative that was investigated was a dual cycle power plant, where a geothermal ORC was used as a bottoming cycle in a waste combustion plant (fig.1.14(c)). The thermal efficiency of such a cycle reached a maximum around 22% and was stable for different geothermal temperatures. The waste combustion cycle countered the variation in geothermal temperature. Using a geothermal ORC as bottoming cycle yields a slightly higher thermal efficiency compared to a system where it is used as pre-heat, however the dual cycle concept is also more complex.

Choice of ORC

The optimum ORC design depends on several factors and should be made from economical perspective, it is therefore difficult to recommend a single ORC design. The combination of geothermal energy and other renewable such as waste combustion is interesting and could give several advantages compared to a standalone ORC. However, a hybrid cycle requires that there are other energy sources available in the area. The combination of a ORC and district heating or process heat is also interesting and should be investigated if there are heat demands in the area surrounding the geothermal power cycle.
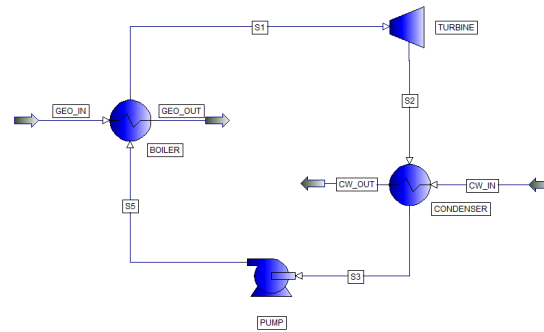
(a) Organic Rankine Cycle (ORC)
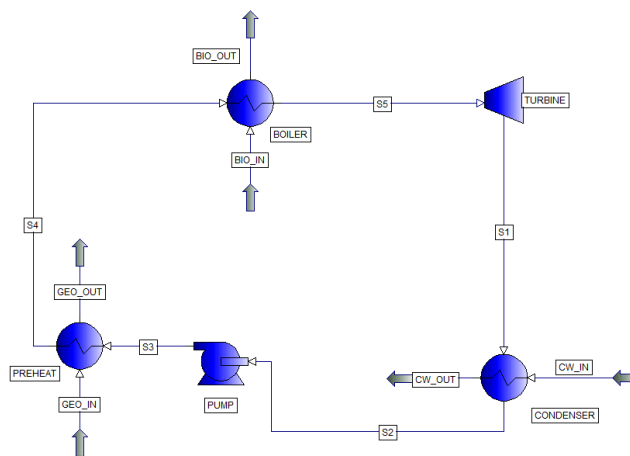
(b) Hybrid cycle with geothermal heat as preheat (HYB)
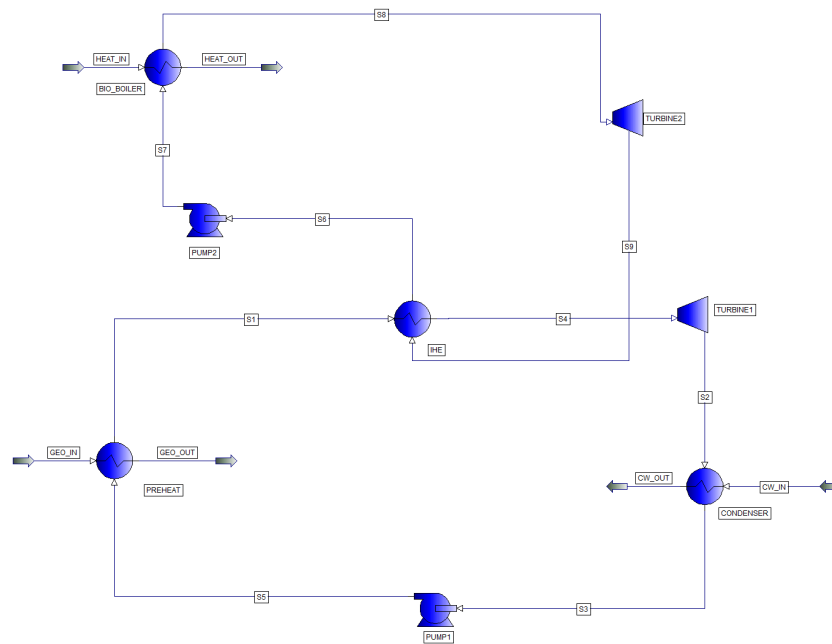
(c) Hybrid cycle with ORC as bottoming cycle (DFH)

Figure 1.14: Potential power cycles for large scale power generation

Operating binary plants of sizes larger than 10 MWe (data from various open-file sources).

Plant	Location	Installed capacity[a] (MWe)	Plant type	Type of cooling tower
Miravalles 5	Costa Rica	(18)	Combined cycle (binary)	Wet
Leyte	Philippines	(61)	Combined cycle (binary)	Wet
Mak-Ban	Philippines	(15.7)	Combined cycle (binary)	Wet/dry
Sao Miguel	Azores (Portugal)	16	Binary	Dry
Pico Vermelho	Azores (Portugal)	11.5	Binary	Dry
Mokai	New Zealand	(18)	Combined cycle (binary)	Dry
Rotokawa	New Zealand	13.5	Binary	Wet
Wairakei	New Zealand	(15)	Combined cycle (binary)	Dry
Zunil	Guatemala	28.6	Binary	Dry
Olkaria III	Kenya	12	Binary	Dry
Puna	Hawaii (USA)	(30)	Combined cycle (binary)	Dry
Heber (SIGC)	California (USA)	40	Binary	Wet
East Mesa	California (USA)	89.4	Binary (five plants)	Wet
Casa Diablo (Mammoth)	California (USA)	42	Binary (three plants)	Dry
Steamboat Spring	Nevada (USA)	34	Binary	Dry
Salt Wells	Nevada (USA)	14	Binary	Dry
Soda Lake	Nevada (USA)	12	Binary	Dry
Stillwater	Nevada (USA)	15.3	Binary	Dry
Stillwater 2	Nevada (USA)	48	Binary	Dry
Blundell	Utah (USA)	11	Binary	Dry

[a] Capacities shown in parentheses correspond to bottoming plants.

Figure 1.15: Operating binary power plants of size larger than 10MWe worldwide [6]

1.7 Theory: Organic Rankine Cycle

The Organic Rankine Cycle is a rankine cycle that uses a working fluid with a relative low critical point. This allows the cycle to convert heat into electricity at low temperatures (100^0C - 200^0C). The drawback is low thermal efficiencies, however since geothermal energy could be viewed as a free energy sources is the most important parameter cost per produced MW ($/MW) and not thermal efficiency.

Thermal efficiency of a ORC

The Organic Rankine Cycle is a heat engine and the thermal efficiency is therefore restricted by the theoretical limit given by the well known Carnot efficiency (equation 1.9).

The thermal efficiency of a closed system is given by

$$\eta_{cycle} = \frac{W_{net}}{Q_{in}} \tag{1.8}$$

Carnot assumed a cycle without any looses, depicted in figure 1.16(a). Solving the first law of thermodynamics using the assumptions employed by Carnot yields

$$\eta_{carnot} = \frac{T_H - T_C}{T_H} \tag{1.9}$$

The Carnot efficiency over predicts the maximum thermal efficiency of a ORC by several factors. A more realistic theoretical limit is the triangular process shown in figure 1.16(b) [7]. This process assumes a gliding temperature profile, which means gradual heating of
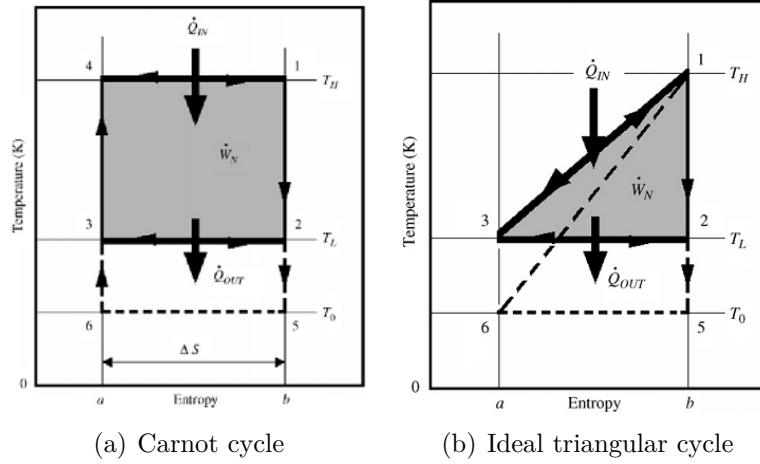
(a) Carnot cycle (b) Ideal triangular cycle

Figure 1.16: Theoretical heat engine cycles [7]

the working fluid as in ORC (no other losses are accounted for). The theoretical maximum efficiency for a gliding temperature cycle (triangular cycle) is given by

$$\eta_{tri} = \frac{T_H - T_C}{T_H + T_C} \tag{1.10}$$

DiPippio [7] presented a relationship for the thermal efficiency of a typical binary geothermal power plant based on actual power plant performance, the relationship is given in equation 1.11. By comparing the relationship to equation 1.10 is it obvious that a the typical thermal efficiency of a geothermal power plant is only 60% that of the theoretical maximum.

$$\eta_{typ} = 0.58 \frac{T_H - T_C}{T_H + T_C} \tag{1.11}$$

The different relationships given for the thermal efficiency can be seen in figure 1.17.

The thermal efficiency of the ORC is effected by several factors. Most important are losses in the pump and turbine and pinch point/match between temperature profiles in the heat exchangers. The isentropic efficiency of a turbine and pump in ORC is typically around 80% and 70% respectively [7]. The match between the temperature profiles in the heat exchanger is obviously dependent on the working fluid and temperature of the geothermal fluid. The working fluid in a ORC is discussed in subsection "ORC working fluid".
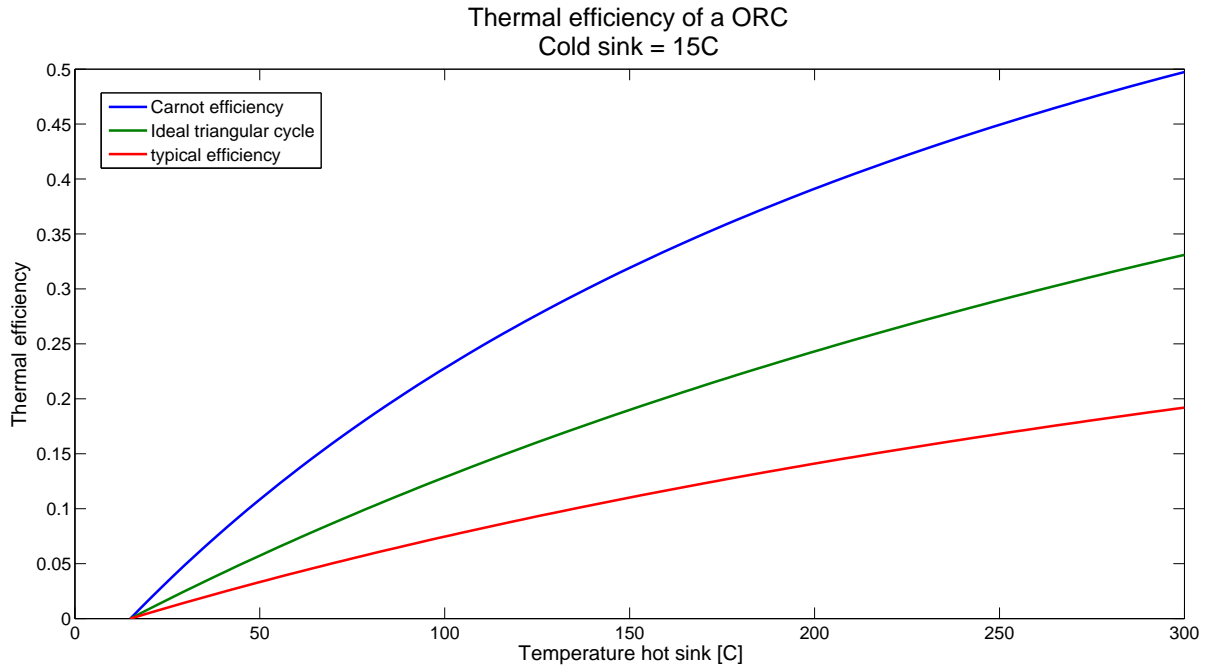
43

Figure 1.17: Theoretical and typical thermal efficiency of a ORC

ORC working fluid

The physical properties of the working fluid is of critical importance to the efficiency of the ORC. Several studies have been conducted on the choice of ORC working fluid, the working fluid that maximizes the thermal efficiency of the system have been found to vary depending on system parameters. A single working fluid have therefore not been identified as the optimum fluid in ORC used with geothermal energy. The best working fluid depends on site specific factors. Based on studies found in the literature is the thermal efficiency difference between 1% - 3% for different working fluids in a optimized cycle [46, 48, 6].

Chen et al (2010) [48] classified the different working fluids after the slope of $\frac{\delta s}{\delta T}$. Three groups were identified; wet, isentropic and dry fluids. The three groups are depicted in figure 1.19(b). Chen investigated around 50 different working fluids that could be applicable for low temperature ORC. The different working fluids where plotted in a $T - \xi$ diagram (figure 1.19(a)), where ξ is given by equation 1.12. A ξ value smaller than zero indicates a dry fluid, $\xi = 0$ indicates a isentropic fluid while ξ larger than zero indicates a wet fluid.

$$\xi = \frac{\delta s}{\delta T} \tag{1.12}$$

where s is entropy and T is the temperature.

(a) Subcritical cycle
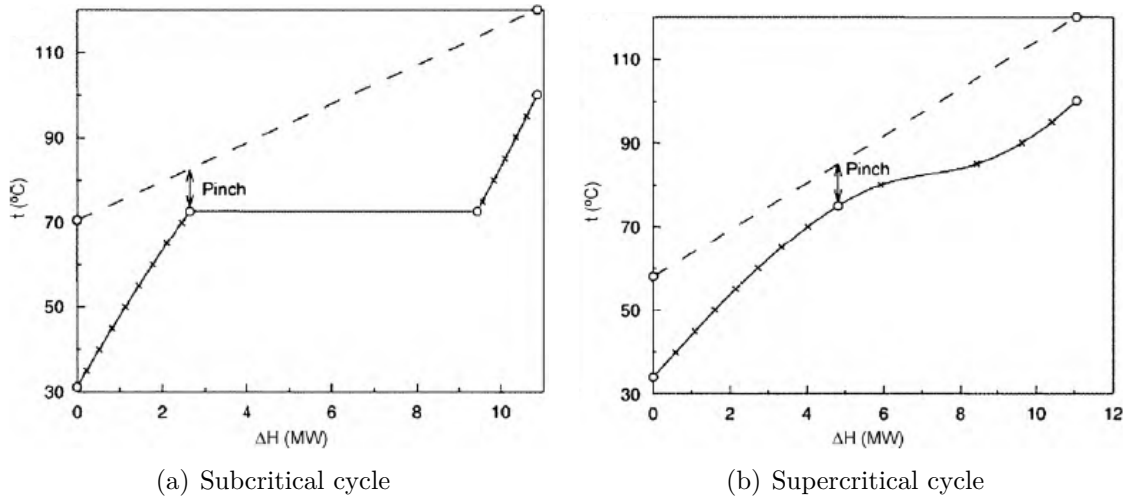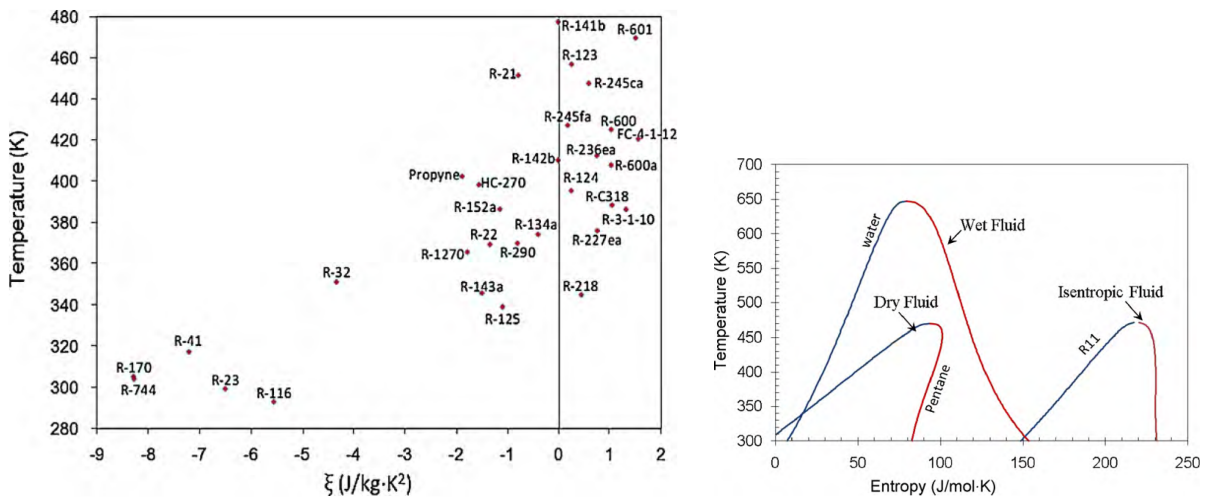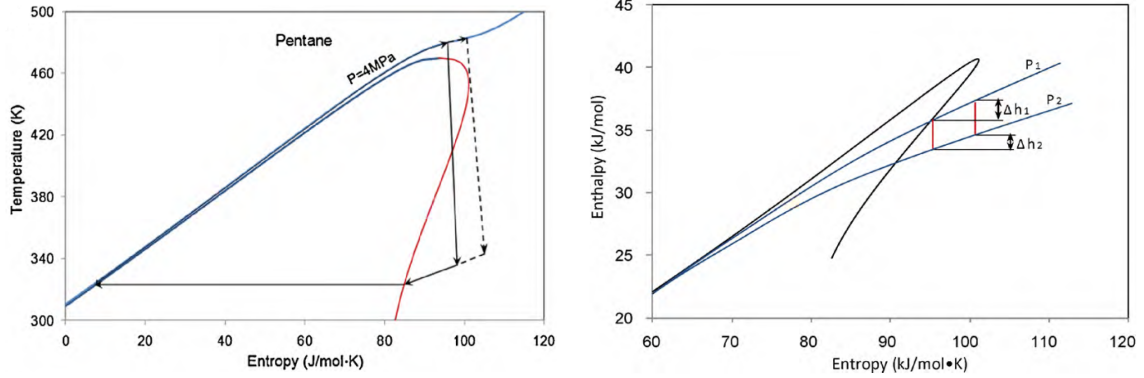
(b) Supercritical cycle

Figure 1.18: T - ΔH diagram showing the thermal match in an subcritical and supercritical ORC [48]

(a) Three types of working fluid: dry, isentropic and wet [48]

(b) Working fluids in a $T - \xi$ chart. The temperature is the temperature at the critical point for each fluid

Figure 1.19: Grouping of working fluids

(a) Organic Rankine Cycle using a dry fluid. Solid (b) Enthalpy - entropy diagram of dry fluid pen-
line = cycle passes through two phase region [48] tane demonstrating the effect of superheat [48]

Figure 1.20: Dry working fluid that passes through two phase region and the effect of
superheat shown in a Ts diagram

A dry working fluid may leave the turbine with a substantial amount of superheat, which
typically require a recovery process in order to keep thermal efficiency from dropping. Wet
fluids on the other hand require higher a higher turbine inlet temperature in order to
avoid the two phase region, which could damage the turbine and reduce the isentropic
turbine efficiency. The working fluid is typically kept outside the two phase region, since
condensation and droplet formation damages the turbine blades and interrupts the flow
scheme in the turbine causing the isentropic efficiency to drop. However, a study by
Demuth [49] found that if a dry fluid passes through the two phase region (solid line in
figure 1.20(a)) should the turbine isentropic efficiency not degrade significantly as long as
no condensation occurs. A dry working fluid that passes through the two phase region
could increase the fluid efficiency by 8%. To this end, dry fluids may server better than
wet fluids in supercritical states if the turbine expansion involves two-phase region [48].

The effect of superheating on the thermal efficiency of the system depends on the
working fluid. The rate at which the constant pressure lines diverges determines the impact
of superheat [48]. A incremental efficiency ($\dot{\eta}$) can be defined as the ratio of incremental
work and heat, given by equation 1.13.

$$\dot{\eta} = \frac{\Delta \dot{w}}{\Delta \dot{q}} = \frac{\Delta h_1 - \Delta h_2}{\Delta h_1} \tag{1.13}$$

h_1 and h_2 is defined in figure 1.20(b).

The choice of working fluid should take into consideration the following points [48]:

- Critical point of the working fluid

46

- Stability if the fluid ad compatibility with materials in contact

- Environmental aspects

- Safety

- Availability and cost

In a commercial EGS power plant is the cost per MW the most critical parameter, and not the thermal efficiency. The reason is that geothermal energy could be regarded as free once the initial investments have been made (the investment costs is large compared to the operational cost). The cost of the power cycle is therefore critical and the choice of working fluid should be based on a economical analysis of the system and not only a thermodynamic analysis.

1.7.1 Thermal design of a ORC

Madahawa et al (2007) [50] investigated a cost-effective optimum design of a ORC that uses a low-temperature geothermal heat source. They used the size of the heat exchangers as a measure of plant cost and optimized the design with respect to thermal efficiency and heat exchanger size. Ammonia was found to yield the minimum objective function (heat exchanger area/thermal efficiency) [50], however extra cost related to safety regulations when building a ammonia plant was not taken into account.

Franco et al (2009) [6] proposed a optimization approach that decomposes the binary cycle into three subsystems; cooling system (CS), heat recovery cycle (HRC) and recovery heat exchanger (RHE). The problem is further organized into two hierarchical levels. A schematic of the approach is shown in figure 1.21. The method is further discussed in the paper by Franco [6].

Based on the optimization process briefly described above was several working fluids and several geothermal temperature ranges investigated. The results are shown in figure 1.22, a interesting aspect is that the thermal efficiency differs little between the investigated working fluids for any optimized solution. From a thermodynamic perspective is the difference between different working fluids small as long as the cycle have been optimized for the given temperature range, which leads to the conclusion that the choice of working fluid should be based on other than thermodynamic factors. Franco et al (2009) [6] identifies the brine consumption per MW of produced energy ($kgs^{-1}MW^{-1}$) as a measure of
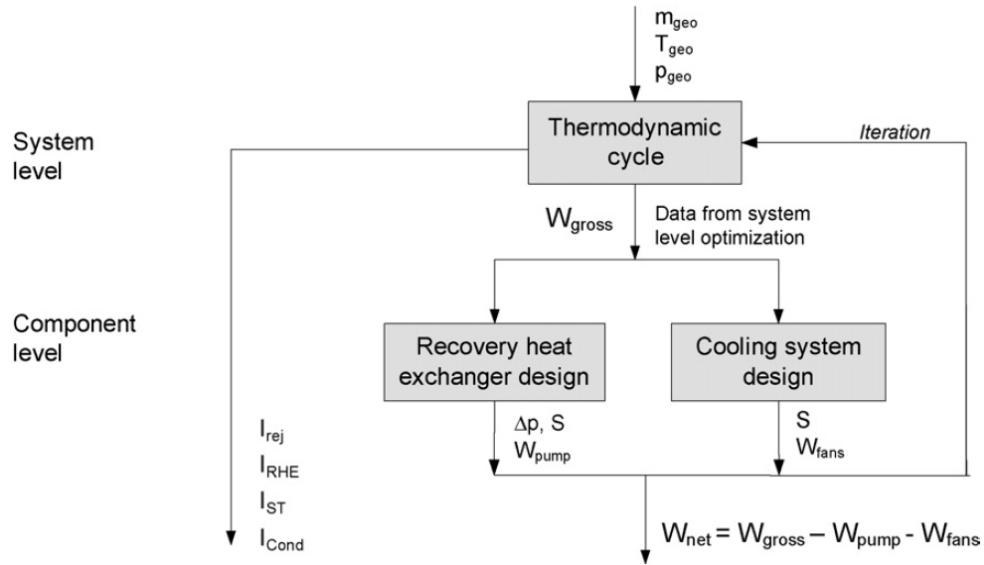
Figure 1.21: Hierarchical organization for the optimal design of binary plants

cost of the system and stresses the importance of keeping the specific brine consumption (β) to a minimum in order for geothermal binary plants to be economical.

$$\beta = \frac{\dot{m}_{brine}}{\dot{W}_{net}} \tag{1.14}$$

Effect of geothermal fluid and rejection temperature differences ($T_{\text{geo}} - T_{\text{rej}}$) on computed results (condensation temperature: 40 °C).

Case 1:	T_{geo} = 160 °C T_{rej} = 70 °C								
	Rankine			Rankine with superheater			Optimized solution		
	β (kg MJ^{-1})	η_{I} (%)	η_{II} (%)	β (kg MJ^{-1})	η_{I} (%)	η_{II} (%)	β (kg MJ^{-1})	η_{I} (%)	η_{II} (%)
Working fluid									
R134a[a]	31.1	8.42	31.98	26.79	9.74	37.11	23.61	11.09	42.11
R152a[a]	28.2	9.28	35.7	23.39	11.20	42.50	23.29	11.24	42.69
Isobutane[b]	27.7	9.45	35.9	29.8	8.79	33.30	24.03	10.91	41.43
n-Pentane[b]	29.73	8.80	33.45	31.2	8.39	31.87	24.66	10.71	40.65
R401A[a]	30.31	8.64	32.82	25.74	10.17	38.63	24.47	10.70	40.63
R407C[a]	38.7	6.76	25.7	33.97	7.70	29.27	26.31	10.02	38.05

Case 2:	T_{geo} = 130 °C T_{rej} = 70 °C								
	Rankine			Rankine with superheater			Optimized solution		
	β (kg MJ^{-1})	η_{I} (%)	η_{II} (%)	β (kg MJ^{-1})	η_{I} (%)	η_{II} (%)	β (kg MJ^{-1})	η_{I} (%)	η_{II} (%)
Working fluid									
R134a[c]	50.3	7.84	31.29	43.99	8.98	35.77	43.99	8.98	35.77
R152a[b]	47.48	8.32	33.14	52.40	7.53	30.03	42.68	9.25	36.87
Isobutane[b]	53.1	7.44	29.63	56.70	6.95	27.71	43.90	9.00	35.84
n-Pentane[b]	55.26	7.15	28.48	58.20	6.78	27.02	44.60	8.86	35.27
R401A[c]	49.43	7.99	31.84	51.23	7.70	30.72	44.18	8.94	35.62
R407C[a]	53.43	7.40	27.38	53.43	7.40	27.38	49.99	7.91	31.48

Case 3:	T_{geo} = 150 °C T_{rej} = 80 °C								
	Rankine			Rankine with superheater			Optimized solution		
	β (kg MJ^{-1})	η_{I} (%)	η_{II} (%)	β (kg MJ^{-1})	η_{I} (%)	η_{II} (%)	β (kg MJ^{-1})	η_{I} (%)	η_{II} (%)
Working fluid									
R134a[a]	43.1	7.81	26.53	35.09	9.60	32.60	30.94	10.89	36.98
R152a[a]	37.72	8.93	30.33	31.25	10.78	36.61	31.04	10.85	36.86
Isobutane[b]	34.07	9.89	33.57	36.38	9.27	31.45	29.36	11.47	38.97
n-Pentane[b]	35.19	9.57	32.51	37.39	9.00	30.60	29.75	11.33	38.46
R401A[a]	39.23	8.60	29.16	34.28	9.83	33.36	31.36	10.74	36.48
R407C[a]	51.94	6.48	22.02	44.14	7.63	25.92	38.99	8.64	29.34

[a] Optimized solution: supercritical cycle.
[b] Optimized solution: dual-pressure level Rankine cycle.
[c] Optimized solution: Rankine cycle with superheater.

Figure 1.22: Effect of geothermal fluid and rejection temperature difference on different ORC designs (condensation temperature = $40^0 C$) [6]

1.8   Summary

Different aspects of a geothermal power plant was reviewed, from different EGS concepts, how to model a fractured EGS and top site power cycles.

A fractured geothermal reservoir situated in granite was identified as the most common EGS concept. The optimal well configuration was found to be governed by local geological conditions, such as the direction of the stress field, amount and size of natural fractures and required energy production. It is therefore critical to predict the fracture network and flow regime accurately.

Low to moderate geothermal temperature fields exist in Norway, it is not a cold spot as previously believed. However, temperatures are extrapolated from 800m deep wells and the uncertainty is therefore large. Hurdal was identified as one of the possible sites for geothermal energy in Norway, with a temperature between $100^0C - 190^0C$ at 5km. A potential reservoir is believed to be situated in granite, with low porosity and permeability.

It is difficult to model the complex fracture network encountered in EGS. The simulation software used are therefore based on a simplified representation of the fracture network. The most common software uses a dual porosity model with discretized blocks (MINC method), where the flow regime is calculated using an effective permeability. Chemical reactions, thermal effects, pressure effects and two phase flow are typically accounted for. TOUGH2 is a widely used computer code for EGS simulation. However, the thermal behavior of the reservoir could be captured by simple horizontal fracture model.

A Organic Rankine Cycle is typically used as top site cycle in a low to moderate temperature field. The optimum design of the ORC is site specific, it is therefore difficult to recommend a design before a site is specified. Combining geothermal energy with other renewable energy sources, such as waste combustion, looks favorable and should be pursued if possible. The advantage is a higher thermal efficiency (almost a factor of 2) and a more stable power output (with respect to variation in geothermal temperature).

Part 2

EGS simulations

This part of the master thesis studies the temperature and heat output from a fractured EGS, and how those two parameters are effected by variations in reservoir and operating conditions. A numerical model was developed in matlab, see subsection "EGS model", Appendix A and Appendix B. The model was used to evaluate the fractured geothermal reservoir under different conditions, the results are presented in section 2.2. A discussion of the results and a summary is found at the end of this part.

A brief overview of the EGS model used is presented in section 2.1, giving the reader a insight into how the model works. The model is presented in detail in Appendix A and Appendix B. Thereafter is the results from the analysis presented, divided into subsections. First are graphs showing the circulation fluid and rock matrix temperature profile, showing the general behavior of the system. Followed by three sections; reservoir conditions, operating conditions and short circuiting. Where the outlet temperature and extracted heat is investigated as function of the parameters in the respective subsections.

2.1   EGS model

There exists several program packages that can model the behavior of a fractured EGS. Perhaps the most popular one being TOUGH2. A overview of the different numerical programs used to model EGS and their characteristics can be found in [44]. Most of these models require extensive amounts of reservoir data in order to yield reasonable estimates, and is therefore best used at site specific studies. At a conceptual level, where the effect of different parameters on the overall heat production is studied is a simple numerical model often the best choice. One advantage of a simple model is low computational costs

compared to more complex models, which makes it possible to run numerous studies in a relative short time. Another aspect is that the error induced by uncertainties in input parameters is often small compared to the error induced by the simplifications of the geothermal reservoir. Resulting in estimates that can describe the general behavior of a system and how it is effect by different parameters, however due to the simplifications done are the results only guiding and should only be used to draw general conclusions.

A numerical model using a simplified representation of a geothermal reservoir (fig. 2.1) with temperature dependent rock properties and average circulation fluid properties was developed in this thesis. The reason for choosing such a model is a lack of detailed geological data which makes advanced models unreliable, garbage in equals garbage out. The other reason is that the aim for this thesis is to draw general conclusions on the behavior of a EGS, and not a optimized design. Comsol could be used, however due to reports of stability problems at long time periods in EGS simulations [24] was it decided not to use Comsol. Therefore was a numerical model based on a simplified representation of a fractured geothermal reservoir chosen.

The model was constructed in Matlab r2010a, and is based on the finite volume method. The rock formation is modeled as a transient 2D heat conduction problem. The flow through the fracture is modeled as a 1D steady state flow between flat plates, and is fully coupled with the rock matrix model using the heat flux across the interface. The fractured network is assumed to consist of equally spaced horizontal fractures with a constant aperture, see figure 2.1. Due to the symmetry in the reservoir is only half the rock matrix between each fracture modeled, see figure A. The heat flux on all sides, except at the interface between the rock and the fluid, is assumed to be zero. Temperature dependent properties is used for the rock matrix, while average properties are used for the circulation fluid. The temperature difference in the circulation fluid in y-direction (fig. 2.2) is assumed to be negligible, as the aperture of the fracture is very small compared to the length of the fracture.

More details regarding the program structure, equations used, boundary conditions and mesh adjustments can be found in Appendix A. The heat transfer in the wellbore is modeled using the classical analytical equation derived by Ramey [51], see appendix B. The model has been validated against analytical solutions, see Appendix A. The model shows excellent agreement with analytical solutions, such as a semi-infinite solid and constant surface temperature solution of flow between two flat plates (Appendix A). The model is therefore assumed to be a correct representation of the simplified geothermal reservoir.
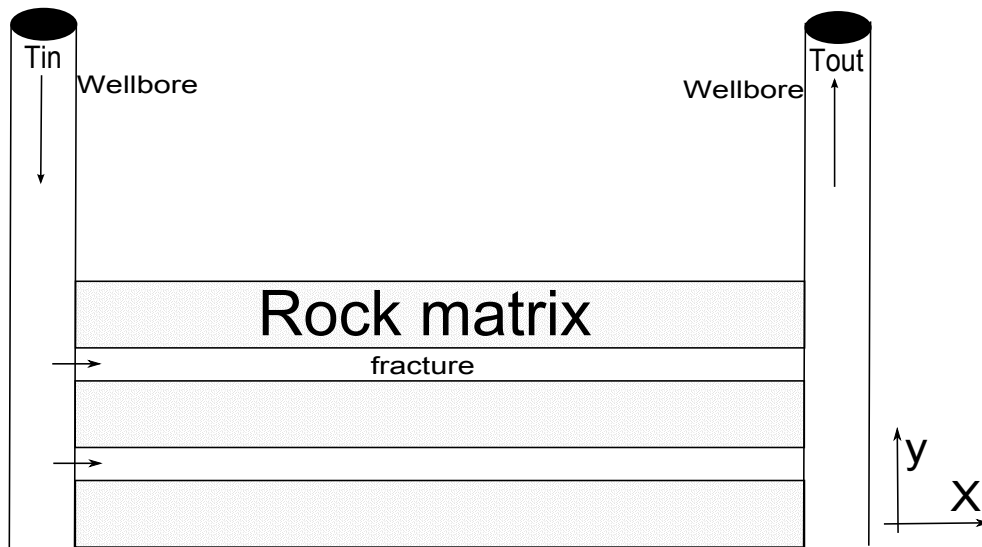
Figure 2.1: Simplified representation of a EGS used in the model

2.1.1 Model assumptions and simplifications

Several simplifications were done. Probably the most important one is that a EGS consisting of a complex network of fractures was modeled as a horizontal fractures with constant aperture and constant fracture spacing (figure 2.2). Which of course is not a physical correct representation, however a single fracture model adequately captures thermalrecovery through heat conduction from the rock surrounding the reservoir [27]. A single fracture representation of a fractured EGS should therefore be adequate to study the impact of different reservoir and operating parameters on the total heat output from a EGS.

Chemical reactions, thermal and pressure effects on the fracture aperture have not been included in the model. The extra accuracy introduced by such models is deemed unnecessary at this stage, and therefore not included. However, mineral deposition and dissolution, shear deformation, fracture opening and thermo elastic effects could have a major impact on a operating EGS and should therefore be included in any site specific design and optimization.

The rock matrix are assumed to be impermeable granite with zero porosity. This is a simplification, however since granite typically can be treated as impermeable should the error be small. Such an assumption could of course not be made in porous sedimentary layers, where fluid flow through pores in the rock matrix could contribute significantly to the heat transfer in the system. The specific heat and thermal conductivity of the rock matrix are temperature dependent, and could vary 50% in the temperature range under consideration. The temperature dependent properties have been model using the method

developed by Clauser et al (1995) [52] and Waples et al (2004) [53].

The circulation fluid is assumed to be uncontaminated water and in single phase (liquid). Fluid properties have been assumed to be constant, and set to an average value between 80^0C and 160^0C. Specific heat of water changes little, below 10% in the temperature range under consideration. Since a average value is chosen should the effect of constant properties be small, compared to using temperature dependent properties.

The convective heat transfer resistance is assumed to be negligible in the time scale under consideration (30 years). Ogino et al (1999) [38] found that the forced convection between flowing water and the fracture surface has an important role in the heat transfer mechanism only in the early stage of heat extraction. The heat transfer resistance between rock and water can therefore be assumed to be negligible in any practical case [38]. This topic is further discussed in section 1.5.1.

The wellbore model is based on the classical analytical expression by Ramey. Ramey's solution is frequently used in the oil and gas industry and has proved to be a good approximation of the heat transfer in a vertical wellbore. However, due to the simplifications done by Ramey is the model not accurate in the early transient period (which depends on rock properties and wellbore geometry). Therefore is the wellbore temperature assumed to be constant, and equal to the inlet temperature, in the first 0.1 years. This causes a error in the production wellbore temperature in this period, however the impact on the total system performance is small since the time scope is 25-30 years. Ramey's solution is prioritized before a accurate numerical solution since it provides a good approximation in the time period under consideration at low computational costs.

The early period in a operating EGS is not captured well in the model. Mathematical errors are introduced by Ramey's wellbore model and since the heat transfer resistance at rock/fluid interface is assumed to be negligible. Flow and heat transfer in the fracture close to the wellbore is not modeled well, since this area is not captured well by the physical model used in the model and the boundary conditions used. However, since this is a small part of the model should the error induced be negligible compared to the other assumptions in the model. The same is true for error in the early period, since this period is negligible in the time scale under consideration (25 - 30 years).

The pressure drop across the length of the fracture is estimated based on a solution of the Navier Stokes equation for horizontal fractures with constant aperture. The flow is assumed to be linear, incompressible and with constant physical properties (average values used). The model is based on a paper by Cibich et al (2008) [40], and the model
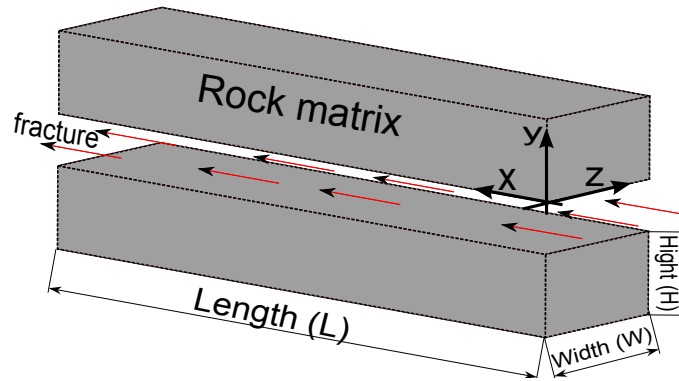
Figure 2.2: 3D representation of idealized fracture

have been used by the Petroleum and Geothermal Group of the Department of Primary Industries and Resources of South Australia (PIRSA). The ratio between fracture aperture and surface roughness elements have been assumed to be constant and set to 0.7. The pressure drop estimation is discussed in detail in Appendix A.

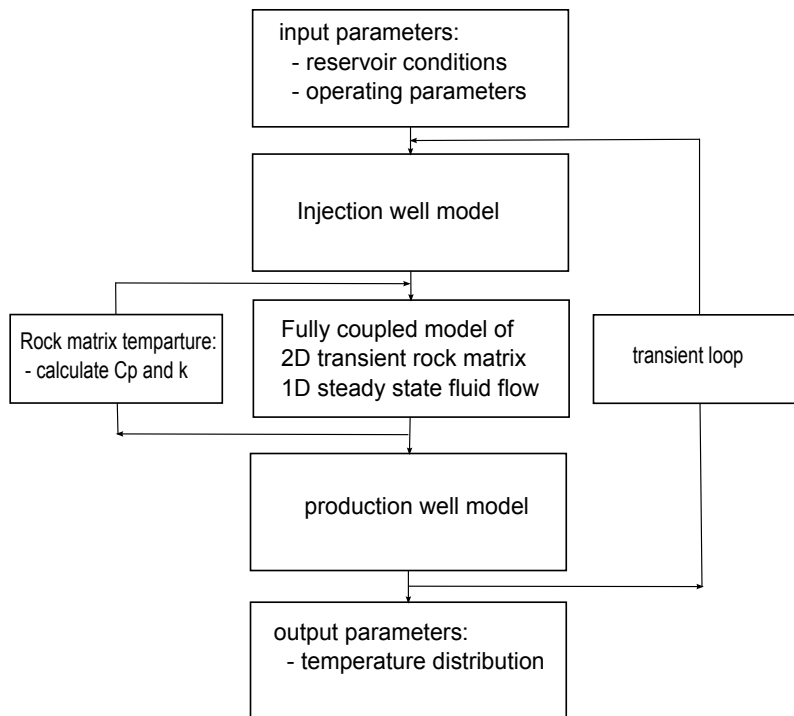Further information about the model can be found in Appendix A and B.

Figure 2.3: Graphical representation of matlab program

2.2   Simulation and Results

The results from the numerical matlab model are presented in the following sections. Different parameters are varied in order to see the effect on matrix temperature and circulation fluid temperature, which is a critical parameter in a EGS power plant. The results show the same physical behavior as reported by Bodvarson et al (1982) [32] (see section 1.4), as expected.

The section is divided into subsections after which group of parameters that are investigated. First is the temperature profile in the rock matrix and circulation fluid shown as a function of fracture length, matrix height, mass flow and time. This is in order to give the reader a understanding of how the temperature profiles develop and behaves. After that is the outlet temperature and heat extracted investigated, as these two parameters are critical for the operation of a geothermal power plant. This is done in three sections; "The effect of changing reservoir parameters", "The effect of changing operating conditions" and "Effect of fracture short circuiting".

2.2.1   Behavior of the temperature profiles in a EGS

The temperature profile in the modeled section of the rock matrix (fig.A) is seen in figure 2.4 and figure 2.5. Figure 2.4 shows the both the vertical temperature profile at 400 meters in to the fracture and the rock matrix temperature profile at the interface between water and rock at different times. The fluid temperature is assumed to be equal the rock matrix temperature at the interface, the figure on the left side in figure 2.4 is therefore also the temperature profile of the fluid. Figure 2.5 shows the temperature at any given location in the rock matrix after 10 and 30 years. The temperature distribution in the rock matrix corresponds with the behavior described by Bodvarson [32], as described in section 1.4.
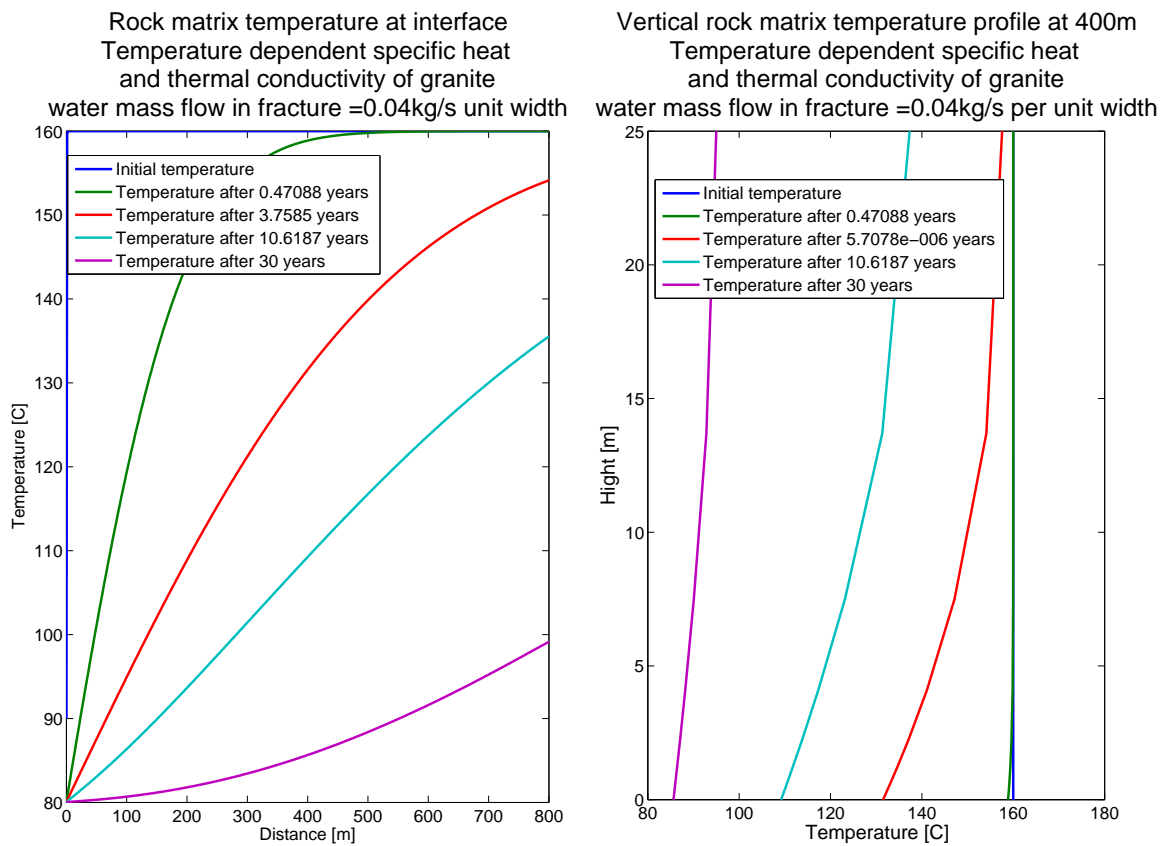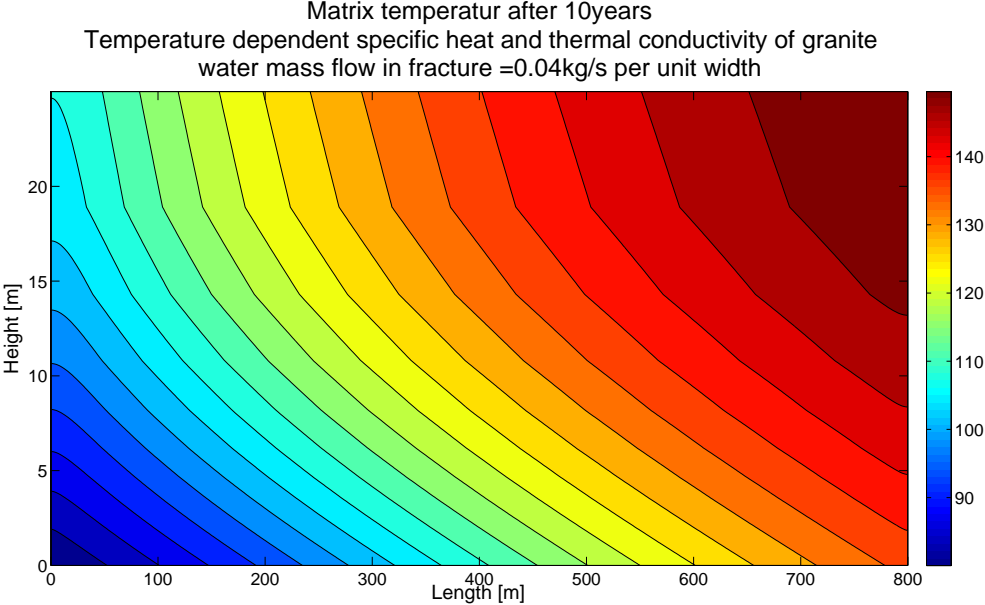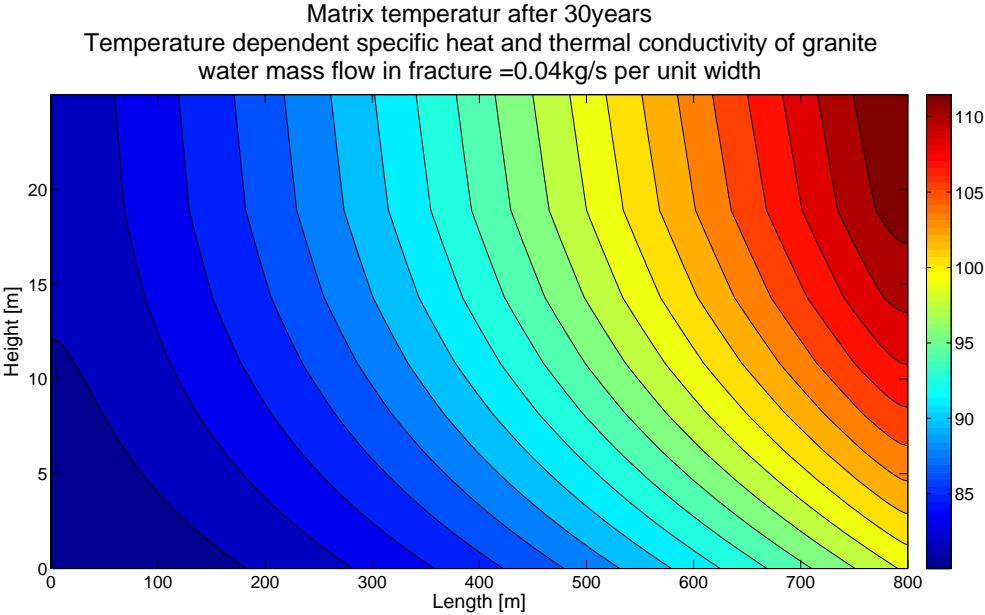
Figure 2.4: Temperature profile of circulation fluid (left) and rock matrix (right) as a function of time

(a) Matrix temperature after 10 years

(b) Matrix temperature after 30 years

Figure 2.5: Matrix temperature at 10 and 30 years

Wellbore model

During steady state operation without thermal breakdown of the geothermal reservoir will the wall temperature in the injection wellbore and production wellbore gradually approach the injection temperature of the respective well. This will cause a gradual temperature change in the fluid exiting the wellbore, this can be seen from figure 2.6. The first period, less than about 0.1 years (depending on actual system parameters), gives a unstable solution and should be disregarded. This is known issue with Ramey's wellbore solution and is discussed further in Appendix B. However, the implication on the overall system performance during the expected life time (30 years) is negligible. The effect of heat transfer in the wellbore increases with a decrease in mass flow and wellbore insulation (casing). A more detailed investigation of the wellbore model is conducted in Appendix B.
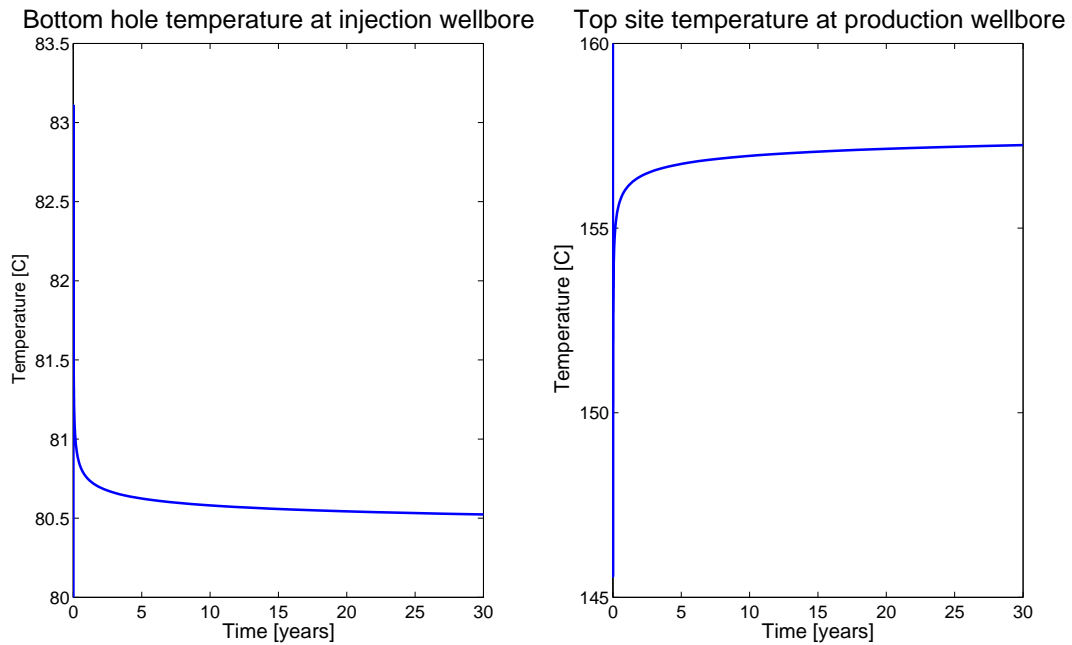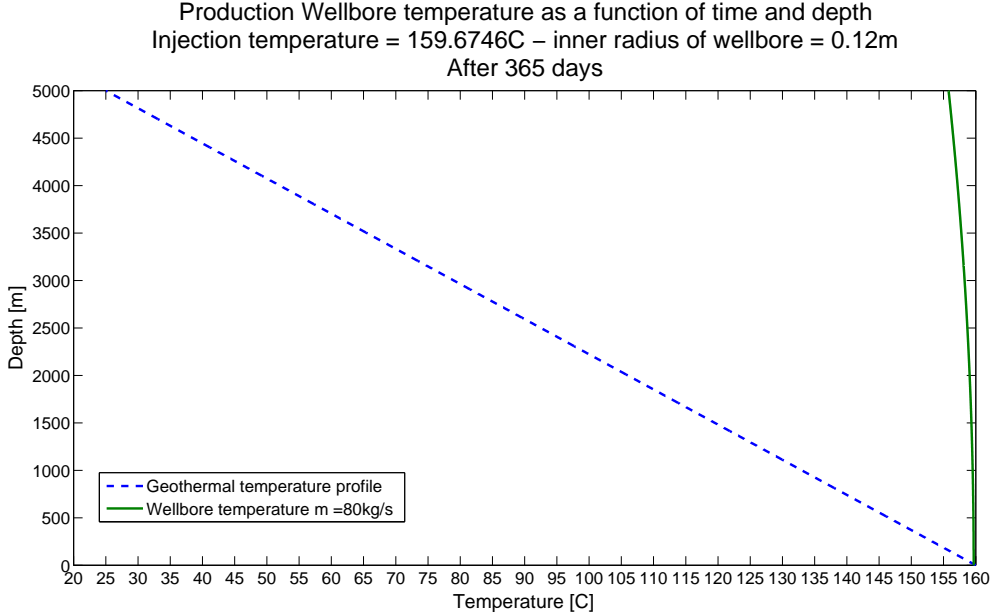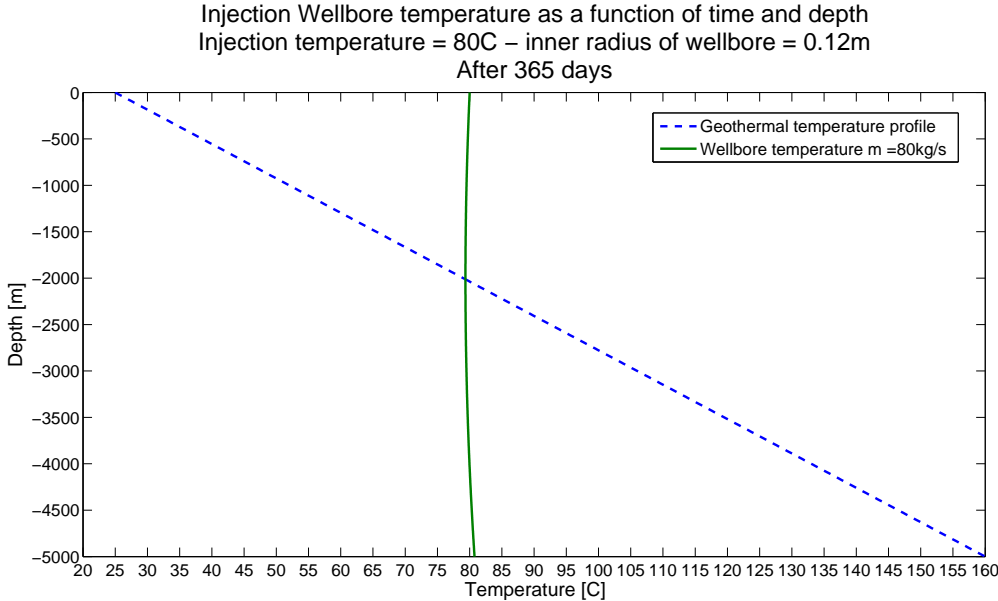

Figure 2.6: Temperature development at the bottom of the injection well (left) and temperature development at the top of the production well (right) as a function of time

(a) Injection wellbore

(b) Production wellbore

Figure 2.7: Temperature profile of the circulation fluid in the injection and production wellbore

2.2.2 The effect of changing reservoir parameters

In this section is the effect of different reservoir parameters on the outlet temperature investigated, such as thermal conductivity, specific heat, fracture length and fracture spacing. All studies are done with a mass flow rate of 0.008 kg/s per unit width, fracture length of 800m and a fracture spacing of 50m if nothing else is stated in the figure text. The low mass flow will in some instances yield small differences, this is due to the low amount of energy extracted from the system. However, the general effect is visible and should increase with a decreasing ratio between rock matrix volume and mass flow rate.

The effect of a change in specific heat and thermal conductivity can be seen in figure 2.8 and figure 2.9 respectively. How different initial rock matrix temperatures effect the outlet temperature is shown in figure 2.10. The top site production temperature as a function of fracture length and fracture spacing is shown in figure 2.11 and 2.12.
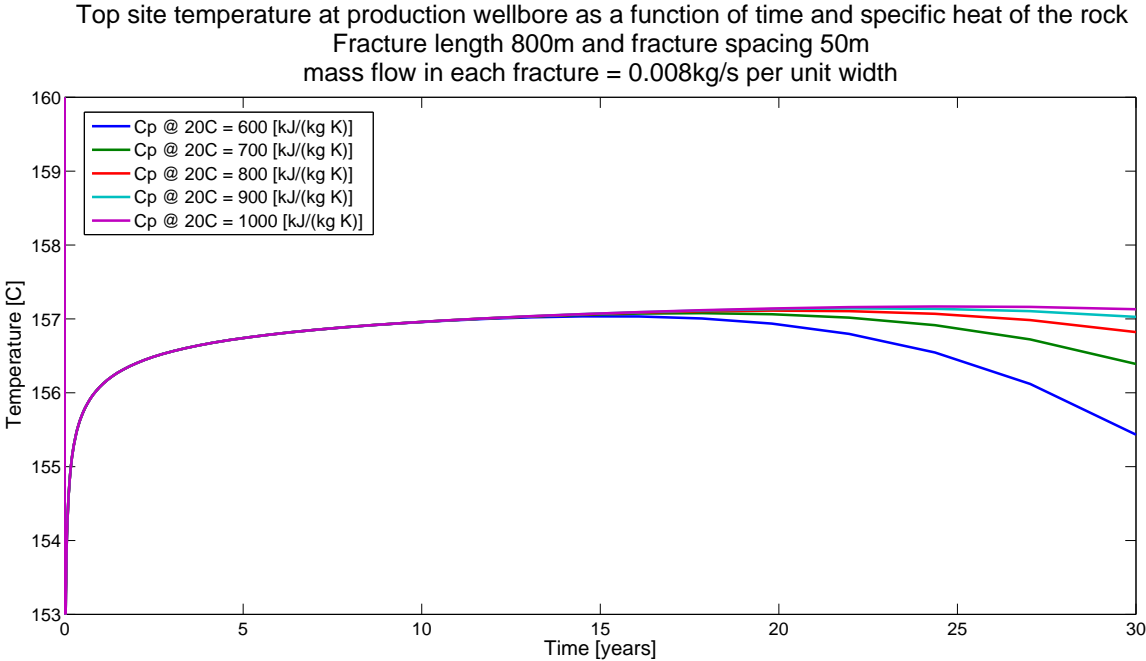
Figure 2.8: Production temperature as a function of time and specific heat of the rock matrix
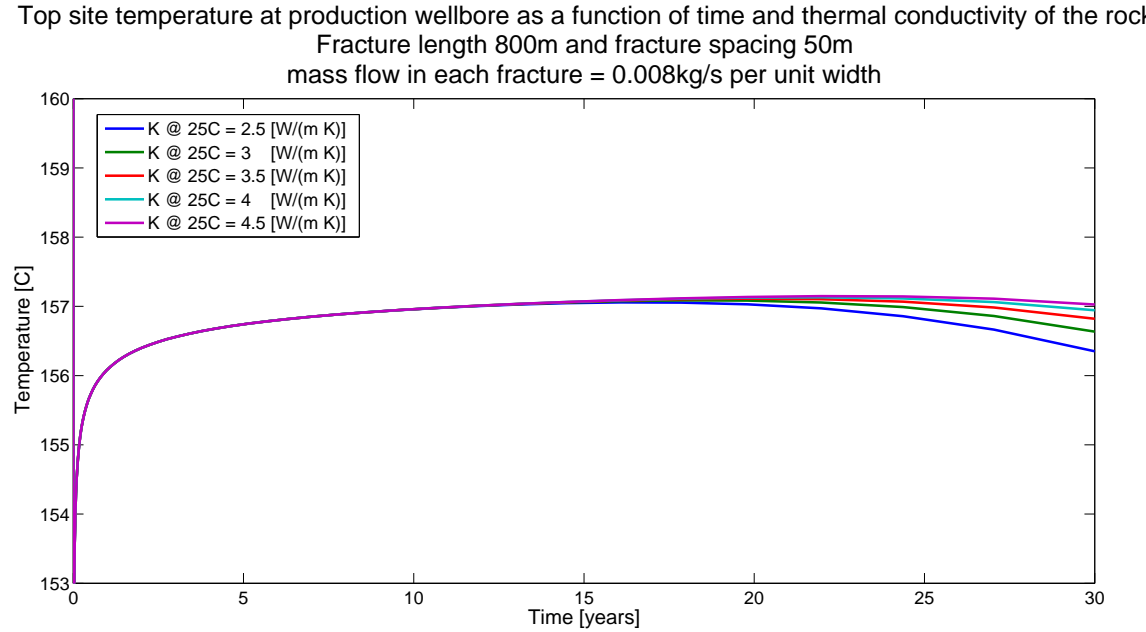

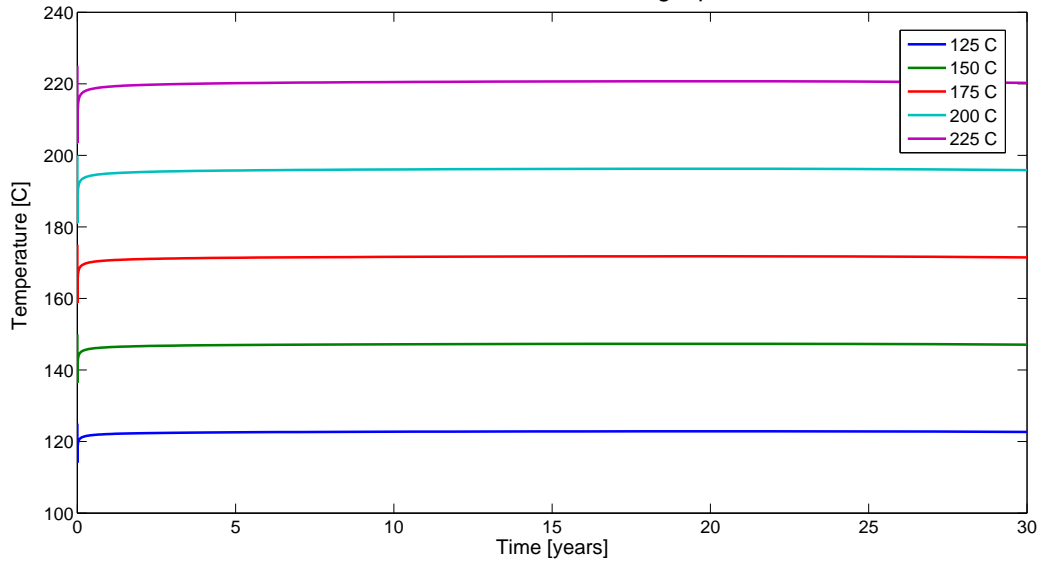**Figure 2.9:** Production temperature as a function of time and thermal conductivity of the rock matrix

Figure 2.10: Production temperature as a function of time and initial temperature of the rock matrix
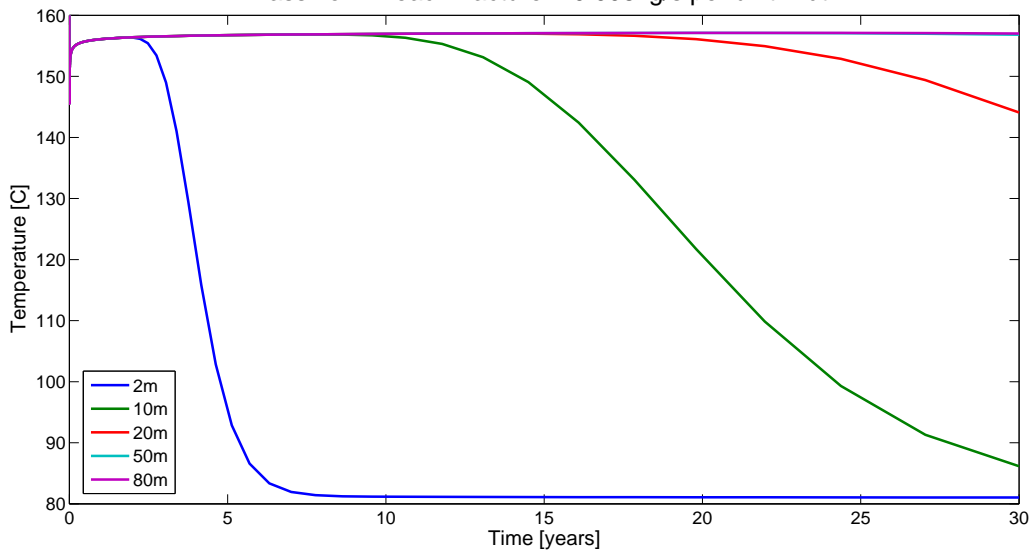

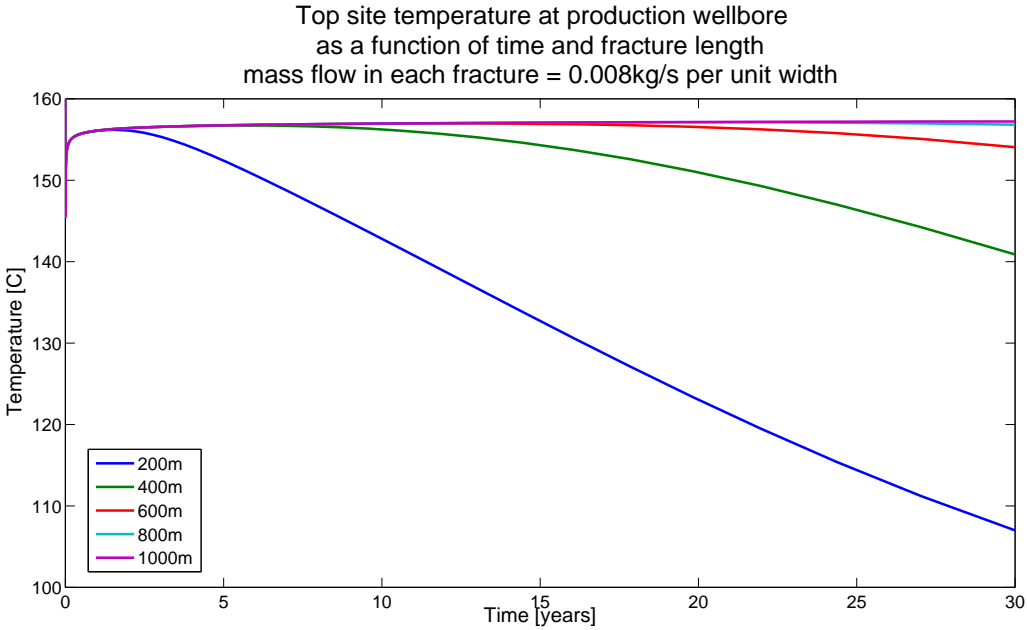**Figure 2.11:** Production temperature as a function of time and fracture spacing

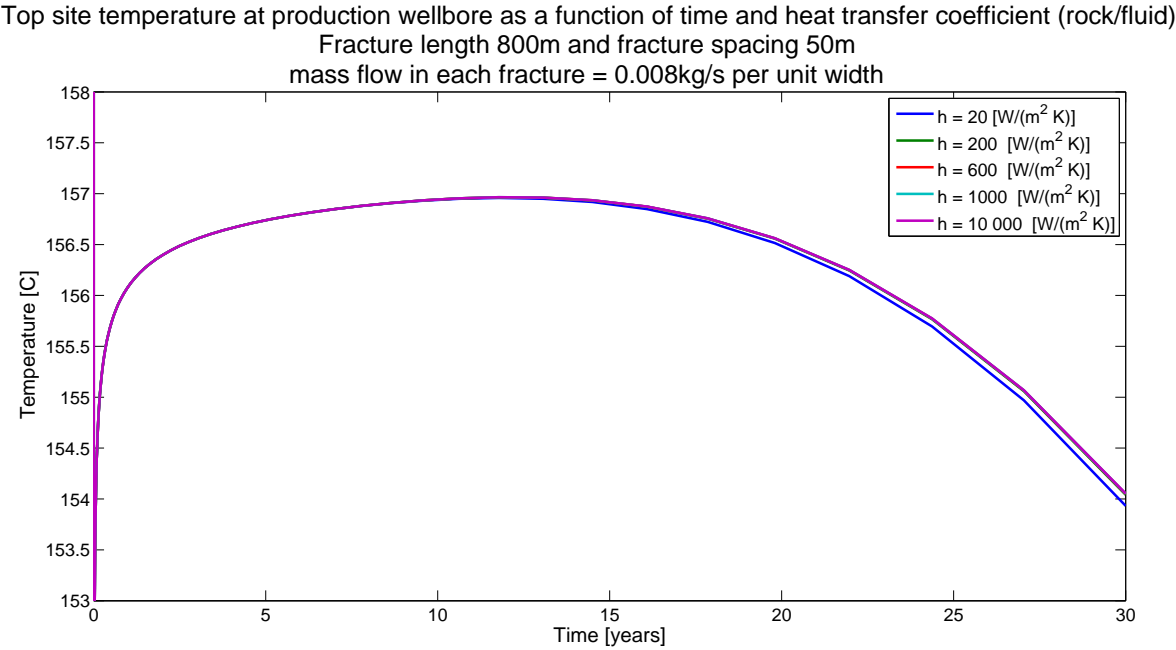**Figure 2.12:** Production temperature as a function of time and fracture length

Figure 2.13: Effect of variation in heat transfer coefficient

2.2.3 Effect of changing operating conditions

How different operating conditions, such as mass flow and inlet temperature, effect the production temperature is investigated in following section.

The top site temperature and extracted heat as a function of time and inlet temperature is shown in figure 2.14. The effect of a low inlet temperature is further investigated in figure 2.15, where the temperature profile is shown for both the circulation fluid and rock matrix after 30 years of production. The top site production temperature for different mass flows and initial rock matrix temperatures is shown in figure 2.7. Figure 2.17 shows the temperature development at end of the fracture. The effect of the heat transfer in the wellbore can be seen by comparing the figure 2.16(b) and 2.17.

The fracture outlet temperature as function of mass flow and fracture spacing after 30 years is shown in figure 2.18.
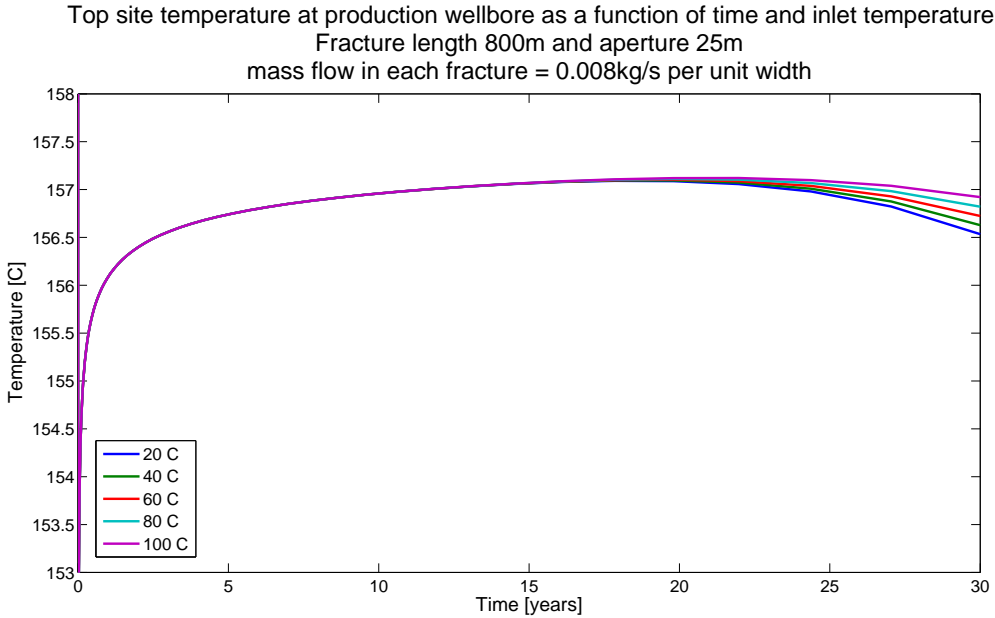
(a) Production temperature as a function of time and inlet temperature of the circulation fluid
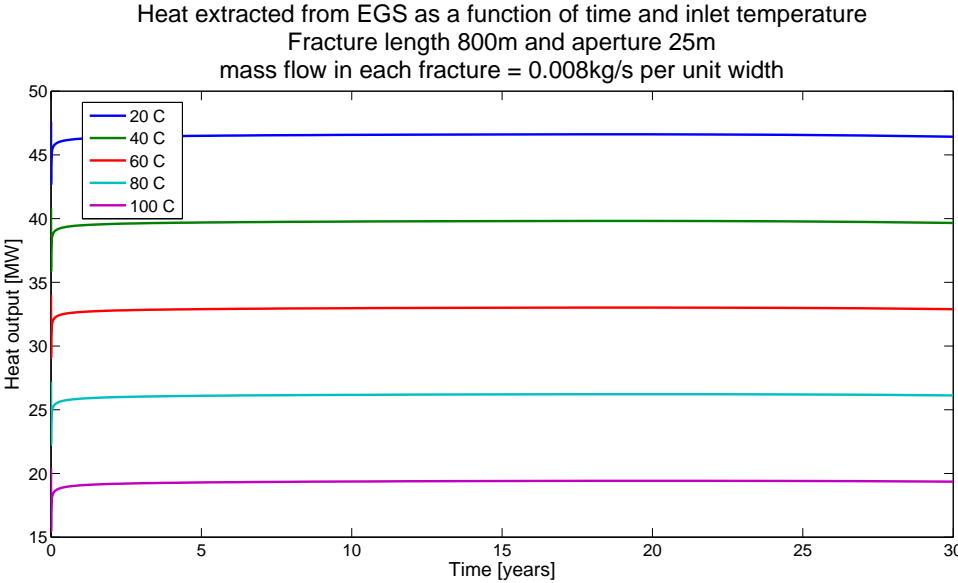
(b) Extracted heat as a function of time and inlet temperature of the circulation fluid

Figure 2.14: Production temperature and extracted heat as a function of time and inlet temperature of the circulation fluid
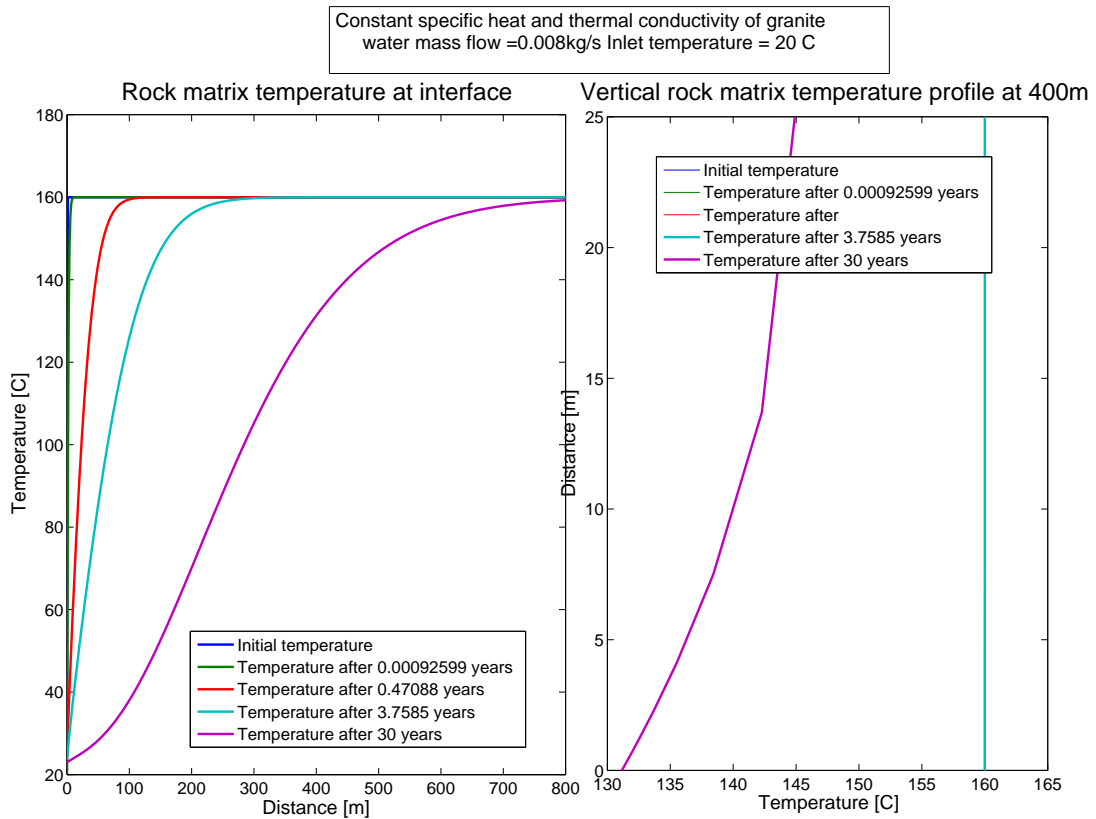
(a) Circulation fluid temperature profile through the fracture and vertical rock matrix temperature
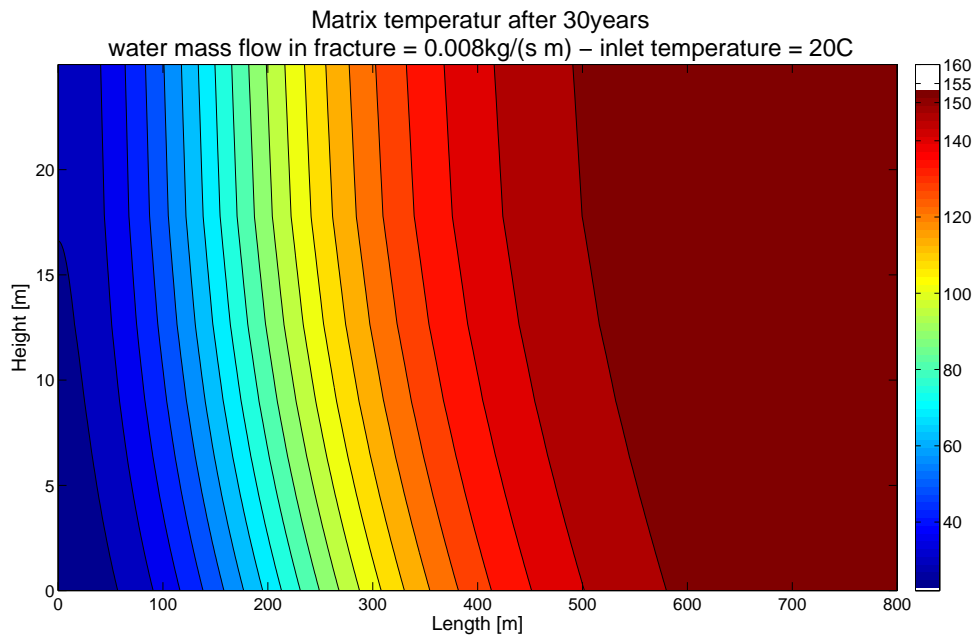
(b) Matrix temperature distribution after 30 years with a fracture inlet temperature of 20^0C

Figure 2.15: Circulation fluid temperature profile and matrix temperature distribution with fracture inlet temperature of 20^0C
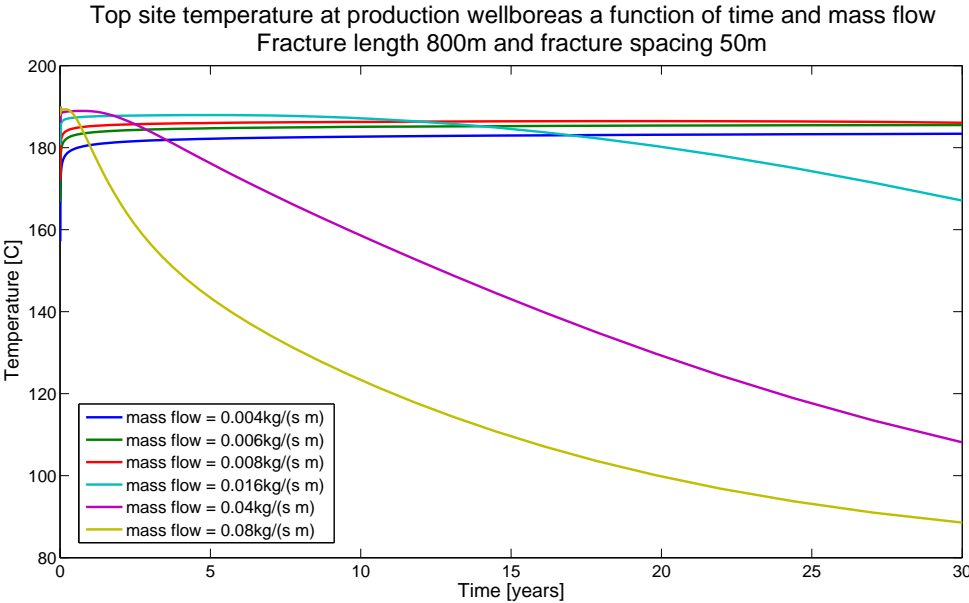
(a) Initial rock matrix temperature 190 ^0C
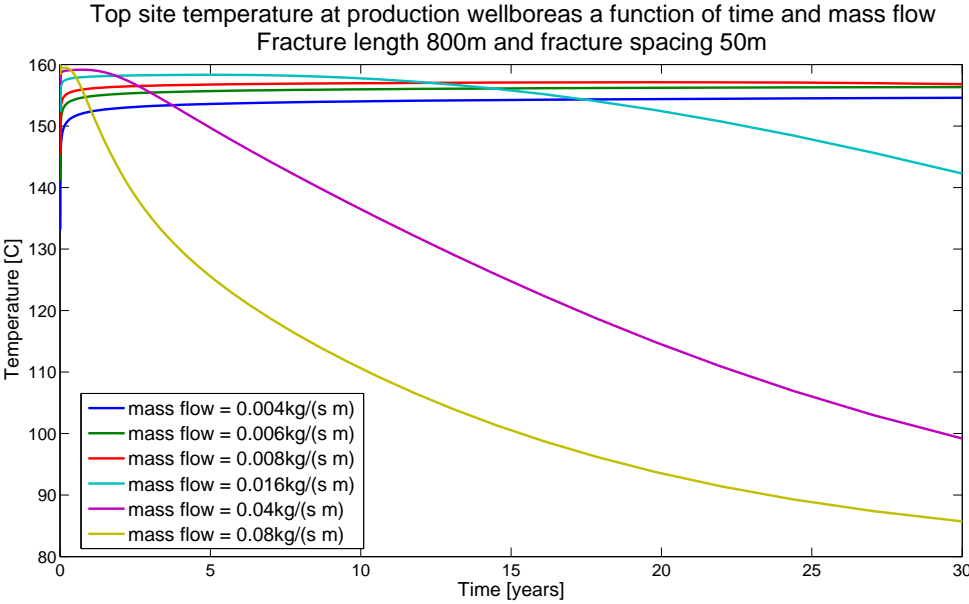
(b) Initial rock matrix temperature 160 ^0C

Figure 2.16: Production temperature as a function of time and mass flow through each fracture
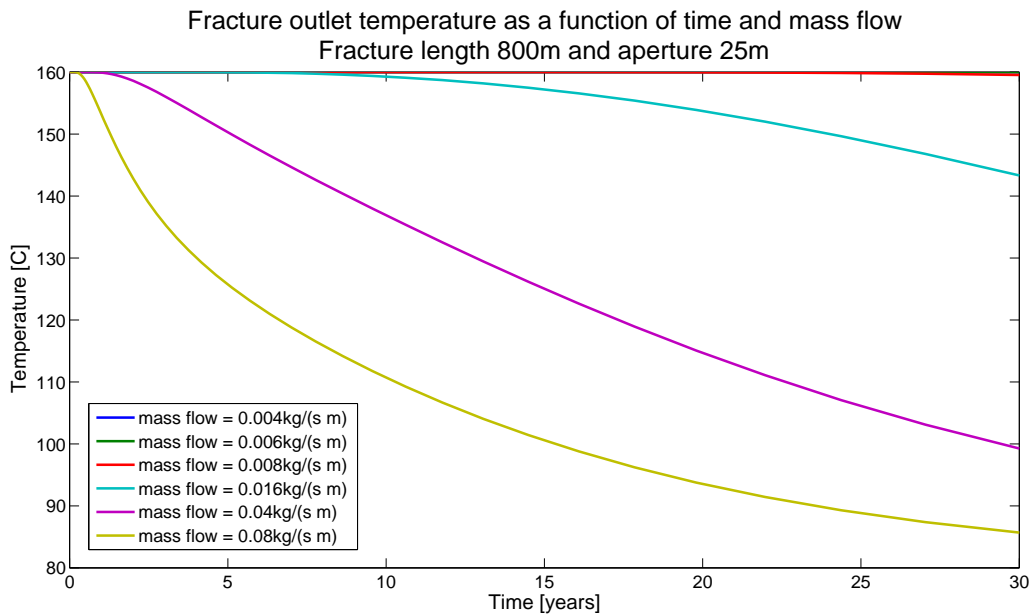
Figure 2.17: Fracture outlet temperature using the same conditions as in figure 2.16(b)
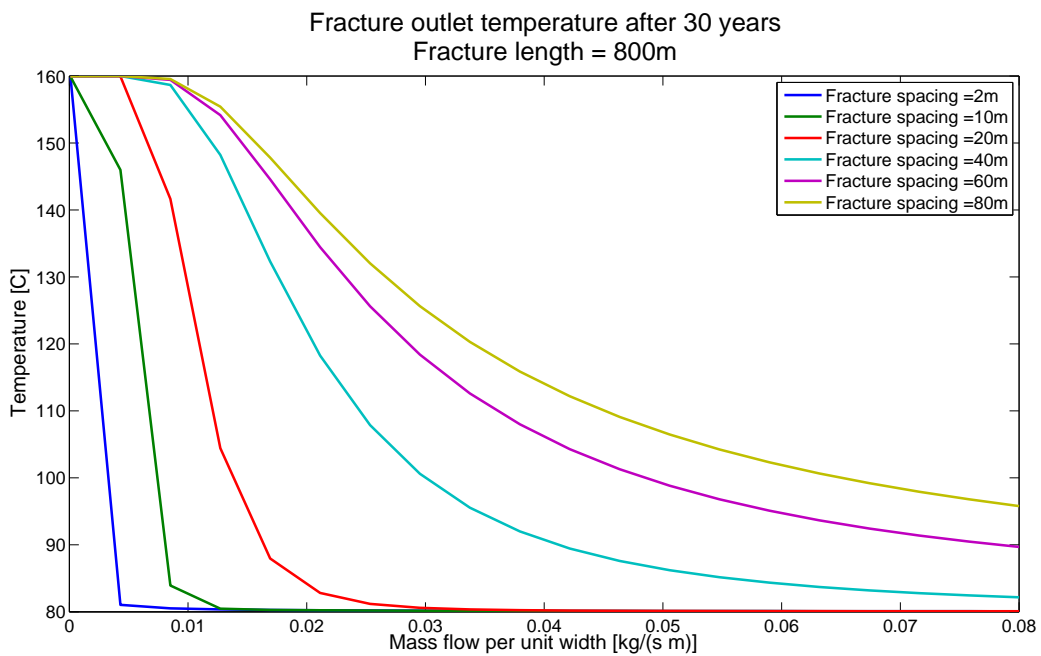
Figure 2.18: Fracture outlet temperature as function of mass flow and fracture spacing

2.2.4 Effect of fracture short circuiting

In order to investigate the effect of a fracture short circuiting on the performance of a EGS was a pressure drop modeled that estimates the mass flow distribution between different fracture apertures developed. The pressure drop model is based on the honors thesis of Cibich [8] and presented in detail in Appendix A.

The pressure drop model assumes a laminar incompressible flow and incorporates the inertia effects due to radial acceleration near the wellbore. The fracture is assumed to be horizontal and of constant surface roughness and fracture aperture. The model is based on a analytical solution of flow between flat plates ("cubic law")and adjusted for non-ideal flow conditions (e.g. surface roughness) using a friction factor developed by Louis (1969)

$$f_l = 1 + 3.1 \left(\frac{\epsilon}{h_f} \right)^{1.5} \tag{2.1}$$

where ϵ is the fracture roughness and h is the fracture aperture. The ratio ϵ/h have been set to a arbitrary value of 0.5 in the pressure drop calculations in this section.

The relationship between mass flow, pressure drop, fracture length and fracture aperture is shown in figure 2.19 and figure 2.20.

The effective permeability as a function of ϵ/h and fracture aperture is shown in figure A.10 and the Reynolds number for different mass flows are shown in figure A.9, both figures are found in Appendix A.

Figure 2.19: Pressure drop as a function of mass flow per unit width

Figure 2.20: Pressure drop as a function of fracture length

Investigation of short circuiting

The effect of different combinations of fracture apertures on the bulk fracture outlet temperature is shown in the following section.

The pressure drop across the fractures is assumed to be equal for all fracture apertures in the same reservoir. The mass flow is calculated from the pressure drop equation

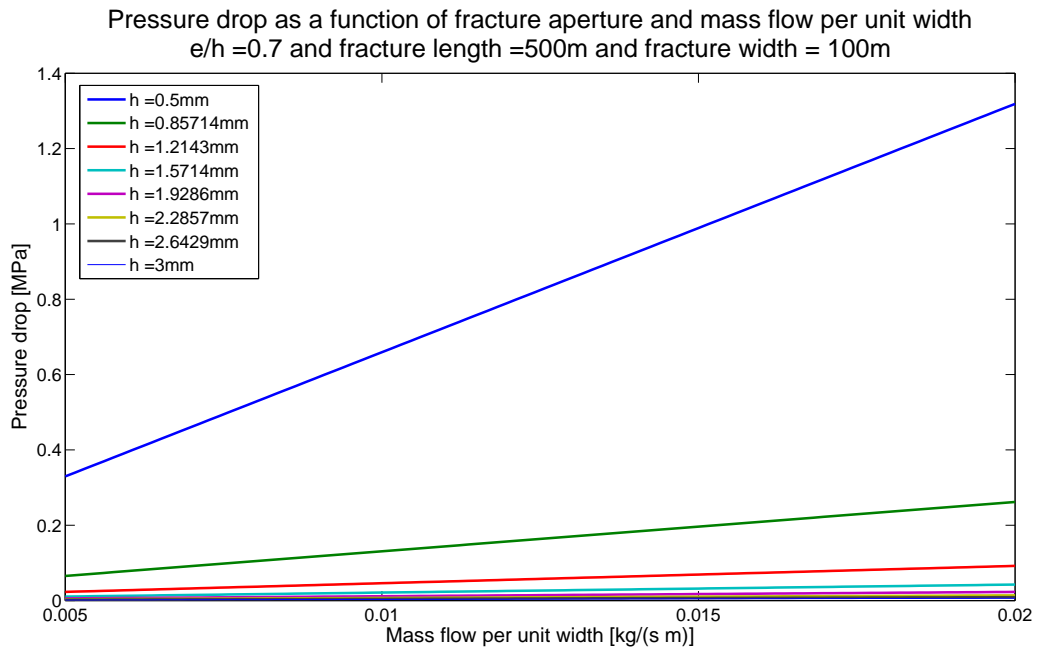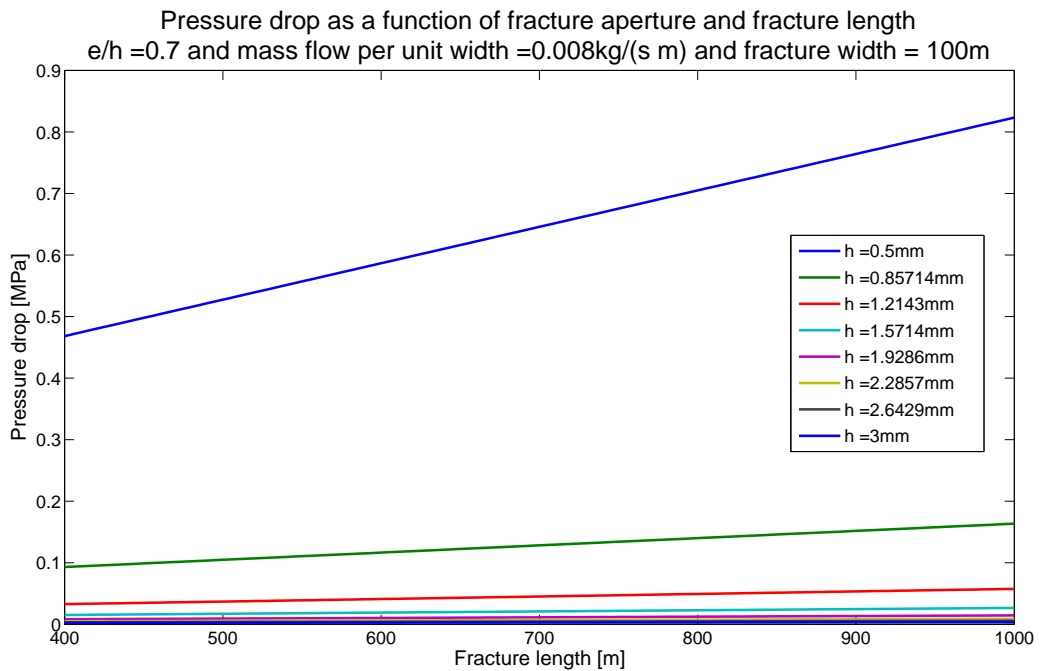$$\Delta P_{total} = \frac{\mu q 12 f_l}{h_f^2} \left[\frac{2 ln \left(r_e / r_w \right)}{\theta} + \frac{2\delta L + L}{w} \right] \tag{2.2}$$

$$\dot{m}_{total} = \rho q = \rho \frac{\Delta P_{total} h_f^3}{12 \mu f_l} \left[\frac{2 ln \left(r_e / r_w \right)}{\theta} + \frac{2\delta L + L}{w} \right]^{-1} \tag{2.3}$$

The heat transfer model developed in matlab uses the mass flow per unit width as input, the mass flow was therefore divided by the fracture width

$$\dot{m}_{width} = \frac{\dot{m}_{total}}{wX} \tag{2.4}$$

where $\dot{m}_{width}$ is mass flow per unit width, w is fracture width and X is number of well pairs.

The heat transfer calculation is therefore based on an average mass flow per unit width.

Short circuit mass flow distribution

For a fracture system that experiences a short circuit is the total mass flow assumed to be constant and equal to that of a reservoir with uniform fracture aperture with a given pressure drop, which can be found using equation 2.3. It is assumed that one of the fractures in the reservoir experiences a increase in fracture aperture (e.g. due to mineral dissolution or shear stress), thus will the total number of fractures in the reservoir be constant ($n_{total} = n_{frac1} + n_{frac2}$). Where n_{frac1} is the number of fractures with the original fracture aperture and n_{frac2} is the number of fractures that have experienced an increase in fracture aperture.

Since the pressure drop model only calculates the mass flow in one fracture is the total mass flow given by

$$\left(n_{frac1} + n_{frac2} \right) \dot{m}_{total} = n_{frac1} \dot{m}_{frac1} + n_{frac2} \dot{m}_{frac2} \tag{2.5}$$

where n_{frac1} is the number of fractures with aperture 1 and n_{frac2} is the number of

fractures with aperture 2. $\dot{m}_{total}$ is the total mass flow calculated from a reservoir with uniform fracture aperture of size aperture 1 and a given pressure drop. The new pressure drop can be calculated by substituting equation 2.3 into equation 2.5 and solving for the new pressure drop

$$\Delta P_{new} = \frac{(n_{frac1} + n_{frac2}) \dot{m}_{total}}{n_{frac1}\dot{B}_{frac1} + n_{frac2}\dot{B}_{frac2}} \tag{2.6}$$

where (δL is the pseudo length, defined in Appendix A)

$$\dot{B}_{frac1} = \frac{h_{f1}^3}{12\mu f_l} \left[\frac{2ln\,(r_e/r_w)}{\theta} + \frac{2\delta L + L}{w} \right]^{-1} \tag{2.7}$$

$$\dot{B}_{frac2} = \frac{h_{f2}^3}{12\mu f_l} \left[\frac{2ln\,(r_e/r_w)}{\theta} + \frac{2\delta L + L}{w} \right]^{-1} \tag{2.8}$$

$$\tag{2.9}$$

Once the new pressure drop across the reservoir is found can the mass flow per unit width in each fracture be calculated from equation 2.3 and the bulk temperature at the bottom of the production well found from (assuming constant Cp value)

$$Q_{total} = Q_{frac1} + Q_{frac2} \tag{2.10}$$

$$T_{bulk} = \frac{n_{frac1}\dot{m}_{frac1}T_{frac1} + n_{frac2}\dot{m}_{frac2}T_{frac2}}{(n_{frac1} + n_{frac2}) \dot{m}_{total}} \tag{2.11}$$

Plots

The effect of different combinations fracture apertures, pressure drop and ratio between "original" fractures and short circuit fractures are presented in the following graphs.

In figure 2.22 to 2.21 is the temperature profile for a reservoir with uniform fracture aperture shown, with different pressure drop and fracture aperture. The mass flow for a specific pressure drop and fracture aperture can be seen in figure 2.19 and figure 2.20. In figure 2.23 to figure 2.28 are the effect of different short circuit scenarios on the bulk temperature presented.

It is assumed that the total mass flow is constant when a short circuit develops, and not the pressure drop. The mass flow will be distributed between the different fracture apertures based on the pressure drop calculation, which is based on the assumption that the cubic law is applicable. The fracture aperture will therefore have a tremendous effect
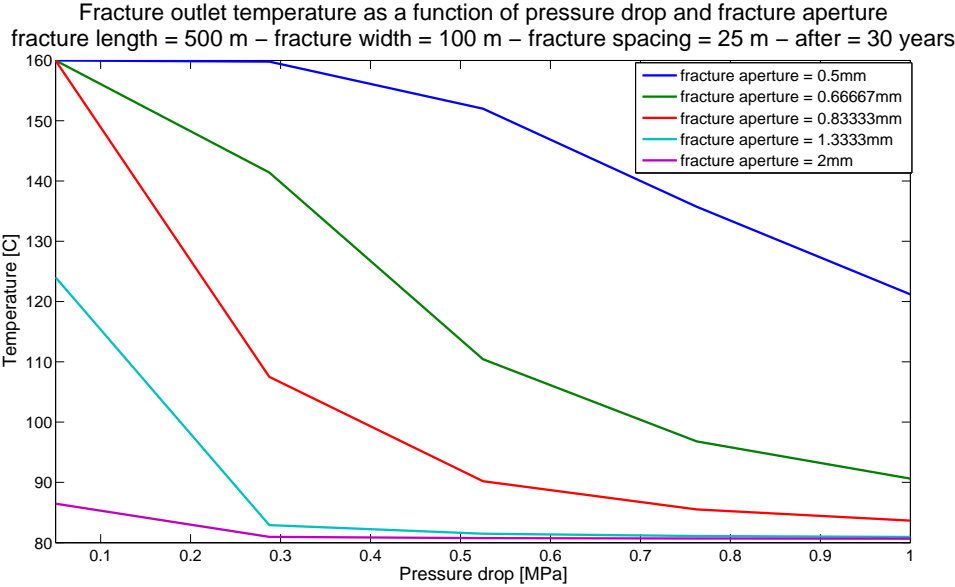
Figure 2.21: Fracture outlet temperature as function of pressure drop and fracture aperture after 30 years of production

on the mass flow in the fracture. The reservoir will also experience a pressure drop, since the flow resistance have decreased due to the short circuit. The effect on the mass flow distribution, temperature profile and pressure drop is shown in figure 2.23 to figure 2.26, where a short circuit fracture (one out of eleven fractures) with aperture of 3mm develops in reservoir with uniform aperture of 0.8mm and a pressure drop of 0.1MPa.

Figure 2.23 shows the temperature profile for a reservoir with uniform fracture aperture (0.8mm) and for the same reservoir if one out of eleven fractures is short circuit fracture with a aperture of 3mm. The mass flow in the original fracture aperture will decrease (assumed that total mass flow is constant) which causes the temperature profile to increase.

From figure 2.24 can we see that the short circuit fracture has a major impact on the bulk temperature. The bulk temperature follows the temperature profile of the short circuit. Which is logical since the mass flow in the short circuit fracture is several factors larger than the mass flow in each original fracture aperture (0.8mm), the mass flow distribution is shown in figure 2.25.

Figure 2.26 shows the normalized temperature profile. Which is the bulk temperature profile (shown in figure 2.24) divided by the original temperature profile (shown in figure 2.23).

In figure 2.27 is the normalized temperature profile shown for several different short circuit fracture apertures.
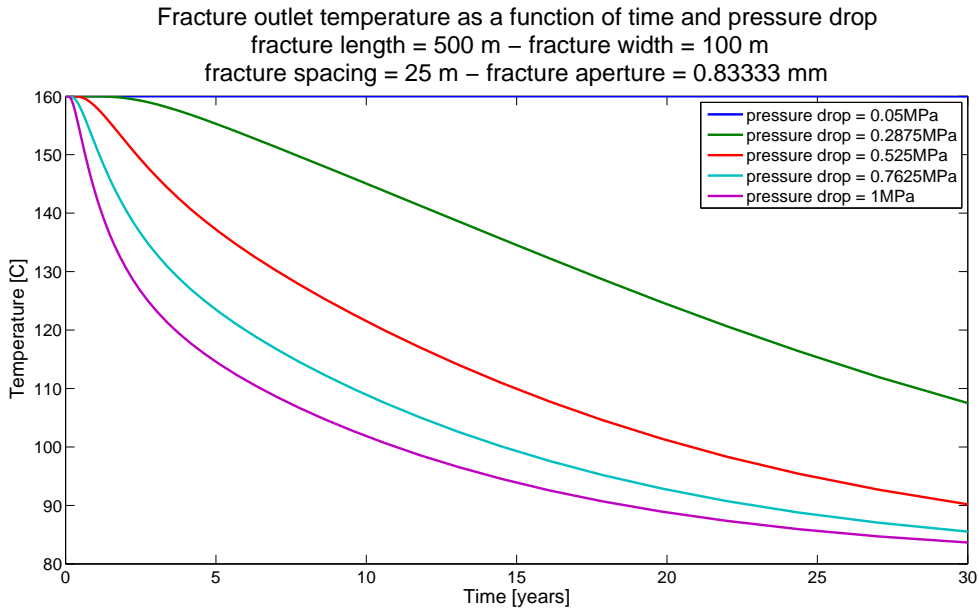
(a) Fracture outlet temperature as a function of pressure drop and time
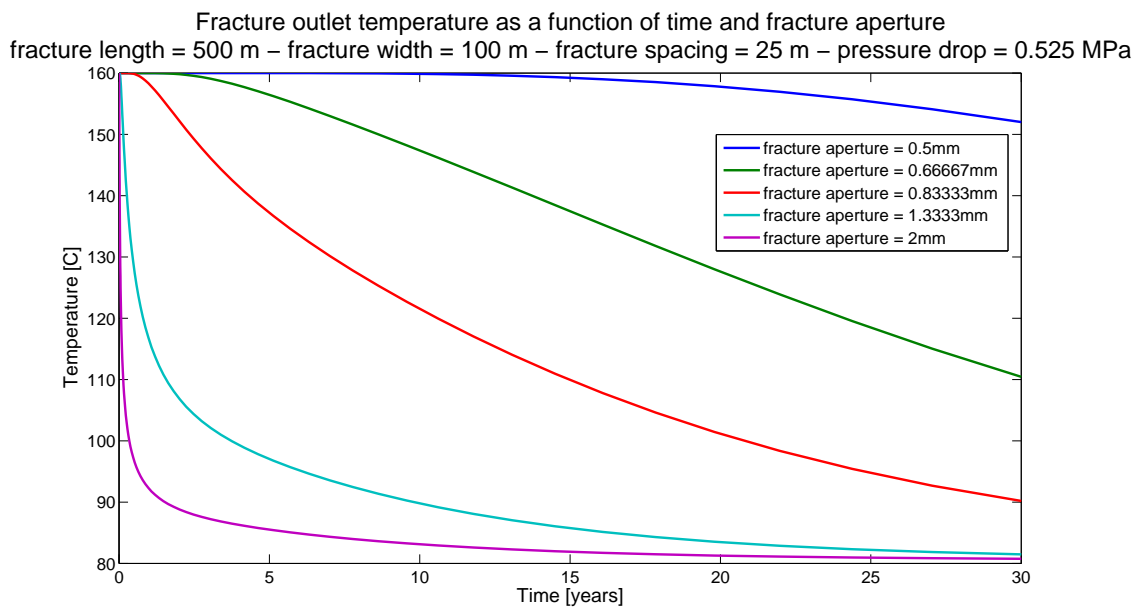
(b) Fracture outlet temperature as a function of fracture aperture and time

Figure 2.22: Fracture outlet temperature for uniform EGS with uniform fracture aperture. Mass flow calculated with pressure drop model
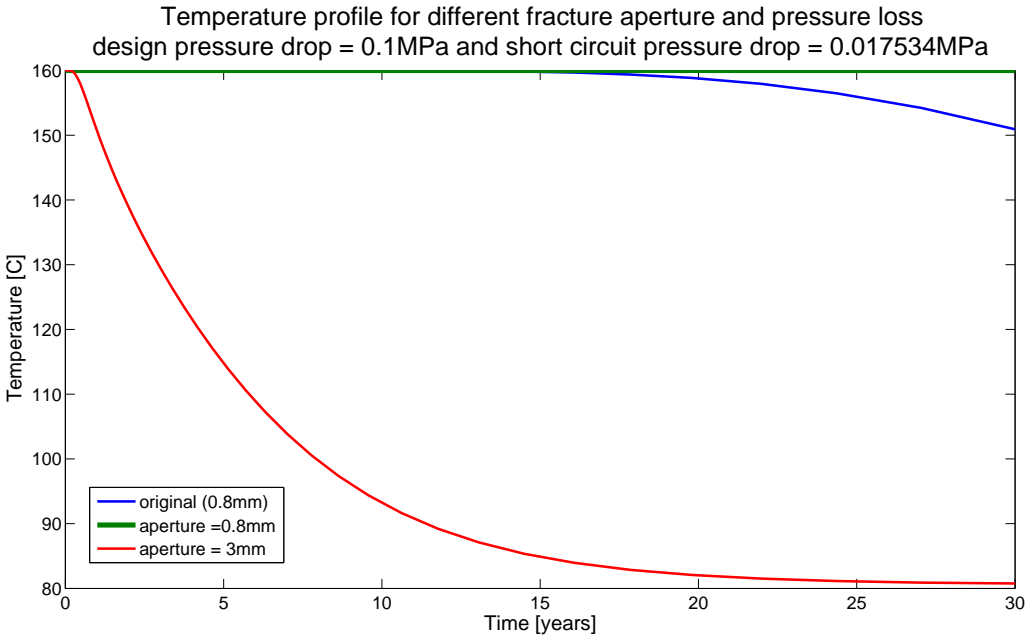
Figure 2.23: Temperature profile for a uniform fracture aperture of 0.8mm compared to the temperature profile in each fracture if a short circuit develops
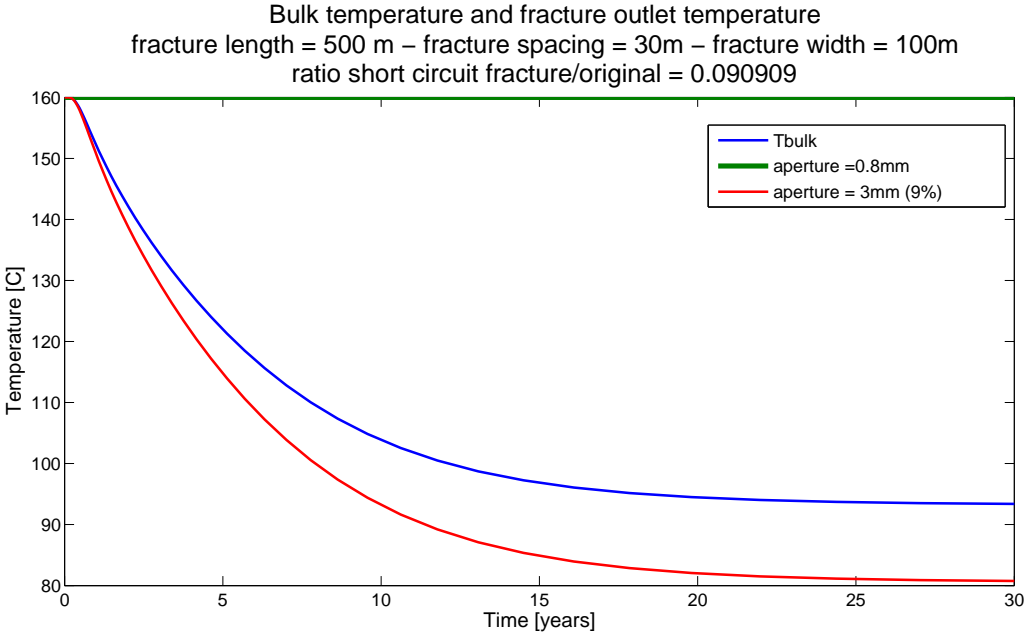
Figure 2.24: Bulk temperature at the bottom of the production well with a short circuit.
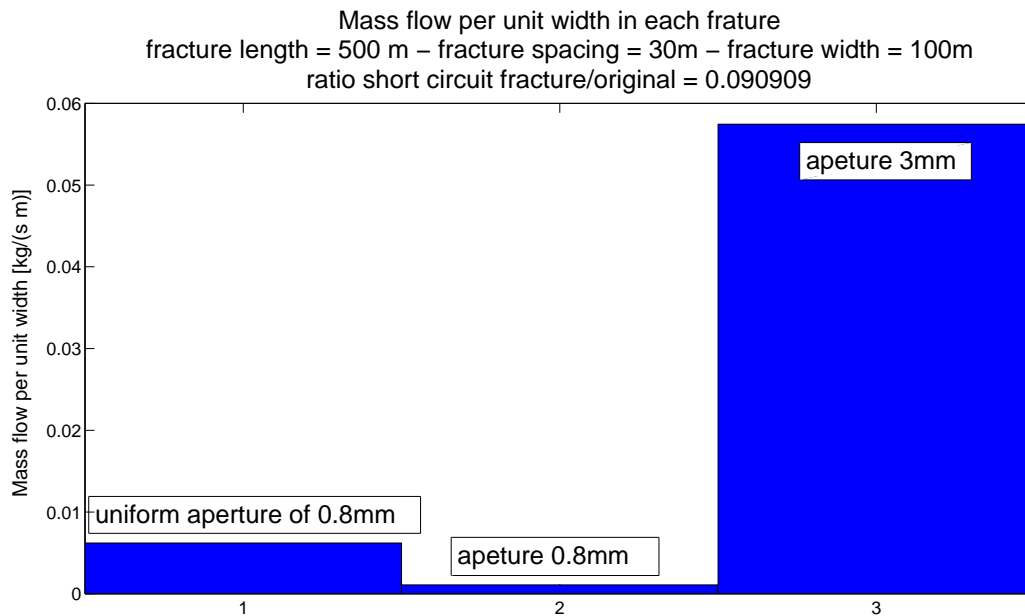
Figure 2.25: Mass flow distribution per unit width in each fracture for a uniform reservoir and if a short circuit develops
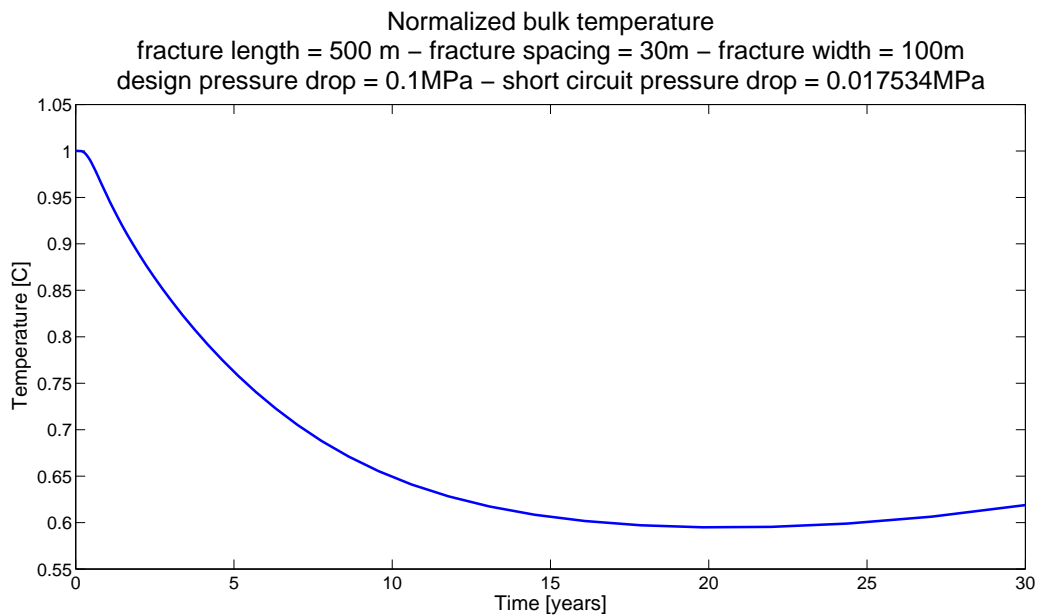
Figure 2.26: Normalized temperature profile. Temperature profile of short circuit reservoir divided by the temperature profile of a reservoir with uniform fracture aperture
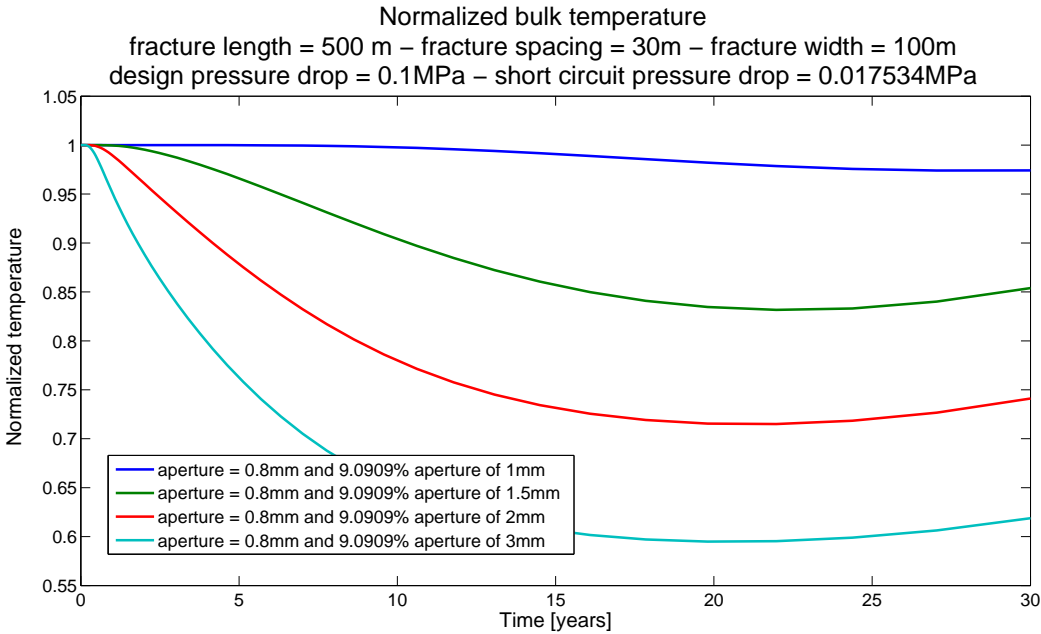
Figure 2.27: Normalized temperature profile for several different combinations of short circuit aperture
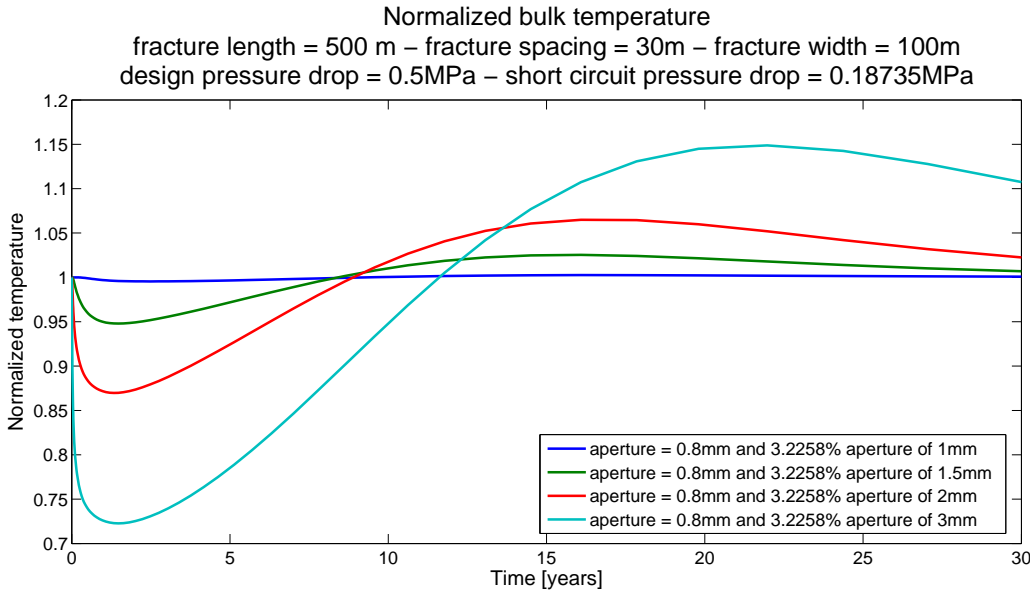
Figure 2.28: Normalized temperature profile with same operating conditions as figure 2.27, the difference being ratio between original fractures and short circuit fractures and a larger pressure drop

2.3 Discussion

The discussion is divided into subsections after which parameters that are studied, following the same organization as previously used in this part.

Effect of changing reservoir parameters

An increase in specific heat of the rock increases the time before a thermal breakthrough occurs. This can be seen in figure 2.8. An increase in specific heat will increase the amount of energy that can be extracted from the rock for the same temperature difference, this is evident from equation 2.12.

$$Q_{rock} = m_{rock}Cp_{rock}\Delta T = V_{rock}\rho_{rock}Cp_{rock}\Delta T \tag{2.12}$$

The same effect is observed for a increase in thermal conductivity of the rock. An increase in thermal conductivity decreases the thermal resistance in the rock, which improves the heat transfer. The result is that more heat can be extracted from the rock before a thermal breakthrough occurs, the vertical (y-direction) temperature difference in the rock decrease as the thermal conductivity increases.

Both of these results are logical and expected. Based on comparison between figure 2.8 and figure 2.9 does a change in specific heat have a bigger impact on the production temperature than the same percentage increase in thermal conductivity, due to earlier thermal breakthrough. A increase by a factor of two on the specific heat and thermal conductivity caused about a 2 and 1 degree Celsius change in the production temperature, which is negligible. However, the effect would increase for a decrease in rock matrix mass and a increase in mass flow since relative more heat would be extracted from the reservoir causing the thermal front to advance faster.

If the initial rock temperature increases will the production temperature increase by the same amount, if no thermal breakthrough has occurred. This can be seen in figure 2.10. The reason is straight forward, the temperature of the circulation fluid approaches the rock matrix temperature and will reach the rock matrix temperature as long as the fracture is long enough.

The time before a thermal breakthrough occurs increases with fracture spacing. Which also is logical, since a increase in fracture spacing increases the amount of energy stored in the rock matrix, and more heat can therefore be extracted. The amount of stored energy increases linearly with a increase in matrix volume/fracture spacing. The effect is shown

in figure 2.11. The same argument is also correct for a increase in fracture length, this can be seen in figure 2.12.

Due to the uncertainties related to the heat transfer coefficient, as discussed previously. Was the effect of the heat transfer coefficient on the production temperature investigated. With the flow rate and rock matrix parameters used is the effect small. From figure 2.13 is a temperature difference of 0.3^0C found for a heat transfer coefficient of 10 and 10 000. A increase in the heat transfer coefficient will decrease the heat transfer resistance between the rock and fluid, thus will the fluid temperature approach the rock matrix temperature as the heat transfer coefficient increases. This means that the fluid temperature profile as a function of fracture length will change as with a change in heat transfer coefficient. However, as long as no thermal breakthrough occurs will a change in heat transfer coefficient not affect the production temperature. A decrease in heat transfer coefficient will decrease the time before a thermal breakthrough occurs. The reason is that a increase in thermal resistance will cause a larger temperature difference between the rock surface and the average fluid temperature, causing the production temperature to drop faster for a smaller heat transfer coefficient. Another aspect is that most of the heat transfer resistance is in the rock matrix, due to a low thermal conductivity. Which means that the heat transfer resistance, heat transfer coefficient, is not important on the total heat transfer since the heat transfer is limited by the thermal conductivity of the rock (this can be seen from equation 2.13). This however, is not true at early times since the thermal front advances as if no rock is present [32]. Therefore will the heat transfer coefficient act as a bottle neck on the heat transfer at early times while it can be neglected at medium to long times [32].

A simplified expression of the heat transfer resistance.

$$R = \frac{1}{hA} + \frac{H}{k_r A} \tag{2.13}$$

where R = heat transfer resistance, h = heat transfer coefficient, k_r is the thermal conductivity of the rock, A is the surface area between rock and fluid (assumed constant cross sectional area in the rock matrix) and H is the hight of the rock matrix.

Effect of changing operating conditions

How different operating conditions effects a fractured EGS is discussed in this subsection.

Figure 2.14 shows how different inlet temperatures effect the outlet temperature. From the figure is it evident that a lower inlet temperature increases the amount of extracted heat

while the production temperature is fairly constant. As long as the production temperature reaches the initial rock temperature, which depends on fracture length, height, mass flow and operating time, is it clear from equation 2.14 that a lower inlet temperature increases the extracted heat. A higher mass flow would have caused the thermal breakthrough to happen earlier and the difference in production temperature would have been larger.

$$Q_{fluid} = \dot{m}_{fluid} Cp_{fluid} \Delta T \qquad (2.14)$$

By decreasing the inlet temperature is more heat extracted from the reservoir, and the point of thermal breakthrough is only slightly effected by decrease in inlet temperature. Based on figure 2.14 should the circulation fluid be cooled down as much as possible in the top site cycle. This would increase the extracted heat from the system while only decreasing the time before thermal breakthrough by a small amount. The reason is that the heat transfer in the rock matrix is mostly vertical [27], mostly due to a larger temperature difference in vertical direction (y-direction) than in horizontal direction (x-direction). When the inlet temperature decreases will the temperature difference increase and more heat will be extracted from the rock, however due to the near vertical heat transfer in the rock matrix will the effect in horizontal direction be small compared to the effect in vertical direction. This can be seen by comparing figure 2.15(b) and figure 2.29, which shows the rock matrix temperature after 30 years for a inlet temperature of 20^0C and 80^0C respectively.

A decrease in inlet temperature will cause the temperature to drop faster after the thermal breakthrough have taken place, which is logical since more heat is extracted. However, the thermal breakthrough occurs at almost the same time regardless of inlet temperature, see figure 2.14. The optimal inlet temperature depends on the top site utilization. Low inlet temperature means that more heat is extracted at a higher production temperature. A high inlet temperature would results in a longer lifetime, however the production temperature will decrease before the same amount of energy is extracted as for system with a low inlet temperature. Based on this argument should a EGS power plant cool the circulation fluid to as much as possible before injection, since this would give the largest amount of extracted energy at the highest temperature (which is critical for the efficiency of the power cycle). The relationship between production temperature and extracted heat can be seen in figure 2.30.

The amount of extracted heat in a given time periode is governed by the thermal diffusivity of the material (eq. 2.15. The larger the thermal diffusivity the faster the propegation of heat in the medium. Typical values for the thermal diffusivity of granite
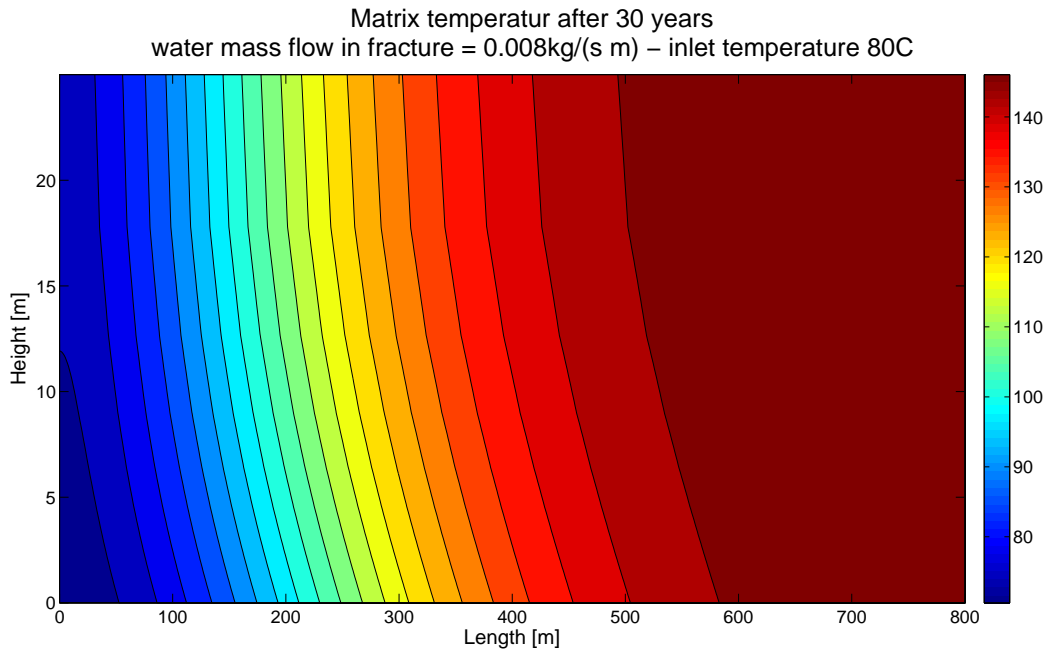
Figure 2.29: Matrix temperature after 30 years with flow rate of 0.008 kg/(s m) and inlet temperature of 80^0C

is 1.3E-6 m^2/s, in comparison is the thermal diffusivity of copper 113E-6 m^2/s and wood 0.13E-6 m^2/s. The thermal diffusivity of granite is therefore relatively low and the heat flow from the granitic rock is therefore relatively small.

$$\alpha = \frac{k}{Cp\rho} \tag{2.15}$$

Figure 2.16 shows the production temperature for different mass flows and two different initial rock matrix temperatures. The effect of a increase in initial rock matrix temperature is a higher production temperature, which corresponds to the increase in initial rock matrix temperature. The shape of the production temperature profile stays the same regardless of initial rock matrix temperature. The effect of the heat transfer in the wellbore is evident from figure 2.16. The heat transfer in the wellbore will have almost no effect on a large mass flow, since a large amount of energy is needed in order to change the bulk temperature. The opposite is true for a small mass flow. The effect can be seen by comparing figure 2.16 and figure 2.17, the larger mass flows are not cooled by the geothermal gradient while the smaller mass flows are cooled. After some time is the wellbore heated up and the cooling effect decreases, resulting in a small temperature increase in the production temperature as long as the a thermal breakthrough has not occurred. It is evident that the decrease
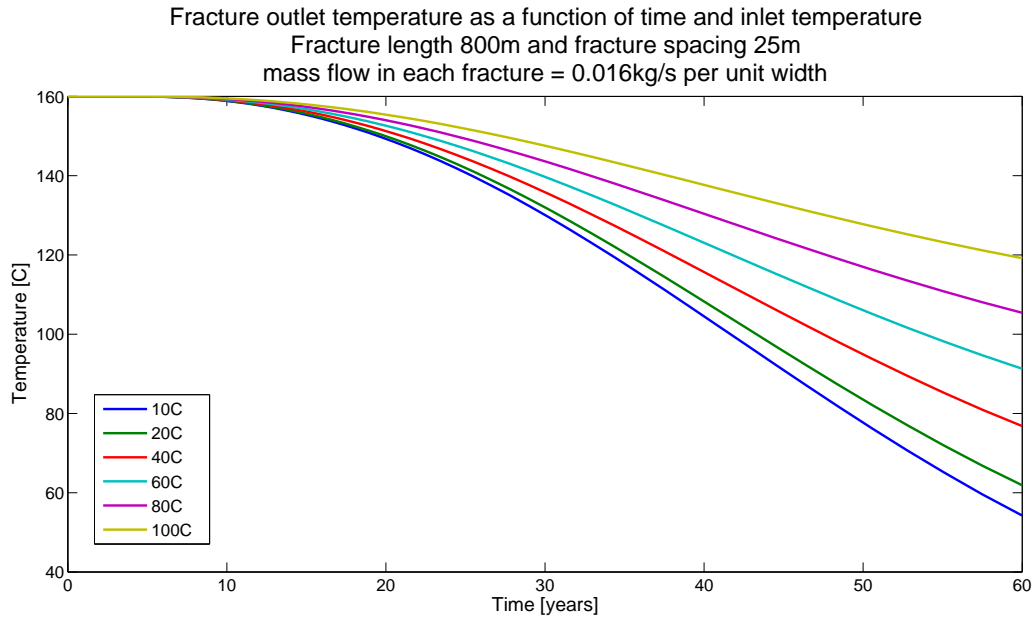
(a) Effect of short circuiting on fracture outlet temperature for a pressure drop of 1MPa
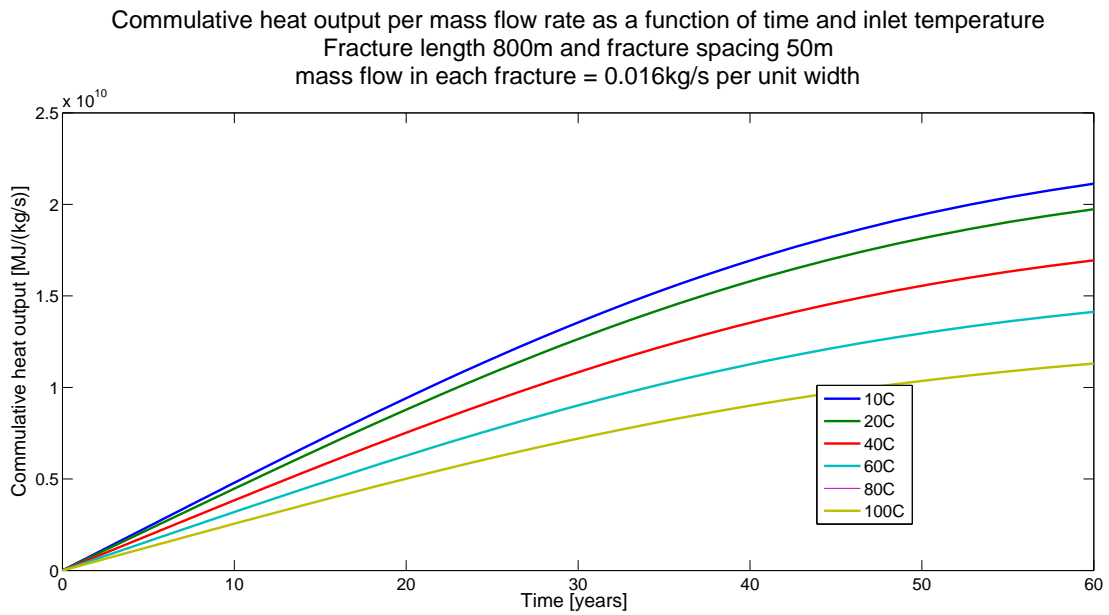
(b) Effect of short circuiting on fracture outlet temperature for a pressure drop of 0.1MPa

Figure 2.30: Extracted heat (per kg/s) and production temperature over time for different inlet temperatures

in temperature for the three largest mass flows is due to a thermal breakthrough in the reservoir.

Figure 2.18 shows the production temperature after 30 years for different mass flows and fracture spacing. There are no surprises in the figure, the production temperature increases with an increase in fracture spacing and a decrease in mass flow rate.

Short circuiting

If short circuit with a aperture of 3mm develops in a fractured EGS with uniform fracture aperture of 0.8mm and a original pressure drop of 0.1MPa is a decrease in production temperature of 40% observed if the short fracture constitute about 9% of the fractures (see figure 2.27). The reason for the large decrease in production temperature is that large difference in mass flow in the respective fractures (see figure 2.25). The mass flow is calculated using the "cubic law" and the mass flow in a fracture is related to the fracture aperture cubed, thus will a difference in fracture aperture have a substantial effect on the mass flow distribution.

The decrease in production temperature due to a short circuit increases with the size of the fracture aperture, which is logical since a larger fracture aperture transports more of the total fluid mass flow. This is seen in figure 2.27. Due to the large difference in mass flow distribution between fractures with different fracture aperture is production temperature governed by the temperature profile in the short circuit even if the short circuit only constitute a small portion of the total number of fractures. If the number of short circuits only constitute 9% of the total number of fractures is the production temperature governed by the temperature in the short circuit (see figure 2.24).

The increase in the normalized temperature profile after about 20 years that can be seen in figure 2.27 is related to the thermal breakdown of the reservoir without a short circuit. The production temperature of the short circuit reservoir stabilizes at a given temperature when the outlet temperature reaches the inlet temperature and the outlet temperature of the original fracture aperture fractures is at the initial rock temperature. This can be seen in figure 2.24, where the bulk temperature stabilizes after about 20 years. If one compares figure 2.23 and 2.24 can we see that the thermal breakdown of the fractures with a aperture of 0.8mm happens earlier in the reservoir with uniform fracture aperture (the 0.8mm aperture fractures in the short circuit reservoir does not experience a thermal breakdown at all in the time period shown). The reason is that the mass flow in the uniform fracture aperture reservoir is larger than for the same fractures in the short circuit

reservoir. The mass flow distribution can be seen in figure 2.25. The decrease in mass flow in the same fracture aperture is a result of a decrease in pressure drop due to the development of the short circuit.

The effect of mass flow distribution on the production temperature is taken to a extreme in figure 2.28. The pressure drop is increased so that the uniform reservoir experiences a thermal breakdown fairly early in the time period. The effect seen in figure 2.27 is therefore increased. The development of the production temperature of the uniform reservoir and the short circuit reservoir can be seen in figure 2.31. The development in the first 5 years corresponds to the development in the time period (30 years) shown in figure 2.27. The reason for the increase in normalized temperature can be seen when comparing the bulk temperature profile and the original temperature profile shown in figure 2.31. The short circuit causes the production temperature to stabilize at a low temperature (due to the thermal breakdown of the short circuit) while the original temperature profile decreases constant once it has reached thermal breakdown. This causes the normalized temperature profile to first drop below 1 and then increase above 1 once the bulk temperature stabilizes and the original temperature profile decreases. When the thermal breakdown of the 0.8mm fractures in the short circuit reservoir becomes significant does the normalized temperature profile start to approach 1 (since both temperature profiles approaches the inlet temperature).
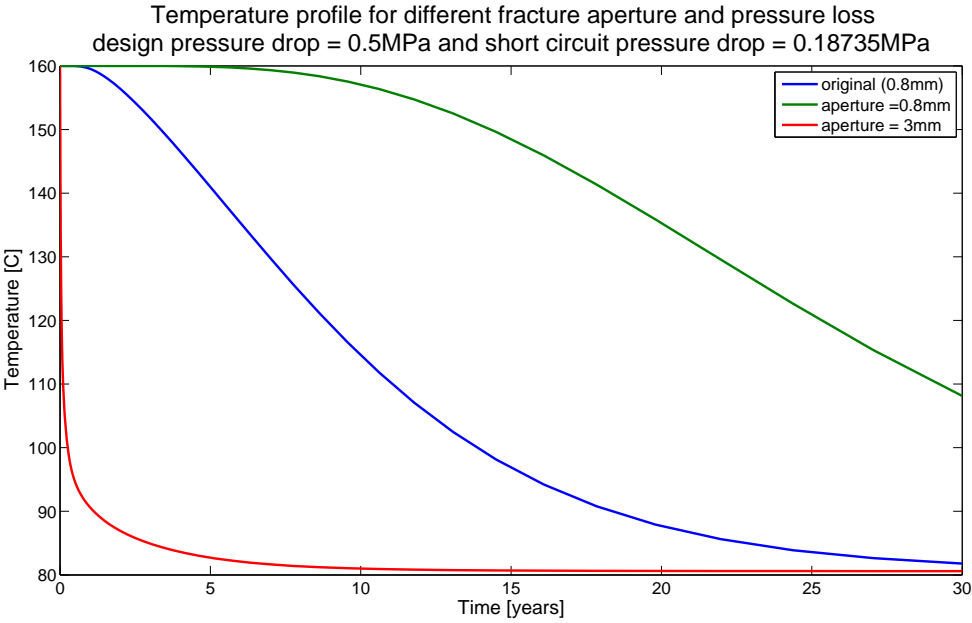
(a) Temperature profile for uniform fracture aperture and temperature profile for each fracture aperture if a short circuit is present
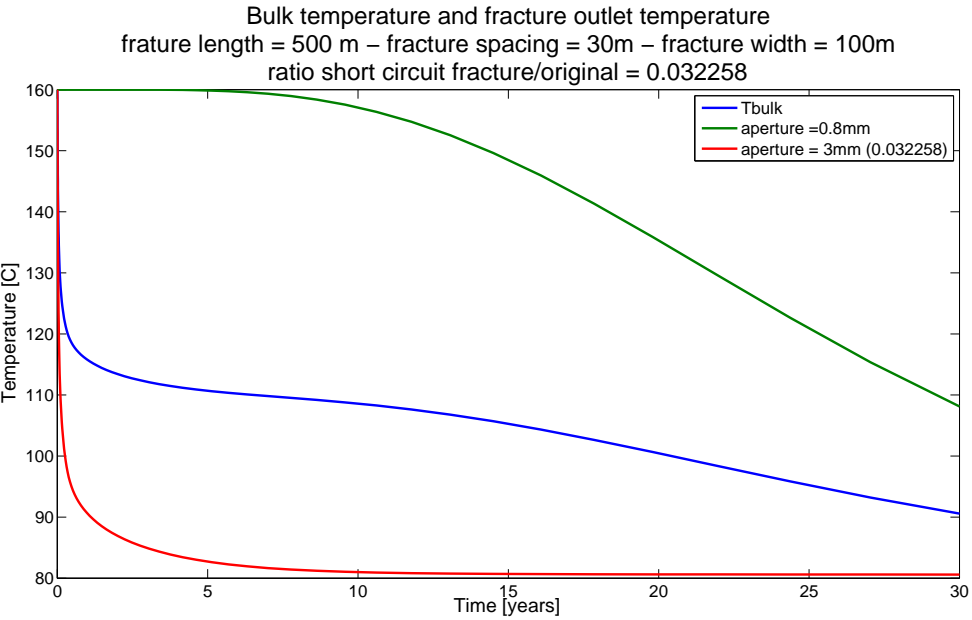
(b) Bulk temperature at bottom of production well and temperature profile for each fracture aperture

Figure 2.31: Temperature profiles for EGS with parameters given in figure 2.28

Additional uncertainties

Due to the assumptions used when developing the fractured EGS model should the specific values from the simulation be used with care. The implications of the assumptions have been discussed before, both in section 2.1 and Appendix A. However, a few aspects have not been discussed.

- The estimated pressure drop is very low compared to values found in the literature of operating EGS sites. The reason is believed to be that the friction factor is based on groundwater joints with small apertures and it underpredicts the friction factor in fractures with large apertures. However, the effect should be the same on all fractures presented in this thesis, the mass flow distribution should therefore not be influenced by the exact value of the pressure drop. The pressure drop values estimated in this thesis should be treated with extreme care since they probably underpredicts the pressure drop by several factors. However, the pressure drop value is not used directly in this thesis and the error could therefore be disregarded.

- The thermal behavior of a EGS with short circuiting have been found by superpositioning the solution for the respective fracture apertures. This is not entirely correct since the short circuit will communicate with the surrounding fractures, which will affect the heat transfer of the surrounding fractures. This effect have not been accounted for in the model, however since the short circuit only constitute a small portion of the total fractured reservoir is the effect believed to be small.

2.4   summary

A numerical model that describes the thermal behavior of a fractured EGS was developed. The model was based on the finite volume method and programmed in Matlab. The fracture network was simplified as horizontal fractures with constant aperture and equally spaced. The pressure drop was estimated using the approach by Cibich [8], and follows the "cubic law". The model was used to investigate how different parameters effect the heat transfer in a fractured geothermal reservoir.

The production temperature and extracted heat were used to measure the effect different parameters. The ratio between circulation fluid mass flow and fractured volume has a large impact on how the system reacts to a change in different parameters. If the system has not experienced a thermal breakthrough is the effect of changing a parameter small, since the outlet temperature is near the initial rock matrix temperature. The general effect should be the same for a system that has experienced a thermal breakthrough, however it is expected that the effect will be larger. Short circuiting was found to have a critical impact on the production temperature. Measures to control the fracture aperture propagation should therefore be taken.

Part 3

System analysis

In this part of the thesis is a complete EGS power plant investigated, combining the geothermal reservoir and the top site cycle. The goal is to identify how a change in reservoir conditions effect the overall thermal performance of the system. For example how a short circuit effect the thermal performance of the top site cycle. A baseline case is designed in order to measure the effect of varying reservoir conditions. The baseline EGS power plant is designed using reasonable parameters regarding a EGS power plant found in the literature. Due to time constraints will the system not be subjected to a optimization process.

3.1   System design (baseline case)

A set of probable system design parameters found in the literature [1, 12] was used as constraints for the EGS power plant. The results from the simulation should therefore yield results that are in the same range as an actual EGS project.

Since it is desirable to look at large/medium scale power production was the power output from the top site cycle set to $5MW_e$. The electrical power output from a EGS can be roughly estimated by the volume of fractured rock [1]. The electrical power output per volume of fractured rock is roughly $26MW_e/km^3$, this relationship holds for a wide variety of injection and production wells and fracture spacing between $3 - 30m$ [1]. Thus is roughly $0.2km^3$ of fractured rock required to produce $5MW_e$. The system was designed for a life time of 20 years and a maximum temperature drop between 10^0C and 15^0C.

	unit	value
Power output	MW	5
Reservoir temperature	C	10 - 15
Maximum temperature drop	C	105
Lifetime	years	20
Well spacing	m	400 - 600
Vertical depth	km	5 - 6
Stimulation zone	m	300 - 1000
Fracture width	m	100 - 200
Fracture spacing	m	3 - 30
Fracture volume	km^3	0.2

Table 3.1: Reasonable system parameters [1, 12, 13]

3.1.1 Fracture system design

The stress regime in the rock matrix will determine the fracture pattern and direction, and this will influence the optimal arrangement of injectors and producers [1]. No data regarding local stress regimes at the desired depth in Norway could be obtained. The well configuration was therefore based on how well the configuration can be simulated using the numerical model developed in this thesis. It was therefore decided to use a five spot system (fig.3.1).

The parameters tabulated in table 3.1 was found by looking at system parameters used in other papers.

It should be noted that the heat transfer close the wellbores is not capture well in the numerical model, since the effect of radial flow on the heat transfer has not been accounted for. The assumptions and simplifications done in the numerical model have been discussed before, in section 2.1 and Appendix A. The model should be able to capture the general thermal behavior, however the exact value from the simulation should be treated with care.
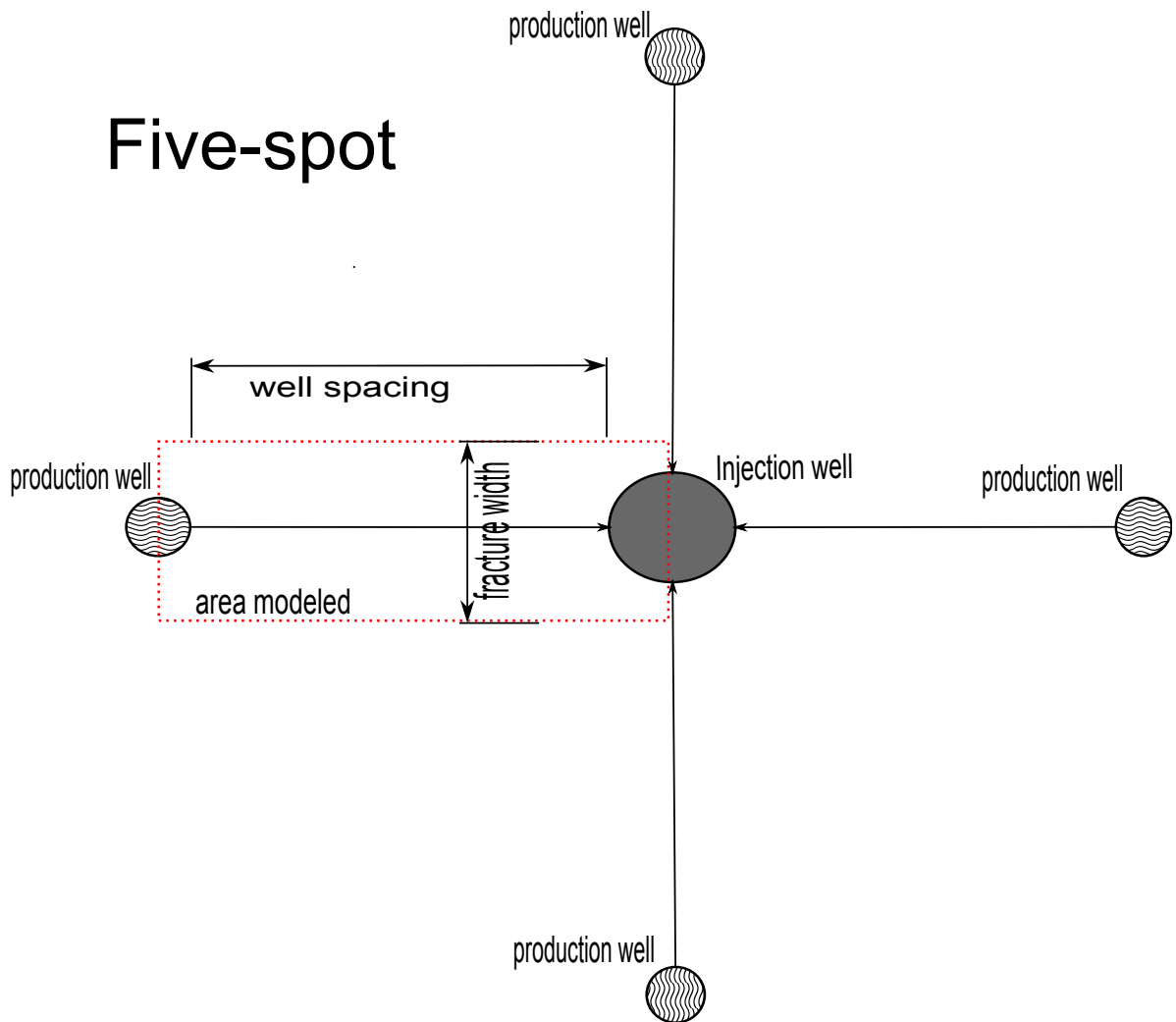
Five-spot

Figure 3.1: Well configuration (five spot)

	Minimum	Maximum
Turbine inlet pressure [bar]	40	80
Pinch Point [C]	5	-
geothermal mass flow rate [kg/s]	70	105
geothermal rejection temperature [C]	40	80
Temperature cooling water [C]	15	15
Turbine isentropic efficiency [54]	80	80
Compressor isentropic efficiency [54]	70	70
Working fluid entering compressor is saturated liquid		

Table 3.2: ORC parameters

## 3.1.2 Top site system design

A supercritical Organic Rankine Cycle that used r134a as working fluid was chosen as top site cycle. The cycle was chosen because the ORC is a relative mature technology and widely used in low to medium temperature geothermal fields. r134a was used since it is a well known working fluid, it has been used in operating ORC's and the difference in thermal efficiency between different working fluids for a optimized solution is small (see figure 1.22) [6].

Auxiliaries, such as a down hole pump and cooled water circulation pump, have not been accounted for in the analysis. The cooling water is assumed to be water at 15^0C. PRO/II have been used as a simulation tool. The geothermal reinjection temperature is allowed to vary as long as the temperature drop in the EGS not exceeds 15^0C for the given mass flow.

The working fluid mass flow, turbine inlet pressure and turbine exit pressure have been optimized with respect to thermal efficiency, given the constraints in table 3.2. The geothermal temperature and mass flow is calculated using the numerical EGS model developed in this thesis given the parameters in table 3.1.

working fluid	critical pressure [kPa]	critical temperature [°C]
r134a	4067	101,10

Table 3.3: Properties of r134a
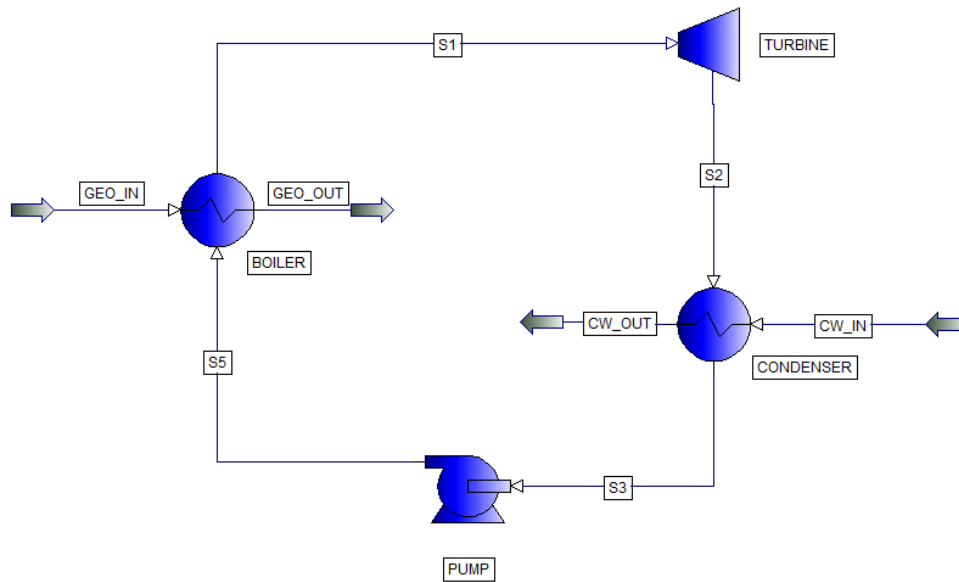
(a) Schematic diagram of a ORC
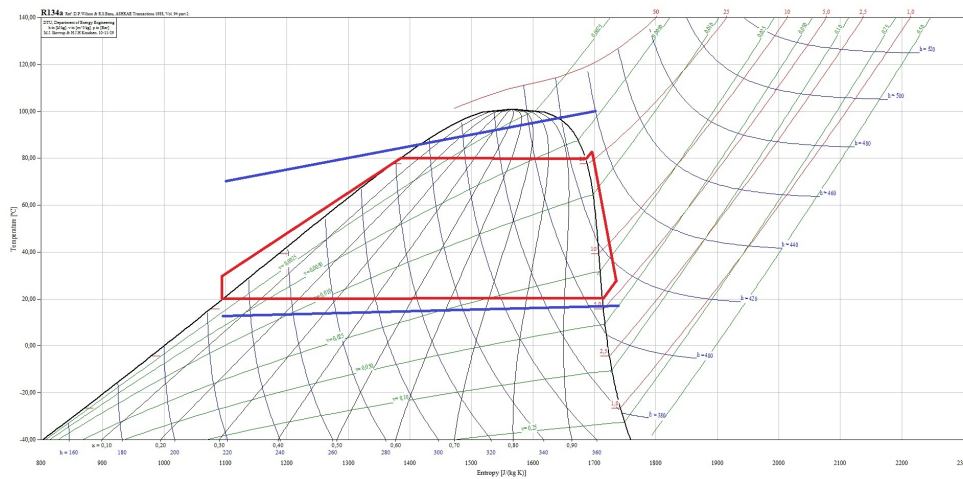
(b) Ts diagram of sub-critical ORC

Figure 3.2: Organic Rankine Cycle

3.1.3   Baseline EGS power plant

The parameters for the baseline EGS power plant was determined using a iterative procedure between the top site model and the geothermal model. The design was restricted by the parameters given in table 3.1 and table 3.2.

Table 3.4 shows the different parameters used in the baseline case.

The geothermal rejection temperature is determined by the temperature profile match in the boiler in the ORC. The pinch point is located between the geothermal inlet temperature and the working fluid exit temperature, it is therefore impossible to cool the geothermal temperature down to cooling water temperature. The optimal geothermal rejection temperature was found to be 62^0C. The UA value of the boiler is large, a higher pinch temperature should probably be used in order to decrease the size of the heat exchanger. However, this is not of concern in this thesis. The temperature profile match in the boiler and condenser can be seen in figure 3.3.
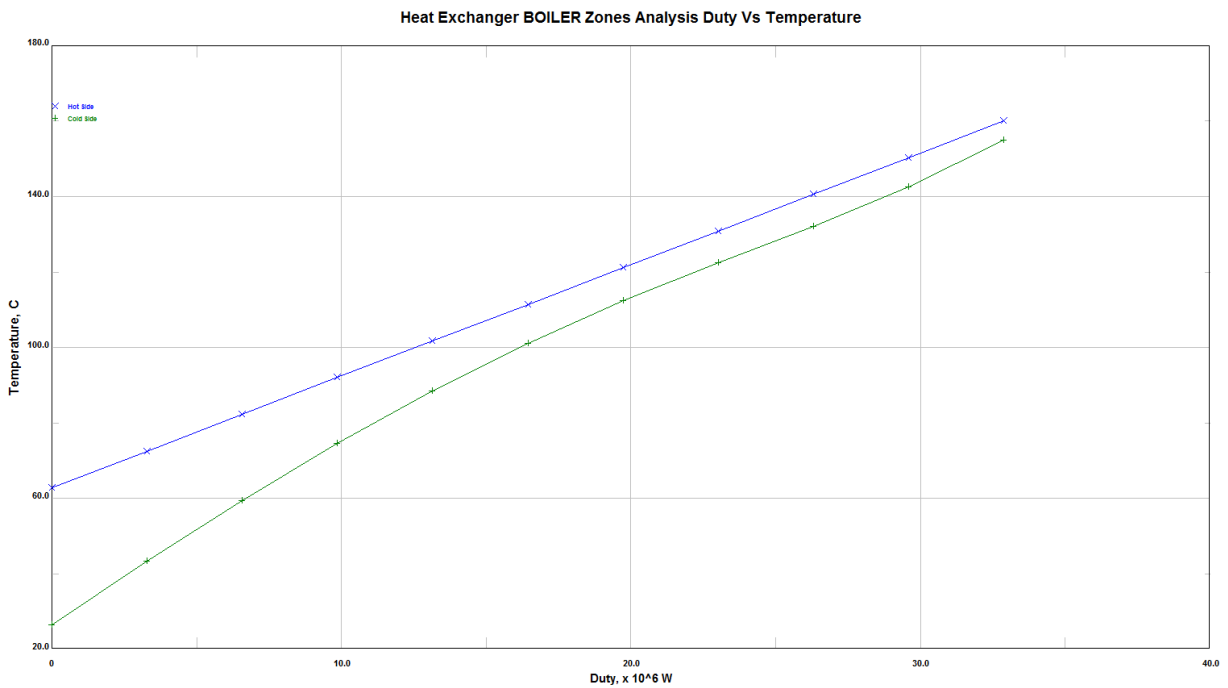
(a) Temperature profile match in boiler
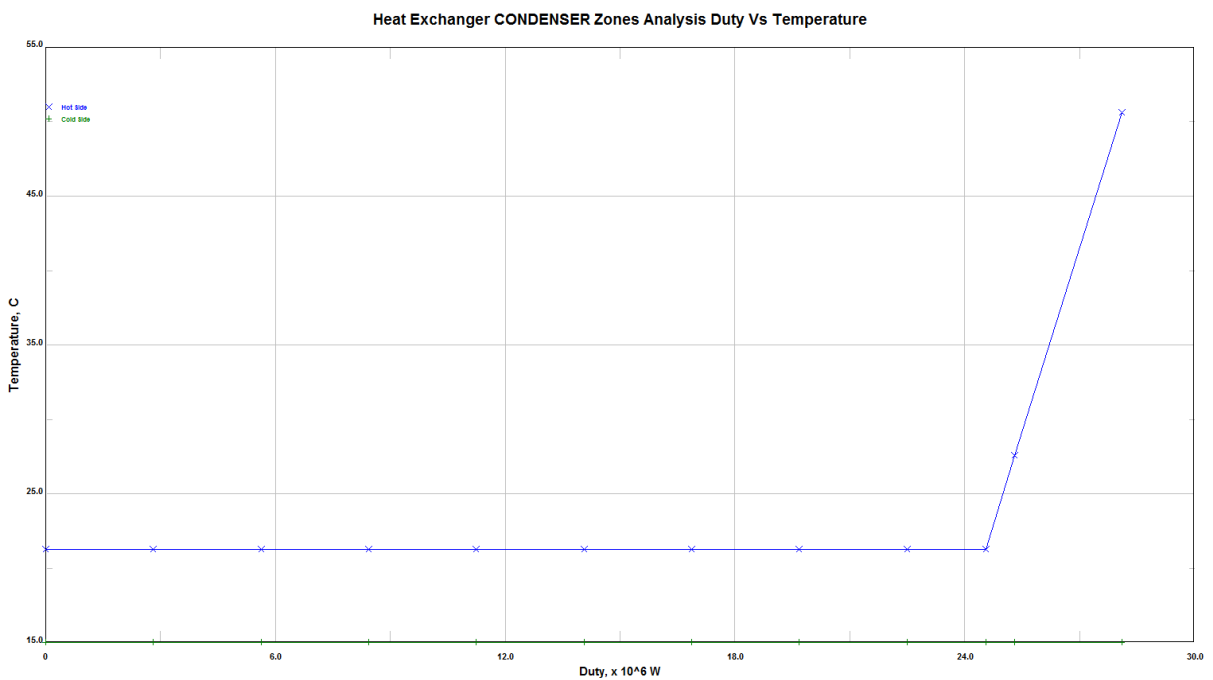
(b) Temperature profile match in condenser

Figure 3.3: Temperature profile match in boiler and condenser (pinch point). Temperature on y-axis (180^0C - 20^0C) and heat duty on x-axis (0MW - 30MW and 40MW)

	unit	value
Geothermal		
Geothermal mass flow	kg/s	81
Geothermal production temperature	C	160
Geothermal rejection temperature	C	62
Fracture aperture	mm	0.8
Fracture pressure drop	MPa	0.25
Fracture width	m	150
Fracture length	m	600
Stimulated zone	m	510
fracture spacing	m	30
number of production wells		4
number of injection wells		1
flow rate per unit width	kg/(s m)	0.0113
Top site		
Thermal efficiency		0.137
Turbine Work	MW	5.4
Pump Work	MW	0.98
Boiler duty	MW	32.2
Boiler UA value	kW/(m^2 K)	20 820 600
Condenser UA value	kW/(m^2 K)	3000
Turbine inlet pressure	MPa	7
Turbine pressure drop	MPa	6.36
r134a mass flow	kg/s	131

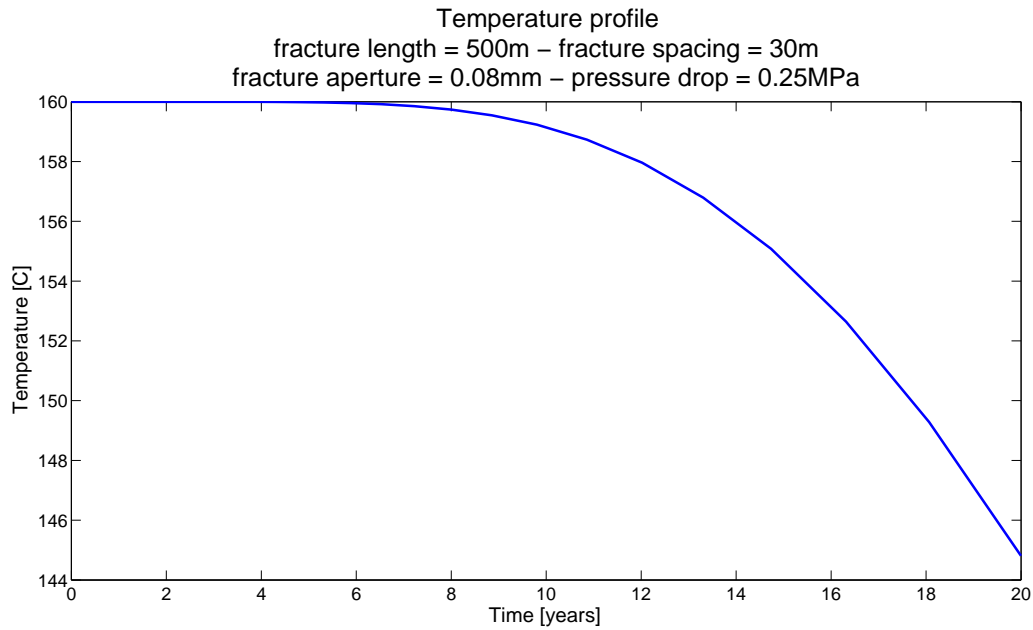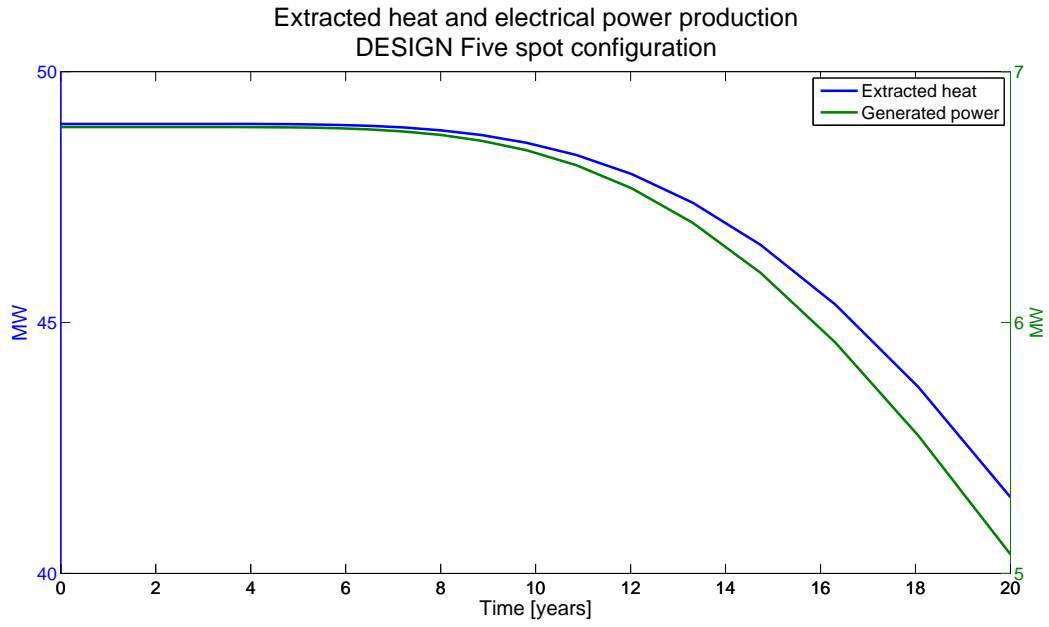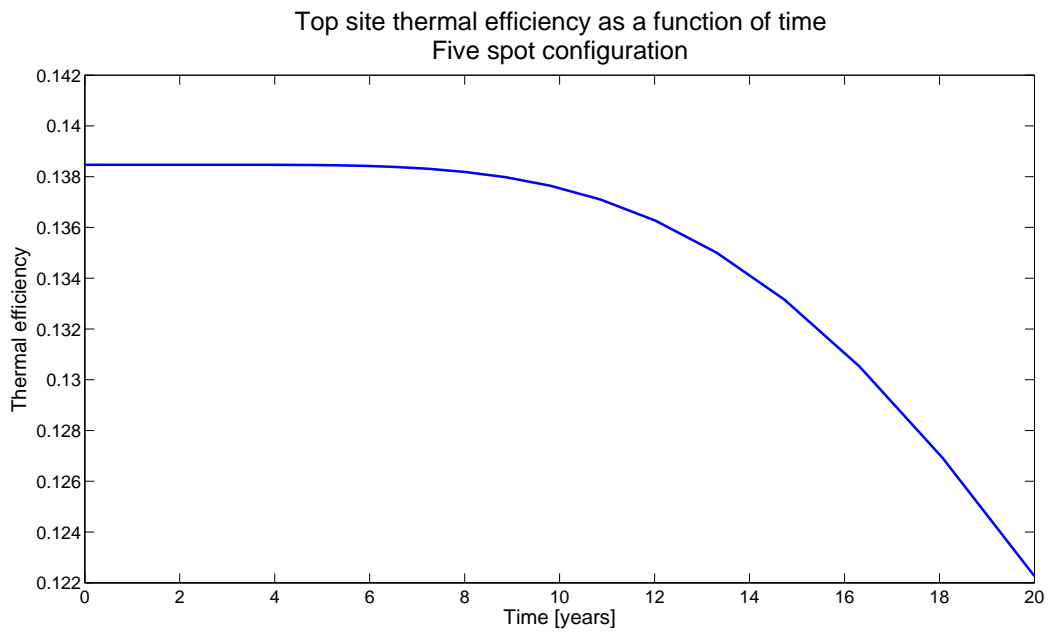**Table 3.4:** Baseline design parameters of ORC

Figure 3.4: Production temperature profile for baseline EGS reservoir

Performance of baseline EGS power plant

The thermal performance of the baseline EGS power plant is shown in figure 3.4 and figure 3.5. The geothermal production temperature profile is shown in figure 3.4 over a time period of 20 years. The amount of extracted heat from the geothermal reservoir is seen in figure 3.5, together with thermal efficiency and net work output from the cycle. The extracted heat is calculated from equation 3.1 using constant properties. This explains the difference in extracted heat between table 3.4 (which is based on PRO/II) and figure 3.5. The calculation process is further discussed in the next subsection, "Calculation procedure".

Extracted heat and electrical power production
DESIGN Five spot configuration

(a) Extracted heat and net power production

Top site thermal efficiency as a function of time
Five spot configuration

(b) Thermal efficiency

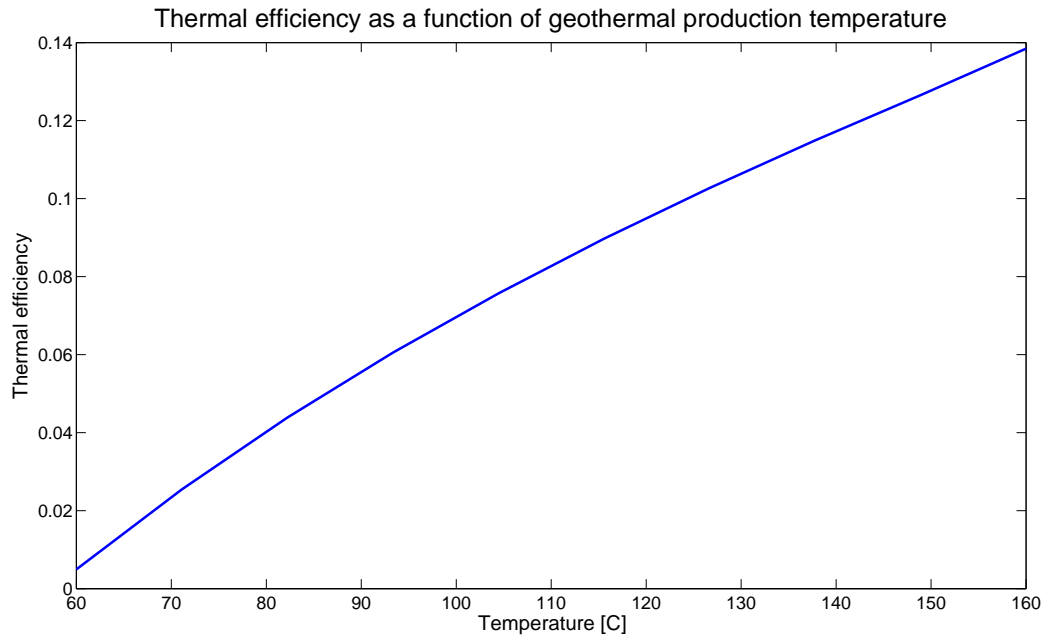**Figure 3.5:** Baseline performance of EGS power plant

Figure 3.6: Thermal efficiency of top site power cycle (ORC) as a function of geothermal production temperature

Calculation procedure

The complete EGS power plant is simulated using two different programs; PRO/II (top site) and matlab (geothermal reservoir). The thermal efficiency of the top site cycle was investigated with respect to changes in the geothermal production temperature. In order to simulate off-design performance of the top site cycle were the governing top site values held constant, such as: the UA values, the working fluid mass flow, cooling water temperature, isentropic efficiency of turbine and pump, pressure drop/rise across turbine/pump and geothermal mass flow, while the geothermal production temperature was varied. The effect on the thermal performance of the top site cycle should therefore be the same as for a real EGS experiencing a change in the geothermal reservoir. The isentropic efficiency of the turbine and pump changes as the cycle is in off-design performance, however no data have been obtained regarding off-design performance of a ORC turbine and pump, it was therefore decided to keep the isentropic efficiency constant. The isentropic efficiency should not change much with variation in the turbine inlet temperature, the isentropic efficiency of a turbine is mostly governed by the pressure drop, mass flow and fluid velocity. A change in inlet temperature could indirectly effect the pressure drop and working fluid mass flow, however since these two quantities are held constant in the off-design analysis should the

assumption of a constant isentropic efficiency be reasonable. The off-design performance could be optimized by controlling the mass flow, that was however not taken into account and the isentropic efficiency of the turbine would decrease with change in mass flow. The assumptions of constant isentropic efficiency and constant mass flow should therefore yield optimistic results.

The effect of a varying geothermal temperature on the thermal efficiency of the top site cycle can be seen in figure 3.6. The thermal efficiency for a discrete number geothermal production temperatures was imported into the matlab model, the thermal efficiency for the top site cycle could then be interpolated for any geothermal production temperature. The amount of extracted heat was found using the temperature values obtained in the numerical matlab model and equation 3.1. The net produced work from the top site cycle was then calculated using equation 3.2, where η_{th} was found by interpolation using the table imported from PRO/II.

$$Q_{extracted} = \dot{m}_{geo}Cp_{geo}\Delta T \qquad (3.1)$$

$$W_{net} = \eta_{th}Q_{extracted} \qquad (3.2)$$

Since the simulation is done using two separate models are a few simplifications introduced. For example does the geothermal rejection temperature decrease as the geothermal production temperature decreases, this is not accounted for since the matlab model uses a constant inlet temperature. The bedrock would therefore experience a more rapid cooling than estimated.

3.2 Parameter study

The effect of varying different geothermal reservoir parameters is investigated in the following sections. Only parameters that are expected to vary, or are uncertain, are investigated. For example is the initial rock matrix temperature not investigated. However, a general sensitivity analysis of several reservoir parameters was conducted in section 2.2.2.

The results will be presented in normalized form, where the baseline scenario is the benchmark.

3.2.1 Short circuit

The effect of a short circuit on the thermal performance of the system was investigated. It is assumed that one out of the seventeen fractures in each production wellbore experiences a increase of fracture aperture. Such an event is likely to happen in a geothermal reservoir, most probable either due to shear stress or mineral dissolution. It is therefore important to investigate the effect on the thermal performance of the system given such a scenario. It is further assumed that the short circuit develops immediately once the EGS is in operation. Several fracture apertures are investigated.

The bulk temperature profile is seen in figure 3.7, while the normalized extracted heat and net power production can be seen in figure 3.8.

Discussion

The effect of a fracture short circuit is evident on the temperature profile and extracted heat from the reservoir. The physical behavior of geothermal reservoir with a short circuit was discussed in detail in section 2.3. The large effect on the temperature profile is due to the fact that the flow is governed by the "cubic law", and the flow in fracture given a pressure drop is proportional to the fracture aperture cubed (eq.2.2), if the friction factor is disregarded.

A interesting observation is that the normalized net work output from the cycle is several percentage lower than the normalized extracted heat, given the same fracture apertures. For the case of a short circuit aperture of 1.5mm is the normalized work output 10% lower than the normalized extracted heat. The reason is that the thermal efficiency of the cycle is dependent on the geothermal temperature, see figure 3.6. The effect is that the net power production decreases more than the difference in geothermal production temperature alone.
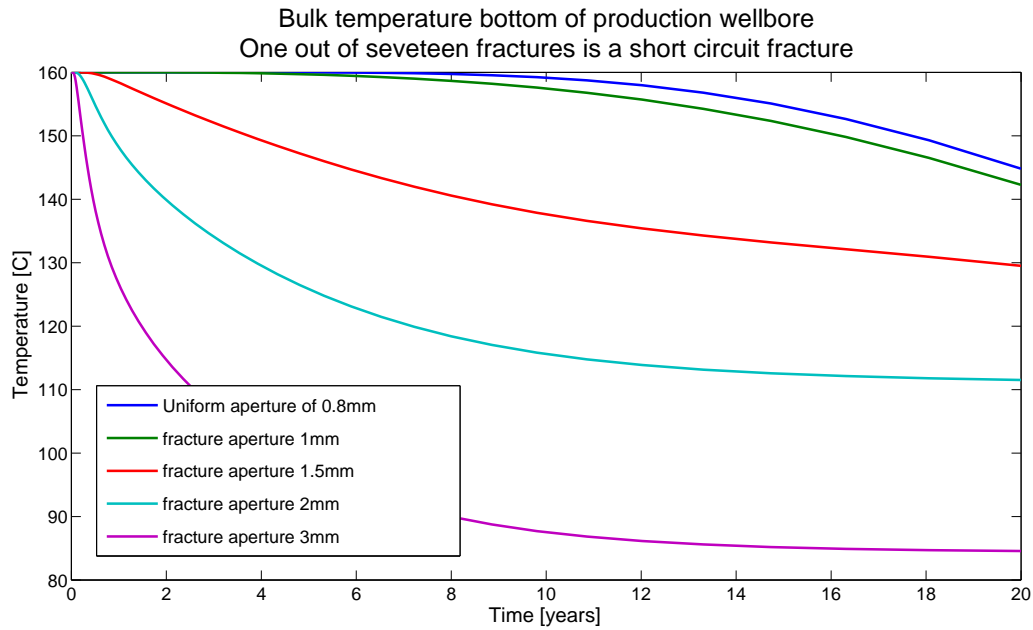
Figure 3.7: Temperature profile for different short circuit fracture apertures

A short circuit is critical for the thermal performance of the system. If one out of seventeen fractures increases from 0.8mm to 1.5m will the net work output from the system decrease with 20% - 30%, which is substantial. A fracture aperture of 2mm decreases the net work output by about 60%. It is therefore critical to control the fracture aperture in the reservoir and be able to close short circuits effectively.
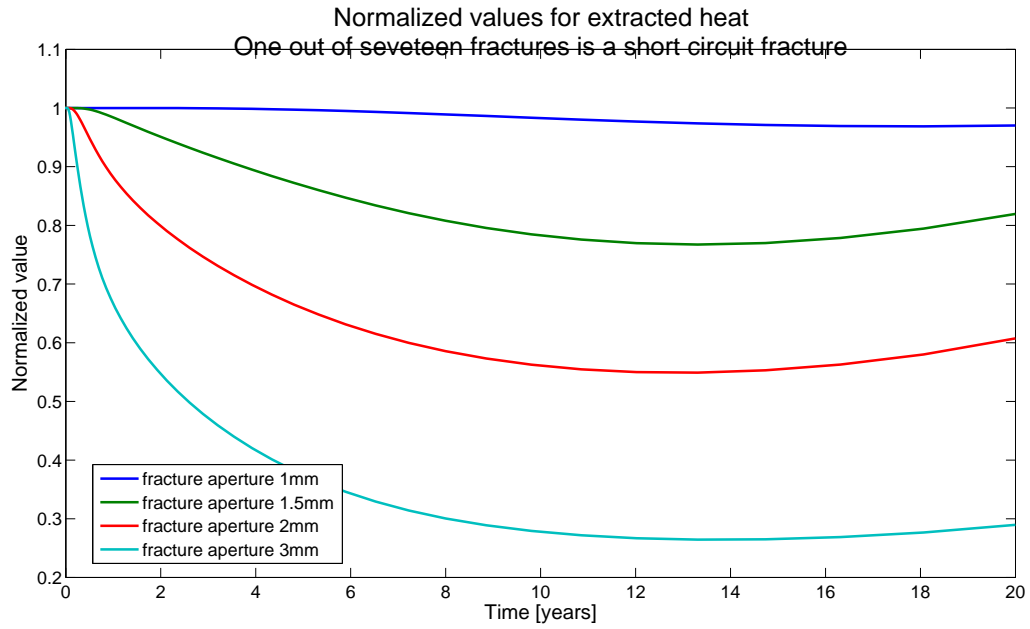
(a) Normalized extracted heat
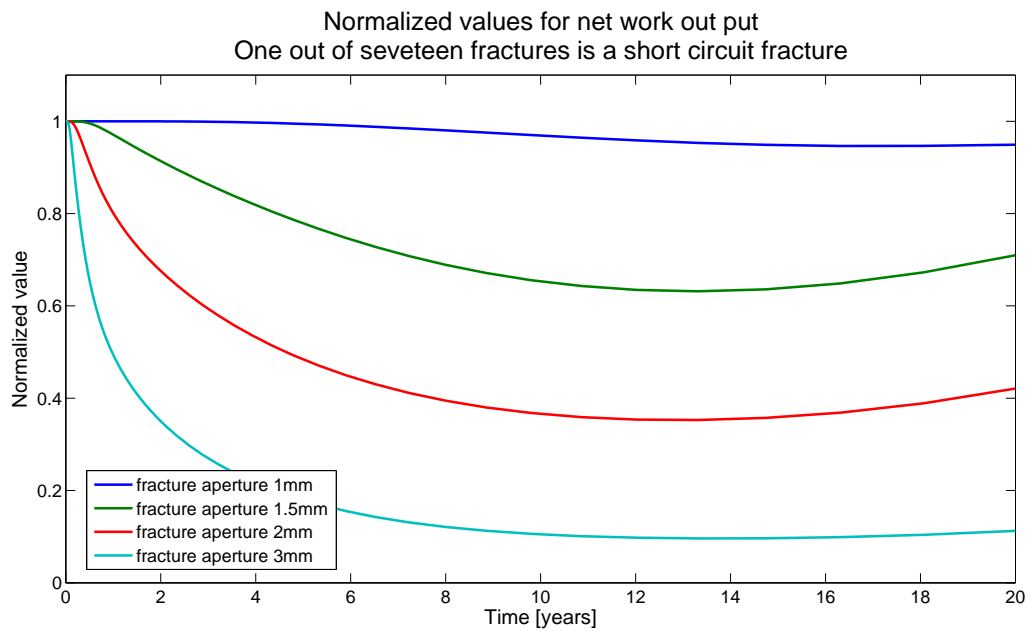
(b) Normalized net power production

Figure 3.8: Normalized thermal performance values for a fracture with a short circuit

3.2.2 Fracture spacing

The effect of a different fracture spacing than what the system was design for is investigated in this section. It is difficult to predict which fractures that will transport the circulation fluid, it is therefore interesting to see what effect a miscalculation in fracture spacing has on the thermal performance of a EGS power plant.

The baseline case assumes a fracture spacing of 30m. The height of the stimulation zone was held constant, and equal to the total number of fractures times the fracture spacing. The total mass flow is held constant and assumed to be distributed equally between the total number of fractures.

Discussion

A strong relationship is observed between the fracture spacing and the net work output from the system. A 66% decrease in fracture spacing results in roughly 30% higher net work output after 30 years. There is no effect before the thermal breakthrough (after about 8 years in the baseline case) occurs in the system, before the thermal breakthrough is the production temperature equal to that of the initial rock temperature. A increase in number of fractures increases the total heat transfer area between rock and fluid, which will increase the heat transfer. Another advantage with closely spaced fractures is that the relatively more heat is extracted from the rock, compared to a reservoir with large fracture spacing. This is due to the fact that most of the heat transfer resistance in a geothermal reservoir is in the rock matrix, therefore would a decrease in fracture spacing improve the total heat transfer from the rock. The temperature difference between the center of the rock matrix and the fluid would be smaller for a decrease in fracture spacing.
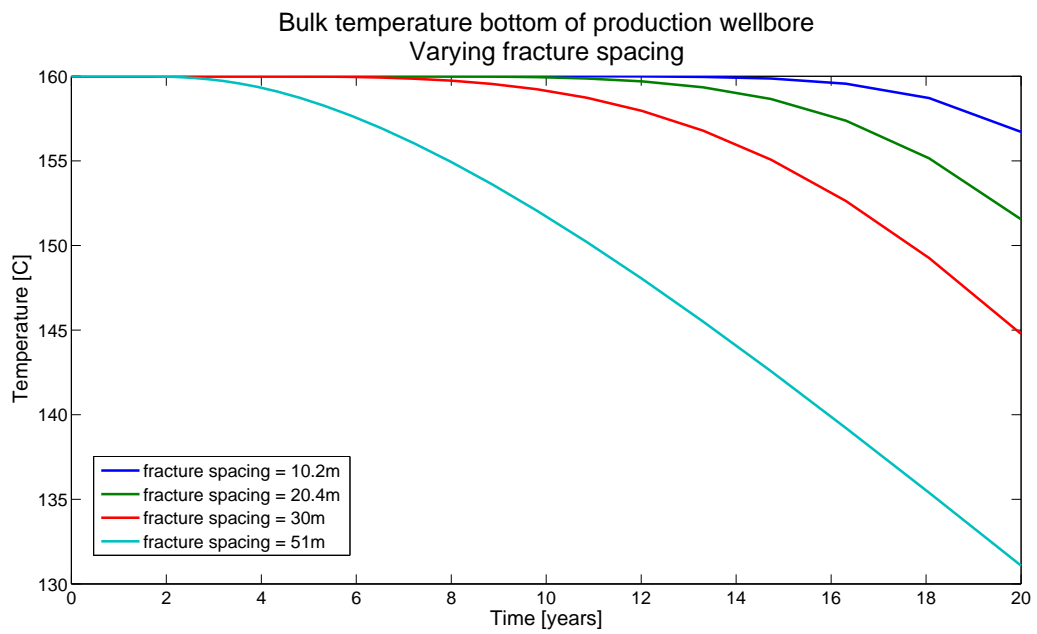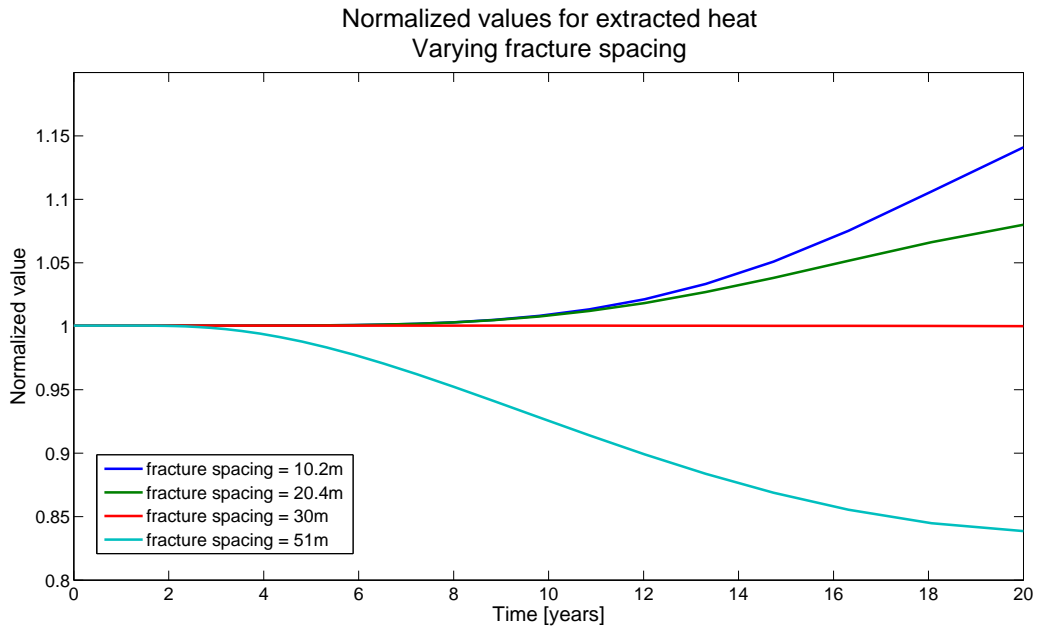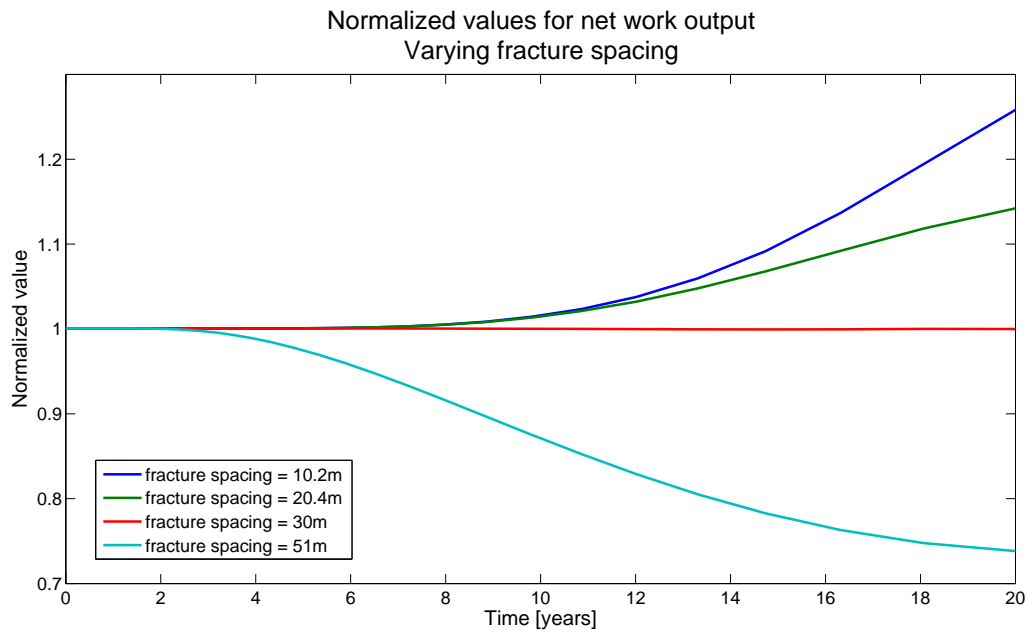
Figure 3.9: Temperature profile for a reservoir with different fracture spacing

(a) Normalized extracted heat

(b) Normalized net power production

Figure 3.10: Normalized thermal performance values for a reservoir with different fracture spacing

3.2.3   Fracture length

The effect of a different fracture length was investigated in this section. The fracture network is a complex network with irregular fracture paths, it is therefore difficult to estimate the fracture length or the effective fracture length. A change in fracture length is compared against the baseline case, using the same top site cycle.

The mass flow is held constant and at the same value as the mass flow in the baseline case. The pressure drop will therefore vary depending on the fracture length. All other parameters are held equal to that of the baseline case.

Discussion

The fracture length directly effects the volume of fractured rock that is available for heat mining, and it also effects the contact surface area between rock and fluid. A increase in fracture length will therefore cause the thermal breakthrough to be delayed, and the opposite is true for a decrease in fracture length. The effect can easily be seen in figure 3.11.

A 17% decrease in fracture length (from 600m to 500m) causes a decrease of about 25% in net work output from the cycle, while a decrease of 33% in fracture length causes a decrease of 55% in the net work output. The net work output from the cycle is highly dependent on the fracture length, is therefore critical to have good estimates on the fracture length/contact area between fluid and rock.

The reason for the sharp decrease in fracture outlet temperature is that the thermal breakthrough occurs earlier for a short fracture, due to less contact area. The total fractured volume is also smaller for decrease in fracture length, and less energy is available for mining.
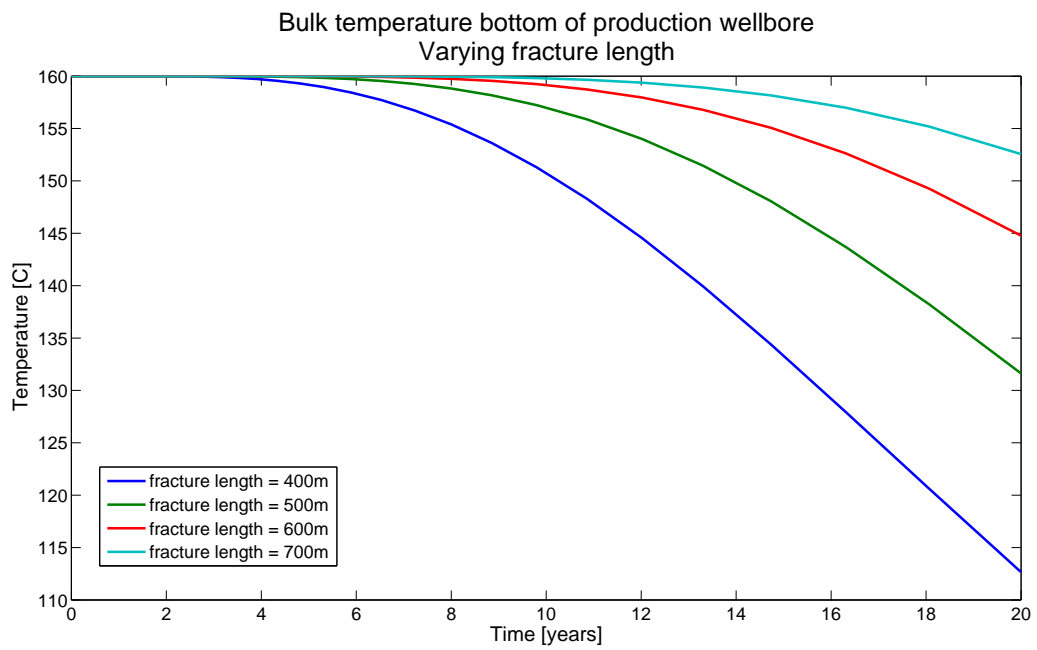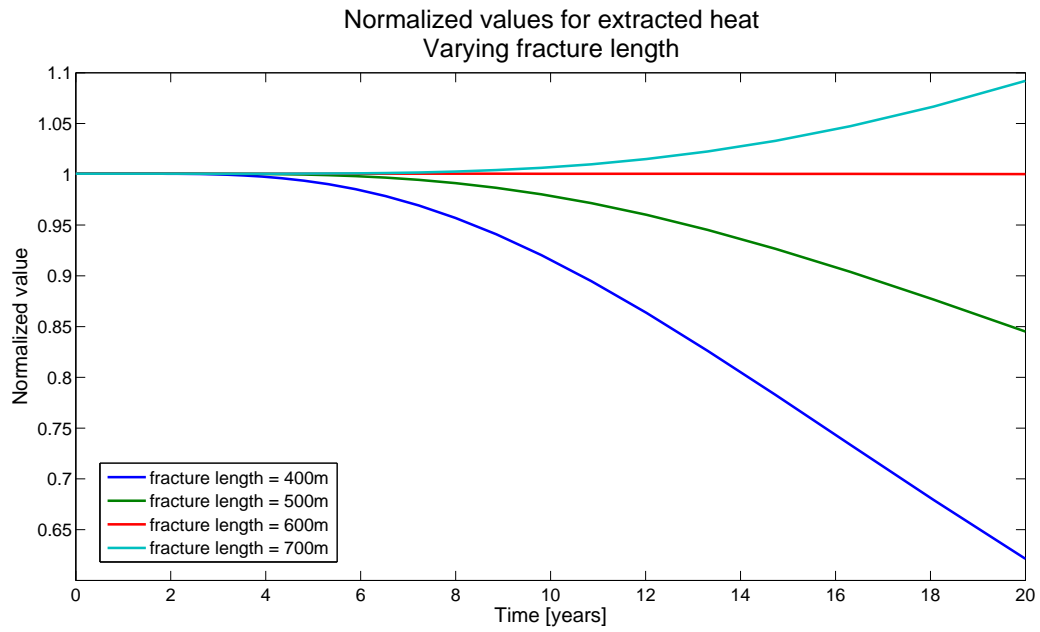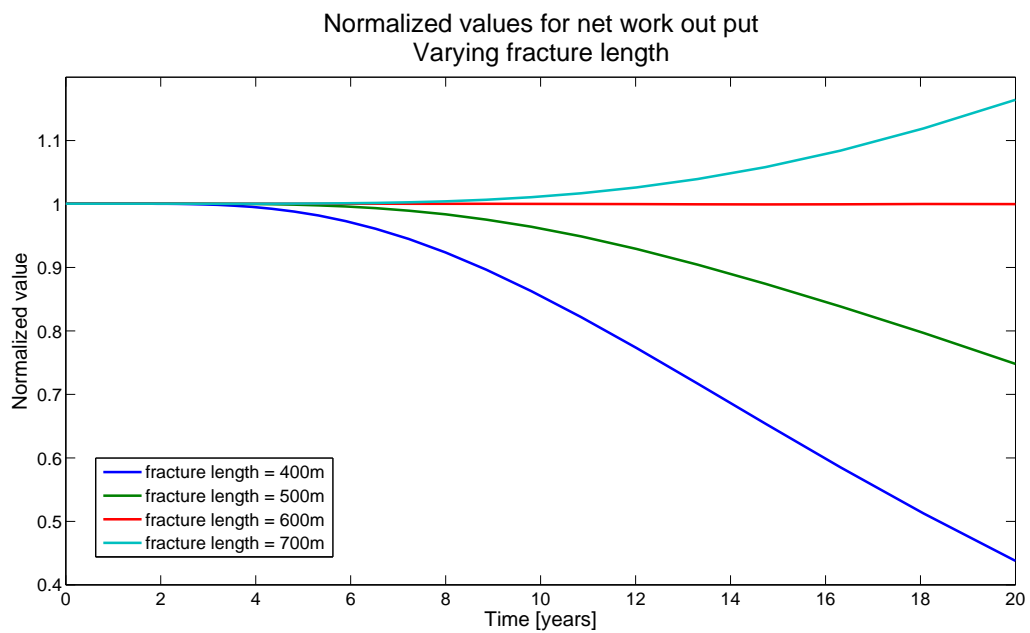
Figure 3.11: Temperature profile for different fracture length

(a) Normalized extracted heat

(b) Normalized net power production

Figure 3.12: Normalized thermal performance values for different fracture length

3.2.4 EGS used in power production: a discussion

The effect of change in reservoir conditions and operating parameters have been discussed before, in section 2.3 and in each subsection in section 3.2. The assumptions used when modeling behavior of the EGS and the top site cycle have also been discussed in detail in section 2.1, 1.6, 1.5, 2.2, 3.1, Appendix A and Appendix B. This discussion will therefore concentrate on the effect of the uncertainty in the geothermal production temperature and different possible options to mitigate the problem.

The sensitivity analysis conducted in this thesis clearly reveals that a fractured EGS combined with a ORC power cycle is vulnerable for a decrease in geothermal production temperature, especially if the EGS is designed for a temperature drop of 10^0C - 15^0C or more. Accurate estimates of the behavior of the reservoir over the entire life time of the system is therefore essential. However, mitigation options should be investigated, such as top site design that minimizes the risk related to a drop in geothermal temperature and reservoir management. Thus making the system less sensitive to changes in geothermal temperature. There will not be conducted a separate analysis of such options, however different possible mitigation options will be briefly discussed which could form a basis for further investigation.

A active reservoir management is essential to mitigate short circuit and fracture propagation effects. Possible measures could be proppants, packers and other zonal isolation tools. Accurate and good measurements of the reservoir during operation are crucial in order appropriate combat developing short circuits and unwanted fracture propagation. Downhole data is also important in order to calibrate simulation tools and numerical models. Such tools are frequently used in the oil and gas industry, however deep geothermal energy typically have higher temperature requirements and cost is critical, further development is therefore important.

The top site utilization should also be designed to cope with drops in geothermal temperature during the life time of the system. One possible approach is to combine geothermal energy and a waste combustion plant (if possible), studies show (section 1.6 and appendix F) that such an approach would yield a higher thermal efficiency and a stable work output with changes geothermal temperature. However, one presumption is that the amount of waste heat can be varied. Hybridization with other alternative energy resources should also be investigated, if available in the vicinity of the geothermal power plant.

If a single ORC is chosen should the design take into consideration the potential for a drastic drop in geothermal temperature, and the system should be able to operate at lower

temperatures. Another possibility is regulate the mass flow of the circulation fluid and the working fluid to compensate a short circuit or altered flow path, this would however take the turbine and compressor into off-design operation which could drastically effect the net work output from the cycle.

A financial decision should account for the risk of short circuiting and uncertainties in the estimates of the production temperature during the life time of the power plant.

3.3 Summary

A complete EGS power plant was designed and used as a baseline, from which the effects of off-design conditions in the geothermal reservoir effects the thermal performance of the system.

A decrease of ten degrees in (from 160^0C to 150^0C) was found to give a decrease in thermal efficiency of about 2%, a decrease of 40^0C gave a 50% decrease in thermal efficiency. The net work output from the system is therefore highly sensitive to a decrease in geothermal production temperature.

Accurate estimates of the fracture network is therefore critical for commercial operation of a EGS power plant. A 17% shorter fracture length than expected results in a 25% decrease in net power output, while a 30% shorter fracture spacing than expected yields a 15% increase in net power output. A short circuit results in a large decrease in net power output. Even if one out of seventeen fractures increases by only 1mm is the result a 60% decrease in net power output. And the decrease is fairly constant over the expected life time of the plant. It is therefore crucial to have to accurate estimates of the hydraulic fracture aperture and have measures to prevent fracture short circuiting.

Conclusion

Potential EGS sites in Norway are believed to be located in granitic basement rocks at 5km or deeper. Temperature estimates suggest temperatures between $100^0C - 190^0C$ at 5 km vertical depths, which are low to moderate temperatures. The highest heat flux is found in the southern parts of Norway [13].

Based on a literature review of different EGS concepts it was decided that a fractured geothermal reservoir would be best suited for medium to large scale power production in Norway. Since there are little information available regarding geological conditions at 5km depths at potential sites was no further specification made. The well configuration in a fractured EGS is highly dependent on local geological conditions, such as the stress field, size and number natural fractures present and rock types. A specification of a fractured EGS can therefore not be conducted before a site is chosen.

The low thermal conductivity of the rock matrix acts as a bottleneck on the thermal performance of a fractured EGS. A thermal front will develop in the reservoir and propagate from the injection point to the production point. Once the temperature at the production point starts to drop, the reservoir is said to have reached thermal breakthrough. Due to the thermal gradient that develops in the rock, the outlet temperature will be lower than the temperature at the center of the rock matrix. The time before a thermal breakthrough occurs is dependent on several factors; temperature difference between rock matrix and fluid, fluid mass flow, fractured reservoir volume and surface area between rock matrix and fluid. The rate at which the temperature decreases once thermal breakthrough has been reached also depends on the same parameters.

The development of a fracture network in a EGS during stimulation is governed by the existing conditions in the reservoir. The thermal performance of a given reservoir is therefore to a large extent dependent on pre-determined factors that cannot be altered, such as the direction of the stress field, existing fractures and joints. It is therefore important to know the local geological conditions before a fractured EGS reservoir is constructed.

An Organic Rankine Cycle is typically used as top-site cycle for low to moderate geothermal fields. The thermal performance of the cycle is highly dependent on the geothermal temperature, and sensitive to changes in reservoir parameters. The net power output from a ORC decreases drastically in off-design conditions, such as a change in geothermal temperature. Geothermal energy projects typically have small margins, it is therefore critical to operate at maximum performance. To this extent it is crucial to obtain accurate estimates of the geothermal reservoir, such as fracture spacing, fracture length, fracture aperture, flow pattern and surface area. If the fracture length is 17% shorter than expected the net power output will decrease with 25%.

The development of a short circuit is critical for the performance of the geothermal reservoir. If 6% of the fractures experiences a 1mm increase in fracture aperture will the net power output from the ORC decrease with about 60%. Controlling the fracture aperture is therefore critical for a fractured EGS. See figure 3.7 and figure 3.8.

The geothermal temperature is highly sensitive with respect to changes in geothermal reservoir conditions, which could drastically effect the thermal performance of the power cycle. It is therefore vital to obtain accurate estimates of the fracture network and be able to handle short circuit if present.

One alternative in order to reduce the risk concerning the geothermal temperature is to combine geothermal energy with other renewable energy resources. Combining a waste combustion plant and geothermal energy looks promising, and offers a stable energy output for a wide range of geothermal temperatures and a higher thermal efficiency. Geothermal energy should therefore be combined with other alternative energy resources, if possible, in order to reduce the risk related to uncertainties in geothermal reservoir conditions.

Further Work

Areas that need further work are specified below, together with a brief explanation of each area. As specified in the master thesis are areas of technological development emphasized. The critical factor in order to obtain a commerical EGS is reservoir managment, and technological advancments in that area should therefore be prioritized.

- **Ability to predict fracture network and flow pattern** Develope fully coupled hydrological-thermal-mechanical-chemical models that accuratly predicts flow pattern and heat transfer over the life time of the reservoir.

- **Control fracture development** Develope high temperature packers, or other zonal isolation tools, that can mitigate short-circuiting, reduce leakage and target specific fractures and zones for stimulation.

- **Temperature hardened tools** Temperature hardened tool for real-time downhole monitoring of temperature, pressure and flow should be developed. This would increase the ability to track reservoir evolution and provide appropriate data for validating and updating reservoir models and simulators.

- **Cost analysis of a complete EGS power plant** In order to further explore the possibility of EGS in Norway should a cost analysis be conducted in order see if commerical operation of a EGS is possible given Norwegian conditions.

- **Use of technology form oil and gas industry** Map which parts and to what extent technology from the oil and gas industry could be used in geothermal reservoir managment.

Bibliography

[1] Jefferson W. Tester. The future of geothermal energy impact of enhanced geothermal systems (egs) on the united states in the 21st century. Technical report, MIT, 2006.

[2] G. L. Mines G. Nalla, G. M. Shook and K. K. Bloomfield. Parametric sensitivity study of operating and design variables in wellbore heat exchangers. *Elsevier*, 2005.

[3] T. Tischner J. Orzol, R. Jung and P. Kehrer. The genesys-project: extraction of geothermal heat from thight sediments. In *World Geothermal Congress 2005*, pages 1–9, 2005.

[4] Mark W. McClure Zhe Wang and Roland N. Horne. Modeling study of single well-well egs configuration. In *Proceedings World Geothermal Congress 2010*, pages 1–12, 2010.

[5] Trond Slagstad. Radiogenic heat production of archaean to permian geological provinces in norway. *Norwegian journal of geology*, 2008.

[6] A.Franco and M.Villani. Optimal design of binary cycle power plants for water-dominated, medium-temperature geothermal fields. *Elsevier*, 2009.

[7] Ronald DiPippo. Ideal thermal efficiency for geothermal binary plants. *elsevier*, 2007.

[8] William Cibich. An analytical model for enhanced geothermal systems (egs). Honours thesis at the University of Adelaide, 2009.

[9] Mark W. McClure. Fracture stimulation in enhanced geothermal systems. Technical report, Stanford University, 2009.

[10] A.Genter and H.Traineau. Analysis of macroscopic fractures in granite in the hdr geothermal well eps-1, soultz-sous-forets, france. *Elsevier*, 1995.

[11] Halliburton. Basic petroleum geology and log analysis. Technical report, Halliburton, 2001.

[12] S.K. Sanyal S.J. Butler and A.Robertson-Tait. A numerical simulation study of the performance of enhanced geothermal systems. In *Twenty-Ninth workshop on geothermal reservoir engineering*, pages 1–6, 2004.

[13] H. Elvebakk C. Pascal and O. Olesen. An assessment of deep geothermal resources in norway. In *World Geothermal Congress 2010*, pages 1–3, 2010.

[14] US department of Energy. Geothermal tomorrow 2008. Technical report, US department of Energy - Energy efficiency and renewable energy, 2008.

[15] Lars Anders Drange. Utilization of geothermal energy, project thesis. Project thesis at the Norwegian University of Science and Technology, 2010.

[16] E.E.Michaelides A.P.Davis. Geothermal power production from abandoned oil wells. *Elsevier*, 2009.

[17] N. Cuenot D. Fritsch A. Genter, K. Evans and B. Sanjuan. Contribution of the exploration of deep crystalline fractured reservoir of soultz to the knowledge of enhanced geothermal systems (egs). *Elsevier*, 2010.

[18] S.Davidson D.Wyborn, L.de Graaf and S.Hann. Development of australia's first hot fractured rock (hfr) underground heat exchanger cooper basin, south australia. *Proceedings world geothermal congress 2005*, 2005.

[19] B.R. Bendall P.W. Reid and L. McAllister. Developing large scale, base load egs power - the parlana project, south australia. In *Proceedings World Geothermal Congress 2010*, pages 1–3, 2010.

[20] S.J. Butler S.K. Sanyal, E.E. Granados and R.N. Horne. An alternative and modular approach to enhanced geothermal systems. In *World geothermal congress 2005*, pages 1–7, 2005.

[21] P.Kehrer R.Jatho S.Wessling K.Hofmeister H.Evers H.Sulzbacher R.Junker, T.Tischer and R.Jung. The genesys project: Single-well-concepts for deep geothermal energy from the northern german basin. Poster, ?

[22] M. W. McClure Z. Wang and R. N. Horne. A single-well egs configuration using thermosiphon. In *Thirty-fouth Workshop on Geothermal Reservoir Engineering*, pages 1–12, 2009.

[23] Arbeidsgruppe Geotermisk Energi. Innsatsgruppe fornybar termisk energi - arbeidsgruppe geotermisk energi. Technical report, Energi 21, 2010.

[24] Knut-Erland Brun. Potensial for dyp geotermisk energi i norge. Master's thesis, Universitetet i Bergen, 2010.

[25] Andreas Reinicke Gunter Zimmermann. Hydraulic stimulation of a deep sandstone reservoir to develop an enhanced geothermal system: Laboratory and field experiments. *Elsevier*, 2010.

[26] T.Gandy P.Hauffe T.Hettkamp H.Menzel P.Penzkofer D.Teza T.Tischner M.Schindler, J.Baumgartner and G.Wahl. Successful hydraulic stimulation techniques for electric power production in the upper rhine graben, central europe. In *World Geothermal Congress 2010*, pages 1–7, 2010.

[27] B.J.Anderson D.L.Koch P.R.Rohr D.Sutter, D.B.Fox and J.W.Tester. Sustainable heat farming of geothermal systems: A case study of heat exctraction and thermal recovery in a model egs fractured reservoir. In *Thirty-Sixth workshop on Geothermal Reservoir Engineering*, pages 1–6, 2011.

[28] D.W. Brown. A hot dry rock geothermal energy concept utilizing supercritical co_2 instead of water. In *Twenty-fifth workshop on geothermal reservoir engineering*, pages 233–238, 2000.

[29] Karsten Pruess. Enhanced geothermal systems (egs) using co_2 as working fluid - a novel approach for generating renewable energy simultaneous sequestration of carbon. *Elsevier*, 2006.

[30] H.Gurgenci A.D. Atrens and V.Rudoplh. Electricity generation using a carbon-dioxide thermosiphon. *Elsevier*, 2010.

[31] B.Moghtaderi A.I. Remoroza and E.Doroodchi. Coupled wellbore and 3d reservoir simulation of a co_2 egs. *Thirty-sixth workshop on geothermal reservoir engineering*, 2011.

[32] C.F. Tsang G.Bodvarson. Injection and thermal breakthrough in fractured geothermal reservoirs. *Journal of Geophysical research*, 1982.

[33] Kambiz Vafai, editor. *Hanbook of Porous media*. Taylor and Francis, 2005.

[34] J.A. Majorowicz A.M. Jassop. Fluid flow and heat transfer in sedimentary basins. *Geological Society, London, Special publications*, 1994.

[35] Karsten Pruess. Modeling of geothermal reservoirs: Fundamental processes, computer simulation and field application. *Geothermics, vol.19. No.1, pp.3-15*, 1990.

[36] Paul Bixley Malcolm Grant. Geothermal reservoir engineering, 2011.

[37] J.Zhao and C.P.Tso. Heat transfer by water flow in rock fractures and the application to hot dry rock geothermal systems. *Pergamon press ltd*, 1993.

[38] T.Fukuda F.Ogino, M.Yamamura. Heat transfer from hot dry rock to water flowing through a circular fracture. *Pergamon*, 1999.

[39] George Moridis Karsten Pruess, Curt Oldenburg. Tough2 user's guide, version 2.0. University of California, Berkeley,, 1999.

[40] M. Malavazos W. Cibich and R. McDonough. A steady state pressure model for egs in the cooper basin. *Australian geothermal energy conference*, 2008.

[41] PIRSA Geothermal Energy. Pirsa publications and reports. http://www.pir.sa.gov.au/geothermal/products__and__data/publications_and_reports, 2011.

[42] A. Ghassemi A.H.D. Cheng and E.Detournay. Integral equation solution of heat extraction from a fracture in hot dry rock. *International journal for numerical and analytical methods in geomechanics*, 2001.

[43] Jian Zhao. Geothermal testing and measurments of rock and rock fractures. *Pergamon*, 1994.

[44] D. Swenson S.K. Sanyal, S.J. Butler and B.Hardeman. Review of the state-of-the-art of numerical simulation of enhanced geothermal systems. In *World Geothermal Congress 2000*, pages 3853 – 3858, 2010.

[45] K.Kitz S.Sanyal and D.Glaspey. Optimization of poewer generation from moderate temperature geothermal system - a case history. *proceedings world geothermal congress 2005*, 2005.

[46] Monica Andrea Borgund. Power production from low-temperature aluminium electrolysis cell off-gases. Master's thesis, NTNU, 2009.

[47] Aleksandra Borsukiewvicz-Gozdur. Dual fluid hybrid power plant co-power by low-temperature geothermal water. *Elsevier*, 2009.

[48] E.K.Stefanakos H.Chen, D.Yogi. A review of thermodynamic cycles and working fluids for the conversion of low-grade heat. *Elsevier*, 2010.

[49] OJ. Demuth. Analysis of mixed hydrocarbon binary thermodynamic cycles for moderate temperature geothermal resources. *Idaho*, 1981.

[50] W.M.Worek H.D.Madhawa Hettiarachchi, M-Golubovic and Y.Ikegami. Optimum design criteria for an organic rankine cycle using low-temperature geothermal heat sources. *elsevier*, 2007.

[51] H.J. Ramey. Wellbore heat transmission. *Society of Petroleum Engineers (SPE)*, 1962.

[52] C.Clauser and E.Huenges. Thermal conductivity of rocks and minerals. *American geophysical Union*, 1994.

[53] D.W. Waples and J.S. Waples. A review and evaluation of specific heat capacity of rocks, minerals and subsurface fluids. part 1: Minerales and nonporous rocks. *Natural resources research*, 2004.

[54] Ronald DiPippo. Ideal thermal efficiency for geothermal power plants. *Elsevier*, 2007.

[55] Schlumberger. Oilfield glossary. http://www.glossary.oilfield.slb.com/, 2011.

[56] Wikipedia. Wikipedia. http://www.wikipedia.org, 2011.

[57] H.K. Versteeg and W.Malalsekera, editors. *An introduction to computational fluid dynamics - The finite volume method (second edition)*. Pearson, 2007.

[58] Aniko Toth and Elemer Bobok. Life time of a doublet in a fractured geothermal reservoir. *Proceedings world geothermal congress 2010*, 2010.

[59] O. Kolditz. Modelling flow and heat transfer in fractured rocks: Conceptual model of a 3-d deterministic fractured network. *Pergamon*, 1995.

[60] J.McLenna T.Stoddard and J.Moore. Fracture conductivity of a bauxite-propped geothermal system at in-situ conditions. In *Thirty sixth workshop on geothermal reservoir engineering*, pages 1–8, 2011.

[61] Zimmermann G and Reinicke A. Hydraulic stimulation of a deep sandstone reservoir to develop an enhanced geothermal system: Laboratory and field experiments. *geotermics*, 2009.

[62] K.Pruess and Yingqi Zhang. A hybrid semi-analytical and numerical method for modeling wellbore heat transmission. In *Thirtieth workshop on geothermal reservoir engineering*, pages 1–5, 2005.

[63] J.Hagoort. Ramey's wellbore heat transmission revisited. *SPE journal*, 2004.

[64] U.Seipold and E. Heugenes. Thermal properties of gneisses and amphibolites - high pressure and high temperature investigations of ktb-rock samples. *Elsevier*, 1997.

[65] M. Crawford W. Kays and B. Weigand, editors. *Convective heat transfer and mass transfer*. McGrawHill, 2005.

[66] N.H. Tran A.R. Shaik, S.S. Rahman and T.Tran. Numerical simulation of fluid-rock coupling heat transfer in naturally fractured geothermal system. *Elsevier*, 2011.

[67] D.Karvounis and P.Jenny. Modeling of flow and transport in enhanced gepthermal systems. *Thirty sixth workshop on geothermal reservoir engineering*, 2011.

[68] H.Tenzer C.I. McDermott, A.R.L Randriamanjatosoa and O.Kolditz. Simulation of heat extraction fom crystalline rocks: The influence of coupled processes on differential reservoir cooling. *Elsevier*, 2006.

[69] Qingfeng Tao and Ahmad Ghassem. Simulation of fluid flow in fractured porothermoelastic reservoirs. *PROCEEDINGS, Thirty-Fifth Workshop on Geothermal Reservoir Engineering*, 2010.

[70] H.Cinco-Ley A.R. Valdez-Perez, H.Pulido and G.G. Munoz. A bew bilinear model for naturally fractured reservoirs with transient interporosity transfer. *Thirty-sixth Workshop on Geothermal Reservoir Engineering*, 2011.

[71] Yue Hao Pengcheng Fu, Scott M. Johnson and Charles R. Carriga. Fully coupled geomechanics and discrete flow network modeling of hydraulic fracturing for geothermal application. *PROCEEDINGS, Thirty-Sixth Workshop on Geothermal Reservoir Engineering*, 2011.

[72] K. Iwai P.A. Witherspoon, J.S.Y. Wang and J.E. Gale. Validity of cubic law for fluid flow in a deformable rock fracture. *eScholarship University of California*, 1979.

[73] J.L. Livesey. Inertia effects of viscous flows. *Elsevier*, 1960.

[74] Arstechnologies.com. What is the self-propping phenomenon? http://www.arstechnologies.com, 2011.

Appendix A

Reservoir model

This appendix goes into detail regarding the fractured geothermal reservoir model that was developed in this thesis. The wellbore model is discussed in Appendix B.

First is the general set up of the numerical model in Matlab presented, followed by how the conduction, advection, pressure loss and temperature dependent properties were modeled. Thereafter is the model validated against different analytical solutions. At the end are the mesh size, time step and different matlab solvers investigated in order to find the optimum tradeoff between computational time and model accuracy.

Brief overview of the model

The fractured EGS was modeled in Matlab r2010a using a Finite Volume Method (FVM). In order to model the physical behavior of a fractured EGS were several assumptions and simplifications applied. The most important are; the bedrock was assumed to be impermeable and isentropic, fractures can be modeled as flow between flat plates using a correct heat transfer coefficient, each fracture is separated by a rock matrix of height H, the fracture aperture is constant and is invariant of pressure changes. Thermal expansion and chemical reactions are neglected. Circulation fluid is modeled as water with constant properties. Temperature dependent properties are used for the rock matrix. The effect of the different assumptions and simplifications is commented further in the subsection labeled " Model uncertainties".

Figure A shows a sketch of the simplified geothermal reservoir, based in this reservoir was the numerical model constructed. Due to symmetry is only a part of the reservoir modeled in Matlab, red area in figure A. The rock matrix have been modeled using a 2D transient finite volume approach, following the approach used by Versteeg and Malalasekera
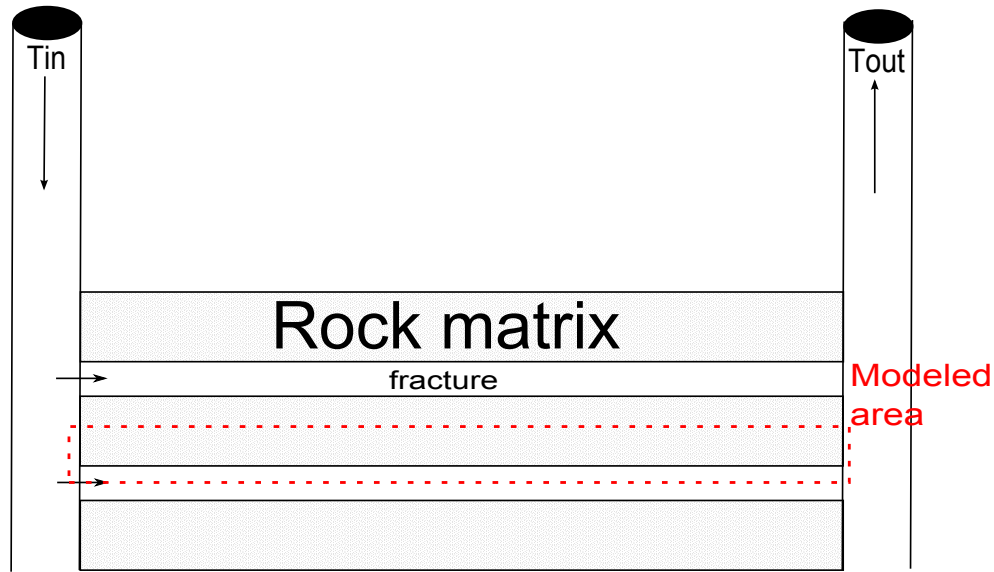
Figure A.1: Representation of a fractured EGS

[57]. The rock matrix model is fully coupled with the advective fluid flow model, which is modeled as a 1D steady state. A fully coupled system, where the rock matrix and fluid flow is solved simultaneously, gave a stable solution in time and large time steps could be used without resulting in a unstable solution. Time and height were discretisation logarithmically in order to save computation time while maintaining accuracy, nodes in length direction were equidistant spaced. This is also discussed in detail in the following section.

Model uncertainties

The different assumptions and simplifications of the physical behavior of the geothermal system are listed and discussed.

- **Uniform fracture network** The geothermal reservoir is assumed to consist of uniform horizontal fractures with constant fracture aperture. The fractures is also assumed to be equidistant spaced. The model of the geothermal reservoir is shown in figure A. This is probably the most important assumption in the model, since the geothermal reservoir in reality consist of a complex network of fractures. The fractures typically align with the stress field, which only in special cases is horizontal. The fracture aperture is not constant, but varies across the fracture length. The spacing between each fracture varies. Thus will the simplified geothermal reservoir used in this thesis not capture the physical behavior of the reservoir well, and the re-

sults should only be used as a general guidance. However, a single fracture model (as used in this thesis) adequately captures thermal recovery through heat conduction from the rock surrounding the reservoir [27]. The general thermal behavior should therefore be correct.

- **Constant fracture aperture** The fracture aperture is assumed to be constant, which is not the case in a real EGS. This assumption will affect the flow regime and pressure loss, however this is of less importance in the model. Since the fracture aperture is very small compared to the fracture length is the fluid temperature assumed to be constant in y-direction. The pressure drop is used to estimate the mass flow rate at different fracture apertures and how the mass flow rate is distributed if more than one fracture aperture is present. Each fracture is assumed to have the same ratio between fracture aperture and roughness, resulting in the same friction factor for all fractures regardless of fracture aperture. However, since the pressure drop is only used to estimate the mass flow distribution between fractures, which in turn are used to make rough estimations on the effect of short circuiting is a correct pressure drop value of less importance.

- **Pressure drop** The pressure drop estimation is based on the work done by Cibich [40], which is used at PIRSA[1] Petroleum and Geothermal Group to model EGS behavior.

  The model is based on the solution of the Navier Stoke equation for a laminar horizontal linearly incompressible flow between flat plates. The friction factor is assumed to be constant. The pressure drop, and thus the mass flow in each fracture, is therefore only a function of total mass flow and the respective fracture aperture. The model is only valid for laminar flow, however based on parameters found in the literature is the flow in a EGS mostly laminar. Radial flow effects near the wellbore have not been taken into account, which reduces the accuracy of the model. The friction factor relationship is taken from Cibich [40], which is modified form of the friction factor found by Louis (1969) for groundwater flow in joints.

  Due to the simplifications and assumptions done should the pressure drop different fracture apertures be treated carefully and only be used as guidance, since the model probably not will predict an very exact value. However, to estimate the exact value of the pressure drop is not inside the scope of this paper. The pressure drop is only

---

[1]Government of South Australia Primary Industries and Resources

used to estimate the mass flow distribution between different fracture apertures and for that purpose should the model be adequate.

- **Negligible heat transfer resistance at the rock/fluid interface** The heat transfer resistance at the interface between the rock and the fluid is assumed to be negligible. This holds true at medium to long time periods, however for short time periods is this assumption wrong. At medium to long time periods is the temperature difference between the rock and fluid small, since the rock matrix have approached the temperature of the fluid. The heat transfer is also restricted by the conduction through the rock, which acts as a bottle neck on the heat transfer regime. The importance of the heat transfer coefficient is therefore negligible at medium to long time periods. At early time periods is the temperature gradient large and the heat transfer coefficient important in order to capture the physical behavior of the system. However, due to the length of the reservoir and the mass flow under consideration is the fluid heated up to the initial rock matrix temperature regardless of heat transfer coefficient. The effect on the production temperature is therefore negligible. As reported by Ogino et al (1999) [38] does the forced convection between flowing water and the fracture surface has an important role in the heat transfer mechanism only in the early stage of heat extraction and the heat transfer resistance between rock/fluid can be assumed to be negligible in all practical cases.

- **No leakage** It is assumed that there is no circulation fluid leakage from the geothermal reservoir. The leakage rate depends highly on the specific reservoir, and rates ranging between 70% and 0% have been reported, see 1.4. If there is leakage of circulation fluid from the reservoir would that decrease the total heat output from the reservoir since some of the water is heated up before it leaves the system. It would also increase costs the circulation fluid needs to be replenished in order for the system to operate at constant mass flows.

- **Chemical reactions and thermal effects are not taken into account** The effect of chemical reactions and thermal effects on the fracture aperture, fracture path and circulation fluid properties have not been taken into account. The effects could however be significant and should be taken into account in any site specific study of a EGS. The most critical effect is the potential for short circuiting as deposition and dissolution can affect the fracture aperture. This could drastically reduce the life time of plant.

- **Circulation fluid temperature is constant in y-direction** The circulation fluid temperature is assumed to be constant in y-direction. Since the fracture aperture is very small compared to the fracture length is this assumption valid and the error induced by the assumption should be negligible.

- **Rock matrix is impermeable** The rock have been assumed to be impermeable, which also often is the case for granite. If there are permeable layers, areas, in the rock matrix could that increase the heat transfer in the rock matrix. Natural occurring fluids or circulation fluid could flow through the permeable layers which would decrease the thermal resistance and aid the heat transfer. However, is it very unlikely that the effect would be substantial except in special cases such as porous and permeable sedimentary layers.

- **Temperature dependent rock/granite properties** The physical properties of granite could change drastically both with temperature and depending on the mineral composition of the granite. Specific heat and thermal conductivity could change as much as a factor of 2-3, see section A.1.4. The effect of temperature dependent properties is accounted for by using relationships developed in the literature, see section A.1.4. However, the effect of different mineral compositions in granite is not accounted for. An average value was used when the specific heat and thermal conductivity of granite was estimated, the value was based on tabulated data found in the literature.

A.1 Model setup

A principal sketch of how the model was programmed in matlab can be seen in figure A.2. Two different methods were investigated; a fully coupled system and a model using two different functions coupled through the heat flux at the interface. Both models gave similar results, however the fully coupled model proved to yield more stable solutions and was therefore preferred. In the fully coupled model are all the nodes shown in figure A.3 solved in the same set of linear equations $AT = b$. The input variables came from the injection wellbore, while the output variables where put into the production wellbore model.

Figure A.3 shows the modeled area and node distribution. The nodes in y-direction is spaced logarithmically. The area shown in figure A.3 is the red area in figure A.
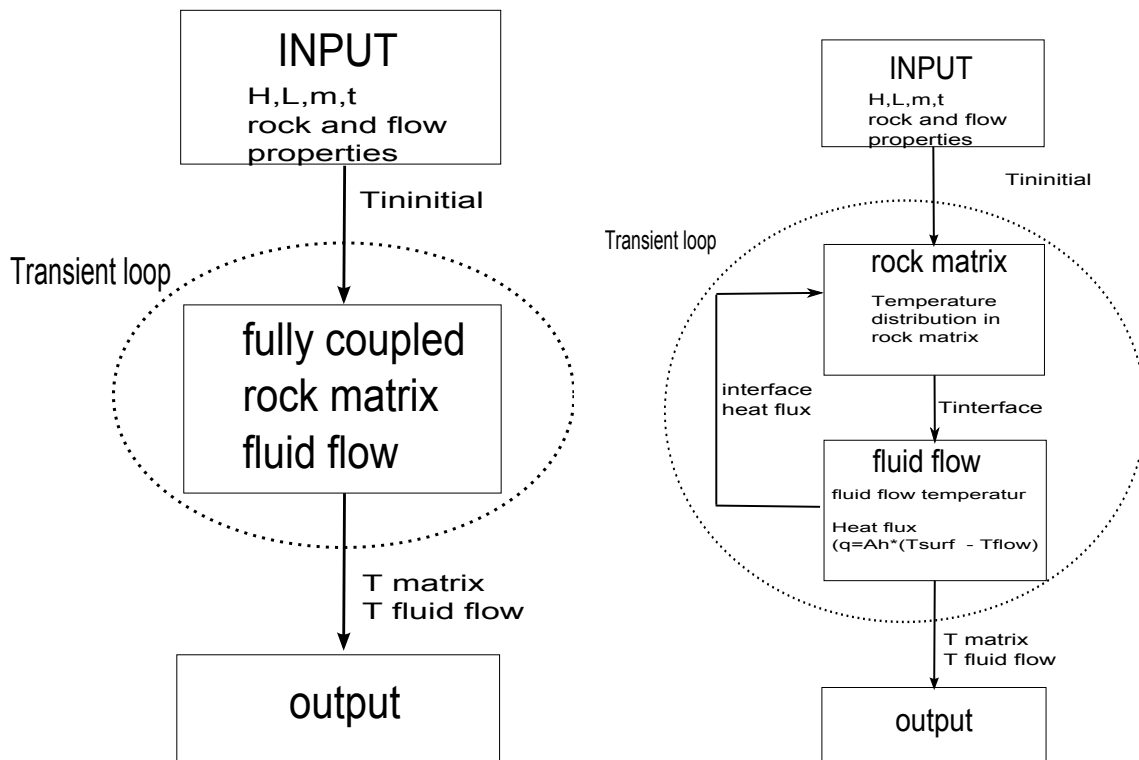
(a) Fully coupled model (USED) (b) Two functions coupled through heat flux

Figure A.2: Principal sketch of matlab program
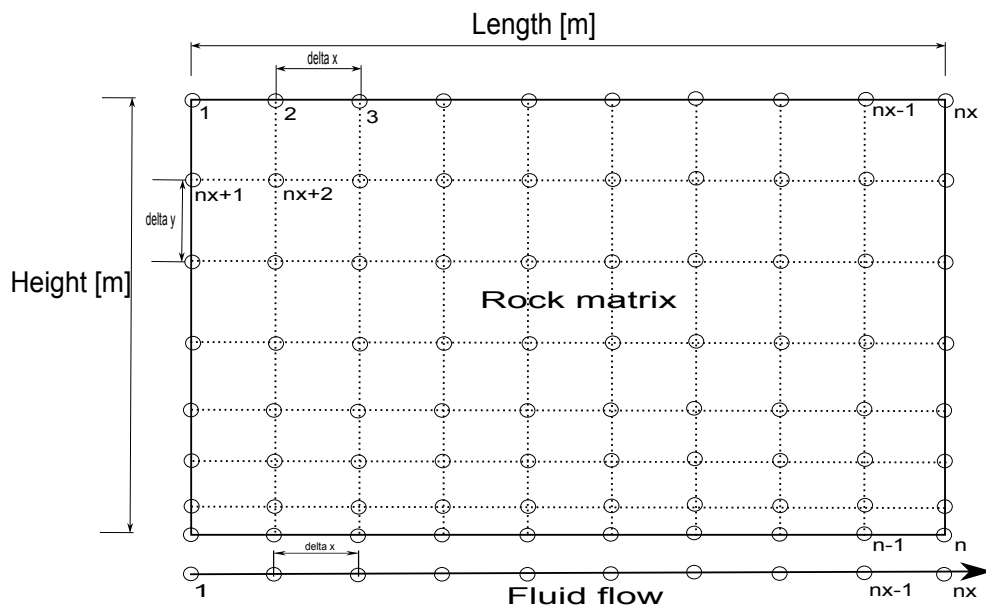
Figure A.3: FVM mesh

A.1.1 Conduction

A 2D transient conductive finite volume model was developed based on the approach used by Versteeg and Malalasekera in the book "Computational fluid dynamics - The Finite Volume Method" [57]. The unsteady energy diffusion equation (eq. A.1) was integrated over time and the control volume surrounding each node. The respective Control Volume can be seen in figure A.4, where W,E,S,N,P refers to the West (W), East (E), South (S), North (N) and P is the node that is being calculated. A with subscript w,e,s,n indicates the cross sectional area. The system of linear equation resulting from the integration and discretisation was then solved using a direct solver in matlab.

Solving the energy equation

The unsteady energy diffusion equation:

$$\frac{\delta \rho C_p T}{\delta t} = div\left(kgradT\right) + S \tag{A.1}$$

Integration over the CV in figure A.4 yields

$$\int_t^{t+\Delta t} \int_{CV} \frac{\Delta T}{\delta t} \delta V \delta t =$$
$$\int_t^{t+\Delta t} \int_{CV} \frac{\delta}{\delta x}\left(k\frac{\delta T}{\delta x}\right)\delta V \delta t + \int_t^{t+\Delta t} \int_{CV} \frac{\delta}{\delta y}\left(k\frac{\delta T}{\delta y}\right)\delta V \delta t + \int_t^{t+\Delta t} \int_{CV} S\delta V \delta t \tag{A.2}$$

Using a implicit solution with a first-order (backward) differencing scheme in time and applying the central differencing scheme to the diffusion terms yields equation A.3 we get

$$\rho C_p \left(\frac{T_P - T_P^0}{\Delta t}\right)\Delta x =$$
$$T_P \Delta t \left[\frac{k_e A_e \left(T_E - T_P\right)}{\delta x_{PE}} - \frac{k_w A_w \left(T_P - T_W\right)}{\delta x_{WP}}\right] \tag{A.3}$$
$$+ T_P \Delta t \left[\frac{k_n A_n \left(T_N - T_P\right)}{\delta y_{PN}} - \frac{k_s A_s \left(T_P - T_S\right)}{\delta y_{SP}}\right] + \bar{S}\Delta x \Delta y'$$

Rewriting equation A.3 using the nomenclature by Versteeg and Malalasekera yields

$$a_P T_P = a_W T_W + a_W T_E + a_S T_S + a_N T_N + a_P^0 T_P^0 - Sp \tag{A.4}$$

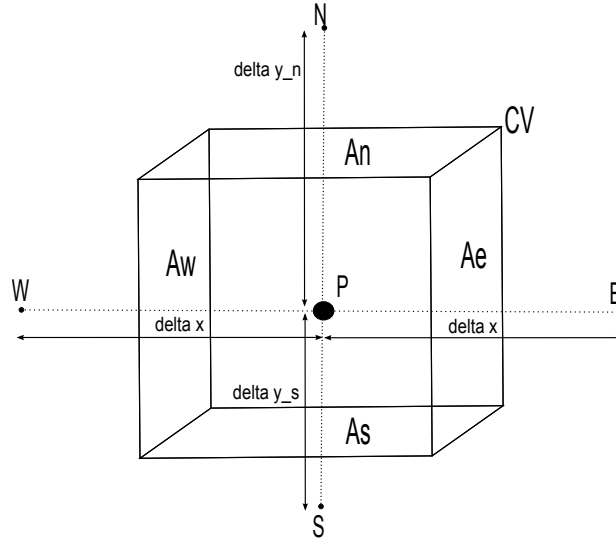**Figure A.4:** FVM nomenclature

where

$$a_P = a_W + a_E + a_S + a_N$$

$$a_P^0 = \rho C_p \frac{\Delta x' \Delta y'}{\Delta t}$$

$$\Delta y' = \frac{\delta y_N P + \delta y_P S}{2}$$

$$a_W = \frac{k_W A_w}{\delta x_{WP}}, a_E = \frac{k_E A_e}{\delta x_{PE}}, a_N = \frac{k_N A_n}{\delta y_{NP}}, a_S = \frac{k_S A_s}{\delta y_{PS}}$$

Y direction (height) is discretisation logarithmically. The length of Δy is therefore not constant and δy_{NP} is therefore not equal to δy_{PS}, however in x-direction is the distance equal due to equidistant spaced nodes and $\delta x_{WP} = \delta x_{PE} = \delta x$. This can also be seen from figure A.4.

Boundary conditions

The boundary conditions used are zero heat flux ($\frac{\delta T}{\delta x} = 0$) at the north, west and east boundary. The heat flux at the north boundary is set to zero due to symmetry. The influence of the heat flux at the east and west boundary is assumed to be negligible on the whole system, since L»H, and is therefore set to zero. The boundary condition at the

south surface is a variable heat flux, determined by the temperature difference between the fluid node and the node at the rock surface $\left(Q = hA_{sur}\left(T_{surface} - T^-_{fluid}\right)\right)$.

Mesh and time scale

A mesh with logarithmic spaced nodes in y-direction and equidistant nodes in x-direction were used, see figure A.3. The nodes in y-direction were spaced logarithmically in order to capture the physical process in the rock near the interface between rock and fluid while keeping the total number of nodes to a minimum. The temperature gradient is large in area close to the interface, closely spaced nodes are therefore needed in order to describe the heat transfer accurately. As the distance from the interface increases will the temperature gradient decrease, thus requiring fewer nodes in order to capture the physical behavior correctly.

Time was also distributed logarithmically. The temperature gradients is largest at the beginning and decreases as time increases, therefore should each time step be smaller at the beginning and increase towards the end. This will decrease the total number of time steps needed in order to capture the physical process accurately, compared to equally spaced time steps.

The time and height discretisation can be seen in figure A.5. The matlab command "logspace" was used to generate the logarithmical spaced nodes and time steps.

A.1.2   Convection

The flow was model as a 1D steady state problem. The heat transport was modeled using the same approach as in the conductive model. Heat generation caused by friction is assumed to be small and is therefore neglected. Integration of the energy equation and applying the previously mentioned simplification and nomenclature yields

$$\dot{m}C_p\left(T_e - T_w\right) = hA_{surface}\left(T_{surface} - T_P\right) + \frac{kA\left(T_P - T_W\right)}{\delta x} + \frac{kA\left(T_E - T_P\right)}{\delta x} \qquad \text{(A.5)}$$

Rewritten using the nomenclature from Versteeg and Malalasekera and using a UP-WIND scheme (eq A.6) yields

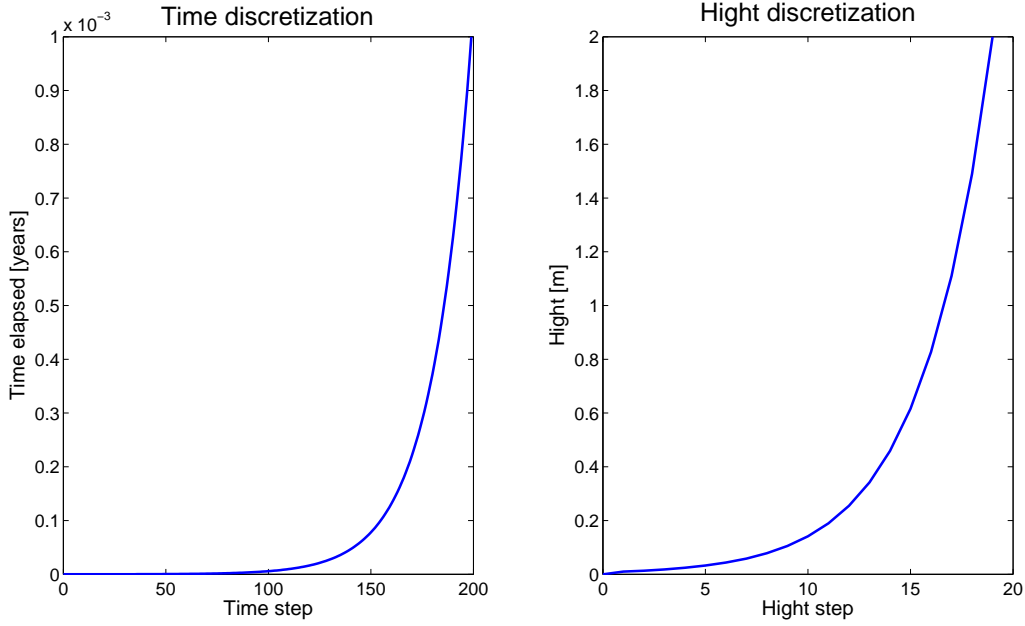**Figure A.5:** Discretisation of time and height

$$a_P T_P = a_W T_W + a_N T_N$$
$$a_P = a_W + a_N$$
$$a_W = \dot{m} C_p$$
$$a_N = h A_{sur}$$
$$T_e = T_P, T_w = T_W \tag{A.6}$$

Heat transfer coefficient

Following the discussion on the heat transfer coefficient from section 1.5.1 is the heat transfer coefficient set to a large number. In other words the heat transfer resistance at the rock/fluid interface is assumed to be negligible.

UPWIND scheme

The UPWIND scheme assumes that the influence from the node upstream is higher than for the node downstream on the node under consideration. This assumptions holds true for one directional flow and flows where the peclet number (equation A.7 is larger than

2 [57]. By using the UPWIND scheme, instead of the central differencing scheme, could the horizontal spacing between nodes be increased without a large increase in error. Thus saving computational time. The assumption of a peclet number larger than 2 typically holds true for a operating EGS.

$$Pe = \frac{\rho u}{k/\delta x} \tag{A.7}$$

where ρ is fluid density, u is flow velocity, k is thermal conductivity and δx is the horizontal spacing between nodes.

Boundary conditions

The inlet temperature is set to a fixed value based on the temperature from the injection wellbore. At the interface between the rock and fluid is the heat flux across the interface used as a boundary conditions. The boundary condition at the fracture exit is set to be zero a heat flux, meaning that the gradient of the temperature profile after the last node is zero.

A.1.3 Pressure drop

The pressure drop model is based on the work done by Cibich in his honors thesis at the University of Adelaide [8], the thesis was done in cooperation with PIRSA[2] Petroleum and Geothermal Group.

Linear flow through the fractures was model as laminar incompressible flow between horizontal parallel plates. Solving the momentum equation and the continuum equation yields

$$\Delta P = \frac{12\mu L q}{h^3 w} \tag{A.8}$$

Where ΔP is the pressure drop across the fracture, L is the fracture length, h is the fracture aperture, w is the fracture width, q is volumetric flow rate and μ is dynamic viscosity of the fluid. Equation A.8 is also referred to as the "cubic law".

In order to account for non-ideal flow conditions (e.g. surface roughness) is friction factor incorporated in equation A.8, resulting in

---

[2]Government of South Australia Primary Industries and Resources

$$\Delta P = f_l \frac{12\mu L q}{h^3 w} \tag{A.9}$$

Louis (1969) developed a friction factor for groundwater flow through joints (eq. A.10)

$$f_l = 1 + 3.1 \left(\frac{\epsilon}{h_f}\right)^{1.5} \tag{A.10}$$

where ϵ is the surface roughness and h is the fracture aperture.

Equation A.8 to A.10 is only valid for laminar flow. The transition from laminar to turbulent in fractures is reported to start at a Reynolds number of 2400 [72].

The pressure drop near the wellbore, due to radial flow, was estimated using equation A.11 and A.12. Equation A.11 is used for converging flow (production wellbore) and equation A.12 is used for divering flow (injection wellbore). The equations are based on Livesey (1960) [73], which is found to correlate best to numerical solutions [8]. Equation A.11 and equation A.12 have been modified to incorporate the Louis friction factor (eq A.10).

$$\Delta P_{rad} = f_l \frac{12\mu q l n \left(\frac{r_e}{r_w}\right)}{h_f^3 \theta} + \frac{3q^2\rho}{5\theta^2 h^2}\left(\frac{1}{r_w^2} - \frac{1}{r_e^2}\right) \tag{A.11}$$

$$\Delta P_{rad} = f_l \frac{12\mu q l n \left(\frac{r_e}{r_w}\right)}{h_f^3 \theta} - \frac{3q^2\rho}{5\theta^2 h^2}\left(\frac{1}{r_w^2} - \frac{1}{r_e^2}\right) \tag{A.12}$$

where q is volumetric flow rate, r_e is external radi of the flow in reservoir, r_w is wellbore radi, θ is degrees of "visible" wellbore in radians ($= \pi$ based on geometry in fig A.6), ρ is fluid density, h is fracture aperture, f_l is Louis friction factor.

The first term in equation A.11 and A.12 account for the viscous effects, whilst the second term accounts for inertia effects as a result of acceleration in radial direction.

The fracture geometry used (fig A.6) results in areas with undefined flow/discontinuities (fig A.7). This can be overcome by defining a correction length δL, that creates a pseudo linear flow flow length to compensate for the area of undfined flow [8]. In this case (following nomenclature in figure A.7)

$$\delta L = 0.5 \left(D - L - 0.5\pi r_e\right) \tag{A.13}$$

The total pressure drop is given by equation A.15, based on the flow geometry given in figure A.7.
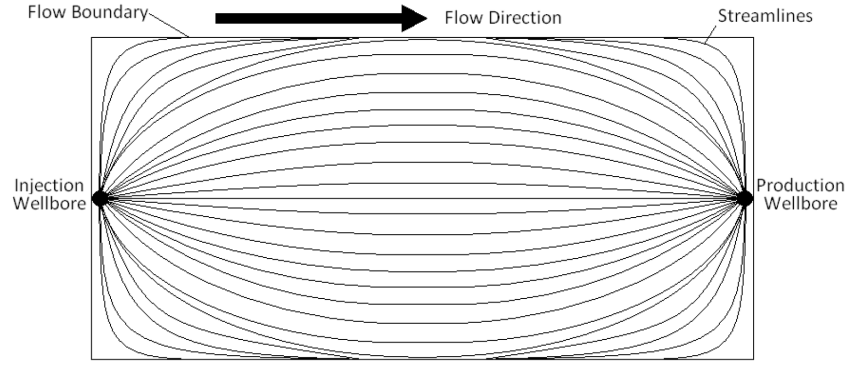
Figure A.6: Idealized fracture geometry with streamlines for source/sink flow, used for pressure drop calculation [8]
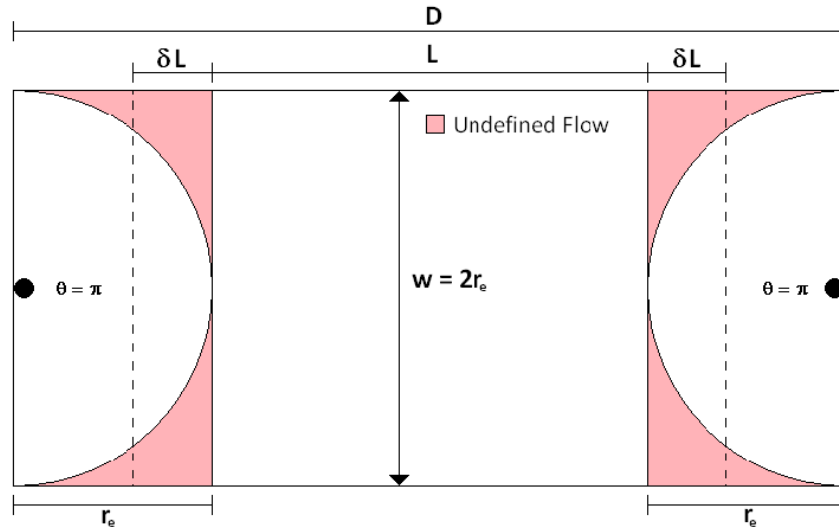

Figure A.7: Approximation of flow geometry [8]

$$\Delta P_{total} = \Delta P_{injectionWell} + \Delta P_{fractureFlow} + \Delta P_{productionWell} \tag{A.14}$$

$$\Delta P_{total} = \frac{\mu q 12 f_l}{h_f^3} \left[\frac{2ln\left(r_e/r_w\right)}{\theta} + \frac{2\delta L + L}{w} \right] \tag{A.15}$$

It can be shown that the effective permeability for such a well configuration is given by [8]

$$k_e = \frac{h_f^2}{12 f_l} \tag{A.16}$$

This approach will not provide accurate estimates of the pressure drop in a fracture.

136

However, that is not the idea either. The total pressure drop is only used to calculate the mass flow distribution between different fracture apertures, the friction factor and flow profile are assumed to identical regardless of fracture aperture. Therefore should the actual value of the pressure drop be of less significance, and some degree of inaccuracy was allowed in order to save computational costs and time.

Mass flow distribution

The mass flow distribution in a reservoir with different fracture apertures was estimated by setting the pressure drop for each fracture equal, and solving for the mass flow.

$$\Delta P_{aperture1} = \Delta P_{aperture2} \tag{A.17}$$

$$\dot{m}_{tot} = \dot{m}_{aperture1} + \dot{m}_{aperture2} \tag{A.18}$$

It is assumed that $\dot{m}_{tot}$ is known. When fracture short circuiting is investigated is the $\dot{m}_{tot}$ determined by the original fracture aperture and pressure drop.

Plots

Figure A.8 to figure A.10 shows the pressure drop, effective permeability and reynolds number for a range of fracture apertures and ϵ/h ratios.
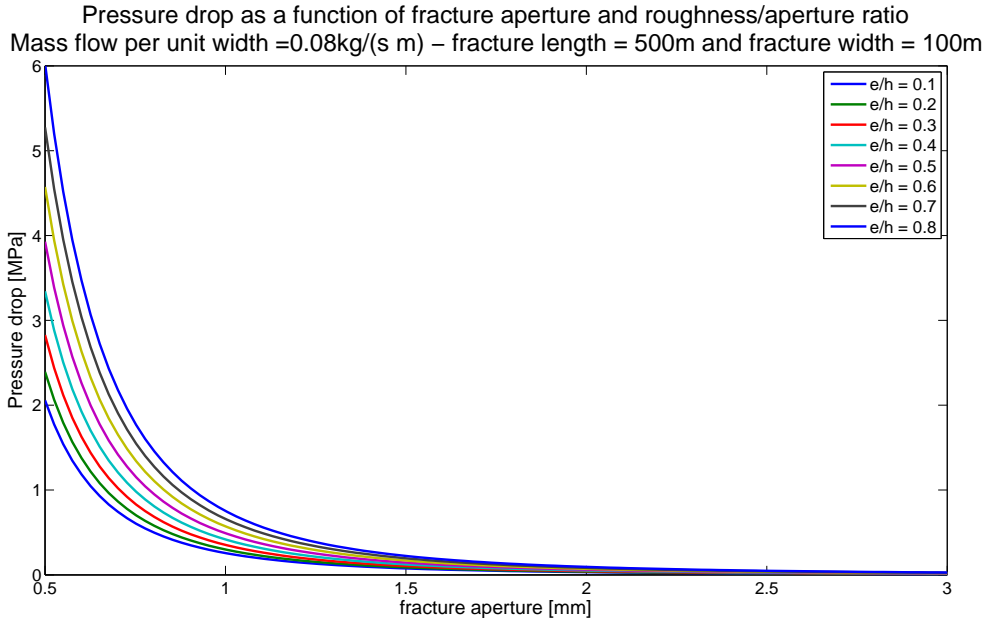
(a) Pressure drop
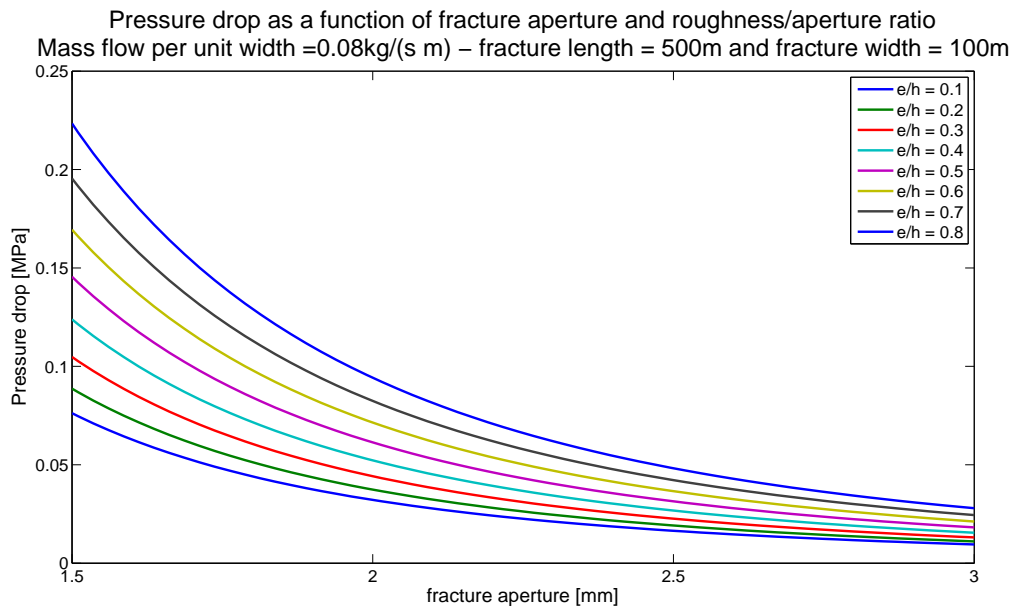
(b) Close up of pressure drop - fracture aperture 1.5 to 3mm

Figure A.8: Pressure drop as a function of fracture aperture and ratio between fracture roughness and fracture aperture
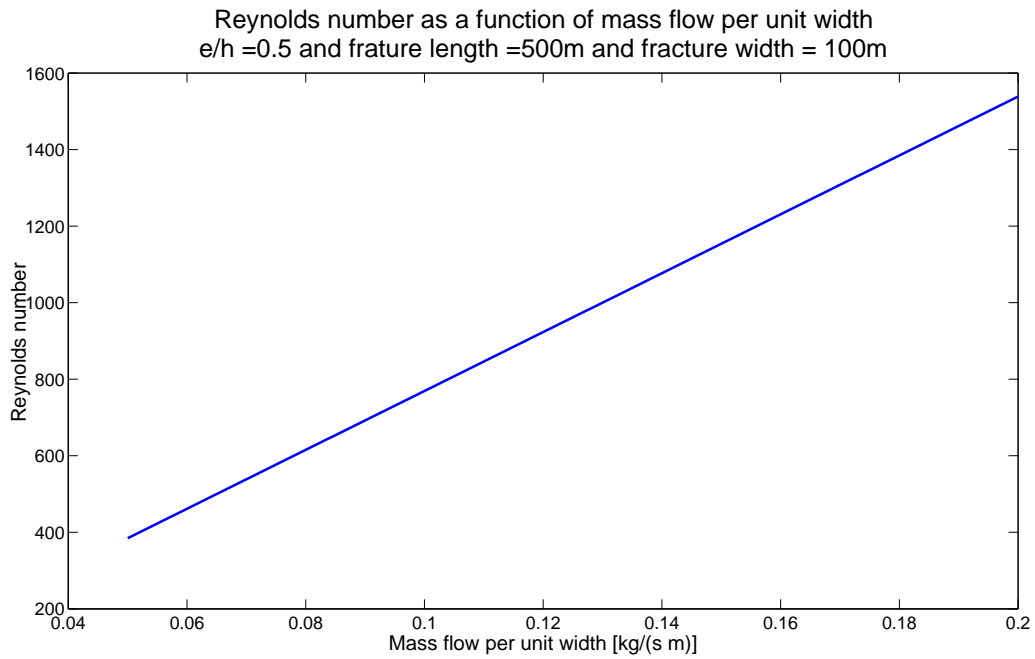
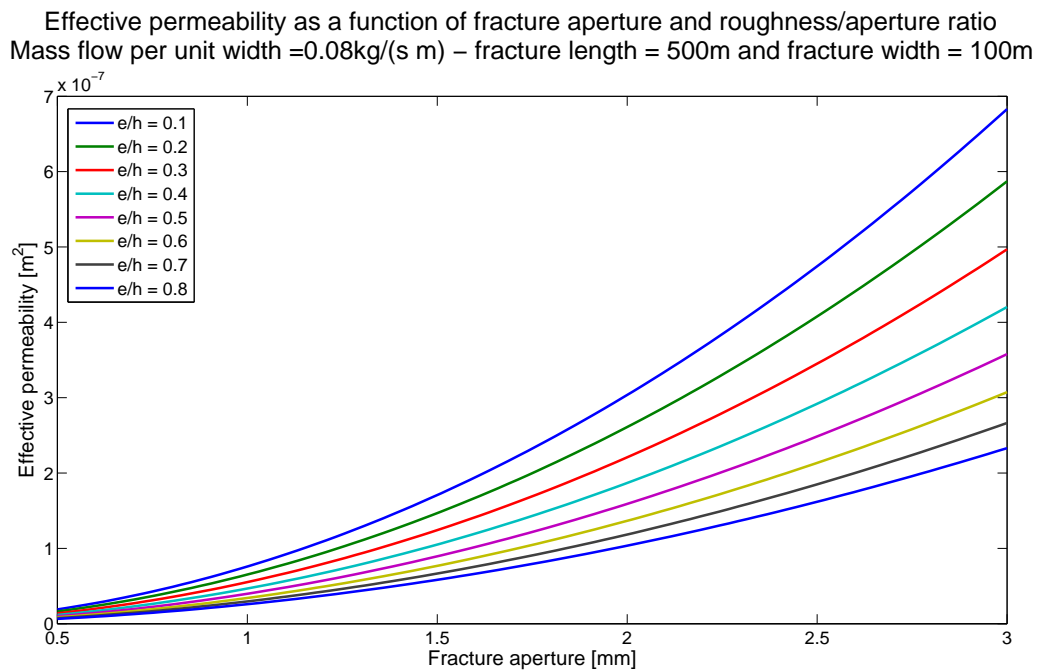**Figure A.9:** Reynold numbers for typical mass flow per unit width flow rates

Figure A.10: Effektive permeability in fracture. Calculated with equation A.16

A.1.4   Temperature dependent properties

The specific heat and thermal conductivity of granite are temperature dependent. The findings by Waples et al (2004) and Clauser et al (1995) are used to estimate the specific heat and thermal conductivity as a function of temperature.

The thermal properties of granite changes little with pressure, compared to temperature, and the effect of pressure changes on properties is therefore neglected in this report [53, 64, 52].

Thermal conduction could vary as much as a factor of two to three [52] at a given temperature, the same is true for specific heat. The reason is the large variation in mineral composition of granite. Since no site specific samples exist from possible locations in Norway is an average value chosen in this study.

The effect of temperature dependent properties, compared to constant properties can be seen in figure A.14(a) and figure A.14(b). Comparing the two figures shows a slightly higher rock formation temperature for temperature dependent rock properties.

Specific heat

Based on the paper by Waples et al (2004) [53] is the following expression used to estimate the specific heat of granite

$$Cp(T) = Cp_{T1}\frac{Cp_{N(T)}}{Cp_{N,T1}} \tag{A.19}$$

where

$$Cp_{N(T)} = 8.95E{-}10T^3 - 2.13E{-}6T^2 + 0.00172T + 0.716$$

where $Cp_{N,T1}$ is measured from experiments at temperature T1. One experimental value is therefore needed in order to estimate the specific heat at any given temperature. Waples et al (2004) [53] provides a table of experimental values of specific heat for granite at 20^0C, with a minimum and maximum value of 600 and 1172 J/kgK respectively.

Equation A.19 is based on a curve fit to normalized Cp values for all nonporous rocks investigated by Waples et al (2004) [53], shown in figure A.11. The values used in the model can be seen in figure A.12.
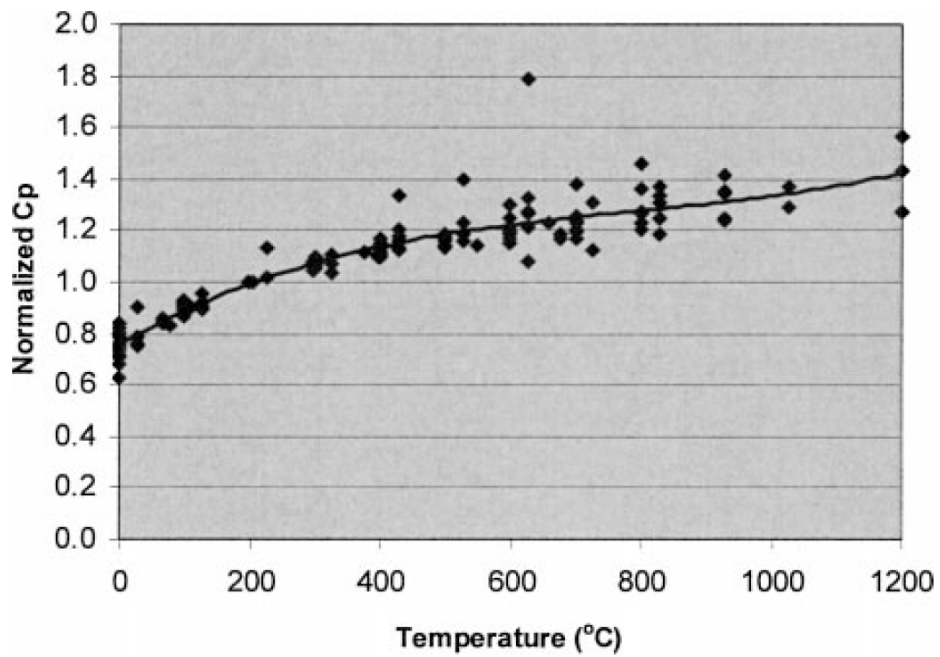
Figure A.11: Normalized specific heat values based on Waples et al [53] - line is based on equation A.19
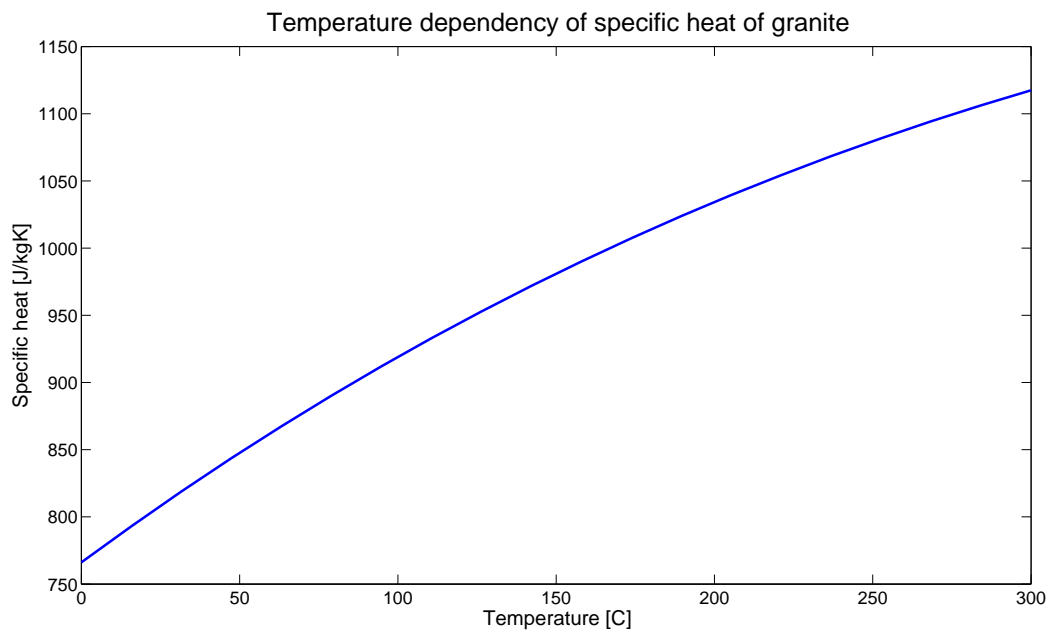

Figure A.12: Temperature dependent specific heat values used in model

Thermal conductivity

Thermal conductivity is assumed to follow the equation developed by Birch and Clark (1940a,b), as given by Clauser et al (1995) [52] (eq. A.20). The equation is believed to yield useful estimates of the temperature dependence of thermal conductivity for crystalline rocks, independent of mineralogy [52].

$$k(T) = \frac{k(0)}{1.007 + T\left(0.0036 - frac0.0072k(0)\right)} \tag{A.20}$$

where

$$k(0) = k(25)\left(1.007 + 25\left(0.0037 - \frac{0.0074}{k(25)}\right)\right)$$

where k(25) is the measured thermal conductivity at room temperature. Based on the paper by Clauser et al (1995) [52] is k(25) assumed to be 3.5 W/mK. How the thermal conductivity changes with a change in temperature can be seen in figure A.13.
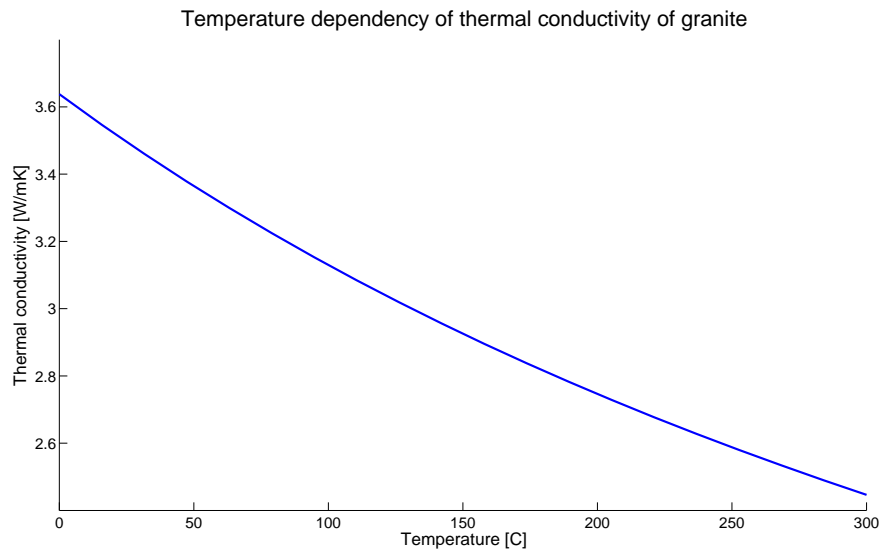
Figure A.13: Thermal conductivity as a function of temperature

Effect on temperature profile

In figure A.14(b) shows the effect of variable parameters compared to using a constant average value for the specific heat and thermal conductivity of granite. In the case shown is the difference small, a few degrees Celsius. However, for other cases could the impact be larger. Temperature dependent properties results in a more realistic model and is therefore used.
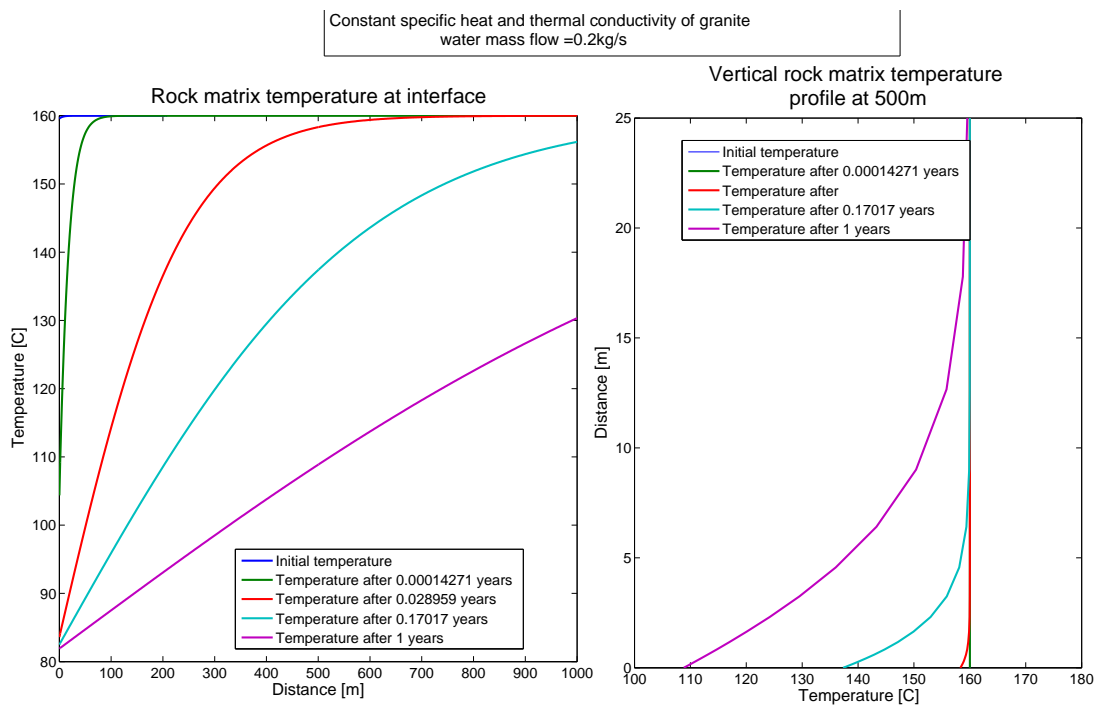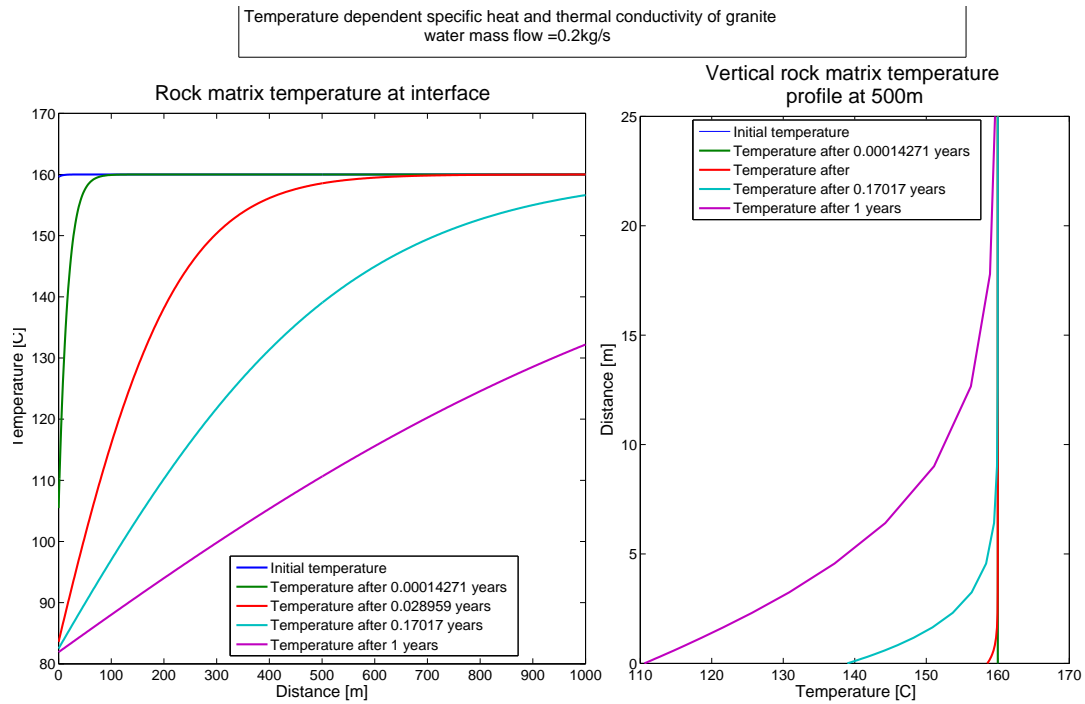
143

(a) Temperature dependent properties

(b) Constant properties

Figure A.14: Effect of constant and temperature dependent properties on rock formation temperature

A.2   Model validation

The model was validated against analytical solutions related that are relevant for a fractured EGS. The results can be seen in figure A.2.1 and figure A.2.1.

A.2.1   Analytical models

In this section are different analytical solutions presented.

Flow between flat plates

The classical heat transfer problem of flow between flat plates at constant temperature was used to validate the convective model. The average temperature of the fluid between two flat plates is given by equation A.21.

$$T = T_{sur} - (T_{sur} - T_{in}) \, exp\left(\frac{-hA_{sur}}{\dot{m}Cp}\right) \tag{A.21}$$

Semi infinite solid

The analytical solution of a semi infinite solid with a convective boundary with a constant temperature fluid was used to validate the transient 2D rock matrix model. The classical solution of a semi infinite solid with a convective boundary is show in equation A.22.

$$
\begin{aligned}
&T\left(x, y, t\right) = \\
&T_i + (T_{inf} - T_i) \left[erfc\left(\frac{y}{2\sqrt{\alpha t}}\right) - exp\left(\frac{hy}{k} + \frac{h^2\alpha t}{k^2}\right) erfc\left(\frac{y}{2\sqrt{\alpha t}} + \frac{h\sqrt{\alpha t}}{k}\right)\right]
\end{aligned}
\tag{A.22}
$$

Analytical solution of fractured EGS

There exist a number of analytical solution efforts [42]. The analytical solution presented in this paper is based on the report of Wunder and Murphy (1978), as presented by Sutter et al (2011) [27].

Several assumptions are made in order to derive a analytical expression for the heat transfer mechanism in a single fracture. The following assumptions were made by Sutter et al (2011) [27].

- The rock extends to infinity in y-direction and z-direction. (fig. 2.2)

- Temperature variation in the water in y-direction is insignificant, since fracture height is very small compared to fracture length. The water temperature is equal to the rock temperature at y=0.

- Conduction in the x-direction and z-direction in both the fracture and rock formation is neglected. Heat transfer occurs only by conduction in the rock in y-direction and forced convection along the x-direction in the fracture.

- The rock and water properties is assumed to be constant

- The static fluid pressure in the fracture is set to exceed the vapor pressure of water by a large enough margin to keep the fracture in single phase flow.

The one dimensional differential energy equation within the rock yields

$$\frac{\delta T}{\delta t} - \alpha \frac{\delta^2 T}{\delta y^2} = 0 \tag{A.23}$$

where

$$\alpha = \frac{k_r}{\rho_r C_{p,r}}$$

The heat transfer resistance at the rock/fluid interface is assumed to be negligible. $T(y = 0, x, t)$ will therefore describe both the rock surface temperature and fluid temperature. The temperature dependency on x is introduced with equation A.24.

$$\rho_w C_{p,w} b \frac{\delta T}{\delta t} + \rho_w C_{p,w} U b \frac{\delta T}{\delta x} = k_r \frac{\delta T}{\delta y}\big|_{y=0} \tag{A.24}$$

Where U is the flow velocity of water, b is half-width of the fracture, ρ_w and $C_{p,w}$ is the density and specific heat of water. The boundary conditions used are

$$T(y = 0, x = 0, t) = T_{w,0}$$
$$T(y \to \infty, x, t) = T_{r,0}$$

and the initial condition is

$$T(y, x, t \leq 0) = T_{r,0}$$

The analytical solution of this problem is

146

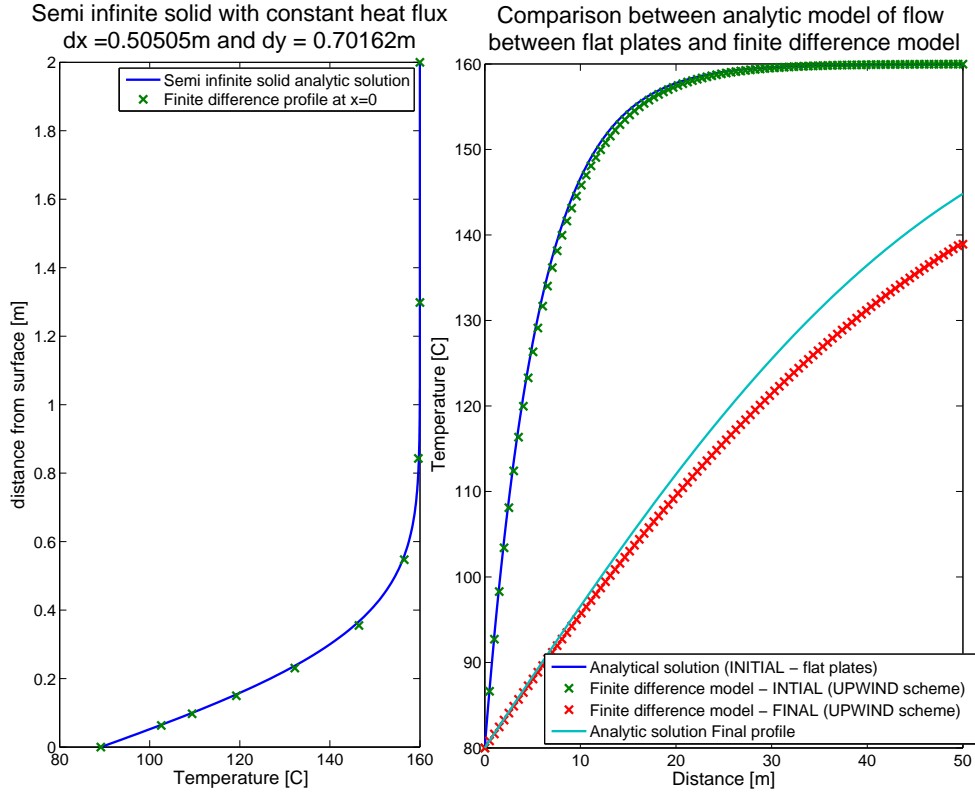**Figure A.15:** Validation of finite volume model

$$\theta(x, y, t) = \frac{T(x, y, t) - T_{w,0}}{T_{r,0} - T_{w,0}} = erf\left(\frac{y + \beta x}{2\sqrt{\alpha t}}\right) \tag{A.25}$$

where

$$\beta = \frac{k_r}{\rho_w C_{p,w} U b} \tag{A.26}$$

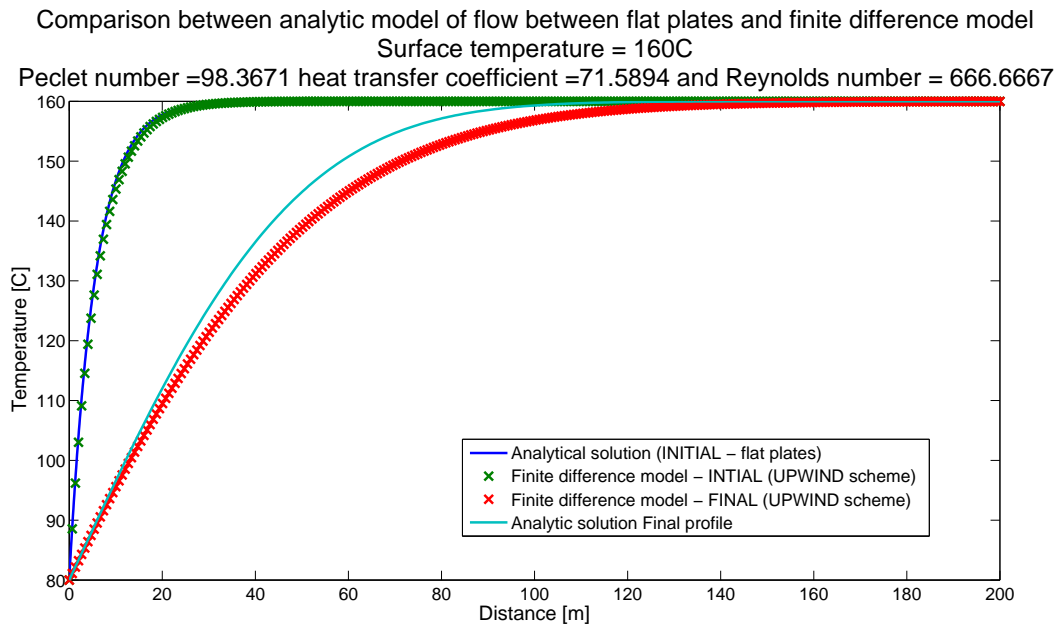Equation A.25 is referred to as the analytical EGS equation throughout this paper.

Figure A.16: Finite Volume model compared against analytical solution of flat plate and analytical solution by Cheng et al.

A.3   Mesh adjustment

Several different mesh sizes were tested in order determine the minimum mesh size that yields accurate results. The number of nodes directly effects the computational time of the model and since several different operating conditions and parameters will be simulated is it critical to keep the computational time at a minimum. The accuracy of different mesh sizes were therefore investigated. The result can be seen in figure A.18. It can be seen from the figure that the temperature profile varies little with a increase in dx and dy, the equidistant spacing between the nodes is therefore kept between 1-2m in x-direction and around 1m in y-direction.

The same type of investigation was conducted in order to keep the number of time steps to a minimum, while maintaining accuracy. A set of simulations where conducted where the number of time steps and mass flows were varied in order to see the effect on the outlet temperature. The number of nodes in x and y direction were kept constant, with average dx and dy within the 2m and 1m respectively. The results can be seen in figure A.17. The effect on the outlet temperature when the number of time steps is reduced from 10 000 to 500 is negligible. The reason is the that the time steps are logarithmically spaced and the steps are small when the temperature gradients are large. When the temperature gradients are small are the time steps large, however since the gradients are small is the error induced by large time steps on the outlet temperature negligible.

The reduction in total number of nodes and times steps due to logarithmic spacing drastically reduced the computational time. Accurate results for a model with a rock matrix of 800m x 25m over 30 years could now be calculated in about 0.5 minutes, which was a drastic improvement compared to linearly spaced nodes.

The analytical and FVM temperature profile starts to deviate around 4 years for a mass flow of 0.2 kg/s and around 7-10 years for a mass flow of 0.02kg/s. The reason is that the analytical profile is based on the assumption of a semi infinite solid, which no longer holds true at the respective times. Since the fractures are spaced a finite length will the temperature profiles interact and the temperature at T(x,y=H,t) start to drop below the initial temperature.
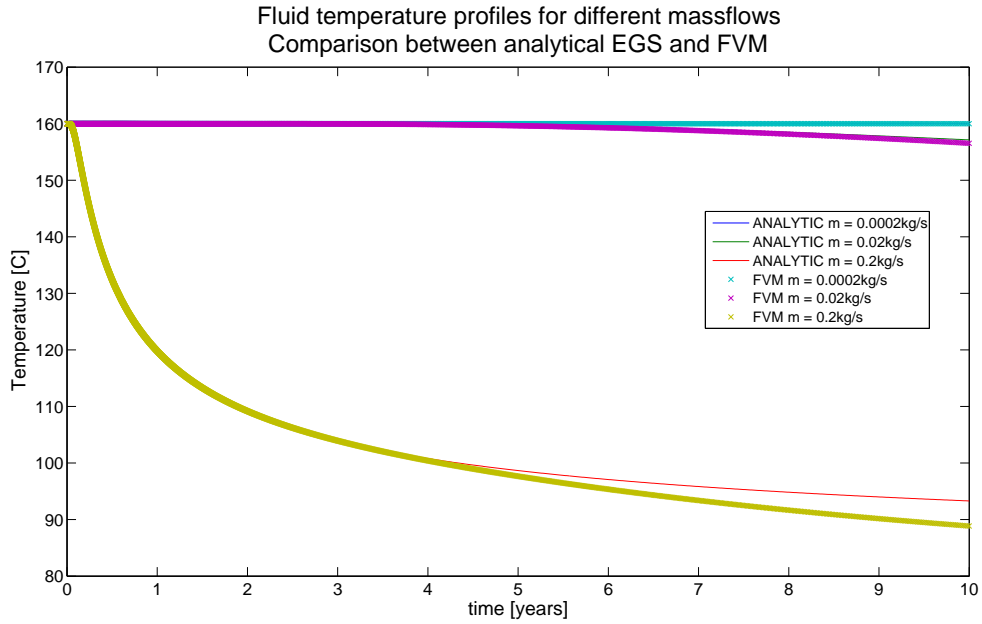
(a) Outlet temperature over 10 years with 10 000 time steps
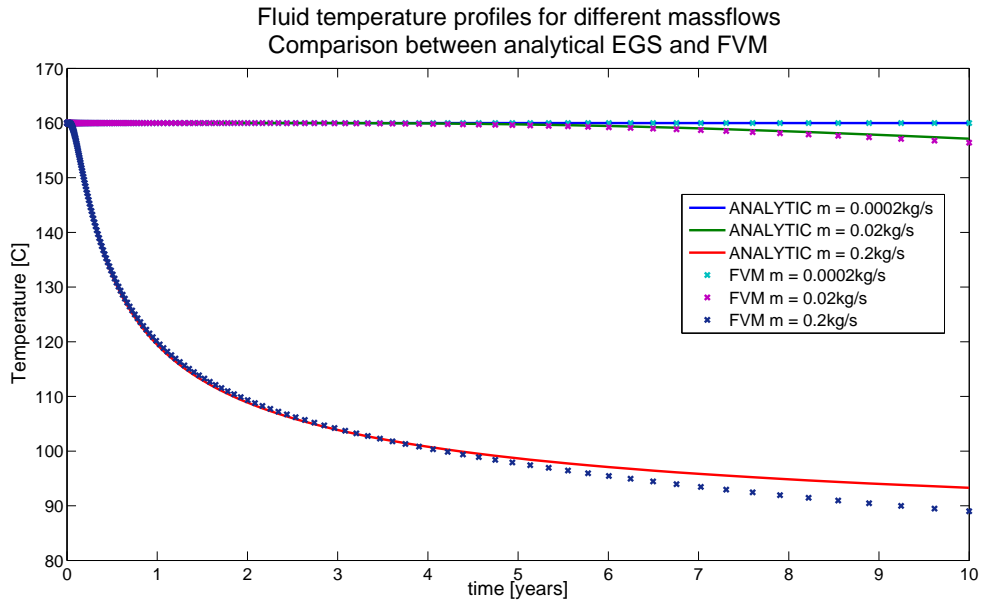
(b) Outlet temperature over 10 years with 500 time steps

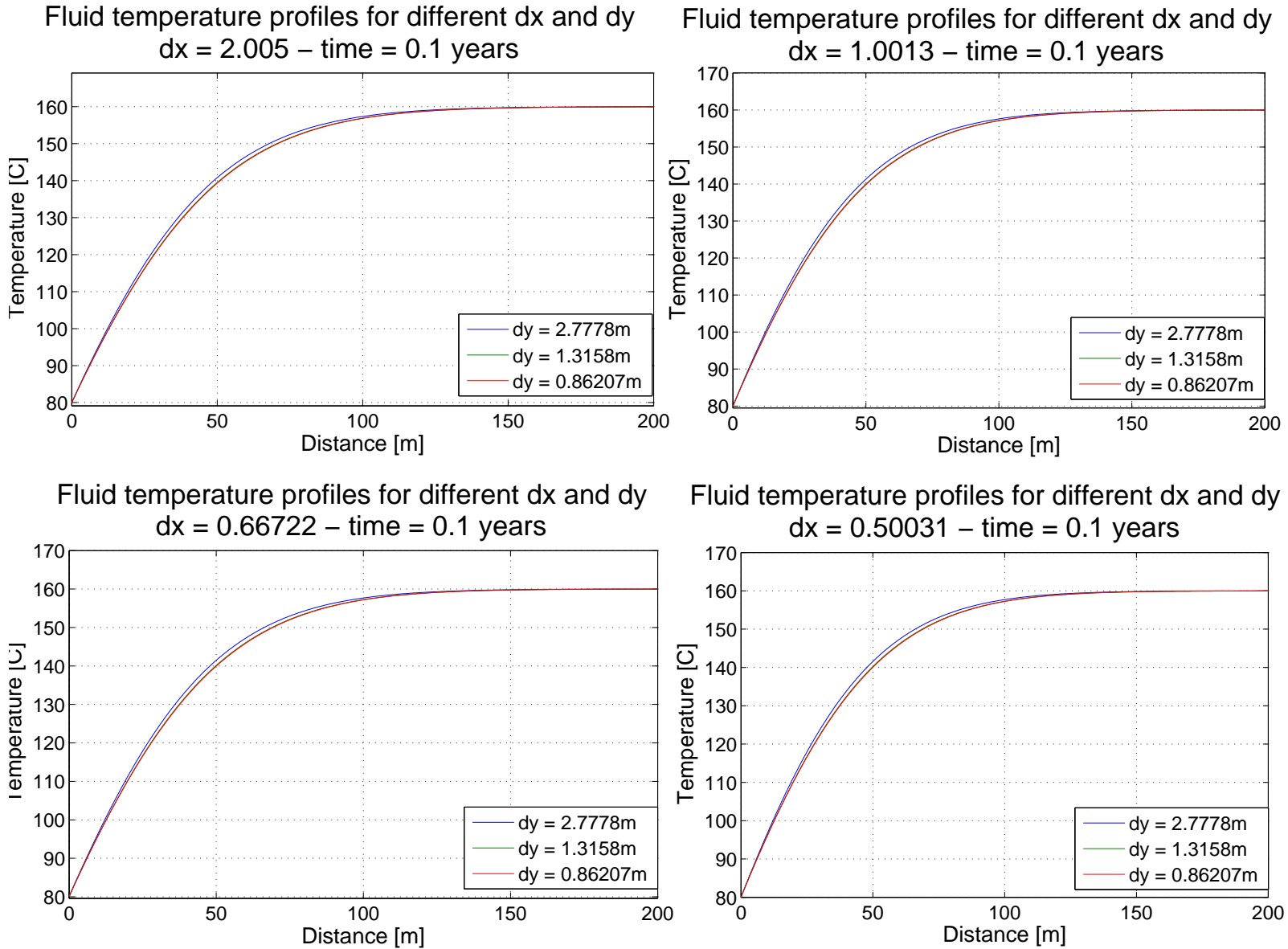**Figure A.17:** Outlet temperature dependency on number of time steps

Figure A.18: Effect of different dx and dy on model accuracy

A.4 Computational time

The computational time per cycle, one solution of the linear system $AT = b$ with n number of nodes, where investigated in order to find the least time consuming solver in matlab. The result for five different solvers can be seen in figure A.19. Based on these results were the direct solution, using the matlab operator "mldivide", chosen.

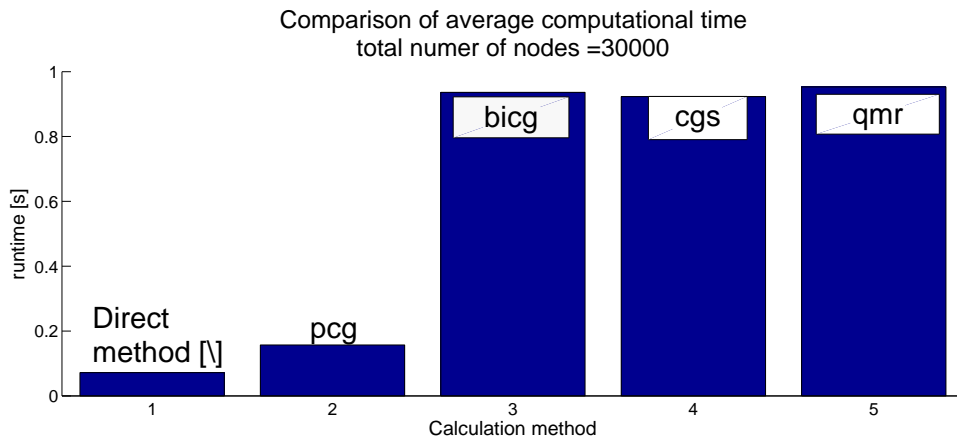Computational time as a function of number of nodes is shown in figure

Figure A.19: Cycle time for different matlab solvers
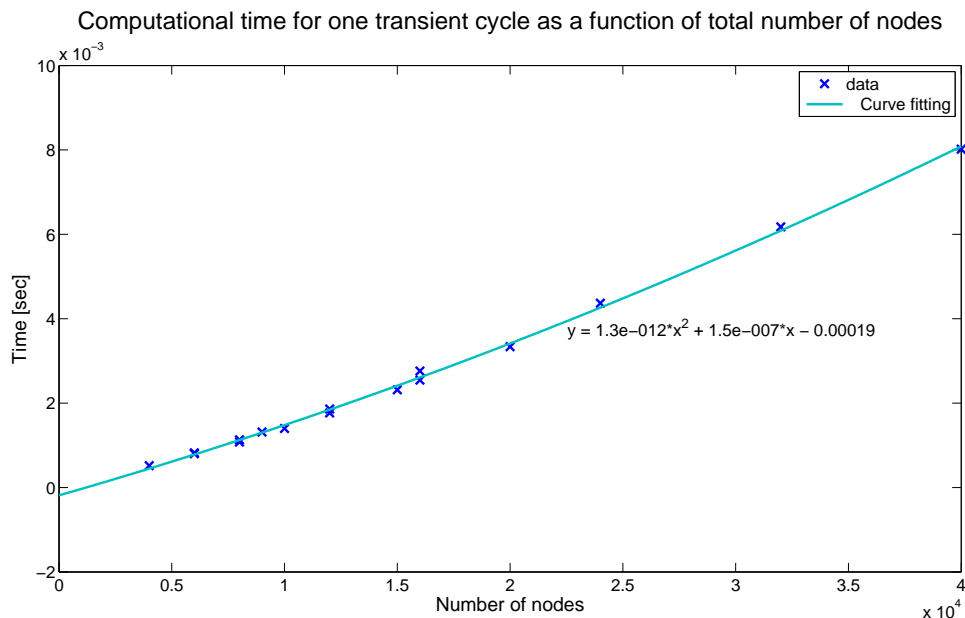

Figure A.20: Cycle time as a function of number of nodes

Appendix B

Wellbore model

Ramey's well known paper [51] on wellbore heat transmission from 1962 was used as basis for the wellbore heat transfer model that was developed in this thesis.

Ramey's solution is simple analytical expression, which requires little computational efforts. Ramey's solution is a excellent approximation for the heat transfer in a vertical wellbore except for at early transient periods [63].

Ramey's analytical solution was used instead of a numerical solution since it gives relative accurate results in the time period under consideration at low computational cost. The alternative would have been a numerical models, however the extra detailed added by such models was deemed unnecessary and would only lead to a more complicated model without increasing the area of application of the model.

Following the original notation and nomenclature of Ramey is the temperature in the wellbore given by (for a liquid)

$$T(y,t) = aZ + b - aA + (T_0 + aA - b) \, exp\left(\frac{-y}{A}\right) \tag{B.1}$$

where

$$A = \frac{\dot{m}C_{p,w}\left(k_r + r_1 U f(t)\right)}{2\pi r_1 U k_r} \tag{B.2}$$

$$T_0 = ay + b \tag{B.3}$$

$$f(t) = -ln\left(\frac{r_2^1}{2\sqrt{\alpha t}}\right) - 0.290 \tag{B.4}$$

T_0 is a linear approximation of the geothermal temperature gradient, however the solu-

tion is not limited to the assumption of a linear temperature profile. A linear geothermal temperature profile was assumed in this thesis. The assumption of linear geothermal profile is not entirely correct, however the error induced by the assumption is deemed negligible compared to the other assumptions done in the model.

Evaluation of the overall heat transfer coefficient (U) is the most difficult step involved on wellbore heat-transmission problems. The overall heat transfer coefficient can be simplified to equation B.5 assuming a simplified wellbore with one casing. This procedure to find the overall heat transfer coefficient is only valid at large values of the Fourier dimensionless time (eq. B.6) [63].

$$\frac{1}{U} = \frac{1}{h} + \frac{r_2 - r_1}{k} \tag{B.5}$$

The heat transfer coefficient between the circulation fluid and the casing was estimated by using the classical analytical solution of flow in a smooth circular tube with variable heat flux boundary. The nusselt number for both a laminar and turbulent flow was taken from "Convective heat transfer and mass transfer" by Kays, Crawford and Weigand [65]. The nusselt number in laminar flow was assumed to be 4.36, thermal entry length was neglected. For turbulent flow was the nusselt number assumed to be that of a constant temperature boundary, this is a valid assumption since the nusselt number for constant surface temperature and heat flux is the same for turbulent flow with prandtl numbers above 1, see figure $14 - 5$ in [65]. The thermal conductivity of the casing was assumed to equal to that of steel (AISI 1000).

Ramey's solution is not valid at early times, as it has a tendency to over predict the temperature [63]. This is a known problem with Ramey's solution, however since it only effects the early times should the implication be small on the total system performance. The length of "Early time" was quantified by Hagoort [63], and is given by the dimensionless Fourier number in equation B.6. Ramey's solution over predicts the temperature for dimensionless Fourier times below 1 [63].

Dimensionless Fourier time is given by

$$t_{DF0} = \frac{k}{r_{cf}^2} \tag{B.6}$$

The equation is based on taken from the paper by Hagoort (2004) [63]. k is the heat diffusivity of the system and r_{cf} is the radius of formation inner boundary (interface casing and formation).

effect of mass flow, time and insulation

The effect of different mass flows and operating times on the wellbore temperature were investigated. From figure B.1 and figure B.2 is it evident that the mass flow have major impact on the temperature profile in the wellbore. Which is natural since less energy is needed to increase or decrease the bulk fluid temperature for small mass flows. An increase in mass flow will therefore make the wellbore temperature profile less dependent of the geothermal gradient and more dependent on the inlet temperature.

As the operating time increases will the rock near the wellbore be either cooled down or heated up depending on the relative temperature difference between rock formation and inlet temperature in the wellbore. The effect can be seen by comparing figure B.1(a) and figure B.1(b). The bottom hole temperature in the injection wellbore approaches the inlet temperature, which is logical since the formation temperature approaches the inlet temperature.
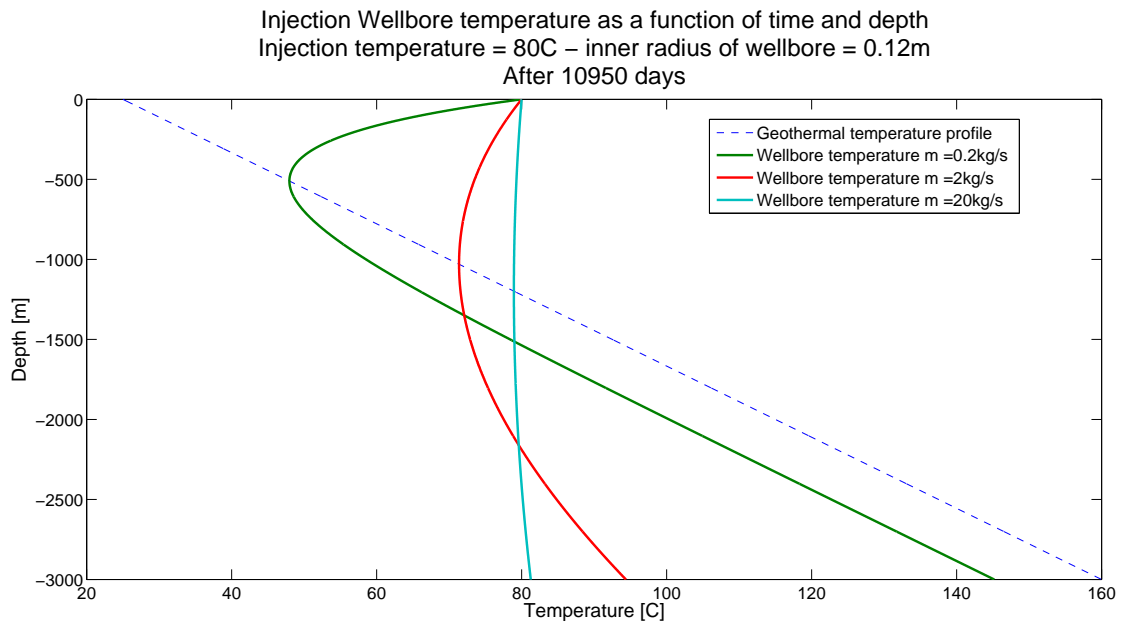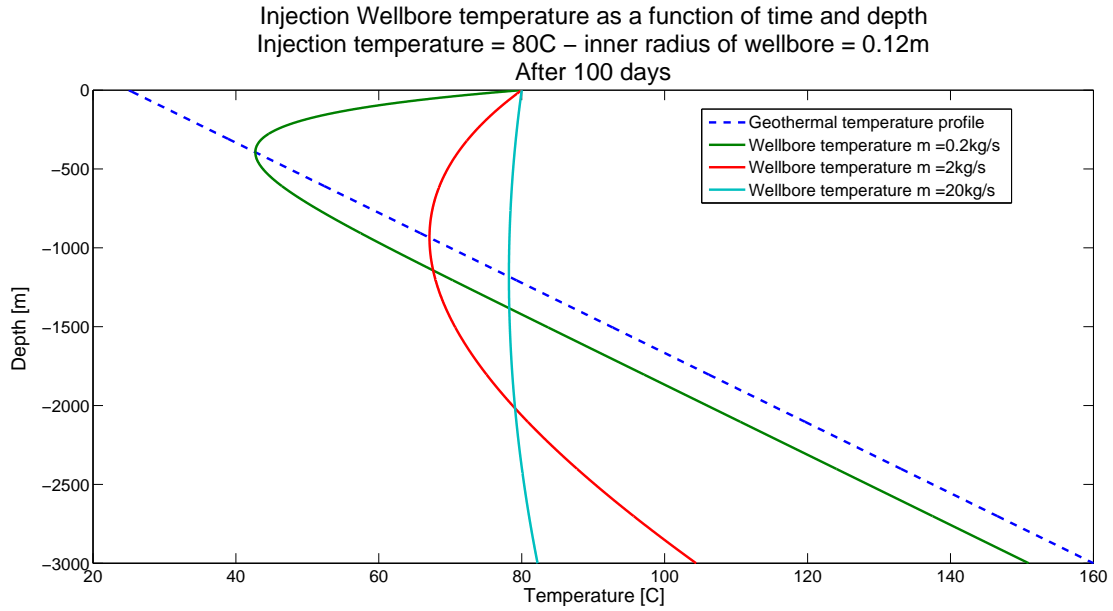
(a) Injection wellbore temperature profiles for different mass flows after 100 days

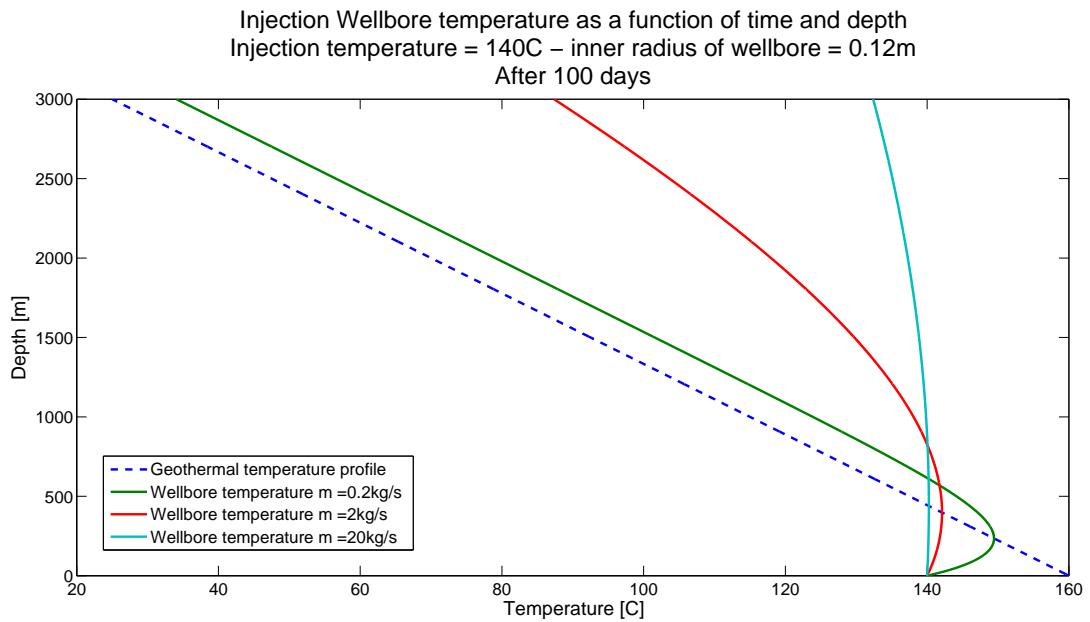(b) Injection wellbore temperature profiles for different mass flows after 30 years

Figure B.1: Injection wellbore temperature profiles for different mass flows and different times

(a) Temperature profile with bottom hole temperature equal to initial formation temperature

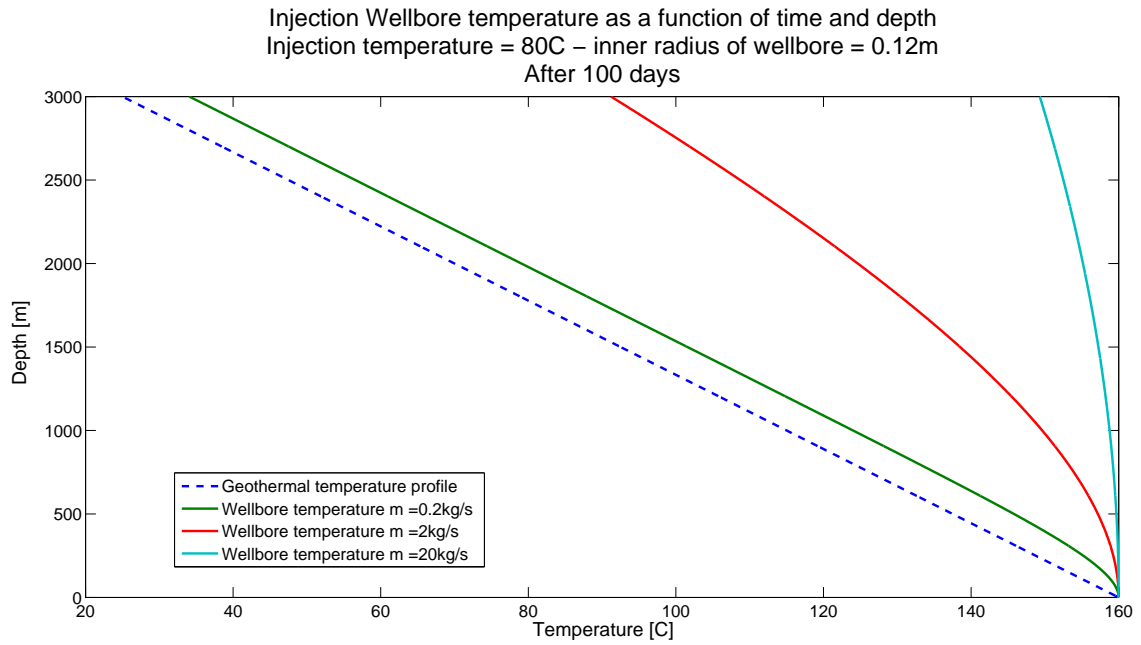(b) Temperature profile with bottom hole temperature lower than initial formation temperature

Figure B.2: Production wellbore temperature profile for different mass flows

Appendix C

Overview of EGS projects

A brief overview of most of the EGS projects world wide are listed in table C.1.

Name	Location	Bedrock type	System type	Purpose
Fenton Hill	New Mexico, USA	Granite	Multiple well w/fracture	General R&D
GeneSys Concept	Northern Germany	Sandstone	Single well w/fracture	Exploitation of old oil and gas wells for direct use
Gross Schöneback	Germany	Sandstone	Multiple well w/Fracture	Fracture in sandstone using proppants
Soultz	Alsace, France	Granite	Multiple well w/Fracture	General R&D and power production
Bruchsal	Germany	Aquifer	two well aquifer	Hydraulic and hydrochemistry
Paralana Project	South Australia	sediments	Multiple well w/fractures	multiple stimulations in sediments
Cooper Basin	South Australia	Granite	Multiple well w/fractures	
Landau	Germany	Aquifers/faults /crystaline basement	Multiple well w/fractures	
Rosemanowes	Penryn, UK	Granite	Multiple well w/Fractures	General R&D
Hijiori	Honshu Island, Japan	Volcanic rock?	Multiple well w/Fractures	Test EGS concept in Japan
Ogachi	HonshuIsland, Japan	Grano-diorite	Multiple well w/Fractures	
Bad Urach	Germany	Crystalline rock	Multiple well w/Fractures	
Falkenberg	Germany	Granite		Hydraulic test
Coso	USA			
Desert peak	USA			
Fjallback	Sweden			
Basel	Switzerland	Granite	Multiple well w/Fractures	
Le Mayet de Montage	France	Granite		
Horstberg	Germany		one well	
Gross Schoneback	Germany	Sandstone	Fracture w/proppants	

Table C.1: Overview of EGS projects

Appendix D

Reservoir and fracture properties

In this Appendix are the parameters used in different studies related to EGS reservoirs presented. The idea is to give the reader a overview the typical values used in a EGS simulation.

D.1   Fractures

There are basically three different types of fractures; opening, sliding and tearing (figure D.1). Observartions at Soultz suggests that most of the transmissibility in a EGS is created when preexisting fractures fail in shear (sliding and tearing fractures) [9]. Opening fractures could occur in the stimulated zone near the wellbore, however they do not correlate with increased fluid flow [9]. The reason is that these fractures typically only extend a short distance from the well and do not contribute significantly to the fluid flow.

Figure D.1 and figure D.3 shows the distribution measured fracture apertures. The fracture aperture distribution shown in figure D.3 are measured based on the thickness of the hydrothermal deposits, which more or less reflect the importance of past fluid circulation. The frequency peaks around 0.5mm and 1mm are largely due a bias introduced by the technique used (as uncertain measurements was rounded off to 0.5 or 1mm).
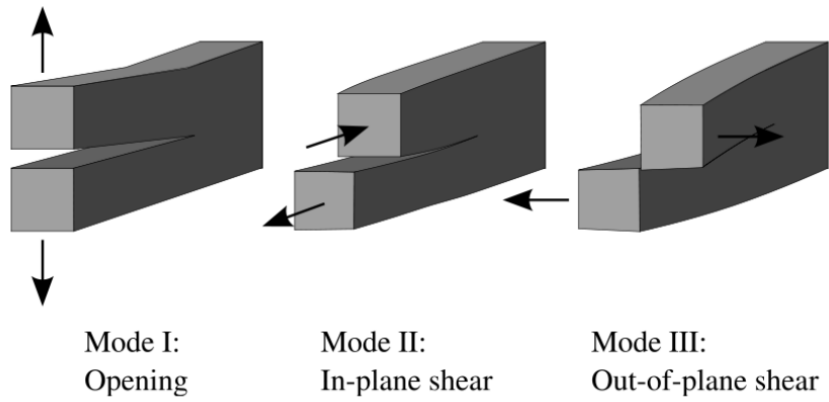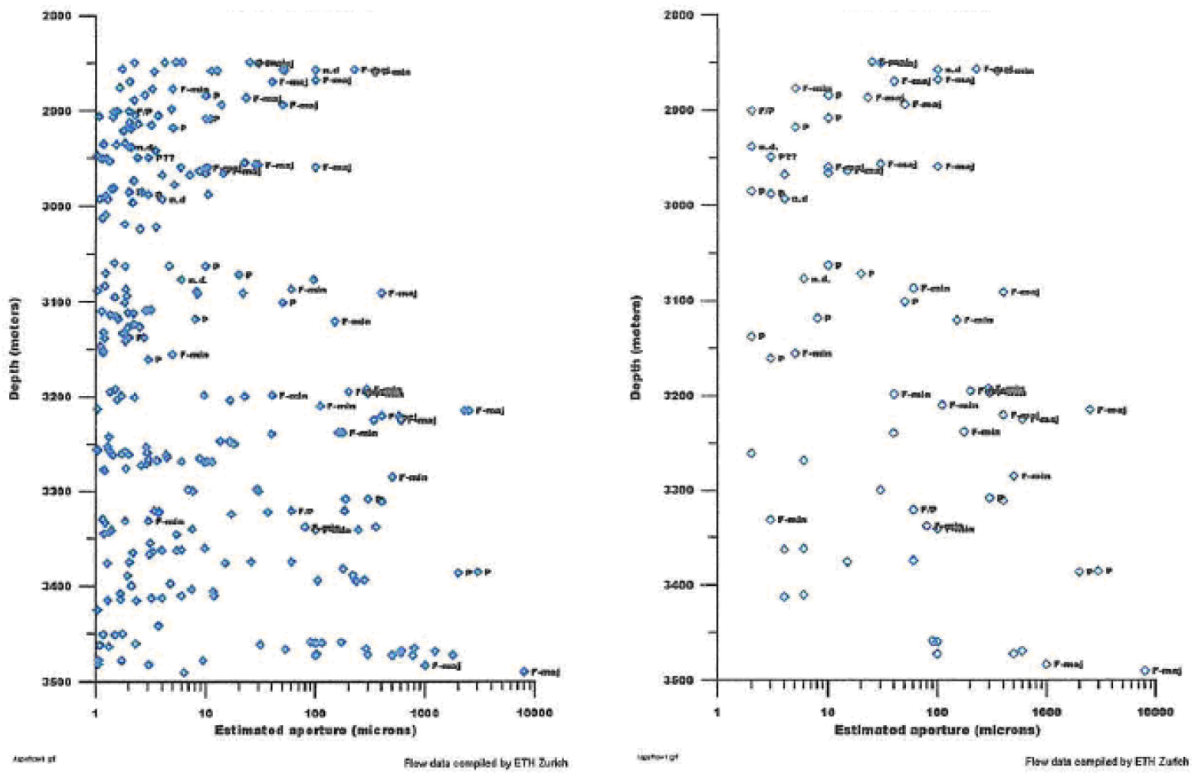
Figure D.1: Different types of fractures [9]

Figure D.2: Fracture aperture (in microns) as a function of wellbore depth (2000 - 3500m). Fractures that were conductive after hydraulic stimulation are labeled. [9]
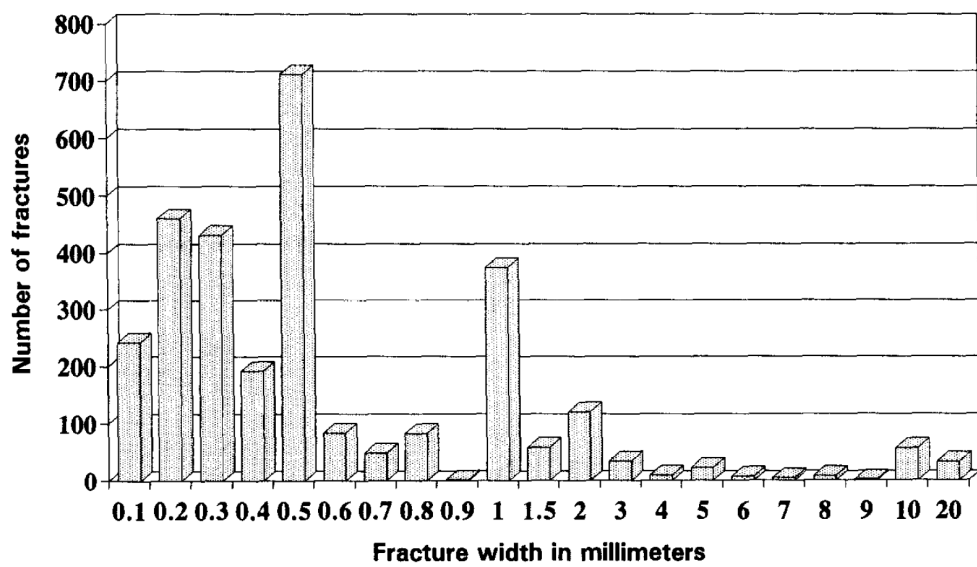
Figure D.3: Frequency histogram of fracture aperture measured on core sections [10]

D.2 Typical parameter values in literature

The data from several papers have been tabulet in order to give the reader a overview of the typical range of different EGS parameters.

Paper	fracture aperture [mm]	flow velocity [m/s]	Pressure drop [MPa]
Bodvarsson et al (1982) [32]	0.1		
Ogino et al (1999) [38]	1		
Remoroza et al (2011)[3] [31]	0.5 - 2		2
Shaik et al (2011)[2] [66]		1.5E-5 - 2.5E-5	14
Sutter et al (2011)[2] [27]		1.33E-4	$10^{-9}m^2$
Karvounis et al (2011) [67]		assumed Re<1	
McDermott et al (2006)[2] [68]	0.0264		20
Pruess (2006) [29]			2
Stoddard [60]	3.25,5		
Zimmermann [61][2]	average 5 - max 10		
Tao et al [69]	1 - 3		
Perez et al (2011)[1] [70]	5		27 125 mD $(2.67E - 11m^2)$
Cheng et al [42]	3	5E-3	
Fu et al[2] [71]	0.5	0.002 - 0.00593 $[m^3/(sm)]$	9 - 15

[1]Pressure drop given as permeability, Darcy's law used to calculate pressure drop

[2]Used Darcy to calculate pressure drop

[3]CO_2 as circulation fluid

Table D.1: Parameters used in different studies

Data used by Cibich [8] to simulate flow in the fractures at the Hijiori site is tabulated below.

Parameter	Unit	Value
fracture width	m	15-65
Aperture	mm	0.15-0.24
roughness	mm	0.1 - 0.15
Louis friction factor		2.68
Volumetric flow rate through fracture	m/s	0.0828 - 0.235

Table D.2: Data from Hijiori HDR project (as given by Cibich [8])

Appendix E

Brief introduction to geology

This appendix gives a brief introduction to the geological terms that are used in this thesis. Most of the information is based on the report: Basic Petroleum Geology and Log Analysis, by Halliburton [11].

E.0.1 Basic geology

First of all, there are three basic rock types; igneous, metamorphic and sedimentary rocks. The three basic categories are grouped after how the rock was formed and they are therefore typically found at distinct places and layers. There are large differences in rock properties between each group, however there are also differences between rocks in the same category. For example will shale and sandstone show large differences in permeability and porosity, even though both are sedimentary rocks.

- **Igneous rocks** are formed from the crystallization of molten rock (magma or lava) from within the earth's mantle. Examples are granite, basalt,

- **Metamorphic rocks**. These rocks are formed from pre-existing rocks, as a result of change in pressure, temperature, shearing stress and/or chemical environment. Examples of such rocks are; slate, marble and schist.

- **Sedimentary rocks** are formed as sediments, either from eroded fragments of older rocks or chemical precipitates. Examples are; shales, sandstone, limestone, dolomites, evaporites. These rock types typically overlay igneous rocks, such as granite. Shales and evaporite layers are typically regarded as impermeable surfaces, which could form traps and boundaries.
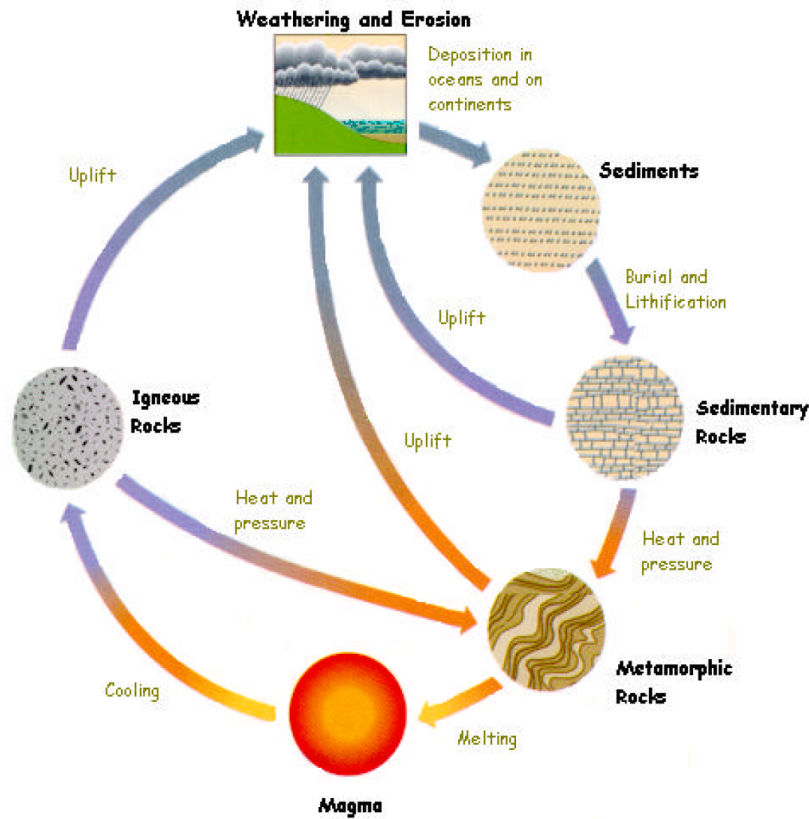
Figure E.1: Geological cycle [11]

Crystalline rock are rocks that have been crystallized. The term is not restricted to a single rock type, both igneous rocks and metamorphic rocks could be crystalline rocks. However, the process and degree of crystallization differ. Granite is a igneous rock that have cooled very slowly under great pressure and have completely crystallized, which is a magmatic process. Meta-schist is a example of a metamorphic rock that have been recrystallized, meaning it have developed from a sedimentary rock through a metamorphic process.

Minerals are the buildings blocks of a rock. Some common minerals are; feldspar, quartz and calcite. Granite, which often is the rock type in geothermal reservoir that could be used for EGS, is rich on feldspar and quartz. However, the percentage of feldspar and quartz in granite depends on the site and physical process that the rock have been subjected to. The difference could be substantial between different locations, which can cause the physical properties of granite to vary by several factors, depending on its specific mineral composition [53].
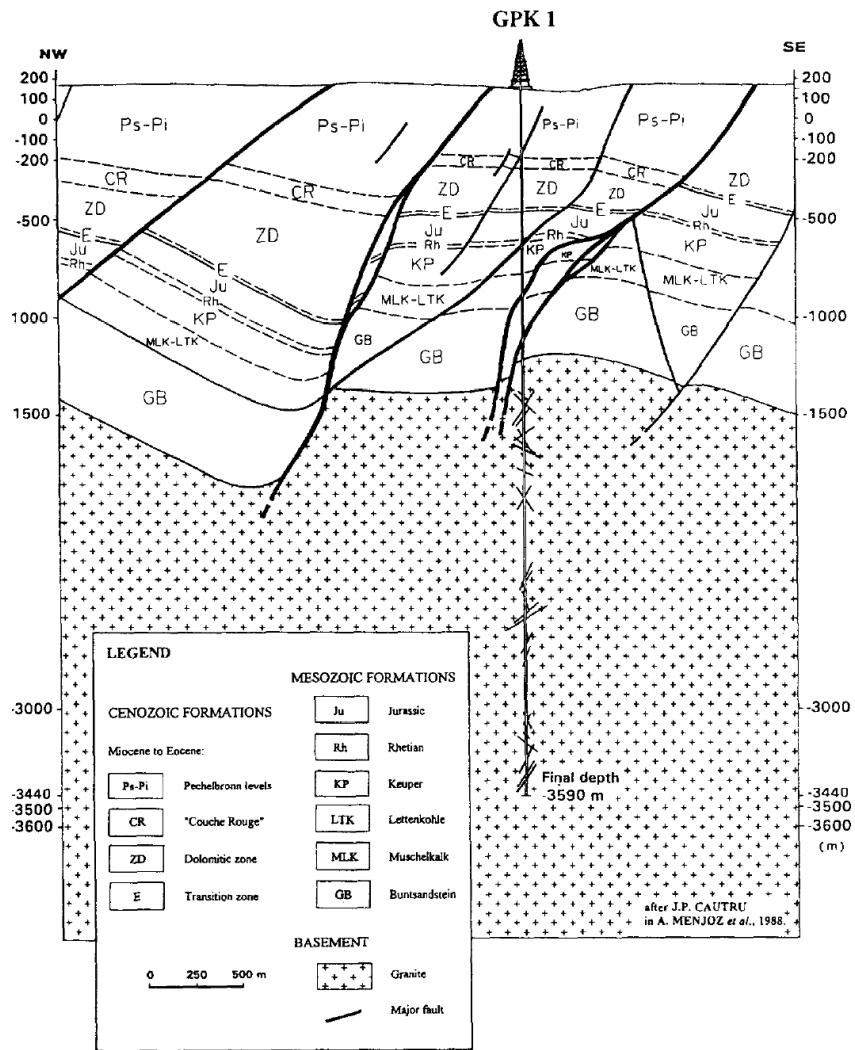
Figure E.2: Typical EGS geology layers [10]

Typical geological conditions at a EGS site is shown in figure E.2.

167

E.0.2 Terms and definitions

- **self-propping** This behavior is attributed to asperities present along the fracture planes, as well as the rock block shifts during injections [74]

- **Porous layer** Is a layer in the rock formation where a relative high degree of porosity is observed.

- **Fracture zones** A layer in the rock formation where a cluster a different fractures are observed.

- **Faults** is a planar fracture or discontinuity in a volume of rock, across which there has been significant displacement. [56]

- **Joints** refers to a fracture in rock where the displacement associated with the opening of the fracture is greater than the displacement due to lateral movement in the plane of the fracture (up, down or sideways) of one side relative to the other. [56]

- **Stimulated** Meaning that the reservoir have been artificially altered to improve permeability

- **Proppants** Sized particles mixed with fracturing fluid to hold fractures open after a hydraulic fracturing treatment [55]

- **Hydraulic fracturing** Water, or other types of fluid, is pumped at high pressures down the wellbore in order to fracture the rock in either shear or tensile stress.

- **Working fluid** is the working fluid in the power cycle.

- **Circulation fluid** is the fluid flowing in a loop between the reservoir and top site heat exchanger.

- **Annulus** The space between two concentric pipe strings, such as between the production tubing and casing in a well. The term may also refer to the space between a pipe string and the borehole wall in an open hole completion or open hole drillstem test (DST).[55]

- **permeability** is measure of easily a fluid flows through the formation/rock. Which depends both on the rock and fluid properties.

168

- **porosity** is the ratio of void space in a rock to the total volume of the rock. Porosity is mathematically expressed as: $porosity(\phi) = V_{void}/V_{total}$

- **resistivity** is a measure of how strongly a material opposes the flow of electric current [56].

- **shear stress** is defined as a stress which is applied parallel or tangential to a face of a material [56].

- **Water saturation** is the ratio between water and void space. Mathematical defined as, $S_w = V_water/V_void$.

- **Hydraulic conductivity** symbolically represented as K, is a property of vascular plants, soil or rock, that describes the ease with which water can move through pore spaces or fractures. It depends on the intrinsic permeability of the material and on the degree of saturation. Saturated hydraulic conductivity, Ksat, describes water movement through saturated media [56].

- **Thermal conductivity** k, is the property of a material describing its ability to conduct heat [56].

Appendix F

ORC and hybrid cycles analysis

The analysis of conducted on top site power cycles in the project thesis fall 2010 is presented in this Appendix. A simple Organic Rankine Cycle and two different hybrid cycles (geothermal energy combined with a waste plant) are analyzed. Enlarged figures of each of the investigated cycles are shown in section 1.6.

Definition of parameters

η_{th} is the thermal efficiency of the system, β is the ratio between net work output from the cycle and mass flow of geothermal circulation fluid and λ measures the exploitation of available geothermal energy.

$$\eta_{th,orc} = \frac{W_{net}}{Q_{geo}} = \frac{m_{r134a}\left(\Delta h_{turbine} - \Delta h_{pump}\right)}{m_{geo}\left(h_{geo} - h_{rej}\right)} \tag{F.1}$$

$$\beta = \frac{W_{net}}{m_{geo}} \tag{F.2}$$

$$\lambda = \frac{T_{geo} - T_{rej}}{T_{geo} - T_0} \tag{F.3}$$

Other variables that are used in this Appendix are: $\eta_{th,sys,85\%}$ refers to the thermal efficiency of the system if only 85% of the total energy from the waste combustion plant is utilized (accounts for losses in the furnace in the waste plant), m_{geo} refers to the mass flow of the geothermal circulation fluid, m_{wf} is the mass flow of the working fluid, T_{rej} is the rejection or injection temperature of the geothermal fluid while $T_{geo}$is the production temperature of the geothermal fluid. The different power cycles are reffered to using the

nomenclature developed by Gozdur [47], where Dual Fluid Hybrid (DFH) plant refers to the cycle where the ORC is the bottoming cycle, Hybrid (HYB) plant uses the geothermal heat as pre-heat in water based rankine cycle.

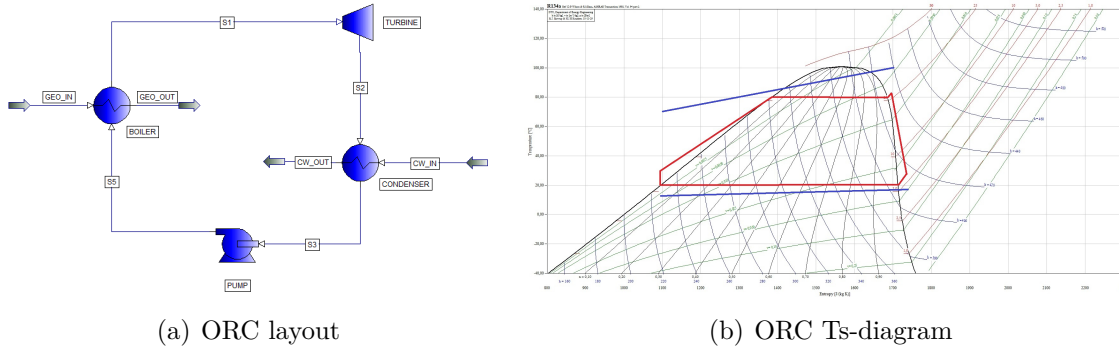# F.1 Analysis of a ORC

(a) ORC layout

(b) ORC Ts-diagram

Figure F.1: Organic Rankine cycle (ORC). Figure a) the simulated ORC configuration, while figure b) shows the cycle in Ts diagram

The cycle can be seen in figure F.1(a). The cycle have been simulated in PRO/II , and parameters like $\eta_{th}, \beta, \lambda$ have been evaluated.

The cycle has been simulated with a inlet (T_{geo}) and rejection temperature (T_{rej}) of the geothermal fluid between 80°C - 160°C and 40°C - 100°C, respectively. The heat exchanger between the geothermal fluid and the working fluid have been set to a duty of 5MW. The pressure at the outlet of the turbine have been set to 600 kPa in order to achieve liquid phase for the working fluid after the condenser. The cooling water have a inlet temperature of 15°C. The pinch point have been set to 5°C in all heat exchangers. PRO/II has been set to optimize the outlet pressure of the pump (up to a maximum pressure of 50bar). The mass flow of the geothermal fluid and working fluid have been calculated based on the given data. The geothermal fluid has been assumed to be water. The isentropic efficiency of the pump has been set to 70% and the turbine have been set to 80%, based on information from [7].

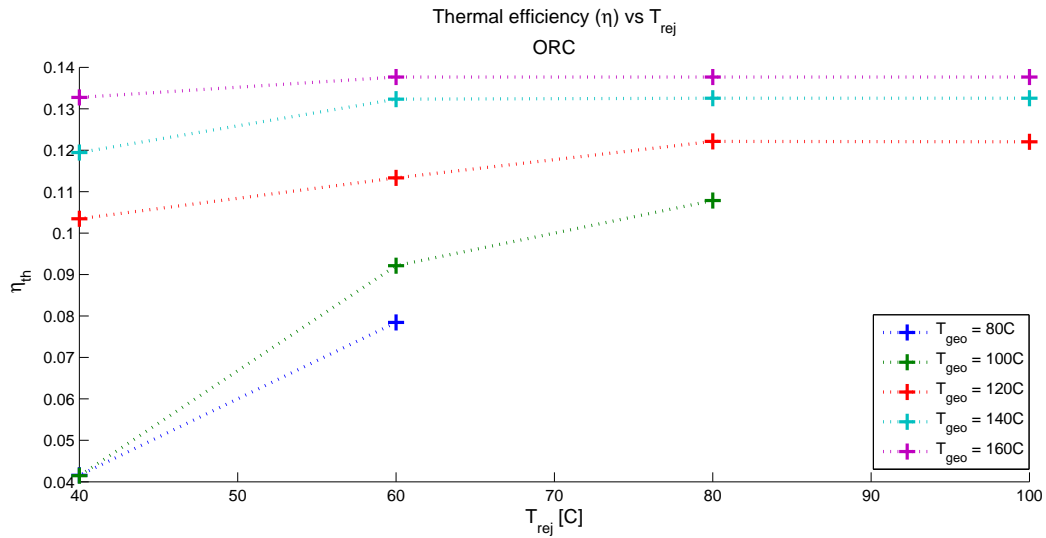The result of the simulation can be seen in figure: F.2, F.3 and F.4

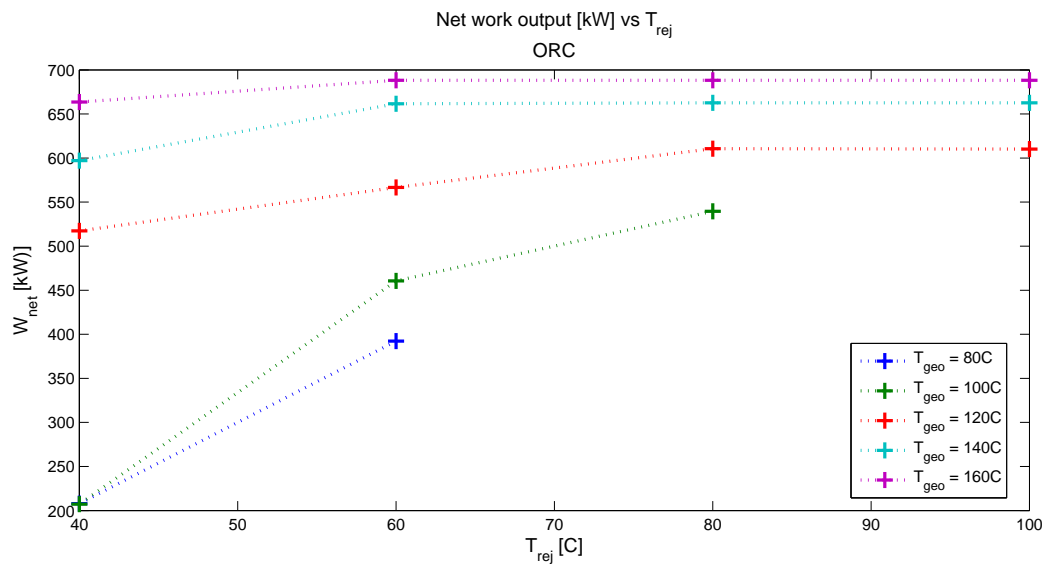**Figure F.2:** ORC: How η_{th} vary with variation in T_{geo} and T_{rej}

Figure F.3: ORC: How W_{net} vary with variation in T_{geo} and T_{rej}
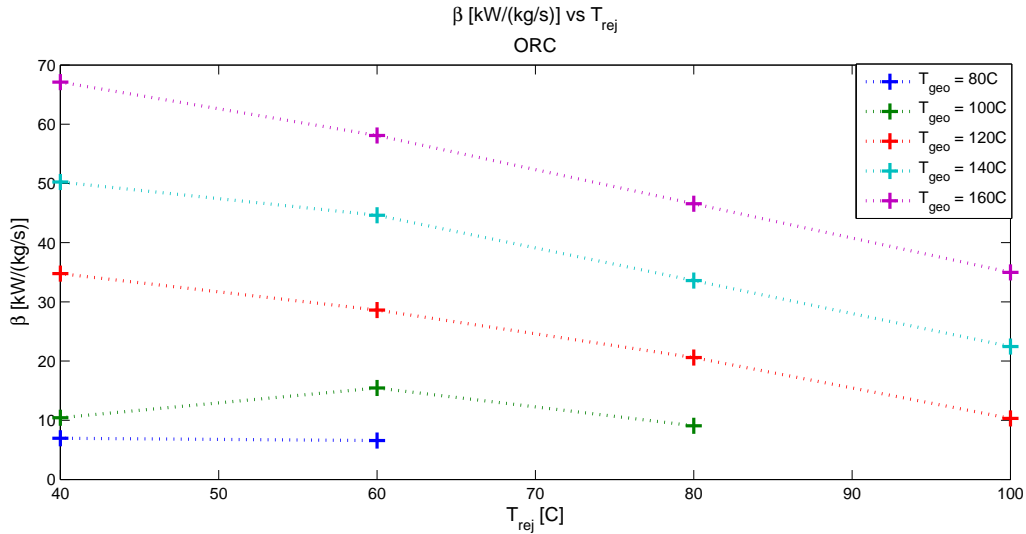
Figure F.4: ORC: How β vary with variation in T_{geo} and T_{rej}

Discussion of the results

The main parameter effecting the thermal efficiency is the match between the working fluid and the geothermal fluid in the boiler. An increase in pressure of the working fluid equals an increase in thermal efficiency, this can be seen from equation (F.1). The increase in pressure, and thus thermal efficiency, is limited by the pinch point, at least from a thermodynamical point of view. A system that is optimized with respect to thermal efficiency will therefore increase the pressure of the working fluid until the pinch point is reached. This implies that the cycle will be transcritical for temperatures and pressure above the critical state, the critical state for r134a can be seen in table 3.3. This is the case for inlet geothermal temperatures above 120°C, where the working fluid pressure is above 4000 kPa.

The thermal efficiency was found to be in the range 4% to about 14%, which is in good agreement with the findings in section 1.6. The reason for the low thermal efficiency for low inlet and rejection temperatures is the limitation imposed on the maximum pressure by the pinch point in the boiler. The thermal efficiency is constant for a geothermal temperature above 140°C and a rejection temperature above 60°C, this is due to the fact that the maximum pressure of the working fluid was set to 50bar. The reason for constant thermal efficiency for T_{geo} at 120°C and T_{rej} above 80°C is that the pinch point is located between the cold product and hot product temperature, seen figure F.5. A increase in T_{rej} will therefore not affect the thermal efficiency of the system, only β. This also explains the invariance in work output at the same geothermal temperatures.
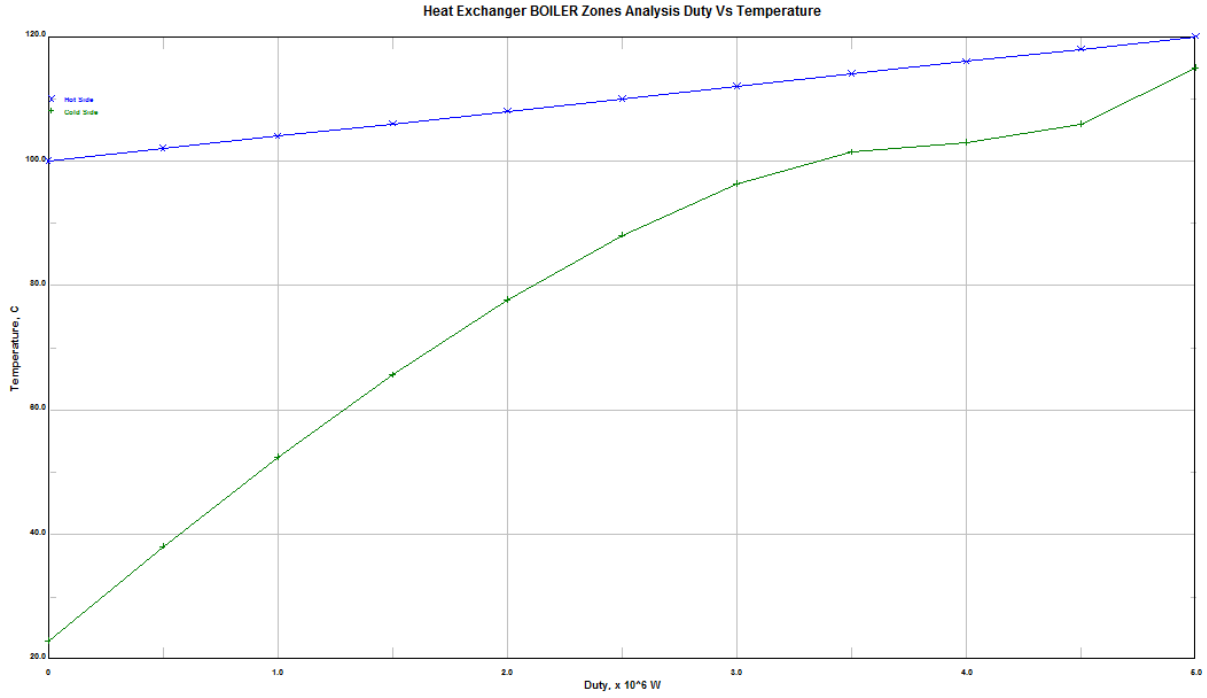
174

Figure F.5: Match between temperature profiles in the boiler for the ORC. Temperature on y-axis (100^0C to 20^0C) and duty on x-axis (0 - 6 MW).

Another perspective is that the limitation imposed by the constant duty of the boiler, 5 MW, causes the stable thermal efficiencies for the conditions given. The only effect of an increase in T_{rej} is an decrease in β, which means that higher mass flow of geothermal fluid is need in order to reach a duty of 5MW. The opposite is true for an increase in T_{geo}, which would decrease the mass flow of geothermal fluid . The effect can be seen from equation F.4, if ΔT decreases must m_{geo} increase, assumed that C_p is constant.

$$Q_{geo} = const = \Delta H = m_{geo}cp\Delta T \tag{F.4}$$

A regenerator can be used in order to increase the thermal efficiency. There a potential for reducing cooling and heating demands by using the available superheat after the turbine as a preheat before the boiler. 0.2 MW is available for use in a regenerator for a inlet and rejection temperature of 120°C and 100°C.

F.2   Waste combustion plant combined with ORC

There are some new factors that should be considered when these systems are analyzed, compared to a single ORC. The main new parameter is the ratio between waste energy and geothermal energy transfered to the system, equation F.5. The other factor is that the temperature of the exhaust gas from the waste boiler should not be increased by the added geothermal energy. This would cause the efficiency of the waste plant to decrease, which is not desirable.

$$\theta = \frac{Q_{waste}}{Q_{geo}} \tag{F.5}$$

$$\eta_{th,sys} = \frac{W_{net}}{Q_{waste} + Q_{geo}} \tag{F.6}$$

F.2.1   Analysis of the dual fluid hybrid plant

This section looks at the dual fluid hybrid plant, where the geothermal heat exchanger and the IHE are connected in series. A schematic of the cycle and the process plotted in Ts diagram can be seen in figure F.6.

In these simulations the rejection temperature of the geothermal fluid has been set to 25°C, in order to exploit all of the available geothermal energy. The idea is that all of the available geothermal energy should be utilized. The same restrictions as for the ORC simulation have been imposed on the ORC cycle in the combined plant, see section F.1. The pressure and the temperature after the waste boiler have been set to 40bar and 400°C, due to limitations caused by fouling, scaling and production of toxic compounds. The waste boiler have been modeled as a heat exchanger with air at 1100°C at the inlet and 150°C at the exit. The mass flow of the geothermal fluid and the ORC working fluid have been calculated based on the restrictions that $T_{rej} = 25$°C and that the ORC working fluid is saturated liquid when leaving the heat exchanger. The exit pressure of the turbine in the waste cycle have been set to 101kPa. The outlet pressure of pump 1 have been varied from 10bar to 40bar and the inlet temperature of the geothermal fluid have been varied from 80°C - 140°C. The efficiency of the pump and turbine in the ORC and waste cycle have been set to 70% and 80%.

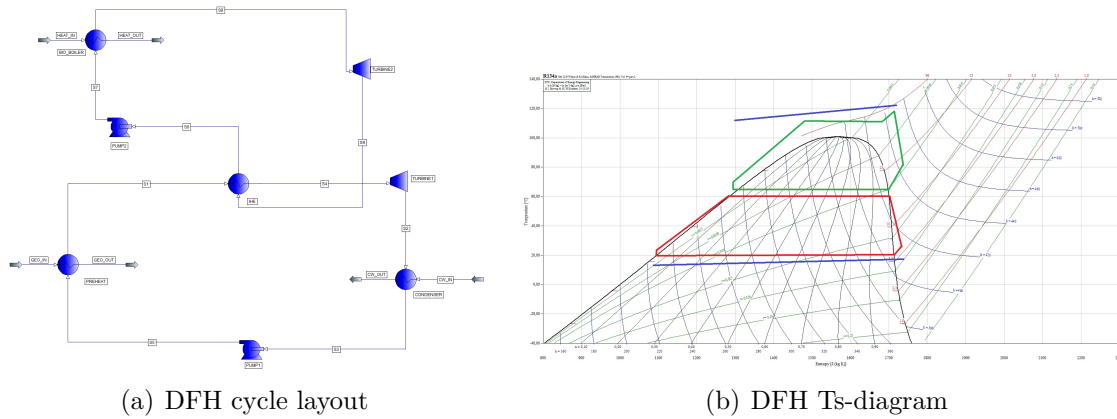The results from the simulation can be seen in figure F.7, F.8, F.9, F.10.

(a) DFH cycle layout

(b) DFH Ts-diagram

Figure F.6: Dual fluid hybrid plant (DFH). Figure a) shows a typical configuration of a DFH cycle, while figure b) shows the cycle in Ts diagram
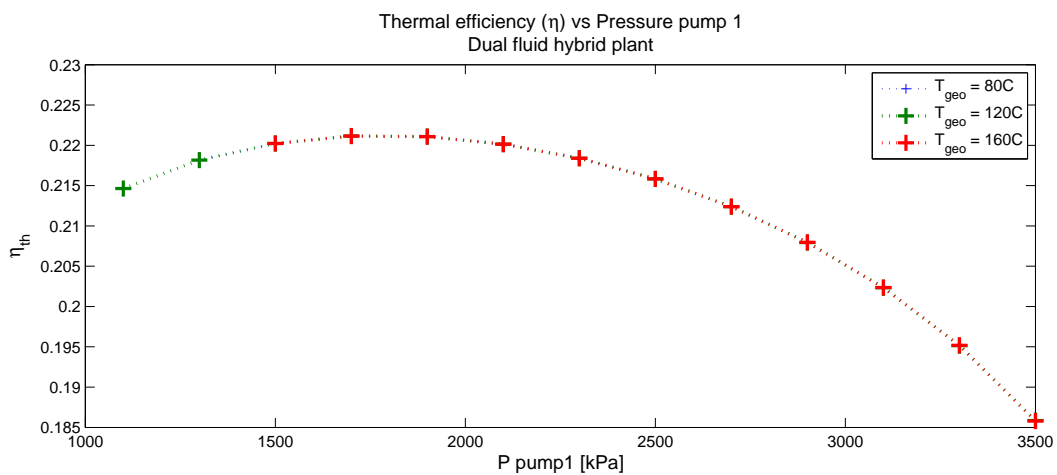

Figure F.7: DFH: How $\eta_{th,sys}$ vary with variation in T_{geo} and P_{pump1}
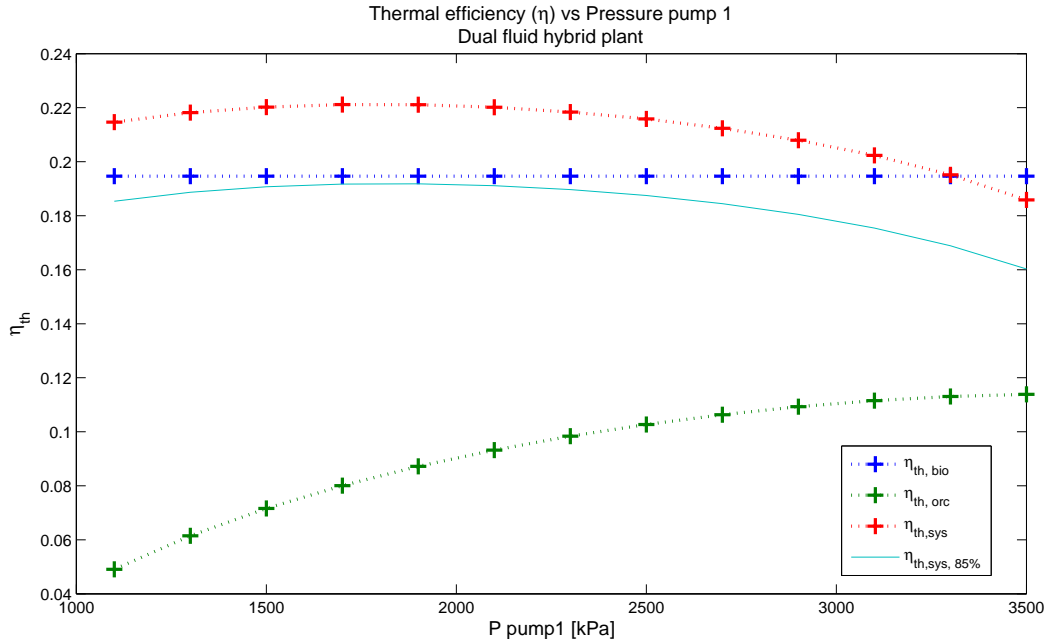
177

Figure F.8: DFH: $\eta_{th,sys}$, $\eta_{th,orc}$, $\eta_{th,waste}$ and $\eta_{th,sys,85\%}$ vary with P_{pump1} @ $T_{geo} = 120°$C
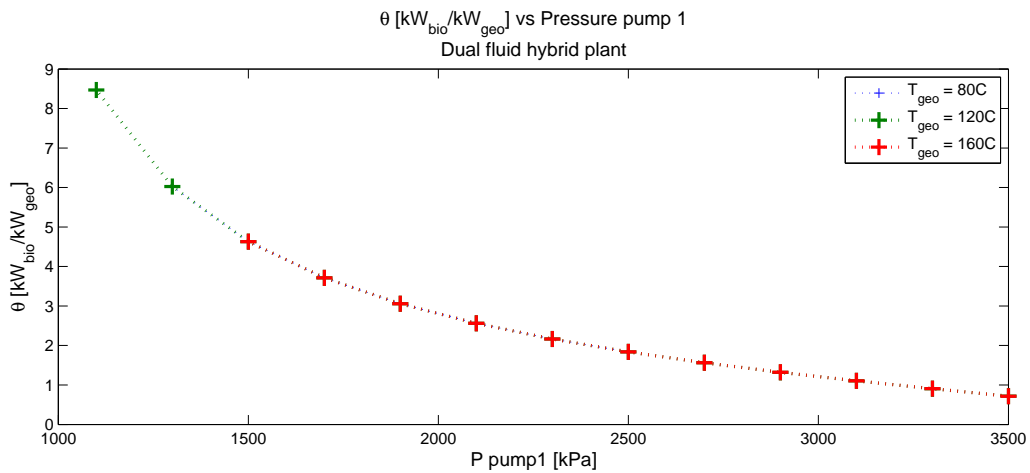

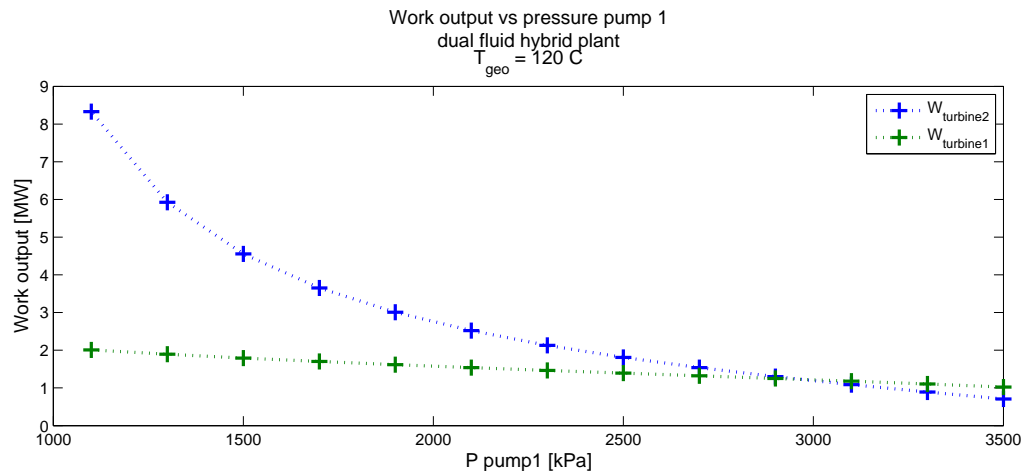**Figure F.9:** DFH: How θ varies with outlet pressure from pump 1 @ $T_{geo} = 120°$C

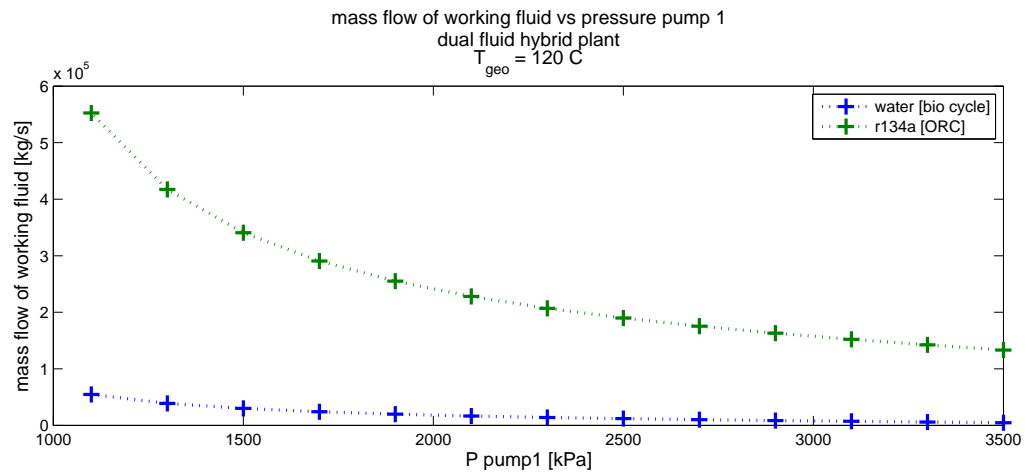**Figure F.10:** DFH: Work out from the system @ $T_{geo} = 120°$C

Figure F.11: DFH: mass flow of r134a and water vs outlet pressure of pump 1 @ $T_{geo} = 120°$C

Discussion of the results

The analysis of the system reveals that the thermal efficiency of the combined cycle is constant with respect to changes in T_{geo}, figure F.7. The reason is that the pinch point is located at between the hot product and cold inlet temperature, see figure F.12. The result is that the temperature and pressure of stream S1 is invariant of T_{geo}, which means that the cycle also is invariant to T_{geo}. The effect T_{geo} is that it limits the maximum pressure of the cycle, due to the pinch point in the boiler.

The thermal efficiency of the waste cycle is constant, which is logical since the conditions are constant, the only variable is the mass flow of water which effects all components equal. The thermal efficiency of the ORC increases as the pressure of the cycle increases, which is also natural, see section F.1.

The thermal efficiency peaks around 1700kPa, figure F.8. The reason being the interaction between available heat of evaporation between the working fluids of the two cycles, r134a and water. This impacts the mass flow of the working fluids, which has an impact on the relative importance of the two cycles, this can clearly be seen from figure F.9. The controlling factor in a DFH is therefore the IHE, due to the variation in available heat of evaporation. The simulation could have been further improved if the outlet pressure of turbine 2 had been allowed to vary and not set to fixed value, since that would have improved the fit between the two working fluids. The effect would have been a reduction in superheat of r134a and an increase in the power output from turbine 2 due to a lower exit pressure.

The mass flow of the geothermal fluid is fairly constant compared to the mass flow of water, which drastically decreases with an increase in pressure of pump 1, see figure F.11. The reason for this is that the mass flow of water is limited by the available heat of evaporation in IHE, which decreases with an increase in pressure of pump 1. This then reduces the work output and heat duty of the boiler in upper cycle, which can be seen in figure F.10 and F.9.

The thermal efficiency of the system varies between 19% - 22%, which is in good agreement with the findings of Gozdur [47] if one considers the fact that this analysis accounts for entropy losses in the turbine and pump. The thermal efficiency should also account for the total waste energy transferred to the waste boiler, and not just the heat duty of the waste boiler. A boiler efficiency of 85% is therefore assumed in order to account for these losses. The effect on the thermal efficiency can be seen in figure F.8, the line marked with $\eta_{th,sys,85\%}$. The maximum thermal efficiency is reduced to 17%.
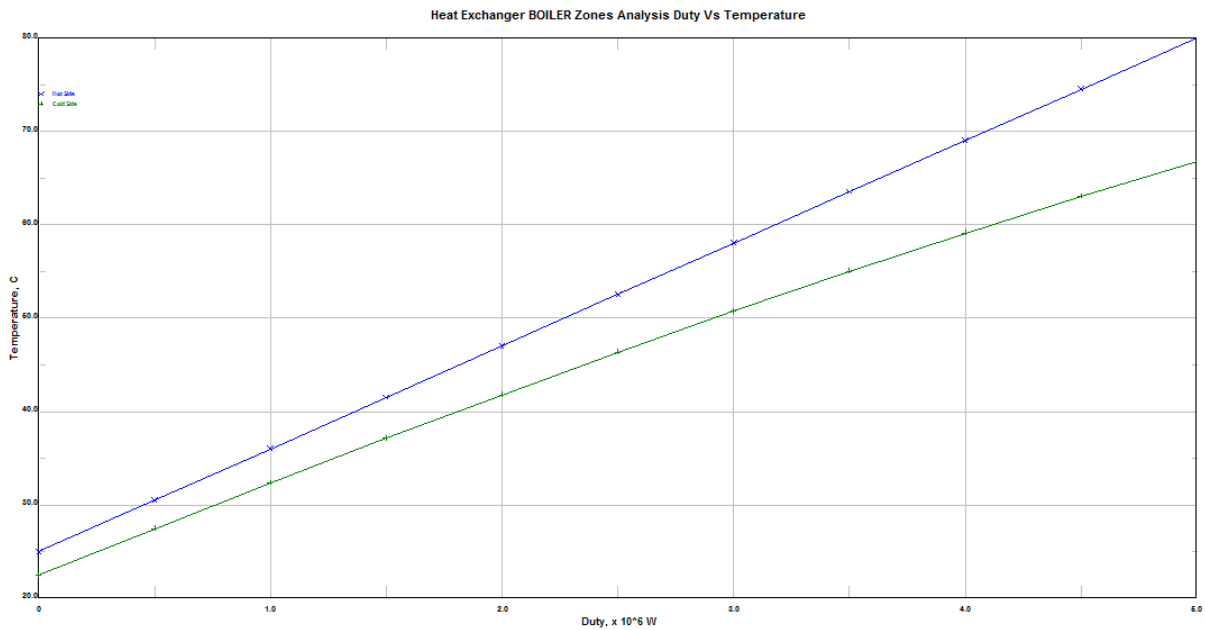
Figure F.12: Match between temperature profiles in the boiler for the fdh. Temperature on y-axis (100^0C to 20^0C) and duty on x-axis (0 - 6 MW).

The combined plant should be compared to a single waste combustion cycle in order to see how the bottoming cycle effect the overall performance. A analysis of a single waste combustion cycle was performedand the gain in thermal efficiency by using the ORC as bottoming cycle is about 2%, calculated with a waste boiler efficiency of 85%.

F.2.2 Analysis of the hybrid plant

The constrictions for the hybrid plant are similar to the ORC analysis, however there are some differences. The working fluid are water, and not r134a. The pressure and temperature at the exit of the waste boiler are 40bar and 400°C, same as for the DFH plant (see section F.2.1). The pressure at the turbine exit is set to 8kPa. The reason is that the working fluid is cooled down to 20°C and the pressure must be 8kPa in order for the working fluid to be water. The geothermal fluid is cooled down 25°C in order to exploit all of the available geothermal energy. The duty of the preheater have been set to 5MW. The mass flow of the working fluid are calculated given the constraint that the working fluid should leave the preheater at 5°C lower than T_{geo}.

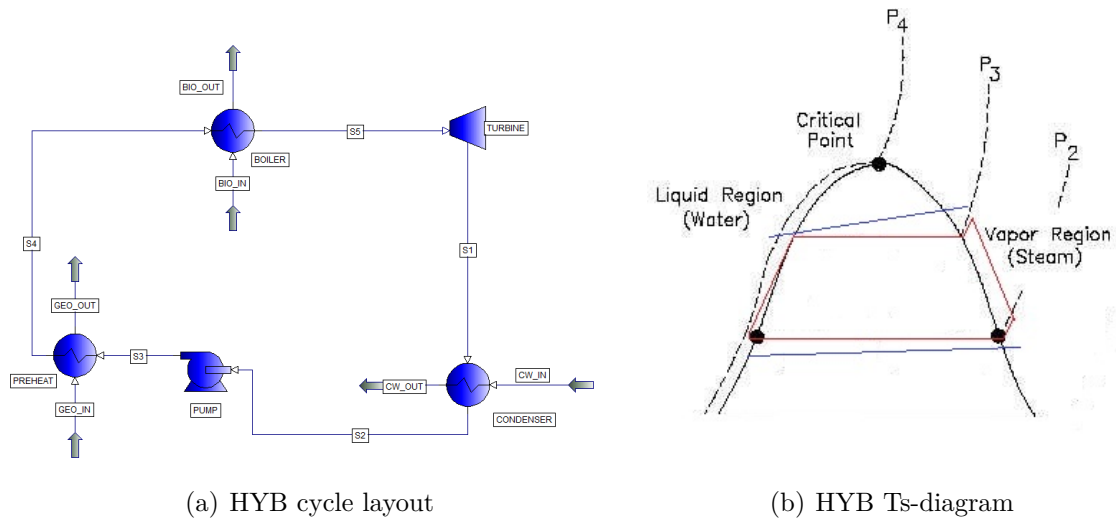The results of the simulation can be seen in figure F.14, F.15, F.16.

(a) HYB cycle layout   (b) HYB Ts-diagram

Figure F.13: Hybrid plant (HYB). Figure a) shows a typical configuration of a HYB cycle, while figure b) shows the cycle in Ts diagram
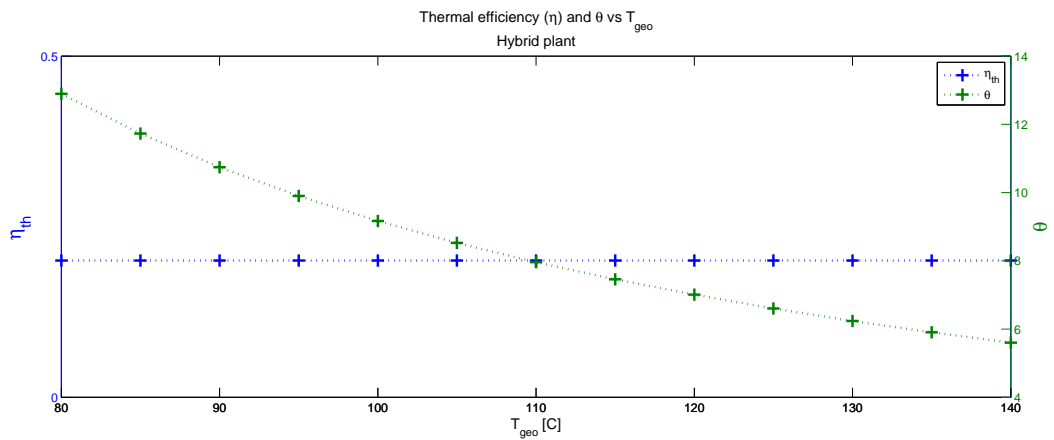
Figure F.14: HYB: Thermal efficiency and θ vs T_{geo}
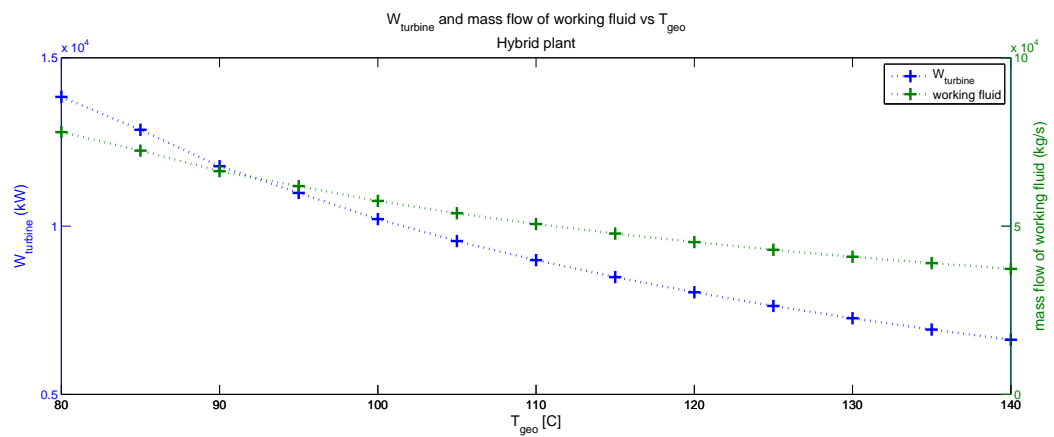

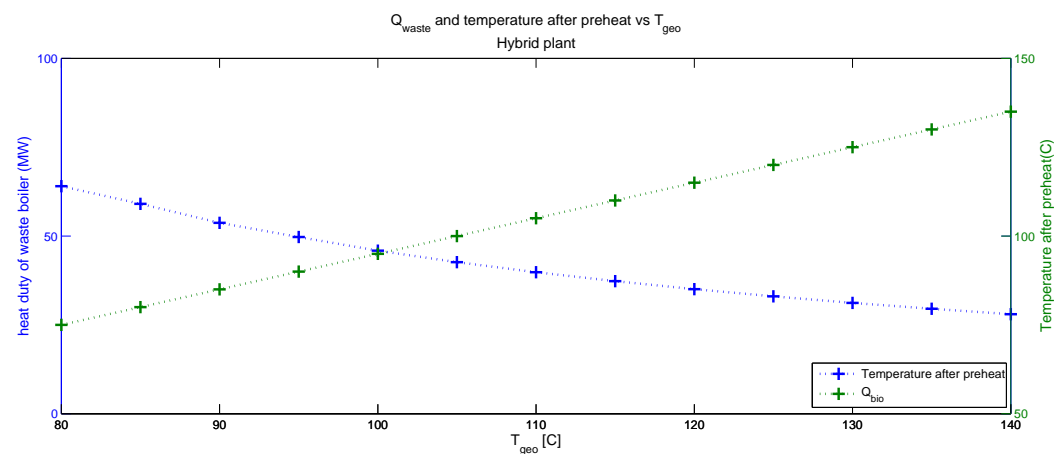**Figure F.15:** HYB: variation in work out vs T_{geo}

Figure F.16: HYB: Q_{waste} and T_{s4} vs T_{geo}

Discussion of the results

The thermal efficiency of the HYB plant is constant, this is natural since the operating conditions are the same for all variations of T_{geo}. The effect of a change in T_{geo} is a change in mass flow of the working fluid and a change in θ. The change in working fluid mass flow is due to the limitation in heat duty of the preheater (5MW) and a change in temperature difference, see equation F.7.

Q_{waste} and $W_{turbine}$ decreases as the temperature of the geothermal fluid increases. The reason for the decrease is that the mass flow decreases, following the argument given above.

$$Q_{geo} = const = \Delta H = m_{wf} cp \Delta T \tag{F.7}$$

Following the argument given before, in section F.2.1 under discussion of the results, should a waste boiler efficiency of 85% be used in order to account for the total energy transferred to the system. The effect is a reduced thermal efficiency. Since the thermal efficiency is constant at 20% will the new thermal efficiency also be constant. The thermal efficiency of the system, accounting for losses in the waste boiler, is 17%. Which is the same as for the case for a single waste combustion plant under the same conditions, this is natural since all the operating parameters are equal.

The results for HYB is in good agreement with Gozdur [47] if one takes into account that the simulation performed by Gozdur is for ideal cycle with 100% isentropic efficiency.

The gain with using geothermal energy as a preheater is that the need for waste, or other renewable combustibles, decreases with the added geothermal energy, for a given power production rate. The system is also very flexible with respect to different energy situations, θ. The HYB cycle is also relatively simple compared to the DFH.